Barts and The London
School of Medicine and Dentistry

Characterisation of a novel *in vitro* model of Basal cell carcinoma (BCC) through stable PTCH1 suppression in immortalised human keratinocytes

PhD Thesis

2013

Muhammad Mahmudur Rahman

Centre for Cutaneous Research

Blizard Institute of Cell and Molecular Science

Barts and The London School of Medicine and Dentistry

Queen Mary University of London

Abstract

Basal cell carcinoma (BCC) of the skin is predominantly associated with mutational inactivation of the *PTCH1* tumour suppressor gene resulting in constitutive activation of the Hedgehog (HH) developmental pathway. Tumour formation is linked to induction of the GLI (GLI1 and GLI2) transcription factors via a pathway that is thought to require the transmembrane protein SMOOTHENED (SMO) and accordingly, SMO is attracting much interest as a drug target in cancer therapy. However, although there has been a high degree of success in treating some BCCs with anti-SMO compounds, many tumours are only partially or unresponsive which indicates that SMO-independent mechanisms may contribute to tumour formation and/or viability.

To further understand how loss of (or reduced) PTCH1 function contributes to BCC, RNAi (retroviral shRNA) was employed to suppress PTCH1 in NEB1 and N/Tert immortalised human keratinocyte cells. Compared to control (shCON) cells, PTCH1 knockdown (shPTCH1) cells displayed more compact colony formation as well as increased GLI1 (but not GLI2) expression however, whereas the increase of GLI1 was suppressed upon transfection with SMO siRNA in shPTCH1 cells, it was insensitive to the presence of the SMO antagonists Cyclopamine-KAAD and SANT1 in shCON cells. The reason for this is unclear but SMO levels were increased and more nuclear in shPTCH1 cells indicating that SMO may have nuclear signalling capability that is unresponsive to certain SMO antagonists. Indeed, cDNA microarray profiling revealed that 80% of the genes that were differentially expressed in NEB1-shPTCH1 cells (>2-fold, $p<0.01$) remained differentially expressed in the presence of Cyclopamine-KAAD; this includes the chemokines CXCL10 and CXCL11 which were recently shown to be over-expressed in BCC thus helping validate the efficacy of NEB1-shPTCH1 cells as an *in vitro* tumour model. In addition, functional gene grouping has predicted novel biological processes downstream of PTCH1 that may be important in BCC biology including NF-κB signalling. In summary, the data presented in this thesis suggests that the mechanism(s) through which the loss of PTCH1 leads to BCC formation may be more complex than has been inferred from previous studies.

Declaration

The work contained in this thesis is the independent work of the author (unless stated otherwise) with the instruction and guidance from my supervisors Dr. Graham Neill and Professor Mike Philpott.

Acknowledgements

I gratefully acknowledge the many people who have helped me to produce this thesis. I thank my supervisors Dr. Graham Neill and Professor Mike Philpott for giving me the opportunity to study under their supervision. In particular, I am indebted to my primary supervisor Dr. Graham Neill for his guidance and patience throughout my course, his enthusiasm for science has demanded that I learn many techniques and scrutinise all aspects of my work ultimately helping me become the scientist that I am today. I thank all of the Neill group and associated members that have contributed to our research: Dr. Diamlee Herath, Dr. Muhammad Pirzado, Margherita Ruocco, Dr. Joanne Selway, Avijit Roy, Dr. Sandeep Nadendla, Dr. Ravi Atkar, Dr. Lia Panagou, Dr. Matt Ward and Allon Hazan. I am also grateful to the British Skin Foundation for their funding.

I would like to acknowledge my family and in particular my wife for supporting me continuously. I apologise to everyone that I have neglected and dedicate my thesis to them. Finally, I reserve special thanks for Dr. Sahira Khalaf who has supported me always in the laboratory and helped me overcome the numerous challenges that I have faced during my time at the institute.

Conferences and awards

William Harvey Day 2010 London: poster prize winner.

William Harvey Day 2011 London: poster presentation.

BSID British society for investigative dermatology 2011: oral presentation, £200 travel grant award winner.

BSID British society for investigative dermatology 2012: poster prize winner.

Hedgehog conference Singapore 2012: poster presentation, £1,500 travel grant award winner.

Contents

Figures and tables list

Abbreviations

ALMS	Alström syndrome
APS	Ammonium persulphate
ATP	Adenosine triphosphate
AU	Protein absorbance
BBS	Bardet-Biedl syndrome
BCC	Basal cell carcinoma
B-CLL	B-cell lymphocytic leukemia
BLAST	Basic local alignment search tool
BMP	Bone morphogenic protein
BSA	Bovine serum albumen
cAMP	Cyclic andenosine monophosphate
cDNA	Complementary deoxyribonucleic acid
CNS	Central nervous system
Cos2	Costal-2
Ct	Cycle threshold
CTS	Connective tissue sheath
Cyc-KAAD	Cyclopamine-KAAD
CXCL	Chemokine (C-X-C motif) ligand
DAPI	4',6-diamidino-2-phenylindole
DAVID	Database for annotation, visualisation and integrated discovery
DEG	Differentially expressed gene
DHH	Desert hedgehog
DISP	Dispatched
DNA	Deoxyribonucleic acid
dNTP	Deoxynucleotide triphosphate
DP	Dermal papilla
dTCF	T-cell factor
DUSP6	Dual specificity phosphatase 6
ECM	Extracellular matrix
EDTA	Ethylenediaminetetraacetic
EGF	Epidermal growth factor
EGFR	Epidermal growth factor receptor
EHH	Echidna hedgehog
EMT	Epithelial-mesenchymal transition

FABP	Fatty acid binding protein
FBS	Foetal bovine serum
FGF	Fibroblast growth factor
FLG	Filaggrin
FU	Fused
Fz	Frizzled
gDNA	Genomic deoxyribonucleic acid
GE	Germinative epithelium
GFP	Green fluorescent protein
GSK3β	Glycogen synthase kinase 3β
HEK293	Human embryonic kidney-293 cells
HH	Hedgehog
HNSCC	Head and neck squamous cell carcinoma
HPE	Holoprosencephaly
HRP	Horseradish peroxidase
HSPG	Heparin sulphate proteoglycans
IFE	Interfollicular epidermis
IFT	Intraflagellar transport
IGF	Insulin growth factor
IHH	Indian hedgehog
IKK	Inhibitor of kappa B kinase
IL	Interleukin
IRS	Inner root sheath
IGFBP2	Insulin-like growth factor binding protein 2
KEGG	Kyoto encyclopaedia of genes and genomes
KGM	Keratinocyte growth medium
KRT	Keratin
L	Litre
LAP	Latent associated protein
LB	Luria-Bertani
LCN2	Lipocalin 2
LEF	Lymophoid enhancing factor
LOH	Loss of heterozygosity
LRP	Lipoprotein receptor
LTBP	Latent TGF-β binding protein
MAPK	Mitogen-activated protein kinases

MCS	Multiple cloning site
MMP	Matrix metalloproteinase
mRNA	Messenger ribonucleic acid
mTOR	Mammalian target of Rapamycin
NBCCS	Nevoid basal cell carcinoma syndrome
NF-kB	Nuclear factor kappa-light-chain-enhancer of activated B cells
nM	Nano molar
ORS	Outer root sheath
PBS	Phosphate buffer saline
PCP	Planar cell polarity
PCR	Polymerase chain reaction
PDT	Photodynamic therapy
PKA	Protein kinase A
PTEN	Phosphatase and tensin homolog deleted on chromosome 10
PTCH	Patched
QHH	Qiqihar hedgehog
qPCR	Quantitative polymerase chain reaction
RISC	Ribonucleic acid-induced silencing complex
RNA	Ribonucleic acid
RNAi	Ribonucleic acid interference
ROS	Reactive oxygen species
SCC	Squamous cell carcinoma
SDS	Sodium dodecyl sulfate
SHH	Sonic hedgehog
shRNA	Short hairpin ribonucleic acid
siRNA	Small interfering ribonucleic acid
SMO	Smoothened
SUFU	Suppressor of fused
TA	Transit amplifying
TAE	Tris acetate ethylenediaminetetraacetic
TEMED	Tetramethylethylenediamine
TGF	Transforming growth factor
TGF-β	Transforming growth factor-β
TGM	Transglutaminase
TLR	Toll-like receptor
TNC	Tenascin C

TWHH	Tiggywinkle hedgehog
UV	Ultraviolet
µM	Micro molar
VEGF	Vascular endothelial growth factor
VIM	Vimentin
WT	Wild-type
ZPA	Zone of polarising activity

Chapter 1

Introduction

Chapter 1 Introduction

1.1 Structure of the skin

The skin encapsulates the whole surface of the body and provides a number of vital functions including barrier formation, synthesis of vitamin D, thermoregulation and protection from ultraviolet (UV) irradiation. The skin is composed of three layers which are the epidermis, dermis and subcutaneous layer (Figure 1.1). The epidermis is the outermost layer of the skin which interacts with the external environment and is mainly consistent of keratinocytes with differing levels of differentiation. The stratum corneum contains the most differentiated cells, the stratum granulosum is followed by the stratum spinosum which contains desmosomes that provide structure and strength and the stratum basale layer which contains undifferentiated keratinocytes that can proliferate and migrate. Differentiation of keratinocytes occurs from the basal layer towards the superficial layer of the epidermis where the terminally differentiated keratinocytes or corneocytes, will shed from the surface.

Melanocytes that are found in the stratum basale contain membrane bound organelles called melanosomes that produce the pigment melanin which is involved in human skin pigmentation. Melanocytes are bound to keratinocytes by E-cadherin which is a cell to cell adhesion protein, allowing the transfer of melanin to the keratinocytes (Freedberg et al., 2003). Melanin pigmentation increases upon UV irradiation as a defence mechanism to prevent DNA damage as the excess melanin is able to absorb UV light (Agar et al., 2005). The stratum basale also contains Merkel cells which are part of the somatosensory system that plays a role in touch response (Maricich et al., 2009). These cells are larger than keratinocytes (to which they are attached) and are present in hair follicles. Langerhans' cells are present in the stratum spinosum and are part of the immune system presenting antigens to T lymphocytes.

The basement membrane divides the epidermis from the dermis and acts as a matrix by which cells may attach for the purpose of differentiation or apoptosis. Also, it can provide a scaffold to allow for tissue repair. The adjacent dermis is rich in collagen to provide stability as well as fibroblasts which play an important role in wound healing. The dermis gives the skin its strength as well as its flexibility which is provided by collagen, elastin and fibrillin proteins. The hypoderm or subcutaneous tissue contains fat that serves to insulate the body and can be utilised for energy storage. The dermis also accommodates hair follicles.

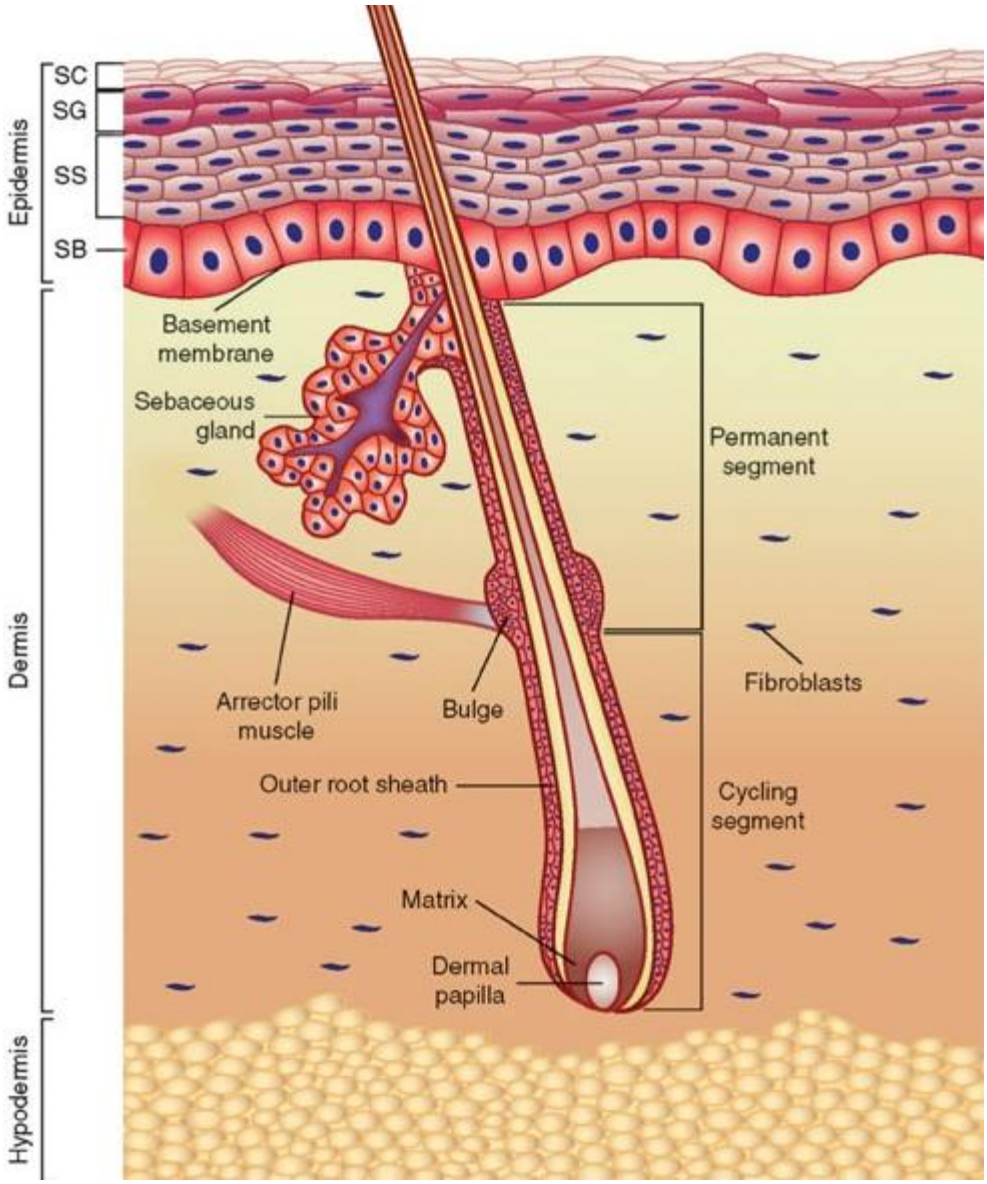

Figure 1.1: Structure of the skin (Wong and Chang, 2009)

SC: stratum corneum, SG: stratum granulosum, SS: stratum spinosum, SB: stratum basale.

1.1.1 Epidermal layers

The epidermal layers are distinguishable based on various levels of keratinisation (Figure 1.2). Keratins are structural proteins which form heteropolymers that give rise to intermediate filaments. In combination with actin microfilaments and microtubules, a cytoskeletal structure is formed. Type I keratins (KRT10 to KRT20) have acidic properties while Type II keratins (KRT1 to KRT9) are basic or neutral. In order to form a heteropolymer filament structure, both Type I and II keratins must be expressed.

The stratum corneum is the most differentiated layer of keratinocytes and is the layer which interacts with the external environment. The thickness of this layer varies depending on age, sex and area of the body i.e. palms of the hand and soles of the feet have a thicker cornified layer. Cells of the stratum corneum are referred to as corneocytes and are the largest form of keratinocyte with a flattened morphology lacking nuclei and cellular organelles (McGrath et al., 2004). Corneocytes contain the filament aggregating protein filaggrin (FLG) which causes the cell to become flattened (Fuchs, 1990; McGrath et al., 2004). These cells that mainly consist of keratins and lipids create a water resistant barrier. The cornified layer has a certain level of elasticity as the plasma membrane surrounding the stratum corneum is stabilised by involucrin cross-linked to keratins and membrane proteins by transglutaminase (TGM) (Eckert et al., 1997). Corneocytes become less compact as desmosomes that keep the cells bound together are degraded leading to shedding of the skin.

Below the stratum corneum is the stratum granulosum layer that contains 3 to 5 layers of granular cells. Granular cells contain enzymes that degrade organelles such as the nuclei, ribosomes and mitochondria as part of keratinisation (Freedberg et al., 2003). Loss of these organelles leads to an accumulation of keratohyalin granules that contain FLG as well as profilaggrin which is a precursor to FLG. During the differentiation of granular cells, profilaggrin is cleaved into smaller FLG units that aggregate the keratin cytoskeleton. TGMs cross-link the cytoskeleton structures to create the stratum corneum. FLG is therefore very important and loss of function mutations to the protein is known to cause Ichthyosis vulgaris which is characterised by dry, scaly skin (Smith et al., 2006).

In areas of thicker skin such as palms of the hand or soles of the feet, a stratum lucidum layer can be found between the stratum granulosum and stratum corneum to reduce friction between the two layers. Keratinocytes of the stratum lucidum contain eleidin which is a

transformation product of keratohyalin and this makes the stratum lucidum hydrophobic (McGrath et al. 2004).

The stratum spinosum that consists of rows of keratinocytes is the next layer of the epidermis. Keratinocytes of this layer are enlarged and cuboidal in appearance forming 4 to 8 layers. Cells from the stratum basale migrate to the stratum spinosum and this is the first point at which keratinocyte differentiation occurs (Fuchs, 1990). Proteins, lipids and keratins are synthesised here. The stratum spinosum consists of lipid containing lamellar granules that make the external epidermis hydrophobic. The stratum spinosum contains KRT1 and KRT10 that form cytoskeletal filaments that are anchored to adhesion complexes called desmosomes; this provides structural support to the skin (Blanpain and Fuchs, 2006).

The stratum basale is a layer of single cells that separates the epidermis from the dermis and is responsible for the constant renewal of epidermal cells. This layer is generally one cell thick consisting of small cuboidal cells (McGrath et al., 2004). Keratinocytes begin proliferation in the basal layer and will differentiate towards the stratum corneum where the cells will eventually be shed. Due to this, it is important to maintain a sustainable rate of cell proliferation in relation to cell death to avoid hyperproliferation or insufficient epidermis development. Melanocytes are also present within the basal layer responsible for the pigmentation of the skin and nails. Markers of the basal layer include KRT5 and KRT14.

Approximately 10% of the basal layer consists of stem cells that have a high reproductive potential and greater life span (Li and Neaves, 2006). As these cells divide, one of the cells will remain in the basal layer as a stem cell while another daughter cell or transit amplifying cell (TA) is committed to differentiate (McGrath et al., 2004). The TA cells maintain the population or differentiate via three lineages to either the interfollicular epidermis, sebaceous gland or the hair follicle (Watt et al., 2006). Epidermal stem cells strongly adhere to the basement membrane and maintain the interfollicular epidermis by replacing differentiating cells (Blanpain and Fuchs, 2006). In contrast, TA cells are limited in their potential to divide and will become less adhesive so that they can ascend through the epidermis, gradually differentiating as they approach the stratum corneum (Fuchs, 2008; Owens and Watt, 2003).

Keratinocytes attach to each other via desmosomes and in the basal layer keratinocytes are secured to the basement membrane by hemidesmosomes. Integrins within the basement membrane bind to laminins that attach the basement membrane to the dermis (Figure 1.3).

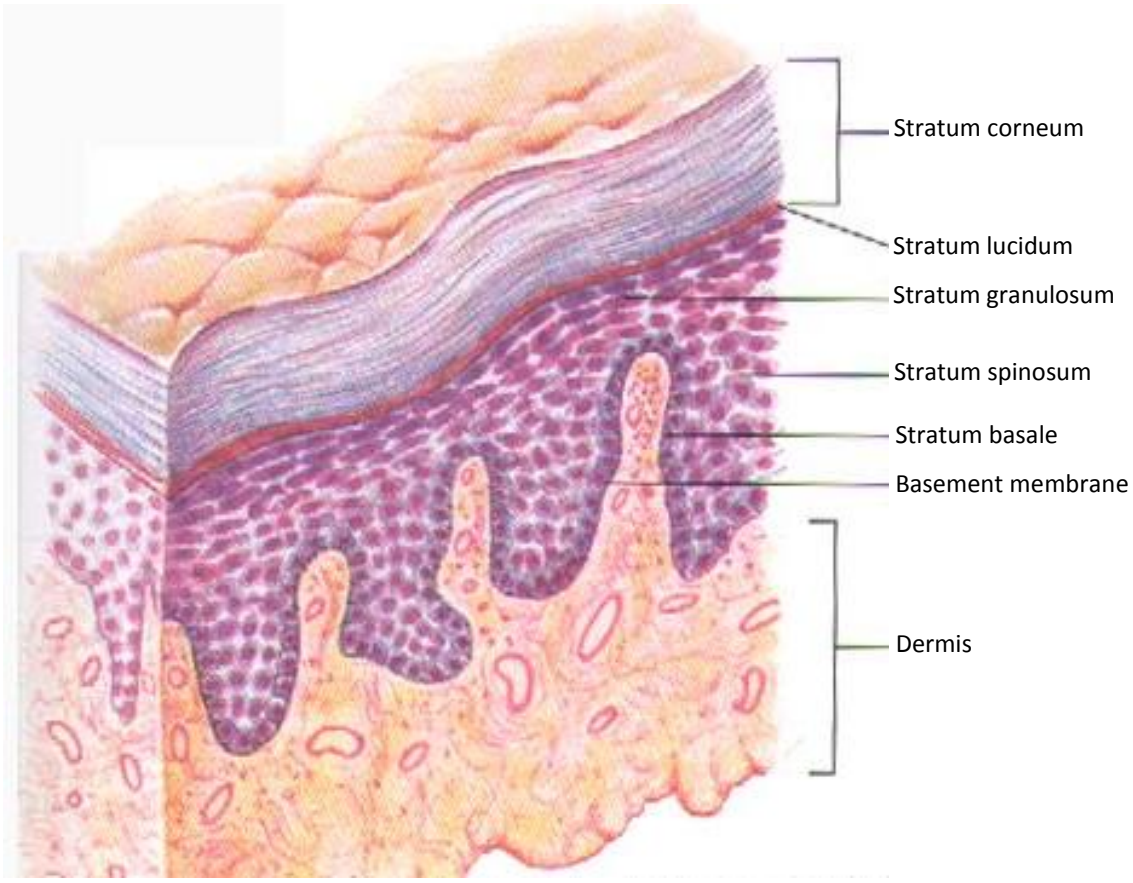

Figure 1.2: Layers of the epidermis (adapted from Shier et al., 1999)

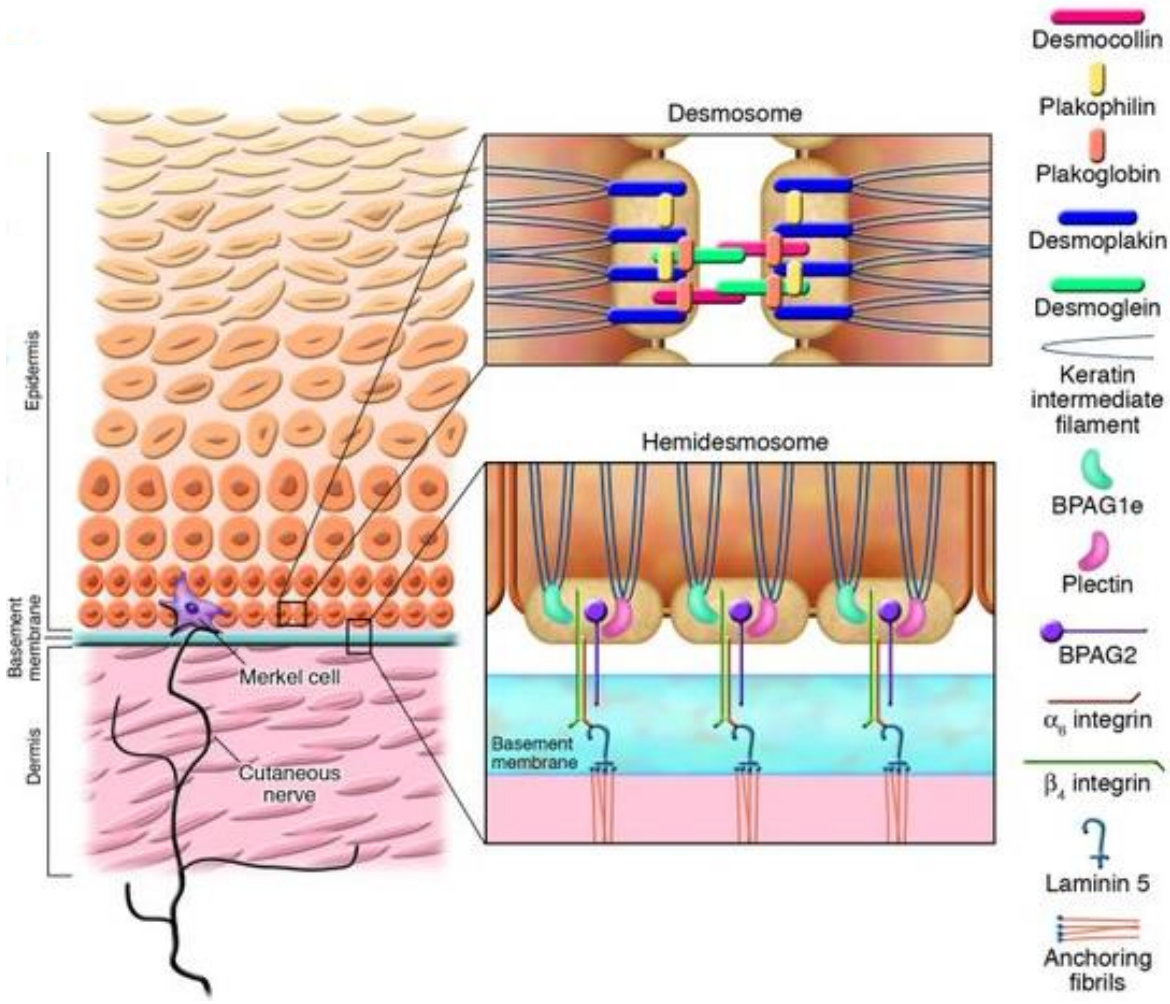

Figure 1.3: Basement membrane (Ross and Christiano, 2006)

1.1.2 Dermis

The dermis provides the skin with its strength as well as its flexibility which is provided by collagen, elastin and fibrillin proteins. The dermis protects the body from injury and helps with thermoregulation via the hypoderm. The dermis also supports hair follicles, nails and both excretory and secretory glands. 75% of the dermis is made up of collagen with the majority being type I and to a lesser extent, types III, IV and V (Frinkel and Woodley, 2001; Goldsmith, 2005). Fibroblasts are the principal cell type of the dermis and are required to synthesise collagen, fibronectin, elastin and laminin; all of which are necessary for the basement membrane and extracellular matrix (ECM) structure. Fibroblasts are mesenchymal cells and form connective tissue and play a role in structure and support of organs such as the skin, lungs and eyes. The dermis also contains a hypoderm layer of fatty tissue and sweat glands both of which are important for thermoregulation. Apocrine and endocrine glands can also be found within the dermis.

1.1.3 Hair follicle

Hair follicles are appendages of the skin that produce hairs which are important for thermoregulation and collecting sensory information from the surrounding environment. The structure of the hair and its three dimensional morphology dictates the shape of the hair produced which characterises different racial hair types. Asians have straight hair follicles that are round in cross section while Caucasian follicles are angled slightly and elliptical in cross section, producing hair with a slight curl. Afro Caribbean follicles are kinked and flat in cross section which produces curly hairs (Montagna and Ellis, 1958). The hair follicle originates in the subcutaneous fat layer that is situated below the dermis intersecting the dermis and epidermis from where the hair shaft extends out. The follicle has a sebaceous gland located within the dermis which secretes the oily substance sebum that gives the skin its water resistant characteristic.

The hair fibre that is made of keratin forms the main body of the follicle. It is surrounded by the inner root sheath (IRS) then the outer root sheath (ORS) (Figure 1.4). The IRS protects and directs the growth of the hair shaft. The IRS itself consists of three concentric layers: a cuticle layer surrounding the hair fibre, Huxley's layer and Henle's layer all characterised by expression of specific keratins. All three layers contain straight protein filaments aligned along the axis of the follicle. The IRS is the first component of the hair follicle to be keratinised which

acts as a template or mould for the emerging hair fibre as the IRS compresses the cortex cells and helps shape the emerging fibre.

The outer root sheath (ORS) surrounds the layers of the IRS and accommodates the bulge region which sits slightly below the sebaceous gland. The bulge contains a niche for epithelial stem cells and attached to the bulge is the arrector pili muscle (Cotsarelis et al., 1990). The sebaceous gland also extends from the ORS. The sebaceous gland consists of a number of sebocyte containing lobes. Sebocytes situated around the periphery of the gland are small flattened cells which divide producing daughter cells that migrate towards the lumen of the gland. Mature sebocytes are large in appearance with large vacuoles that contains sebum which is released into the lumen of the sebaceous gland. Sebum is then secreted via the sebaceous duct, directly onto the skin surface or into the hair canal (Downing et al., 1982; Deplewski and Rosenfield, 2000).

The connective tissue sheath (CTS) or dermal sheath is derived from the dermis and this layer contains fibroblasts and collagen fibrils which provides the follicle with structural stability. Fibroblasts synthesise collagen and play an important role in follicle regeneration as well as renewal of the dermal papilla (DP) after wounding (Jahoda and Reynolds, 2001).

Generation of the hair follicle is directed by the DP. The DP is a collection of mesenchymal derived fibroblasts, pear-shaped in its appearance and is located at the base of the hair follicle. The DP is highly active and consists of cells that induce hair follicle development from the epidermis as well as the root sheaths (Jahoda and Oliver, 1984; Jahoda and Reynolds, 2001).

Surrounding the DP are germinative epithelium (GE) cells and proliferation of these cells affect hair growth (Weinstein and Mooney, 1980). GE cells terminally differentiate to hair follicle matrix cells that are committed to follow one of several differentiation lineages including the IRS and ORS. As cells leave the GE pool, full keratinisation occurs within 2½ days (Weinstein and Mooney, 1980). The interaction between the DP and GE cells is an important factor in hair growth. The larger the size of DP, the greater the number of cells that it contains which correlates with the size of hair follicle therefore the larger the hair follicle, the greater the size of hair fibre produced by the follicle.

DP cells are essential for hair growth as the removal of the DP in rats arrests hair growth. However, the ORS is able to compensate and helps generate a new DP from which hair follicle growth is resumed (Oliver, 1967; Jahoda, 1992). Studies have also shown that the CTS is

capable of supplying cells for DP renewal (Oliver, 1966; Oliver, 1967; Jahoda, 1992). DP cells retain their embryonic functional ability and are able to induce new hair fibre growth in mature adult skin when implanted into previously deactivated hair follicles although the DP cells are required to be in close association with epidermal cells (Oliver, 1967; Horne et al., 1986). DP cells can also interact with the epidermis to induce the development of new hair follicles (Jahoda, 1992).

Hair follicles undergo a cycle of activity whereby the follicle will grow to its maximum length which is then discarded followed by the generation of a new follicle. There are three distinct stages of growth which are anagen, catagen and telogen (Figure 1.5).

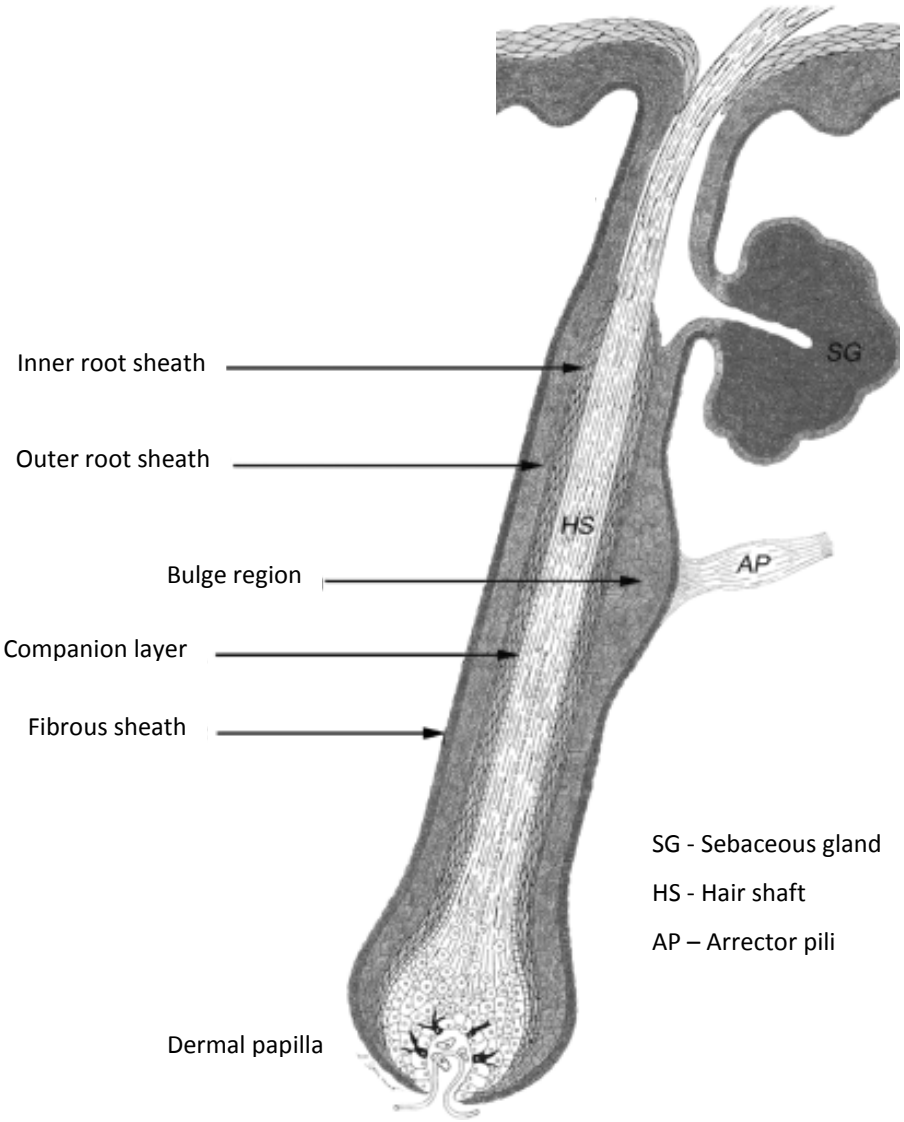

Figure 1.4: Structure of the hair follicle (adapted from Toll et al., 2004)

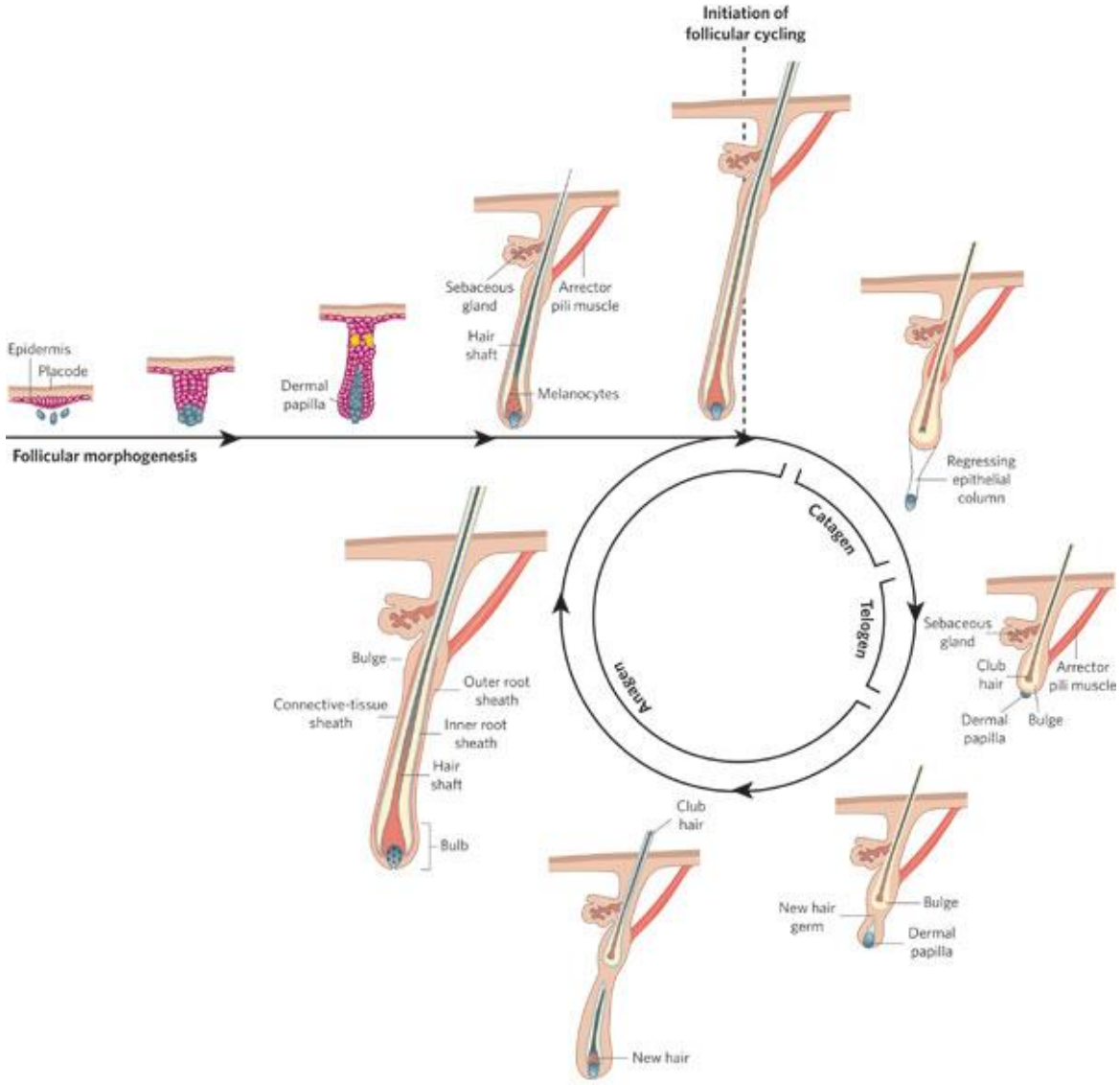

Figure 1.5: Hair follicle cycle (Fuchs, 2007)

Anagen is the initial growth stage of the follicle and hair shaft. The epidermal cells that surround the DP form the shaft and are constantly dividing which will push each layer of cells towards the epidermis. The hair shaft of the previous cycle will also be completely forced out of the follicle and skin which is known as exogen.

The anagen phase can be further separated into six stages. During Anagen I, the DP cell niche will increase in its size. In Anagen II, the follicle anchors itself in the dermis and differentiation of the cells will give rise to the root sheaths. During Anagen III, Melanocytes develop near the DP. At this point, the follicle has grown to its maximum capacity and is attached to a now enlarged DP. Anagen IV marks the point where DP cells start producing melanin. The hair shaft is still within the IRS and during Anagen V the shaft is able to break out of the IRS and travel towards the epidermis. At Anagen VI, the hair shaft is visible at the surface of the skin. The hair shaft from the previous hair cycle is either forced out or compressed in a clubbed hair which will eventually be removed.

During early anagen, CTS is composed of a thin basal lamina and surrounded by collagen. The collagen gradually thickens as the hair follicle grows until late anagen by which time the collagen separates into three layers. The inner layer outside of the basal lamina consists of thin collagen fibres that run parallel to the follicle. The middle layer is thicker with fibres that run transversely against the hair axis. The outer layer contains fibres that run in different directions parallel to the outer surface of ORS cells.

Anagen is followed by catagen which marks the start of degradation. Catagen provides a mechanism whereby the hair follicle stops production of the hair shaft causing it to move towards the epidermis for shedding. The process begins with the DP shrinking and dissociating from the dermis with the ORS of the lower follicle ceasing to proliferate. The ORS located at the mid section of the follicle begins to harden and forms a bulb at the bottom of the hair shaft. The DP shrinks due to the loss of cells allowing the DP to move towards the bulge region which also causes the hair shaft to move towards the epidermis. The GE will also stop proliferating which causes the follicle epithelium to undergo apoptosis. Production of melanin ceases and a number of melanocytes are lost through apoptosis (Slominski et al., 1994; Tobin et al., 1998).

The telogen phase follows catagen and this is known as the resting phase of the hair cycle. With the hair shaft having been dissociated from the DP, the cells below the hair shaft that have now stopped proliferating will form a club shape creating a club hair. This club hair is

shed in the final stage which is known as exogen. If the club hair is not removed by physical means, the onset of the next anagen phase will force out the club hair. The length of the hair cycle varies depending on the location on the body with the duration of anagen determining the type of hair produced and its length (Paus and Cotsarelis, 1999).

1.1.4 Signalling pathways involved in hair follicle development

A number of developmental signalling pathways have been implicated in hair follicle formation including the Wnt, Hedgehog (HH), fibroblast growth factor (FGF), transforming growth factor (TGF) and bone morphogenic protein (BMP) pathways.

The Wnt signalling pathway is involved in the development of embryological systems and is controlled by paracrine Wnt signalling molecules that act via frizzled (Fz) receptors (Cadigan and Nusse, 1997). Wnt signalling exists in canonical β-catenin dependent and non-canonical β-catenin independent modes (Chien et al. 2009) (Figure 1.6). The Wnt ligand binds to a co-receptor complex consisting of Fz and low density lipoprotein receptor 5 and 6 (LRP5/6) to activate Dvl which acts upon the β-catenin complex. This complex consists of β-catenin, APC tumour suppressor, CK1α kinase and GSK3β kinase, all of which are attached to the tumour suppressor protein Axin. As the pathway is inactive, β-catenin is phosphorylated then ubiquitinated leading to its degradation by CK1α (Gao et al., 2002). As Wnt activates the pathway, Dvl blocks the activity of GSK3β which allows dephosphorylated β-catenin to enter the nucleus and activate the transcription of certain target genes by binding with the T-cell factor (dTCF) and lymphoid enhancing factor (LEF-1) transcription factors (van de Wetering et al., 1997; Behrens et al., 1996). Downstream targets of LEF-1 include c-Myc which is a transcription factor as well as the cell cycle regulator Cyclin D1 (Wodarz and Nusse, 1998). Non-canonical Wnt signalling can occur via calcium flux or JNK (Veeman et al., 2003) with functions being described such as planar cell polarity (PCP) in *D. melanogaster* embryos (Seifert and Mlodzik., 2007). Deregulated signalling of canonical WNT signalling leads to the over expression of β-catenin either by stabilising β-catenin or inhibiting the GSK3β complex (Morin et al., 1997; Rubinfeld et al., 1997).

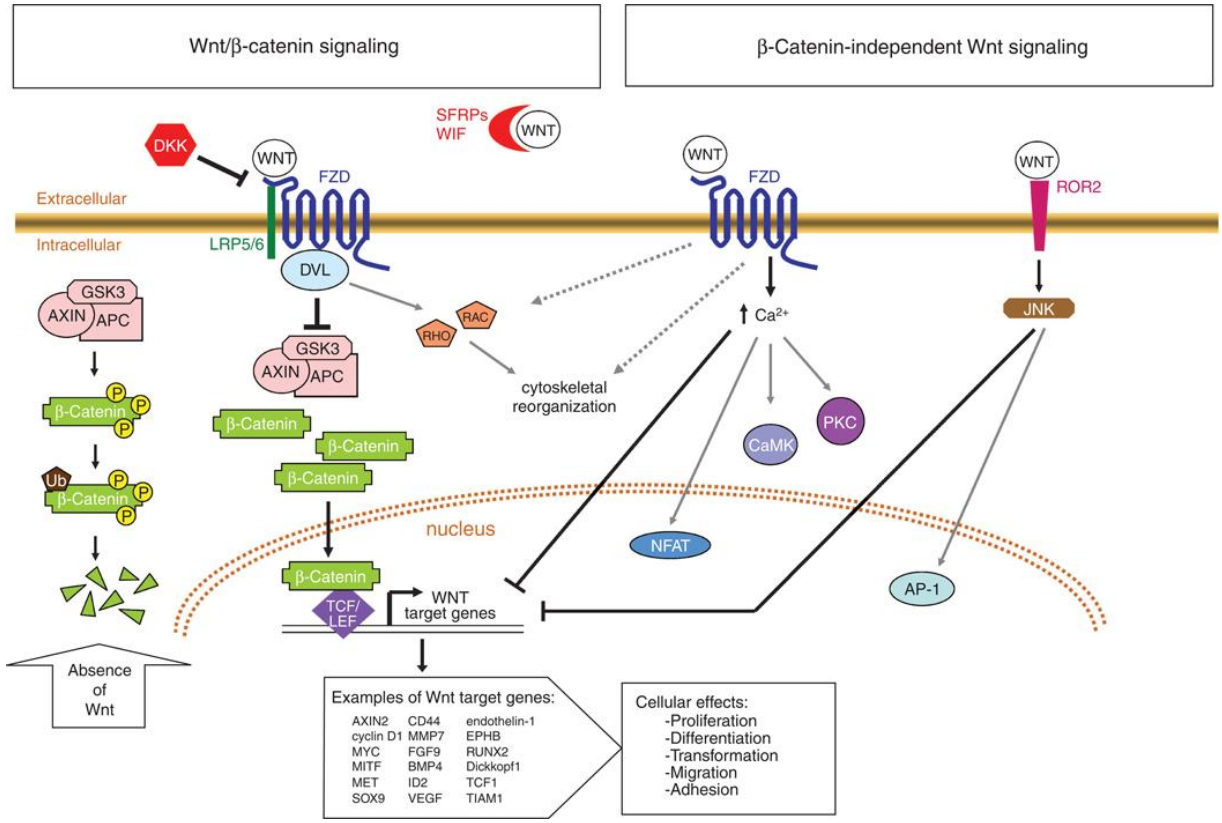

Figure 1.6: Wnt signalling (Chien et al., 2009)

The importance of Wnt signalling in hair follicle has been highlighted in LEF-$1^{(-/-)}$ mice that do not develop hair follicles as seen from histological sections (van Genderen et al., 1994) while over expression of LEF-1 in the epithelium of transgenic mice leads to the aberrant patterning of hairs and the growth of hairs in the oral cavity (Zhou et al., 1995). Suppression of Wnt signalling either by ablation of β-catenin or expression of a truncated form of LEF-1, results in inhibition of hair follicle formation (Huelsken et al., 2001, Merrill et al., 2001).

The Wnt pathway can be activated independently of β-catenin involvement by alternative signalling mechanisms including JNK and calcium flux (Veeman et al., 2003). Wnt-4 is expressed in both embryonic and adult mouse skin while Wnts 5a and 11 are expressed in the dermis of embryonic mouse skin. Although the function is unknown, studies suggest that Wnt-5a may be a downstream target of the HH pathway and plays a role in hair follicle morphogenesis (Reddy et al., 2001).

The HH signalling pathway which will be discussed in more detail later (section 1.3) plays an important role in regulating the development of embryonic structures including limbs (Goodrich et al., 1996). HH signalling also plays a role in hair follicle formation in mammals. The Sonic HH (SHH) ligand is shown to be expressed in the developing whisker of mice (Iseki et al., 1996). It was also reported that *Patched* (*PTCH*) which represses HH signalling, is also present in cells surrounding SHH positive cells of mouse whisker follicles implying that HH levels may need controlling to limit hair follicle development (Goodrich et al., 1996). Further studies in chicks where SHH was over expressed through retroviral transduction resulted in the development of abnormally large feather buds (Ting-Berreth and Chuong, 1996; Morgan et al. 1998). These studies suggest that the HH pathway is involved in the development and the size of hair follicles.

The BMP signalling pathway is involved in embryonic development and has been linked with HH and Wnt pathways in hair follicle morphogenesis. BMP factors work in concurrence with the Wnt and SHH signalling to stimulate the induction of hair follicles during embryogenesis (Botchkarev and Sharov, 2004). SHH expressed in the epithelium has also been shown to induce condensation of the dermis as a precursor to DP formation via TGF-β2 signalling (Ting-Berreth and Chuong, 1996). TGF-β peptides control differentiation and proliferation among other functions (Figure 1.7). TGF-β acts with the TGF-α cytokine to induce cell transformation as well as to initiate apoptosis of certain cell types (Schuster and Krieglstein, 2002). As a TGF-β ligand binds to TGF-β receptor types I and II, type II receptors phosphorylate the type I receptor leading to pathway activation (Massague, 1998). TGF-β signals are mediated via the

SMAD and TAK1 pathways which also mediate BMP signals (Miyazono, 1997). Of the three TGF-β isoforms, TGF-β1 is required for the homeostasis between cell growth and apoptosis. TGF-β1 is expressed and secreted as an inactive complex that consists of latent associated protein (LAP) and a TGF-β1 peptide. LAP-TGF-β1 is linked to latent TGF-β binding proteins (LTBP) which enhance the stability of the cytokine and helps target the signal to the ECM. Latent TGF-β1 is usually stored in the ECM where it can be secreted and activated (Koli et al., 2005).

Members of the TGF-β family play an important role in DP development. The TGF-β2 isoform is required for inducing mouse hair follicle morphogenesis while TGF-β receptors I and II are observed during the hair follicle development and cycling. TGF-β2 has also been shown to play a role in regulating the down growth of keratinocytes that are committed to becoming hair follicles (Paus et al., 1997).

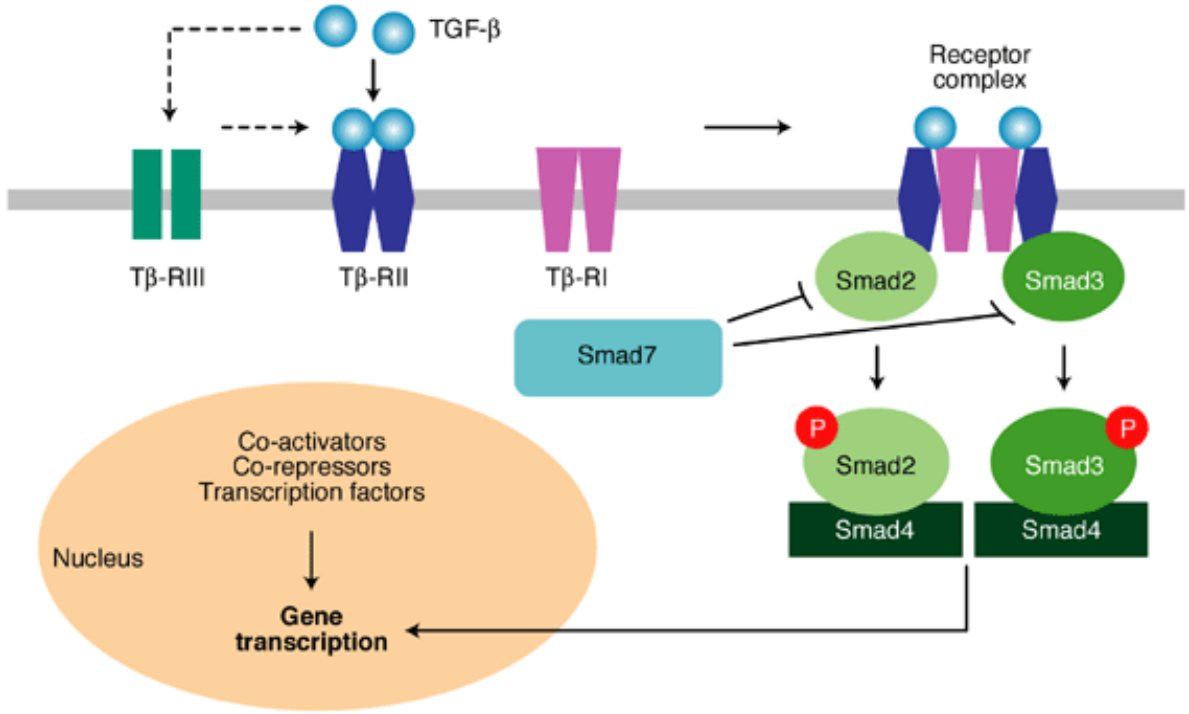

Figure 1.7: TGF-β signalling (Pinzani and Marra, 2001)

1.1.5 Stem cells

Stem cells are defined by three characteristics: the ability to self renew, the regulation of cell number and the ability to differentiate into various cell types that may perform a number of functions based on their cell fate (Stecca and Altaba, 2005). The basal layer contains approximately 10% of stem cells that give rise to differentiating keratinocytes however the main source of stem cells is thought to be the hair follicle (Li and Neaves, 2006; Cotsarelis et al., 1990). Stem cells of the hair follicle can give rise to eight different cell types within the hair follicle. These include the ORS, companion layer of the ORS, Henle's layer, Huxley's layer, IRS cuticle, hair fibre cortex, hair fibre cuticle and the germinative epithelium (Liu et al., 2003). Hair follicle stem cells may also differentiate into sebocytes or form the interfollicular epidermis (IFE) from which sebocyte and hair follicle lineages can be induced depending on the type of mesenchymal signal transduction (Owens and Watt, 2003; Youssef et al., 2010).

A number of hair follicle stem cell markers have been identified including β1-integrin, α6-integrin, CD34, CD71 and p63, however, hair follicle stem cells are difficult to distinguish from daughter TA cells (Ma et al., 2004). Hair follicle stem cells are slow cycling and have a high proliferative potential and clonogenicity (Liu et al., 2003). A slower rate of growth has the advantage of conserving the proliferative potential of the cells as well as reducing the chance of errors occurring during DNA replication.

The division of a stem cell will give rise to another stem cell to maintain stem cell numbers as well as a TA daughter cell which is limited in its proliferative potential (Ma et al., 2004). It has been suggested that the bulge region of the hair follicle is a pool of stem cells (Cotsarelis et al., 1990). Stem cells of the bulge region have been shown to differentiate into the ORS, IRS, hair shaft and sebaceous gland (Oshima et al., 2001).

Keratinocytes and the epidermis act to protect the body from damaging factors such as UV irradiation. As the keratinocytes are subjected to such conditions, there is a high potential of mutations occurring. As such, TA differentiated keratinocytes are shed so there is a limited time in which any mutations can occur. In contrast, stem cells reside in the basal layer for long periods of time and can therefore accumulate a number of different mutations or stresses that may give rise to tumour formation.

It is believed that in cancers, small stem cell niches are responsible for tumour growth and maintenance (Reya et al., 2001). Hair follicle stem cells of the bulge region are pre-

programmed to invade the dermis which is characteristic of the developing hair follicle (Muller-Rover et al., 2001) therefore, a bulge stem cell may be more invasive than other more differentiated cells (Perez-Losanda and Balmain, 2003). However, it is unknown whether tumours arise from stem cells located within normal tissue or if tumour cells develop stem cell characteristics due to genetic changes that may occur (Perez-Losanda and Balmain, 2003).

There are various different tumours that arise from the epidermis such as Basal cell carcinoma (BCC) and sebaceous adenoma (Kore-eda et al., 1998; Owens and Watt, 2003). It is also well established that BCCs arise from mutations that deregulate the HH pathway and it is believed that BCCs may arise from undifferentiated cells of the ORS (Wicking et al., 1999; Owens and Watt, 2003). As the HH pathway has been shown to control certain properties of stem cell niches within the brain (Palma and Altaba, 2004), it is possible that deregulated HH signalling leads to changes in stem cell properties that lead to tumour formation. Other epidermal tumours including tricofolliculomas and pilomatricomas may potentially arise from stem cells that initially differentiate into the hair shaft or IRS (Owens and Watt, 2003). Studies have also shown that blocking of the TGF-β pathway prevents bulge stem cells from forming colonies suggesting that the TGF-β pathway maintains bulge stem cells (Lin and Yang, 2013).

1.2 Skin cancer

Cancer describes the uncontrolled growth of cells that can occur in nearly all types of tissue resulting in tumour formation. Diseases may be inherited or acquired through mutations caused by UV radiation for example. Mutations create an imbalance in the ratio of proliferation to cell death leading to tumour formation and possible metastasis. Various different mutations can affect certain aspects of cell biology that contribute to cancer development for example, mutations of Wnt and HH pathways components may cause hyperproliferation while matrix metalloproteases (MMP) mutations may alter cell invasion. Skin cancer is the most common malignancy as the purpose of the skin is to protect the body from stress such as UV damage therefore the skin is the most susceptible organ to tumour formation.

Age is a major risk factor in skin cancer as there is an accumulation of sun exposure over time. UVA and UVB radiation penetrate the skin and more specifically UVB has been associated with mutations that lead to BCC formation (Kim et al., 2002). Other risk factors include virus infections such as HPV 16 virus which is linked to SCC formation (Eliezri et al., 1990). Genetic factors that give rise to certain characteristics such as freckles, moles, blue eyes and red hair

are known to increase susceptibility to developing skin cancer (Elwood et al., 1985). Skin cancer is classified as either melanoma or non-melanoma cancer.

1.2.1 Squamous cell carcinoma (SCC)

SCC is an epithelial malignancy that can occur in the mouth, lung, prostate as well as the skin which is the second most prevalent non-melanoma skin cancer after BCC. UV radiation is the most common cause of SCCs which produces mutations in DNA, forming thymidine dimers in the p53 tumour suppressor gene (Preston and Stern, 1992; Fears and Scotto, 1983). If the DNA is not repaired or the cells are not targeted for apoptosis, tumours may form (Grossman and Leffell, 1997). As a result, fair skinned people are more susceptible to developing SCCs and people who are born in areas where there are large amounts of UV radiation from the sun are also more likely to develop these tumours (Johnson et al., 1992). The loss of p53 function is also a characteristic of head and neck SCC (HNSCC) (Bonner et al., 2006). Functional inactivation of p16 through deletion or methylation is a common occurrence in HNSCCs (O'Regan et al., 2008). Metastatic SCC of the skin have been shown to have mutations that lead to the over expression of EGFR (Shimizu et al., 2001; Maubec et al., 2005; Krahn et al., 2001). 90% of HNSCCs also show over expressed EGFR protein levels (Ang et al., 2002). Also, mutations of PTCH1 have been identified in cutaneous SCCs of patients who have a history of BCC (Ping et al., 2001).

1.2.2 Basal cell carcinoma (BCC)

Basal cell carcinoma (BCC) accounts for 70% of all skin cancers (Mancuso et al., 2004) and is the most common cancer to affect Caucasians with increasing incidence (Crowson, 2006). Compared to melanomas and SCCs, there are no precursor lesions detected in BCCs (Saldanha et al., 2003). BCCs rarely metastasise and are therefore very rarely fatal despite having a high frequency. There is a high patient morbidity and if tumours are not removed, they can cause extensive scarring and deformity (Elwood et al., 1985).

The prevalence of BCC varies depending on geographical location where the incidence is greater in countries with high sunlight exposure (Holmes et al., 2000; Marks et al., 1993). Although the cure rate for BCC treatment is close to 100% (Svard et al., 2006) (with an extremely rare possibility of metastasis and fatality), the illness can cause substantial disfigurement and scarring. The most common areas where BCCs develop are the head and

neck where tumours can invade locally and cause tissue damage (Shea et al., 1992). The causative factors in BCC development are thought to be both genetic and environmental.

1.2.2.1 Basal cell carcinoma subtypes

Three subtypes of BCCs exist, each identifiable by their histology. These main subtypes are superficial, nodular and morpheic BCCs with morpheic the most aggressive and nodular the most common (Crowson, 2006) (Figure 1.8). Superficial BCCs appear as ulcers on the surface of the skin and histologically, they form a mass of cells below the epidermis. These extend from the dermis to the papillary dermis and have an increased risk of reoccurring if they are not fully removed (Saldanha et al., 2003).

In contrast, nodular BCCs can be clearly seen as a growth on the surface of the skin and through a cross section, tumour islands develop varying in size and number. It is a low risk subtype that commonly occurs on the head, neck and other sun exposed areas. Micronodular BCCs are a subtype of nodular BCCs that are characterised by smaller tumour island usually below 0.15 mm in diameter (Saldanha et al., 2003).

Morpheic BCCs are not particularly visible on the surface of the skin however, these are the most aggressive and infiltrative BCCs that develop. They appear as tumour islands that vary in shape and size but more often as flattened cell masses. Morpheic BCCs display stromal fibrosis which is associated with aggressive local invasion. Other rare forms of BCCs include pigmented types where tumours contain brown or black pigments, more common to dark skinned individuals. The basisquamous form is more difficult to classify as they have characteristics of both BCCs and SCCs (Saldanha et al., 2003).

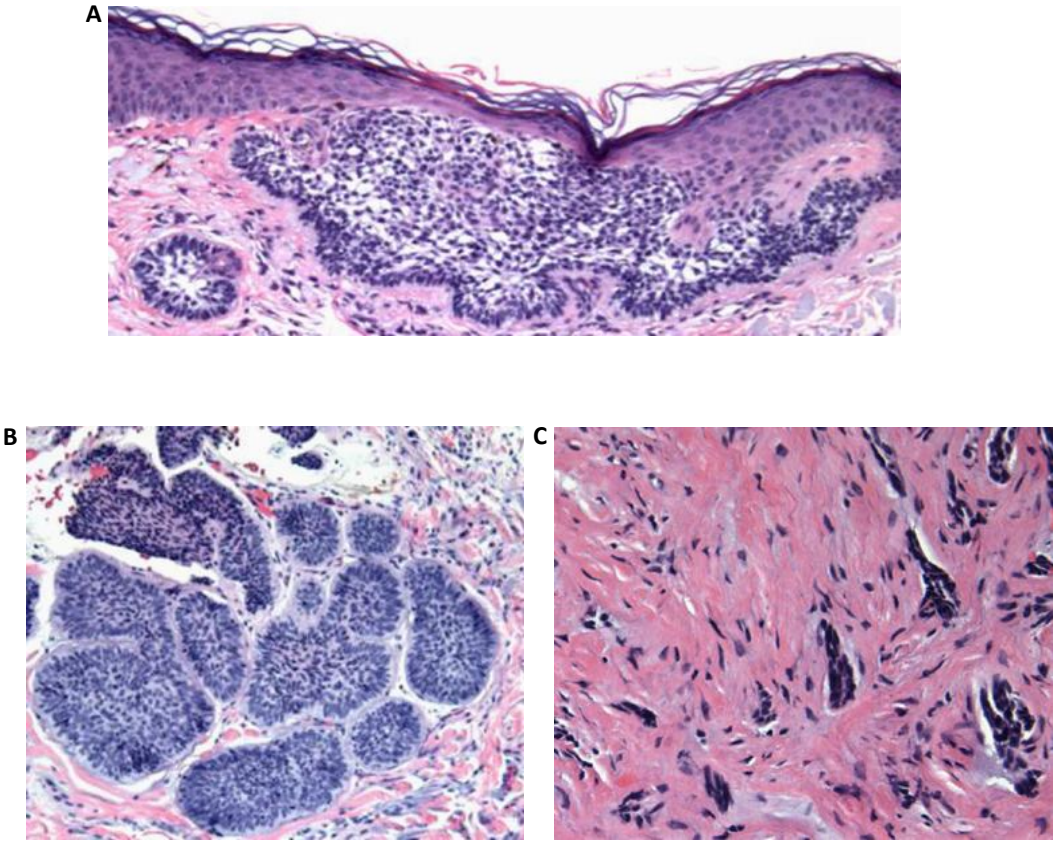

Figure 1.8: BCC histology

Histological section of [**A**] superficial, [**B**] nodular and [**C**] morpheic BCC (Crowson, 2006).

1.2.2.2 Treatment

BCCs very rarely metastasise and are not fatal but they can cause significant scarring and disfigurement especially around the eyes and nose. The most common treatment is to surgically remove the tumour while other common treatments include cryotherapy or radiotherapy while Imiquimod and photodynamic therapy (PDT) are more recent forms. Imiquimod based creams are applied to the tumour in order to cause an inflammatory response to destroy the lesion. 74% of patients reported complete remission of the tumours (Lien and Sondak, 2011); however, this is only used to treat superficial BCCs. PDT involves applying a photosensitive drug to the tumour and upon activation of the drug by light, oxygen radicals are released that induce cell death with a cure rate reported to be 79% (Lien and Sondak, 2011). GDC-0449 (Vismodegib) is a SMO antagonist that has shown a 50% response in metastatic tumours and 60% in advanced local tumours (Göppner and Leverkus, 2011); this and other SMO inhibitors will be discussed in more detail later (see section 1.3.4.4). Other drugs such as Fluorouracil have been used to treat BCCs however it is only effective for superficial and non-invasive BCCs and it results in adverse side effects (Love et al., 2009).

1.2.2.3 Genetics and molecular biology

Our current understanding of BCC genetics stems from studies of patients with a hereditary predisposition to BCC: Gorlin syndrome also known as Nevoid Basal Cell Carcinoma syndrome (NBCCS). NBCCS is a rare autosomal dominant condition where sufferers are predisposed to BCC formation and was first described by Professor Robert J Gorlin in 1960 (Gorlin and Goltz, 1960). Children that suffer from the disease can also develop certain characteristics such as a protruding jaw and a wide set of eyes. The nervous system may also be affected that culminates in an enlarged head as well as suffering from seizures, deafness, blindness and mental retardation (Dicker et al., 2002). The incidence of NBCCS in the UK is 1 in 19,000; NBCCS patients usually develop BCCs from a young age and are prone to developing other tumors including medulloblastomas (Evans et al., 2010).

Familial linkage studies performed on NBCCS patients revealed a mutation located on chromosome 9q22.3, specifically to one allele of the *PTCH1* tumour suppressor gene (Johnson et al., 1996; D'Errico et al., 1997). The formation of BCCs in NBCCS patients occurs after the loss of heterozygosity which is where the remaining, functioning *PTCH1* allele acquires a mutation (Gailani et al., 1996). PTCH1 is a cell membrane receptor specific to HH ligands that suppress the HH pathway therefore, loss of PTCH1 functionality is thought to result in the

constitutive activation of the pathway in BCC tumours. From the results of several studies, up to 90% of sporadic BCCs (i.e. non-NBCCS tumours) also have PTCH1 mutations predicted to reduce protein function while 10-20% have activating mutations of the downstream protein Smoothened (SMO) which renders the protein insensitive to inhibition by PTCH1 (Rubin et al., 2005; Youssef et al., 2010). Mutations of the *PTCH1* locus has also been linked to hair follicle derived neoplasia (Nilsson et al., 2000).

HH signalling has been shown to be important in maintaining the epidermal stem cell populations of the stratum basale and the bulge region of the hair follicle (Blanpain and Fuchs, 2006). BCCs arise from the basal layer of the epidermis with the tumour mass consisting of basaloid cells. BCCs do not become cornified as seen from *in vivo* studies implying that they should not differentiate *in vitro* (Grando et al., 1996). BCCs express KRT5 and KRT14 however, there are no KRT1 and KRT10 differentiation markers suggesting that BCCs arise from basal cells (Leigh et al., 1993). Tumours consist of clusters of basal cells surrounded by a thin cytoplasmic layer. The surrounding basal cells of the tumour mass are arranged in a palisading manner to separate the tumour from the stroma (Vantuchova and Curik, 2006). There is also evidence that BCCs can arise from the hair follicle. Although BCCs are usually negative for differentiation markers, they express components of the HH pathway such as GLI1 which are important for the hair cycle and hair follicle regeneration. Also, Cytokeratin 17 which is a differentiation marker of the hair follicle has been detected in BCCs (Alessi et al., 2008) which supports the idea that BCCs arise from ORS cells (Crowson, 2006; Owens and Watt, 2003).

Mouse studies where oncogenic SMO-M2 is conditionally over expressed reveals that BCC-like tumours form mainly on the ears and tail. These tumours did not originate from the bulge region however, there was strong induction of Ptch1, Gli1 and Gli2 (Youssef et al., 2010). Also, SMO-M2 expression in hair follicle TA cells did not give rise to tumours. The same study showed that the long term expression of SMO-M2 of interfollicular epidermal progenitor cells results in the development of more invasive BCC. This suggests that tumours may not arise from the bulge region although HH signalling is highly active, but more specifically the IFE.

A role of the skin is to protect the body from UV radiation meaning that keratinocytes have a higher risk of acquiring mutations. UV radiation comes in two forms, UVA at 320-400 nm and UVB at 290-320 nm. Cellular exposure to UV radiation results in the generation of reactive oxygen species (ROS) that damage cells. Types of ROS include hydrogen peroxide, hydrogen radical, lipid peroxide and singular oxygen (Farage et al., 2010). Free radicals that are produced damage DNA causing mutations in oncogenes, tumour suppressor genes and can activate

pathways that regulate differentiation, growth, apoptosis and senescence. The effects of UVB damage of skin can accumulate in keratinocytes over a number of years until a certain key mutation occurs or a point at which there are enough mutations that make the cells carcinogenic (Lewis et al., 2008). Mutations of mitochondrial DNA for example are irreversible as the mitochondria have no system to repair the damage making these mutations more common. In contrast, nuclear DNA damage can be repaired or the cell can be targeted for apoptosis.

67% of sporadic BCCs display C to T and CC to TT transitions of DNA coding for PTCH, caused by UVB damage (Rubin et al., 2005). Approximately 40% of BCCs were also shown to carry mutations of p53 which is likely to be due to UV exposure as well as mutations to components of the HH pathway (Reifenberger et al., 2005). People that have type I skin which is characterised by pale, non-tanning and easily burnt skin are at a higher risk of developing BCCs. Also, those who have red or blonde hair with blue or green eyes are more susceptible. UV radiation from sunlight is the largest source however the increased use of sunbeds for cosmetic purposes as well as some dermatological treatments has led to younger females developing sporadic BCCs (Rubin et al., 2005).

Other genetic illnesses including Rombo syndrome (Michaelson et al., 1981), Xeroderma pigmentosum (Kraemer et al., 2007) and Cartilage-hair hypoplasia (Makite et al., 1999) are all associated with a high risk of developing BCC which demonstrates the involvement of other pathways linked to DNA damage and repair. Xeroderma pigmentosum is an autosomal recessive disorder that results in an inability to repair DNA damage caused by UV radiation. Patients were found to have mutations of p16, p53, SHH, PTCH1 and SMO in skin tumours all of which are induced by UV radiation (Couve-Privat et al., 2004). As well as UV being a risk factor, people that are immunosuppressed have an increased incidence of BCC and more specifically, develop infiltrative forms rather than superficial or nodular BCCs (Crowson, 2006).

1.3 The Hedgehog signalling pathway

The hedgehog (HH) signalling pathway plays an essential role in the regulation of proliferation, differentiation, patterning and growth of the embryo (Altaba et al., 2002). The pathway is most active during embryogenesis and involved in pattern formation of the developing limb bud (Towers and Tickle, 2009) as well as the ventral neural tube (Dessaud et al., 2008). The pathway is also required for the control of cell growth, proliferation, differentiation (Wicking

and McGlinn, 2001), stem/progenitor cell renewal, tissue regeneration and repair (Beachy et al., 2004).

1.3.1 Development

HH signalling is important for embryogenesis and tissue patterning. Stem cells can be induced by the HH pathway so that they differentiate into precursor cells which will then follow different cell fates. HH signalling is involved in the patterning, regulation of cell proliferation and differentiation of most tissues during development (Daya-Grosjean and Couve´-Privat, 2005). During development, the embryo relies on various genetic interactions that will specify cell fates within the tissue (Park et al., 2000). HH signalling plays an important role in vertebrate skeletal development, digit formation on the hands and feet, teeth, lungs and nervous system (Mo et al., 1997; Hardcastle et al., 1998; Grindley et al., 1997).

The zone of polarising activity (ZPA) is an important region involved in limb bud development that has strong HH expression (Park et al., 2000). The ZPA is an area of the developing limb bud that instructs its growth and polarity. It is controlled by many different genes and signalling pathways which determine its development into bones, joints, tendons and muscles. Development of embryo cell location, shape, size and differentiation into tissues are managed by HH signalling that varies in its strength, timing and location (Altaba et al., 2003).

HH signalling is strongly involved in development of both the peripheral and central nervous systems (CNS). This pathway has been shown to act as a morphogen which is a substance that forms a gradient by which early neuronal tube development is governed. HH signalling also acts as a mitogen to induce mitosis in brain development. SHH ligand null mouse embryos display small neural tubes due to the lack of ventral differentiation in the notochord (Altaba et al., 2003). The neocortex is part of the cerebral cortex and is responsible for higher functions in mammals. Its development is dictated by HH signal regulation of early ventral patterning of the dorsal brain, a precursor for the neocortex. HH has also been implicated in midbrain expansion and the proliferation of granular precursors in the cerebellum (Palma and Altaba, 2004). HH ligands are secreted from the notochord and its floor plate generating a ventral to dorsal HH signal gradient. This gradient dictates the progenitor cell identity and the fate of neuronal cells within the ventral neural tube (Liem et al., 2000). The HH signal effect on neural development is further controlled by the TGF pathway, more specifically BMP4 and BMP7 (Liem et al., 1995). HH proteins also interact with the RAB23 GTPase to determine dorsal ventral patterning as well as with FGF components (Altaba et al., 2003). RAB23 (small GTP binding protein and part

of the Ras protein family) has been shown to be a negative regulator of HH in mice (Eggenschwiler et al., 2001). The importance of HH signalling in development is further demonstrated by *HH* null mice that have no CNS cell types present and lack any patterning of limbs (Chiang et al., 1996).

1.3.2 Hedgehog signalling in *Drosophila melanogaster*

Much of our understanding of the HH signalling pathway stems from studies performed on the fruit fly, *Drosophila melanogaster*. The origin of Hedgehog as the name for the pathway derives from the phenotypic change in *D. melanogaster* upon the mutation of the *HH* gene (Nusslein-Volhard and Wieschaus, 1980). A large scale screen was performed on fruit flies to identify mutations that may alter the development of the larval body. *HH* in *D. melanogaster* was identified as one of a number of genes that are important in developing the anterior and posterior parts of the individual body segments. The mutation of the *D. melanogaster HH* gene results in a coat of spines to grow on the underside of larvae (Nusslein-Volhard and Wieschaus, 1980). As well as *D. melanogaster*, *HH* genes are also present in a number of invertebrates including *Hirudo medicinalis* (leech) and *Diadema antillarum* (sea urchin) (Chang et al., 1994; Inoue et al., 2002). It is important to note that *Caenorhabditis elegans* (roundworm) have no *HH* ortholog however there are a number of proteins homologous to *PTCH* (Kuwabara et al., 2000). A number of *HH* orthologs vertebrates have been cloned such as mouse, zebrafish and chicken (Echelard et al., 1993; Krauss et al., 1993; Riddle et al., 1993).

HH ligand processing and secretion are very highly conserved between *D. melanogaster* and mammals although there are some differences. *D. melanogaster* has a single *HH* gene whereas vertebrate signalling involves three HH ligands named after different types of hedgehog; Desert (DHH), Indian (IHH) and Sonic hedgehog (SHH); the latter based on the video game (McMahon, 2000). Of the three ligands, SHH is most expressed in mammals as it is involved in the development of the brain, spinal cord and limbs (Chiang et al., 1996). IHH has been reported to regulate bone growth (Lanske et al., 1996) while DHH regulates nerve sheath formation (Mirsky et al., 1999). Zebrafish express a further three types of HH ligand which are Tiggywinkle hedgehog (TWHH), Echidna hedgehog (EHH) and Qiqihar hedgehog (QHH) (Ekker et al., 1995; Currie and Ingham, 1996; Ingham and McMahon, 2001). In both vertebrates and invertebrates, the binding of HH to its specific receptor PTCH starts a signalling cascade that results in the activation of zinc finger transcription factors - GLI in mammals and *Ci* in *D. melanogaster*. This results in the expression of specific target genes (Huangfu and Anderson, 2006; Varjosalo and Taipale, 2007).

1.3.3 The Hedgehog signalling cascade

The HH signalling cascade is initiated by HH ligands and controlled by the tumour suppressor protein PTCH1. Upon the binding of HH to PTCH1, SMO that is suppressed by PTCH1 is free to translocate to a complex consisting of Fused (FU) and Suppressor of Fused (SUFU). This complex releases the GLI transcription factors that translocate to the nucleus where they begin transcription (Figure 1.9).

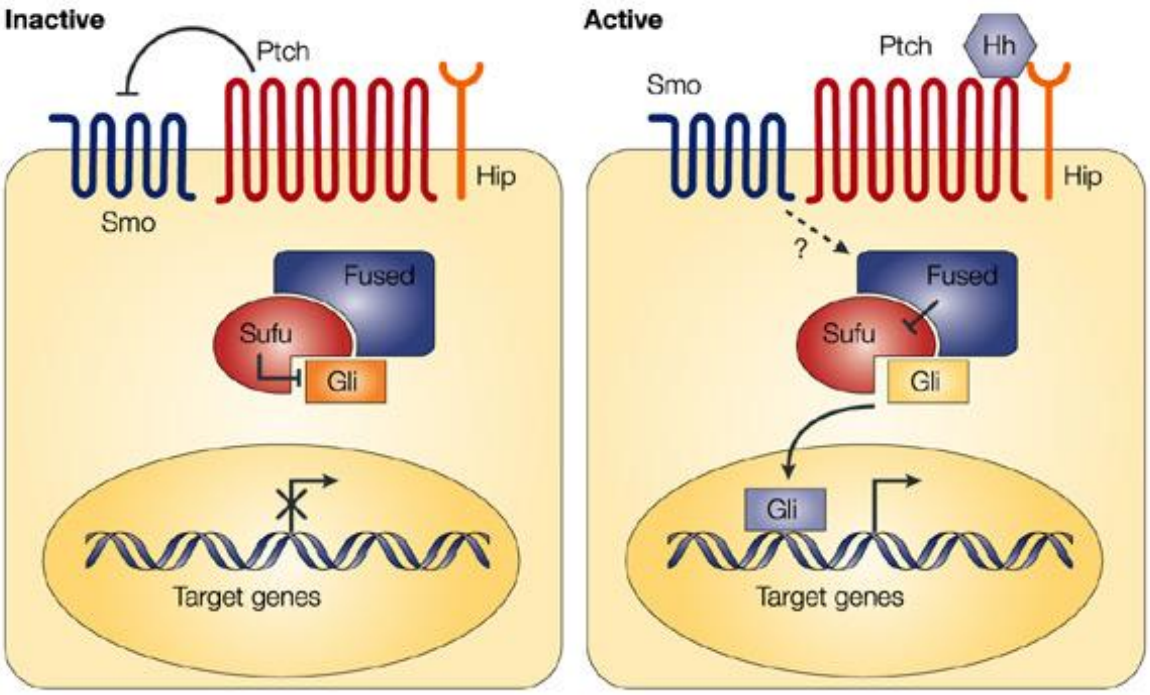

Figure 1.9: The Hedgehog signalling pathway (di Magliano and Hebrok, 2003)

HH ligands are required to initiate the HH signalling cascade with SHH, IHH and DHH all active in mammals. The HH gene encodes a 45 kDa glycoprotein that is cleaved at the C- and N-terminal regions. The N-terminal fragment is post transcriptionally modified to accommodate a hydrophobic cholesterol structure that allows the ligand to bind to the cell membrane (Lodish et al., 2000). A further lipid modification may occur where palmitic acid is added to the N-terminus (Taipale and Beachy, 2001). The difference in modified and non-modified HH ligands was highlighted where it has been shown in mice that over expression of lipid modified HH is more potent than non-modified HH although the mechanism is unknown (Kohtz et al., 2001; Lee et al., 2001). Studies of mice only expressing N-terminal HH fragments that lack lipid modification reveal limb and digit developmental defects (Lewis et al., 2001). HH ligand can be transported by diffusion through extracellular spaces or a concentration gradient. HH can also enter the cell via endocytosis which can be receptor mediated (Ryan and Chiang, 2012). Heparin sulphate proteoglycans (HSPG) have been shown to control a number of signalling pathways such as HH, Wnt, TGF-β and FGF signalling pathways. HSPGs are capable of retaining and stabilising HH ligands by facilitating ligand-receptor interactions (Ryan and Chiang, 2012).

For HH to be released from the cell, a 12-pass transmembrane protein Dispatched (DISP) is required. DISP has a significant sequence similarity to PTCH in particular, the sterol sensing region that is implicated in lipid transport or secretion of lipid modified proteins (Lum and Beachy, 2004). Lipid modified HH is not secreted from cells if there is an absence of DISP. In *D. melanogaster*, DISP releases lipid modified HH from the cell compared to mammalian DISP which is thought to be involved in HH multimer formation (Daya-Grosjean and Couve´-Privat, 2005).

HH signalling is controlled by the tumour suppressor protein PTCH1 and the G-protein coupled receptor SMO (Taipale and Beachy, 2001). PTCH1 contains twelve transmembrane domains and two extracellular loops that bind to HH ligands (Marigo et al., 1996). Mutations of PTCH1 are associated with various birth defects as the HH pathway is heavily involved in embryonic development (Hahn et al., 1996). PTCH2 that was discovered in vertebrates shares a 54% sequence homology to PTCH1 however the amino and carboxylic regions differ which confers a different protein function (Carpenter et al., 1998). HH reception by PTCH1 can be enhanced by HH binding proteins located at the cell surface; these are IHOG and BOI in *D. melanogaster*, BOC and CDO in vertebrates as well as GAS1 (Allen et al., 2011; Beachy et al., 2010; Izzi et al., 2011). Loss of IHOG and BOI in *D. melanogaster* results in a complete loss of signalling and this is also observed in mice that lack BOC and GAS1 highlighting the importance of these cofactors (Allen et al., 2011; Izzi et al., 2011).

Not only does PTCH1 function as the HH receptor, PTCH1 is a negative regulator of the HH pathway by inhibiting SMO. In the absence of a HH signal, PTCH1 localises to the primary cilium and maintains SMO in an inactive form thus preventing its translocation to the cilia (Rohatgi et al., 2007). Early studies of PTCH1 would suggest that it binds directly with SMO (Murone et al., 1999) however more recent studies indicate that the two proteins do not physically bind to each other (Taipale et al., 2002).

In the presence of HH, PTCH1 relieves its inhibition of SMO. SMO is targeted for phosphorylation by CK1α and GRK2 protein kinases at the C-terminal end which induces conformational changes allowing SMO to translocate to the primary cilium (Chen et al., 2011). This translocation is controlled by β-Arrestins and the kinesin 2 motor protein KIF3A that bind to SMO after it has been phosphorylated. Active SMO modifies full length GLI proteins into active transcription factors (Kovacs et al., 2009) (Figure 1.10).

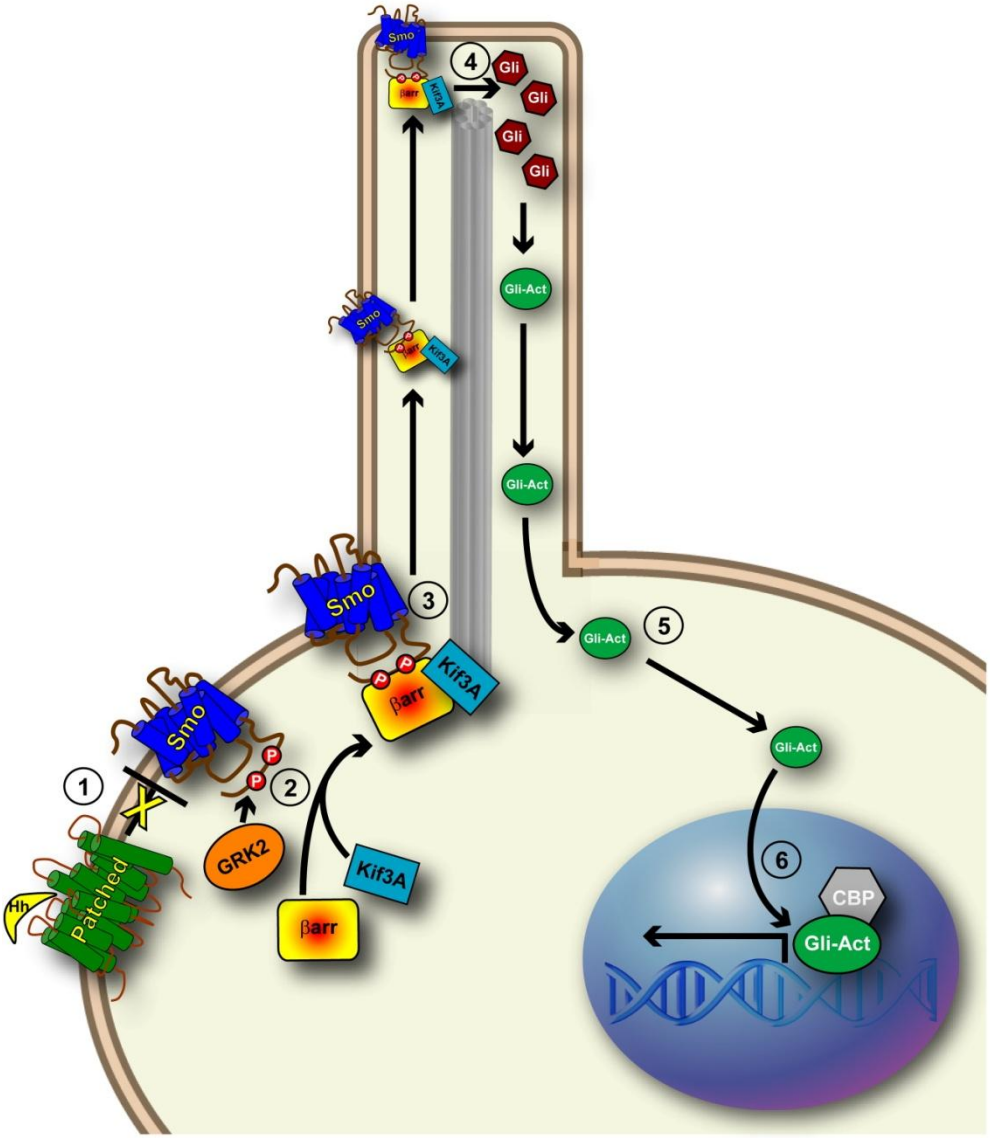

Figure 1.10: SMO translocation to the primary cilium mediated by β-Arrestins (Kovacs et al., 2009)
[**1**] Upon HH binding, SMO is released from PTCH1. [**2**] SMO is phosphorylated by GRK2 that leads to the formation of a complex consisting of SMO, β-Arrestin and KIF3A. [**3**] This SMO complex is translocated to the primary cilium where [**4**] SMO cleaves GLI1 into an active form. [**5**] Active GLI translocates into the nucleus [**6**] where transcription of downstream targets occur.

Inactive GLI proteins are part of a complex consisting of FU and SUFU where the cytoplasmic domain of SMO is able to bind with this GLI/SUFU complex (Beachy et al., 2004). When GLI is bound to the complex, GLI is retained in the cytoplasm through phosphorylation of the C-terminus preventing translocation to the nucleus (Lauth and Toftgard, 2007). There is little known about how SMO interacts with the GLI/SUFU complex but it is thought that GLI/SUFU that accumulates in the cilium, dissociates as a result of interacting with SMO (Zeng et al., 2010). It has also been proposed that the kinesin protein KIF7 can promote the disassembly of GLI from SUFU (Endoh-Yamagami et al. 2009). Further evidence of this comes from mice that are deficient in KIF7 which exhibit decreased HH signalling and reduced *PTCH* expression in the notochord (Liem et al., 2009). It is unknown if KIF7 and SMO interactions are dependent on SMO phosphorylation as this has been shown with Costal-2 (Cos2), the *D. melanogaster* equivalent of FU (Shi et al., 2011; Jia et al., 2003).

Once GLI dissociates from the SUFU complex, it is able to enter the nucleus where it is converted to its activator form, GLI-A (Tukachinsky et al., 2010). Cytoplasmic microtubules are required for this translocation to occur as it has been shown that the addition of Nocodazole (destabilising agent of microtubules) prevents GLI entering the nucleus and also reducing its activity (Humke et al., 2010). GLI is active when in its full length form and repressed when truncated or modified (Bishop et al., 2010). GLI binds to the DNA of HH target genes that contain the consensus binding sequence 5'-TGGGTGGTC-3' (Hooper and Scott, 2005). A negative feedback loop exists between PTCH1 and GLI1 which illustrates the importance of HH pathway regulation (Rahnama et al., 2006).

There are three members of the GLI family all of which have a highly conserved DNA binding domain containing a zinc finger that binds to the consensus sequence (Dennler et al., 2007). GLI1 is the most prominent of the three and its over expression has been observed in many different types of cancers (Altaba et al., 2002). A positive feedback mechanism has been reported between GLI1 and GLI2 (Regl et al., 2002). HH signalling has also been linked to TGF-β (Cretnik et al., 2009), Notch and Wnt/β-catenin pathways (Adolphe et al., 2006).

GLI2 and GLI3 have C-terminal activator domains as well as N-terminal repressor domains while GLI1 only has a C-terminal activator domain (Hooper and Scott, 2005). This means that all three GLI proteins function as activators while GLI2 and GLI3 can act as repressors. PTCH can then inhibit the HH pathway at the cell membrane whereas GLI1 will positively feed back by inducing GLI1 specific genes (Hooper and Scott, 2005). GLI1 has been reported to target a number of genes such as CCND1, FOXM1, PDGFRA and SFRP1 (Katoh and Katoh, 2008).

SUFU is able to stabilise full length GLI2 and GLI3, sequestering both proteins in the cytosol which prevents nuclear translocation and activation (Tukachinsky et al., 2010; Wang et al., 2010). SUFU can also promote C-terminal phosphorylation of full length GLI via protein kinase A (PKA) followed by further phosphorylation via glycogen synthase kinase 3β (GSK3β) and CK1α (Tempe et al., 2006; Kise et al., 2009). *Sufu* deficient mice perish before embryo day 9.5 and display reduced levels of full length and repressed GLI (Svard et al., 2006).

1.3.4 Hedgehog signalling in disease

As the HH pathway is involved in a number of developmental processes, it is unsurprising that mutations of HH pathway genes give rise to a number of diseases. With the HH pathway associated with various major pathways, diseases may arise indirectly.

1.3.4.1 Ciliopathies

Cilia are organelles that can be found on the surface of many cell types, consisting of microtubules. Cilia can either be motile or non-motile primary cilia. Motile cilia are able to generate movement while primary cilia play a sensory role. Both cilia types consist of nine microtubules that run in parallel to each other but with the addition of dyenin arms in motile cilia (Figure 1.11).

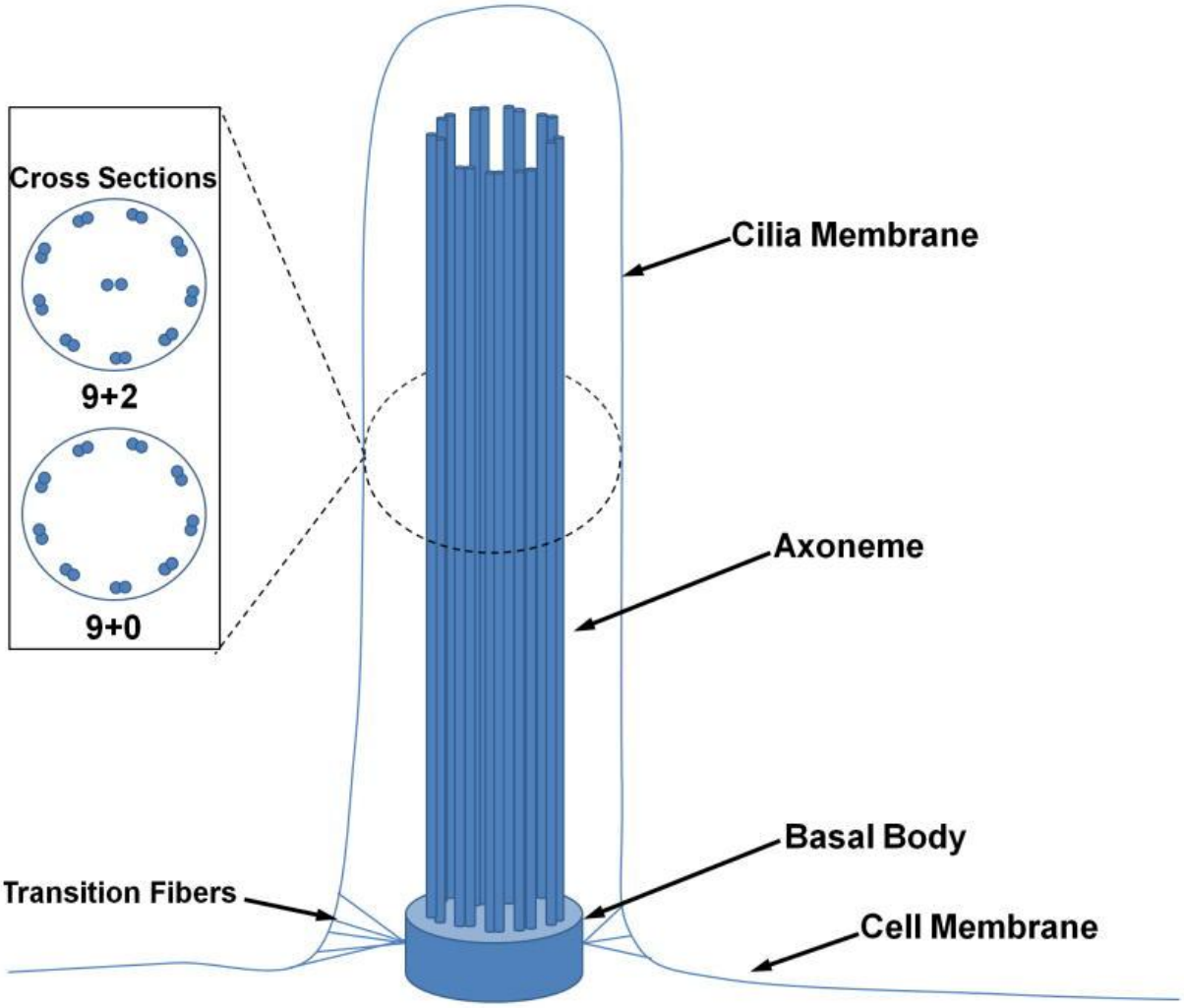

Figure 1.11: Structure of the cilia (Berbari et al., 2009)

Cilia contain a core of microtubules known as the axoneme. The axoneme consists of nine microtubule doublets and in motile cilia, the doublets surround another pair of microtubules. This is referred to as a 9+2 structure as opposed to a 9+0 arrangement in non-motile cilia. Cilia extend from the basal body which is associated with transition fibre proteins that regulate protein exit and entry from the cilia (Reiter et al., 2012). Cilia with the 9+2 arrangement are usually found on the surfaces of epithelial cells in the trachea for example. These cilia move together in tandem for the purpose of moving mucus or fluids.

Proteins are transported to the cilia along the axoneme by the intraflagellar transport (IFT) system. IFT and motor proteins such as kinesin-2 are involved in the transport of proteins from the basal body along the axoneme while dynein is involved in protein transport in the opposite direction, towards the basal body (Gerdes et al., 2009). This process is vital for accurate localisation of proteins to the cilia as well as ciliogenesis.

Non-motile cilia are found in specialised sensory cells such as in the cochlea and photoreceptors where external sensory signals are received. A number of receptors and ion channels are expressed in the cilia including HH which have been discussed, Wnt and PDGFα (Lee and Gleeson, 2010). Cilia involvement in Wnt occurs via the Wnt ligand, Frizzled receptor and Disheveled that regulate migration, proliferation and cell fate determination (Simons et al., 2005). PDGFα is located in the primary cilia and is important in cell migration, growth and survival (Schneider et al., 2005).

The HH signalling pathway is mediated through cilia as demonstrated in mouse embryonic fibroblasts where upon SHH activation, SMO localises at the primary cilium (Corbit et al., 2005). In the absence of SHH, PTCH1 localises at the cilia which in turn prevents SMO accumulating at the cilia. Therefore, the cilia can act as chemosensors that detect extracellular SHH (Rohatgi et al., 2007). It has also been shown that mutations of two IFT proteins, IFT88 and IFT172 gives rise to similar defects of the neural tube as SHH mutant mice. Mice with mutations to both PTCH1 and IFT88 or IFT172 were shown to display identical features to mice with the single PTCH1 mutation which indicates that IFT proteins act downstream of PTCH1 (Huangfu et al., 2003). Disruption of the basal body via the OFD1 gene in mice also showed similar defects to SHH mutant mice (Ferrante et al., 2006). GLI2, GLI3 and SUFU have also been observed at the tip of the cilium (Haycraft et al., 2005).

The Wnt signalling pathway (see section 1.4.3) regulates cell fate, proliferation and migration that can signal in canonical and non-canonical modes. Both modes are regulated by cilia due to

PCP proteins that are localised to the basal body such as Inversin, VANGL2 and FAT4 (Morgan et al., 2002; Ross et al., 2005; Saburi et al., 2008). The disruption of the cilia and the basal body has highlighted the importance of these structures in Wnt signalling. Zebrafish that have disrupted basal bodies via RNAi methods reveal impaired gastrulation and convergent extension. shRNA knockdown of basal body proteins BBS4 or BBS6 in Human embryonic kidney-293 (HEK293) cells also resulted in impaired convergent extension as well as increased canonical Wnt activity. Knockdown of KIF3A using shRNA also gave a similar phenotype with increased Wnt signalling (Gerdes et al., 2007). Other studies have shown that the ciliary protein NPHP3 binds to Inversin to inhibit canonical Wnt signalling which further links cilia to the Wnt signalling pathway (Bergmann et al., 2008).

Primary cilia in fibroblasts play an important role in cellular growth via the PDGF signalling pathway which is involved in processes such as migration, survival and proliferation. PDGF receptors are able to activate MEK and ERK pathways that control gene transcription. PDGF receptor α (PDGFRα) has been shown to localise at the primary cilia in NIH3T3 cells during growth arrest and in mouse embryonic fibroblasts which results in up-regulated PDGFRα phosphorylation and subsequent phosphorylation of MEK and AKT (Schneider et al., 2005; Schneider et al., 2010).

Polycystins 1 and 2 (PKD1 and PKD2) are two proteins that regulate cilia length and signalling, these proteins are also involved in adhesive protein to protein and carbohydrate interactions. Cilia also contain Integrins that work in tandem with PKD1 and PKD2 to allow for cilia to sense the microenvironment which has been associated to wound healing (Lu et al., 2008). Primary cilia of chondrocytes (cells involved in cartilage growth and maintenance) are in direct contact with ECM proteins suggesting that cilia respond to mechanical stimuli (Jensen et al., 2004).

Another pathway that can act via cilia is the Fibroblast growth factor (FGF) pathway that is involved in cell survival, proliferation and migration. FGF ligands have also been implicated in facial and forebrain development (Creuzet et al., 2004) while others have shown that FGF signalling is required for regulating cilia length and function (Neugebauer et al., 2009). The disruption of FGF receptor 1 (FGFR1) leads to reduced expression of IFT88 as well as the transcription factors FOXJ1 and RFX2 that are involved in the control of cilia gene expression.

Ciliopathies describe a class of genetic disease whereby primary cilia do not function. Ciliopathies of motile cilia affect cell motility while non-motile ciliopathies will cause conditions that alter the phenotype due to aberrant cilia function and signalling. Bardet-Biedl syndrome

(BBS) is characterised by postaxial polydactyly (growth of an extra digit on the hand or foot) and approximately 98% of patients are obese (Beales et al., 1999; Tobin and Beales, 2009).

Meckel Gruber syndrome is a lethal autosomal recessive illness that presents in a similar fashion to BBS. Like BBS, there are a number of developmental defects which may be linked to IFT proteins. IFT proteins are required for ciliogenesis as well as the maintenance of cilia and flagella with the HH and Wnt pathways active in this organelle (Pedersen and Rosenbaum, 2008). Studies where IFT proteins are knocked down in mice reveals that there is no GLI activator or repressor activity (Huangfu et al., 2003; Haycraft et al., 2005). IFT proteins are also required for GLI1, GL2 and GLI3 transport as well as SUFU where the proteins localise at the tip of the cilium (Haycraft et al., 2005).

Other ciliopathies such as Alström syndrome (ALMS) are similar to BBS and further characterised by neurosensory hearing loss, cone-rod dystrophy and Type II diabetes. Certain features may emerge including dilated cardiomyopathy, hepatic and renal dysfunction (Tobin and Beales, 2009). Knockdown of the Alström syndrome 1 (ALMS1) gene using siRNA in mice causes defective ciliogenesis where the cilia are stunted in length and are unable to generate a calcium influx when cilia are stimulated (Li et al., 2007).

1.3.4.2 Cancer

It has been well documented that the aberrant activation of the HH signalling pathway can lead to a number of cancers. There are three models proposed for HH pathway activity in cancer (Figure 1.12) (Scales and de Sauvage, 2009). The first classification of cancers that were discovered were type I cancers that harbour activating mutations of the HH pathway and are HH ligand independent such as medulloblastomas and BCC. Type II cancers are defined as autocrine or juxtacrine and ligand dependent. This means that HH ligand that is produced by the cell is to stimulate that same cell or a close neighbour which could be a tumour cell. Cancers that are type III are paracrine ligand dependent which is defined as when epithelial tumour cells release HH ligand and activate the pathway in stromal cells which subsequently feed other signals back to the tumour resulting in growth and survival (Rubin and de Sauvage, 2006; Scales and de Sauvage, 2009).

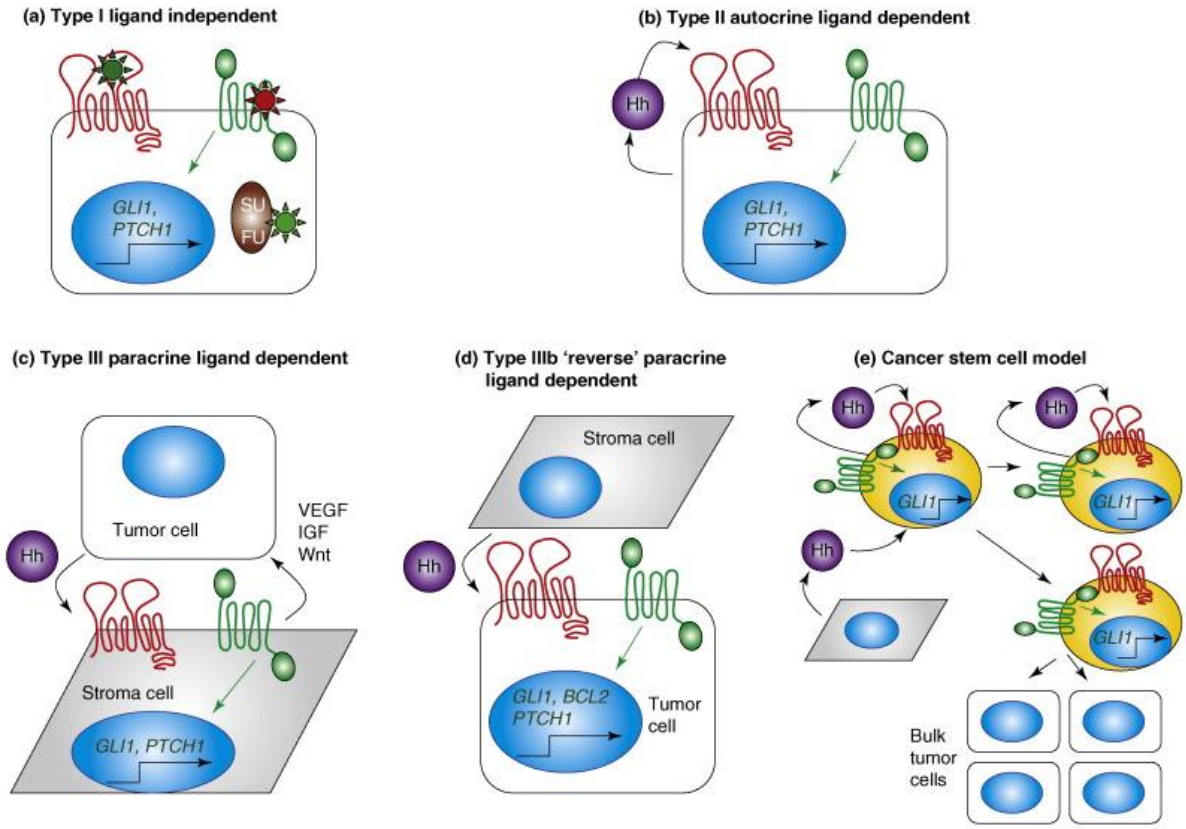

Figure 1.12: Modes of Hedgehog signalling (Scales and de Sauvage, 2009)

[**a**] Type I ligand independent cancer where PTCH1 is inactive or SMO is active resulting in constitutive activation of the HH pathway even when HH ligands are present. [**b**] Type II ligand dependent autocrine cancer cells produce and respond to HH from the same cell. [**c**] Type III ligand dependent paracrine cancer cells secrete HH into the stroma which can feed back to the cancer cell with signals such as Vascular endothelial growth factor (VEGF), Insulin growth factor (IGF) and Wnt. [**d**] Similarly, type IIIb ligand dependent paracrine tumours receive HH from stromal cells resulting in pathway activation in the cancer cells. [**e**] HH signalling in self-renewing cancer stem cells that may come from the cell itself or the stroma. These cancer stem cells may give rise to HH dependent cells or even HH negative tumour cells.

Type I cancer was initially linked to the HH signalling pathway after the identification of PTCH1 inactivating mutations in Gorlin's syndrome that results in the constitutive activation of the pathway that does not require HH ligands to stimulate the pathway (Hahn et al., 1996, Johnson et al., 1996). Studies have shown that up to 90% of BCCs have inactivating mutations of PTCH1 and 10% have SMO activating mutations (Xie et al., 1998). Deregulated HH signalling is also a feature of medulloblastomas and rhabdomyosarcomas which can be due to PTCH1 inactivating mutations and less frequently SUFU mutations (Taylor et al., 2002; Tostar et al., 2006).

Type II autocrine tumours where HH signalling is constantly active affect a wide range organs including the liver, pancreas and prostate (Sicklick et al., 2006; Thayer et al., 2003; Karhadkar et al., 2004). These tumours have increased levels of HH ligand and PTCH1 and GLI expression. HH ligand that is produced by tumour cells will act upon itself or other neighbouring tumour cells in order to promote growth and survival of the cells. To suppress such autocrine tumours, HH neutralising antibodies or downstream inhibitors targeting SMO for example are most effective.

Type III paracrine cancers depend heavily on HH signalling to promote a favourable tumour microenvironment in the stroma (Yauch et al., 2008). It has been shown that in mice, prostate cancer signals to the stroma via paracrine signalling with an increased level of PTCH and GLI detected in mouse stroma in response to human HH production (Fan et al., 2004). It was also observed that HH ligands derived from the tumour as a result of HH over expressing xenografts are able to stimulate PTCH1, GLI1 and GLI2 expression of infiltrative stroma but not in the tumour. Treatment of these tumours with a HH blocking antibody and a SMO inhibitor reduced expression of PTCH1, GLI1 and GLI2 in the stroma as well as slowing tumour growth. This shows that the stromal cells can send growth and survival signals back to the tumour and not just the tumour stimulating the stormal cells (Theunissen and de Sauvage, 2009; Yauch et al., 2008). In pancreatic adenocarcinoma, deletion of SMO in pancreatic cells does not significantly affect PTCH1 and GLI expression in neoplastic pancreatic ductal cells and also do not affect the adenocarcinoma itself (Nolan-Stevaux et al., 2009).

These studies show that paracrine HH signalling that originates from tumour cells activate HH signalling in the stroma which results in the promotion of tumour growth and survival that occur through the stromal expression of certain factors (Theunissen and de Sauvage, 2009). The mechanism by which stromal cells feedback to the tumour cells is still unclear however, it is believed that a number of signalling pathways including IGF and Wnt may be involved (Scales and de Sauvage, 2009, Yauch et al., 2008).

Type IV HH signalling describes a reverse paracrine model whereby stromal cells secrete HH ligands that are received by tumour cells (Theunissen and de Sauvage, 2009). Type IV cancers include haematological malignancies such as B-cell lymphocytic leukemia (B-CLL) where HH secreted from stromal cells was shown to be vital for the survival of the cancer B-cells due to the up regulation of BCL2 which is an anti-apoptotic factor as well as other HH components including GLI1, GLI2 and SUFU (Hegde et al., 2008). With the reverse paracrine signalling model, stromal HH that is believed to be driving tumour growth could be a potential therapeutic target.

1.3.4.3 Hedgehog signalling in Basal cell carcinoma

As the HH signalling pathway plays an important role in development, it is not surprising that dysregulation of the pathway is associated with disease including cancer (di Magliano and Hebrok, 2003; Rubin and de Sauvage, 2006; Altaba et al., 2002; Taipale and Beachy, 2001). HH signalling has also been shown to be required for the maintenance of cancers such as lung and prostate cancer despite the tumours arising from the dysregulation of other signalling pathways (Watkins et al., 2003; Karhadkar et al., 2004).

HH signalling was implicated In BCC biology after the observation that Gorlin's syndrome patients are predisposed to developing BCCs (Johnson et al., 1996). Gorlin's syndrome patients are born with a defective *PTCH1* allele and upon the loss of function of the remaining allele (loss of heterozygosity, LOH) BCCs develop (Gailani et al., 1996). As a result Gorlin's patients are more likely to acquire the LOH mutation of *PTCH1* and develop BCCs at an earlier age than non-Gorlin's patients. Non-Gorlin's patients develop tumours later in life because loss of function mutations to both *PTCH1* alleles takes longer to occur for BCCs to form.

PTCH1 LOH mutations have been observed sporadic BCCs ranging between 11-67% in various studies (Saran, 2010). It has been reported that approximately 90% of sporadic BCCs harbour loss of function mutations of PTCH1 and 10% activating mutations of SMO (Rubin et al., 2005; Youssef et al., 2010). 50% of sporadic BCCs have been shown to carry mutations of PTCH1 that are caused by UVB radiation (Gailani and Bale, 1997). In contrast one study has shown that out of the BCCs examined, *PTCH* mRNA was over expressed in all samples. PTCH protein expression was found in all tumour cells and stronger in palisading cells but not in normal epidermal cells (Tojo et al., 1999).

Downstream of PTCH1, activating mutations of SMO have been described in sporadic BCCs as Arg-562-Gln in SMO-mutant 1 (M1) and Trp-535-Leu in SMO-mutant 2 (M2). Of the two identified mutations the SMO-M2 mutation was found in nearly all BCCs where PTCH1 remained intact. Mice over expressing wild type SMO do not develop any abnormalities whereas SMO-M2 over expressing mice display BCC like characteristics. There are areas of down growth into the dermis, a non-keratinised epithelium and an absence of hyalin granules in the stratum granulosum. There is also a large accumulation of PTCH in basal cells (Xie et al., 1998). The study strongly implicates HH signalling in BCC and that the increase of PTCH mRNA levels is due to do mutant SMO activity.

Non-canonical activation of the HH pathway i.e. the pathway is stimulated by another factor, may also contribute to BCC development. Transforming growth factor-β (TGF-β) has been reported to induce both GLI1 and GLI2 expression in keratinocytes. Furthermore, increased GLI1 and GLI2 expression was maintained in the presence of the SMO inhibitor Cyclopamine suggesting that GLI1 and GLI2 can operate independently of SMO (Dennler et al., 2007). Also, mRNA analysis of BCC reveals elevated levels of TGF-β and SMAD pathway components (Gambichler et al., 2007). The deletion of Notch in mouse skin has been shown to induce GLI2 expression resulting in BCC formation (Nicolas et al., 2003).

A number of mouse models of BCC have been developed to help understand how BCCs may form. As $PTCH^{-/-}$ mice are not viable, $PTCH^{+/-}$ mice were developed with a single allele mutation of PTCH as seen in Gorlin's patients. After the mice were UV irradiated, they develop a large number of tumours that resemble BCCs (Donovan, 2009; Daya-Grosjean and Couve´-Privat, 2005). This is due to UV damage that causes the LOH of the remaining PTCH allele although it is not known why actual BCCs do not develop. Other studies have shown that $PTCH^{+/-}$ mice develop tumours similar to Trichoblastomas which are rare dermal tumours that develop close to the hair follicle and X-ray irradiation of these mice increased the number of tumours and altered their appearance to be more similar to nodular BCCs (Mancuso et al., 2004). There is evidence suggesting that Trichoblastomas share many similarities to nodular BCCs (Schirren et al., 1997).

An *in vivo* study has shown that loss of *PTCH1* function in mouse skin is capable of inducing BCC formation (Adolphe et al., 2006). An inducible *PTCH1* knockout mouse system has demonstrated that the loss of PTCH1 function from the basal cell population is sufficient to induce skin tumour formation that resembles BCC. This system differs to $PTCH^{+/-}$ mouse

models that are UV irradiated to tumours therefore there may be non-specific effects of the UV radiation (Donovan, 2009; Daya-Grosjean and Couve´-Privat, 2005). The Adolphe model shows that the targeted deletion of both *PTCH1* alleles is sufficient to induce BCC-like tumour formation which implies that specifically the loss of PTCH1 function is important for tumour formation.

Further downstream of the HH pathway, mice over expressing GLI1 were able to develop tumours that share a resemblance to BCCs (Nilsson et al., 2000). Interestingly, mice over expressing an activated mutant form of GLI2 which is a positive regulator of GLI1 developed multiple BCCs (Sheng et al., 2002; Grachtchouk et al., 2000). GLI2 studies in mice show that over expression of the protein in hair follicle stem cells leads to nodular BCC formation compared to GLI2 over expression in the IFE which leads to a more superficial BCC phenotype (Grachtchouk et al., 2011).

Other components of the HH pathway have been investigated including SUFU. SUFU knockdown in mice results in embryonic death but $SUFU^{+/-}$ mice develop characteristics that can be found in Gorlin's patients such as jaw keratocysts. Fibroblasts derived from $SUFU^{-/-}$ mice were shown to have elevated levels of GLI1 mediated HH signalling which implies that loss of SUFU function leads to ligand independent HH activity (Svard et al., 2006).

Mouse studies where GLI2 is over expressed reveals the development of multiple BCCs which suggests that GLI2 is a potent oncogene. These tumours strongly resemble human BCCs in their histology and express various BCC markers. HH components such as PTCH1, GLI1 and GLI2 were increased at the mRNA level in the tumours but not the epidermis. As HH ligand is not detected in human BCCs, this suggests that tumours can arise independently of the HH ligand (Grachtchouk et al., 2000).

Some BCC tumours that do not have mutated PTCH, can still have increased HH signalling as a result of SMO activating mutation which negates the repressive function of PTCH on the pathway (Xie et al., 1998). More recent studies show that mutant SMO-M2 over expressing mice do not develop BCCs. The tumours that do emerge are more characteristic of follicular hamartomas (benign tumour) with invasive down growth into the dermis and hyperproliferation of the epidermis (Grachtchouk et al., 2003). In another study, expression of active mutant SMO-M2 in mice did in fact lead to tumour formation (Youssef et al., 2010). Here it was also shown that the tumours originate from undifferentiated basal layer stem cells via increased HH signalling and not from the hair follicle bulge region for example. This may be

a reason as to why the two models differ as the specific area where the mutations occur could determine the type of tumours that form.

Mouse studies regarding Wnt signalling show that the pathway is required for Hamartoma development around the hair follicle and this tumour has been associated with dysregulation of the HH pathway. Expression of an active mutant of SMO induced tumour development in mice via constitutively active HH signalling however, the addition of the Wnt antagonist Dkk1 resulted in the inhibition of Hamartoma development (Yang et al., 2008). This suggests that inhibition of Wnt may serve as a viable therapeutic target and demonstrates a link between HH and Wnt signalling pathways.

1.3.4.4 Therapeutic targeting

Aberrant HH signalling can be caused by the dysregulation of a number of components within the pathway and through different mechanisms. Specific therapies can be selected for autocrine or paracrine ligand dependent cancer which would involve blocking or reducing HH activity however, as BCCs are ligand independent which makes the therapy more difficult administer. The current strategy for treating BCCs would be to treat the tumour with inhibitors that are downstream of the activating mutation such as SMO.

As a potential treatment for BCC there are SMO antagonists currently available, the first being Cyclopamine. Cyclopamine was discovered when pregnant sheep that were eating the *Veratrum californicum* species of lily containing Cyclopamine, would carry embryos with holoprosencephaly (HPE). HPE is a developmental disorder where the midline of the face does not develop resulting in a cyclopic eye which has been linked to HH signalling as Cyclopamine was shown to specifically inhibit SMO (Taipale et al., 2000). $SHH^{-/-}$ knockout mice have also been reported to develop HPE (Chiang et al., 1996). Cyclopamine has been shown to inhibit human medulloblastoma growth (Dahmane et al., 2001) which has led to the proposal for HH antagonists as a valid treatment however non-canonical HH signalling and the development of BCC through this mode of signalling has important therapeutic implications.

Due to the low affinity of Cyclopamine, synthetic derivatives have been developed such as BMS-833923, CUR-61414, HhAntag-691, IPI-926, MK4101, SANT1, SANT4 and Cyclopamine-KAAD with GDC-0449 having undergone phase I clinical trials to treat BCC (Scales and de Sauvage, 2009, Van Hoff et al., 2009) with 50% of metastatic tumours and 60% of advanced local tumours responded to the treatment (Göppner et al., 2010).

Other potential therapies include HH blocking antibodies which prevent the binding of HH ligand to PTCH1 and have shown to be successful (Scales and de Sauvage, 2009). The targeting of other HH components such as GLI with GANT58 and GANT61 are undergoing various phases of development (Lauth and Toftgard, 2007).

The use of SMO inhibitors is an appealing therapeutic target however there are a number of studies that show differing levels of efficacy. NIH-3T3 mouse embryonic fibroblasts that were stimulated with a modified version of SHH ($ShhN_p$) show a 150 to 200 fold increase of GLI reporter activity. Upon the addition of Cyclopamine, GLI reporter activity fell to near normal levels. Also, $PTCH^{-/-}$ mouse embryos that have increased HH expression could be lowered using Cyclopamine which shows that the inhibitor works downstream of PTCH. The NIH-3T3 cells were then transduced with wild type SMO to increase GLI reporter activity by 10 fold that was subsequently reduced to normal levels after Cyclopamine treatment. Interestingly, NIH-3T3 cells that are transduced with an active SMO mutant to induce HH signalling could not be reduced by Cyclopamine. Although mutant SMO NIH-3T3 cells do not respond to the inhibitor, HH signalling was repressed upon the introduction of PTCH. This suggests that certain activating mutants of SMO can make cells resistant to Cyclopamine but can be regulated by PTCH and still respond to SHH (Taipale et al., 2000).

Regarding mouse models of BCC, $PTCH^{+/-}$ mice that develop BCCs after UV irradiation that were treated orally with Cyclopamine for 20 weeks show a reduction in approximately 66% of tumours (Athar et al., 2004). BCC biopsies taken from UV irradiated $PTCH^{+/-}$ mice that were subsequently cultured *in vitro*, were shown to regress upon treatment with the SMO inhibitor CUR61414 (Williams et al., 2003). These studies demonstrate the capabilities of using SMO inhibitors to treat BCCs in mice and from this, valid reason to use such inhibitors to treat human BCCs. A criticism of these studies is that the BCCs occur after the UV irradiation of the mice and not through other mutations such as SMO activation although these are rare.

Studies have shown that not all BCCs respond to SMO inhibitors such as GDC-0449 which is undergoing Phase I trials. Of the metastatic BCCs that were treated, only 30% responded to treatment. 43% of locally invasive BCCs responded to GDC-0449 and of these, 21% showed a total response. Unfortunately, 30% of patients suffered from minor side effects and 25% more serious effects resulting in the death of seven people (Sekulic et al., 2012).

Targeting components downstream of SMO such as GLI1 have been tested. GANT58 and GANT61 both inhibit GLI1 in HEK293 cells. Treatment with GANT61 resulted in the

accumulation of GLI1 in the nucleus but transcriptional activity and DNA binding was suppressed. Interestingly, when 22Rv1 prostate carcinoma cell lines were treated with Cyclopamine *in vitro* there was no inhibition of cell growth however, when these cells are used in xenografts Cyclopamine was able to stop tumour growth. GANT61 treatment of the xenografts shows strong tumour regression (Lauth et al., 2007). The data suggests that tumour growth could be controlled by an external factor such as stromal signalling or that both the tumour and stroma need to be targeted for inhibition.

1.4 Alternative pathways involved in Basal cell carcinoma

1.4.1 The p53 signalling pathway

The p53 tumour suppressor gene plays an important role in cellular regulation (Figure 1.13). Its functions include tumour suppression, metabolic control, stem cell control, DNA damage repair and the initiation of apoptosis (Olivier et al., 2010).

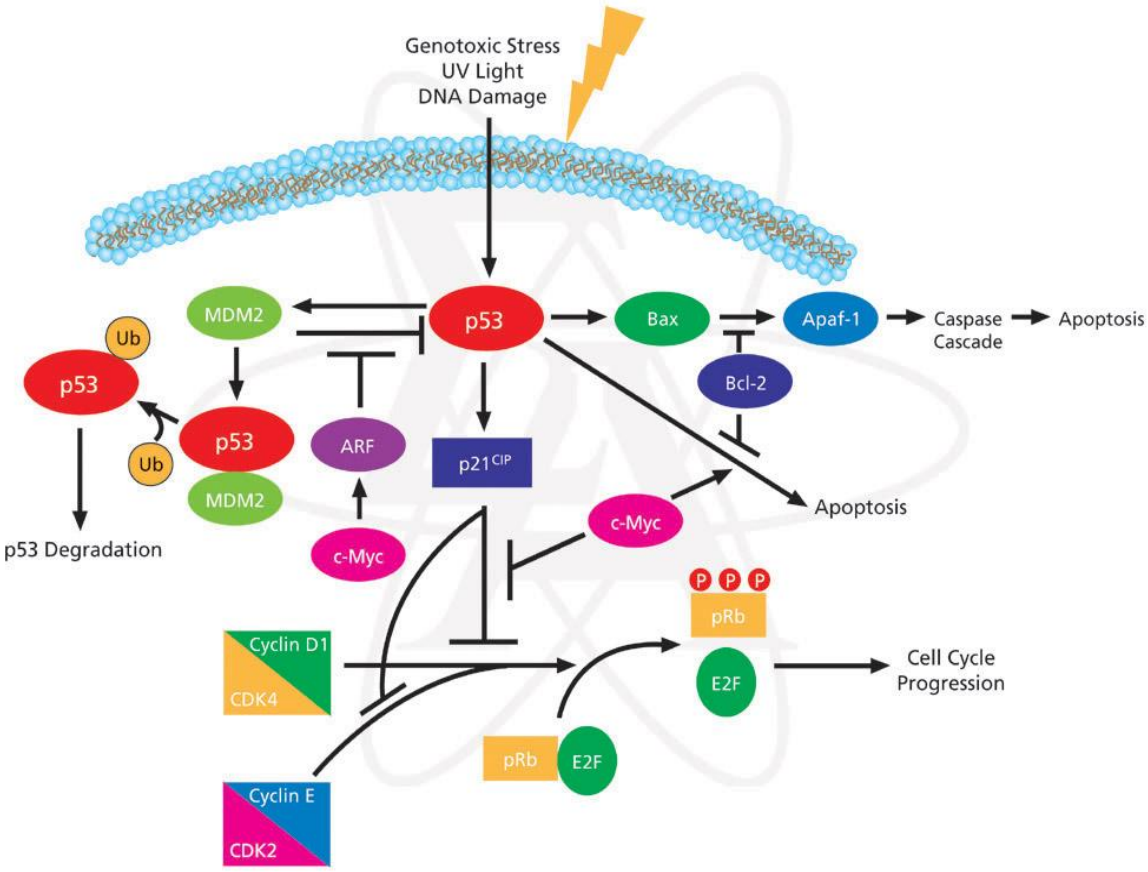

Figure 1.13: p53 signalling (Sigma-Aldrich, 2012)

It is well documented that around half of all BCCs have mutations of the TP53 gene (Mancuso et al., 2004; Soleti et al., 2009; Rady et al., 1992). The frequency of BCCs was shown to increase with patient age which implies that longer exposure to UV light may cause mutations of p53 (D'Errico et al., 1997). CC to TT or C to T transitions at dipyrimidine sites of the p53 gene were found in UV exposed tumours resulting in protein loss of function (Mancuso et al., 2004; D'Errico et al., 1997; Denef et al., 2000; Zhang et al., 2001). Due to this, the cells are unable to repair DNA damage caused by UV exposure and may not undergo apoptosis. Indeed, p53 knockout mice have been shown to develop tumours significantly earlier than wild type mice after UV irradiation (Kim et al., 2002).

Studies of $PTCH^{+/-}$ mice reveal that after UV irradiation, the mice are more susceptible to developing spontaneous tumours. $PTCH^{Neo67/-}$ (heterozygous knockout mice targeting exons 6 to 7) develop BCC precursor lesions and upon UV treatment, these lesions develop into nodular and infiltrative BCCs. Immunohistochemistry also revealed that p53 expression is increased in tumours after UV treatment whereas p53 levels in normal skin were not affected. p53 expression was concentrated around tumour islands (Mancuso et al., 2004). The study shows that the progression from hyperproliferation to nodular to infiltrative BCC formation is a stepwise process which may occur due to an accumulation of sequential genetic alterations. A similar study of $PTCH^{+/-}$ mice shows that X-ray treatment of these mice results in BCC formation but only from KRT15 expressing cells of the bulge region. $PTCH^{+/-}$ $p53^{-/-}$ mice show greater BCC carcinogenesis from the bulge region and develop BCC from the IFE which also has increased levels of SMO. In areas such as the ears and tail of $PTCH^{+/-}$ mice, there was no BCC formation which may be associated with the lack of SMO expression in these regions (Wang et al., 2011).

1.4.2 The EGFR signalling pathway

The epidermal growth factor receptor (EGFR) is a cell membrane receptor that activates a number of downstream pathways and targets with various different functions (Figure 1.14). EGFR is part of the receptor tyrosine kinase family ErbB and is stimulated by several ligands including epidermal growth factor (EGF) and transforming growth factor-α (TGF-α) (Olayioye et al., 2000).

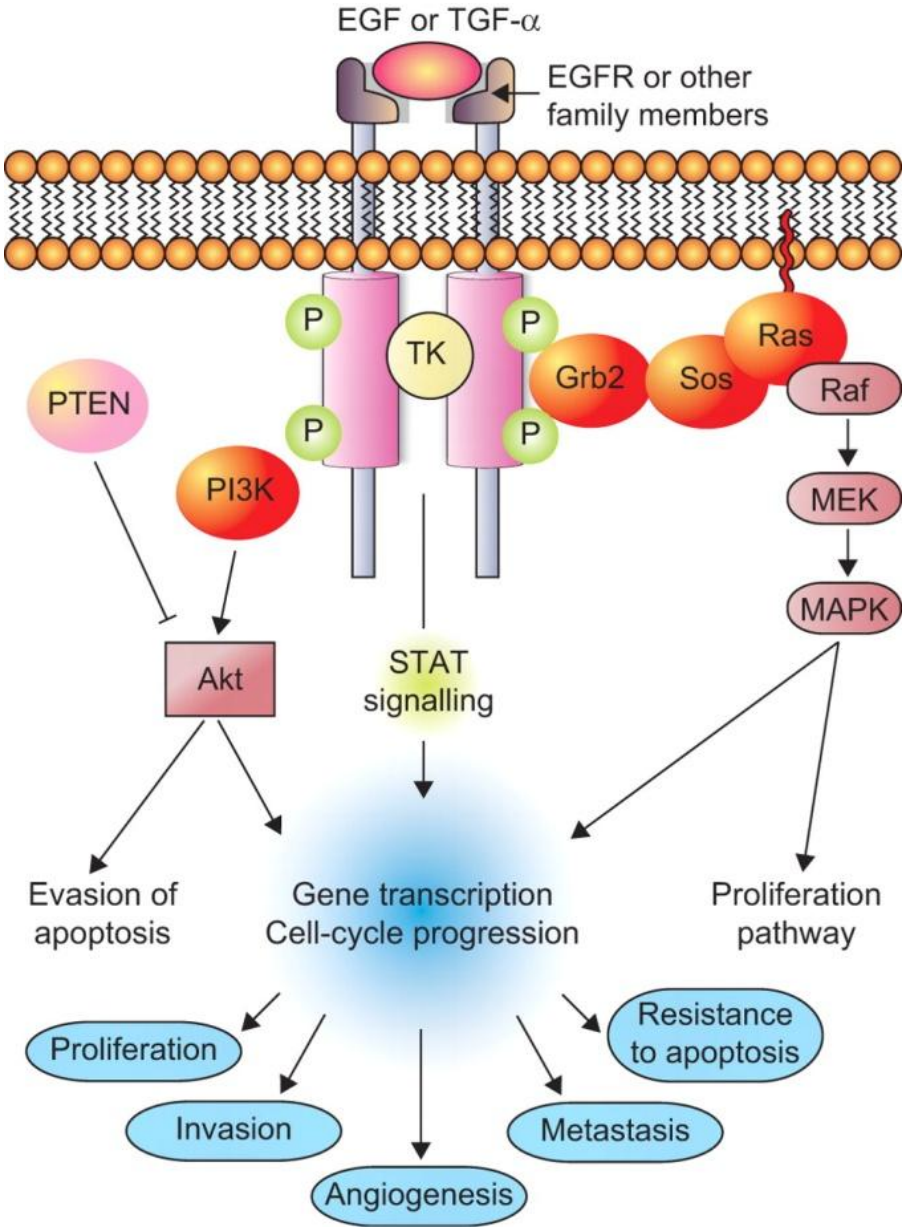

Figure 1.14: EGFR signalling (Brambilla and Gazdar, 2009)

Phosphorylation of EGFR at various residues has been shown to have different effects on downstream signalling targets. Phosphorylation of Tyr845 has been implicated in maintaining activation of EGFR (Hubbard et al., 1994) while Tyr1173 phosphorylation has been linked to ERK activation (Hsu et al., 2011). EGFR can perform auto-phosphorylation to initiate signalling pathways including MAPK, JNK and AKT (Oda et al., 2005).

The PI3K/AKT pathway plays an important role in cell survival by inhibiting apoptosis. As AKT is activated, a number of apoptosis factors such as Caspase-9 and Forkhead transcription factors become inactive (Cardone et al., 1998; Brunet et al., 1999). As well as regulating cell survival, the AKT pathway controls proliferation and angiogenesis via the mTOR (Mammalian target of Rapamycin) and PTEN (Phosphatase and tensin homolog deleted on chromosome 10) signalling pathways (Figure 1.15) (Castellino and Durden, 2007). PTEN is a tumour suppressor protein that negatively regulates the PI3K/AKT pathway (Maehama and Dixon, 1998) and loss of function of this protein has been linked to a number of skin cancers (Ming and He, 2009). There is little known about the role that PTEN may play in BCC biology however as PI3K/AKT activation is required for HH signalling, mutations of PTEN may activate PI3K/AKT which could potentially initiate BCC formation (Riobo et al., 2006 A).

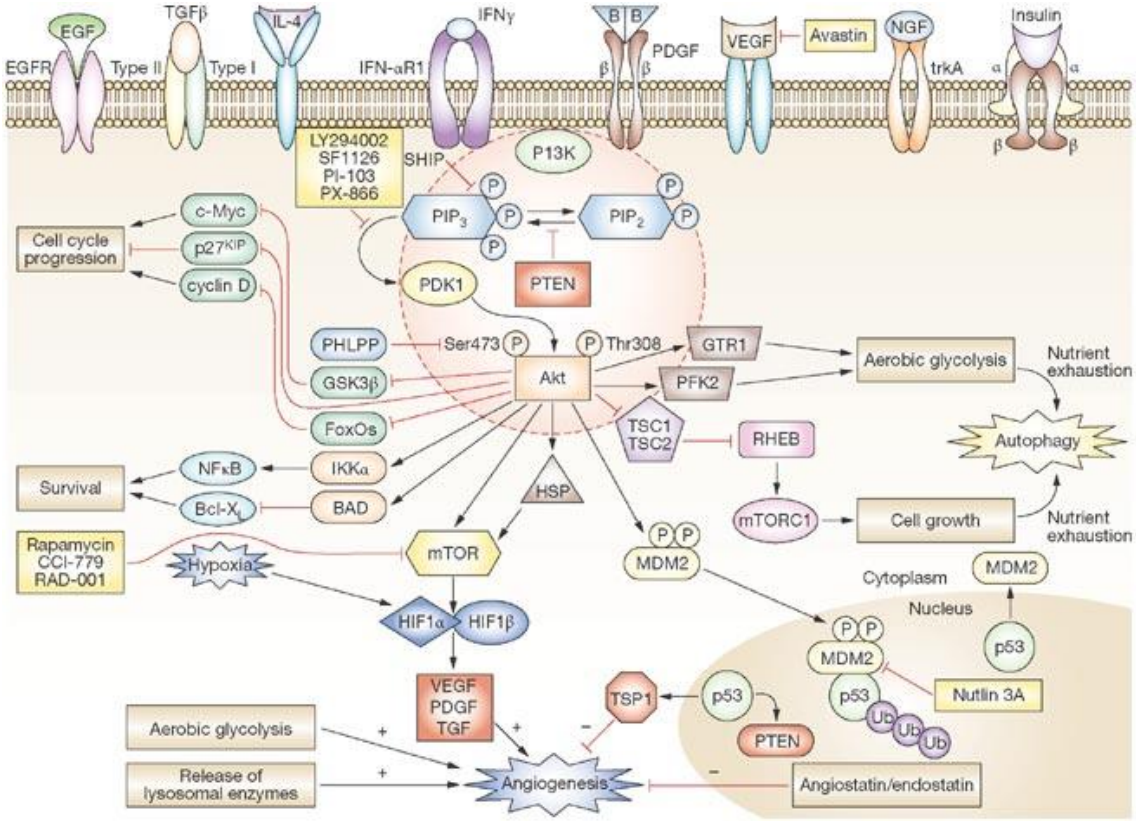

Figure 1.15: PI3K/AKT/PTEN pathway (Castellino and Durden, 2007)

AKT that is activated downstream of PI3K was shown to be important for HH signalling in chicken neuronal development and the stimulation of the PI3K pathway also activates GLI transcription factors. AKT that positively regulates HH signalling suggests that there is a synergistic role of these pathways that is required for embryonic development which may extend to HH dependent tumours (Riobo et al., 2006 A). PI3K/AKT activation has been implicated in BCC development after immunohistochemistry of BCCs were shown to have increased levels of pAKT (Hafner et al., 2010). However, another study has shown a lack of pAKT activation in BCCs (O'Shaughnessy et al., 2007).

HH signalling has been further associated with EGFR signalling as the over expression of SHH in HaCaT immortalised keratinocytes that were grown in organotypic culture, induced a basal phenotype and promoted invasion of the cells into the collagen matrix. SHH expression was shown to increase the phosphorylation of EGFR, JNK and Raf as well as increase Matrix Metalloproteinase-9 (MMP-9) which has been implicated in cell invasion and tumour aggression (Rebecca et al., 2005; Tai et al., 2008). Inhibition of EGFR using the antagonist AG1478 reduced the invasiveness of the cells while supplementing SHH over expressing cells with EGF increased invasiveness. It is not stated whether MMP-9 expression is mediated through SHH, EGFR or both but the data implies that both pathways are linked together and may contribute to tumour invasion by activating MMP-9 (Rebecca et al., 2005).

Studies have shown that EGFR signalling modulates the expression of GLI target genes in N/Tert human immortalised keratinocytes (Kasper et al., 2006). 19 genes were found to be induced synergistically by GLI1 and EGF treatment also; GLI1 target genes were shown to be modulated by EGFR signalling through MEK/ERK pathways.

Studies have also identified that HH and EGFR synergy can induce oncogenic transformation which is mediated through EGFR activation of RAS/RAF/MEK/ERK. EGFR/MEK/ERK pathways are able to induce JUN signalling which is essential for oncogenic transformation. EGFR/MEK/ERK pathways also increase GLI1 and GLI2 expression. In mouse cells where BCCs develop as a result of activated HH signalling, inhibiting both EGFR and GLI signalling shows a reduction of BCC growth and therefore presents a potential therapeutic opportunity (Schnidar et al., 2009).

In contrast, our research group has previously shown that the over expression of GLI1 in N/Tert cells reduces EGFR expression and that compact colony formation (a characteristic of BCC tumour formation) is associated with repressed ERK activity (Neill et al., 2008).

Furthermore, staining of a panel of BCCs reveals no pERK expression in 13/14 tumours whereas pERK was expressed in the epidermis suggesting that its loss is important for tumour formation.

1.4.3 The Wnt signalling pathway

The Wnt signalling pathway has been shown to play an important role in cell proliferation, differentiation and stem cell fate (Angers and Moon, 2009; Ling et al., 2009). Activation of this pathway is frequently observed in human cancers with active Wnt promoting the accumulation of β-catenin. β-catenin is a component of adherens junction complexes that are required to maintain epithelial cell layers and regulate cell growth. The *CTNNB1* gene encodes β-catenin and this gene is thought to be an oncogene (Wang et al., 2008). β-catenin is able regulate gene expression however, *CTNNB1* is not mutated in BCC and it is likely that disregulation of Wnt and/or HH signalling pathways leads to nuclear β-catenin accumulation (Hino et al., 2005; Liu et al., 2005; Saldanha et al., 2004).

The HH and Wnt pathways have been shown to be linked with each other in normal development. Activation of GLI2 was shown to regulate Wnt8 expression while inhibition of Wnt also reduces GLI2 and GLI3 expression (Mullor et al., 2001). The same study also showed that GLI1 induces certain Wnt genes in BCC-like skin tumours.

1.5 Aims of the study

Although BCC genetics have been well established and the involvement of the HH signalling pathway in BCCs recognised, there is some conflicting data regarding the molecular basis of disease. The HH signalling pathway is known to interact with a number of other major signalling pathways so it is unclear how important direct HH signalling is regarding BCC development. Mouse models where PTCH1, GLI1 and GLI2 have been influenced show that BCCs can develop when manipulating this pathway. The over expression of mutant SMO-M2 specifically in the IFE, also leads to BCC formation (Youssef et al., 2010) although others have shown that SMO-M2 over expression in mice does not lead to BCC formation (Grachtchouk et al., 2003). These mouse studies show that manipulation of the HH components play a role in BCC biology however, there are discrepancies in the exact type of tumours that form from each study as not all develop BCCs.

Following on from this, it is also a mystery as to why a large percentage of BCC patients do not respond to SMO inhibitors regardless of whether SMO mutations can or cannot lead to BCC development. This could be because HH is not as important for BCC biology as first thought or there are more complex modes of HH signalling that do not depend upon SMO. Furthermore as seen in NIH-3T3 cells where mutant SMO has been over expressed, HH signalling could not be repressed by Cyclopamine but could be controlled by the reintroduction of PTCH (Taipale et al., 2000).

Regarding the use of clinical SMO inhibitor GDC-0449, one study has demonstrated that 2/33 BCCs show a complete reduction while 16/33 shows partial reduction in tumour growth (74) while others have shown that 50% of metastatic tumours and 60% of advanced local tumours responded to the treatment (Van Hoff et al., 2009; Göppner et al., 2010). Another study has shown that 30% of metastatic BCCs respond to GDC-0449 while 43% of locally invasive BCCs of which 21% showed a full response however there were side effects including the deaths of seven people (Sekulic et al., 2012). In contrast, an amino acid substitution identified in SMO that shows no effect of the HH signalling pathway, has been reported to disrupt the ability of GDC-0449 to bind to SMO and repress the HH pathway (Yauch et al., 2009).

At the molecular level and as noted above, BCC is principally associated with mutational inactivation of the *PTCH1* tumour suppressor gene which is thought to lead to increased expression of the proto-oncogenic GLI transcription factors, GLI1 and GLI2 via a mechanism that requires the protein SMO. Indeed, anti-SMO compounds are effective at suppressing GLI1 expression and tumour formation in pre-clinical mouse models however the results of recent clinical trials have been mixed with some tumours showing regression or stability whereas others demonstrated no response. In addition, the evidence that these SMO inhibitors suppress GLI1 in human tumours is weak and recent research in Dr Neill's group has shown that many BCCs do not actually express high levels of GLI1 as determined by immunohistochemistry (unpublished data). As such, the aim of the study was to:

1- Create a novel *in vitro* model of BCC through targeted suppression of PTCH1 in human keratinocytes with the aim of identifying novel mechanisms that may contribute to the formation and progression of this common skin tumour; these may be SMO-dependent and/or SMO independent.

2- To utilise this model to investigate and delineate the canonical HH signalling pathway in human keratinocytes i.e. does loss of PTCH1 function lead to an increase of GLI1 through SMO or are other factors involved?

Chapter 2

Materials and methods

Chapter 2 Materials and methods

2.1 Immortalised keratinocyte cell culture

The three different types of cell line that were used for the study are HaCaT, NEB1 and N/Tert immortalised human keratinocytes. NEB1 cells originate from early epidermal keratinocytes and were immortalised using HPV16 E6/E7 virus (Morley et al., 2003). N/Tert keratinocytes were generated by retroviral transduction of telomerase (Dickson et al., 2000). HaCaT cells are spontaneously immortalised keratinocytes (Boukamp et al., 1988) with a mutation of the p53 pathway later being identified as the likely cause of immortalisation (Lehman et al., 1993).

NEB1, N/Tert and HaCaT cells were cultured in keratinocyte growth medium (KGM) consisting of Alpha MEM and 10% (v/v) heat inactivated foetal bovine serum of Brazilian origin (Lonza, Slough, UK), 2 mM L-glutamine and 2% o(v/v) penicillin streptomycin (PAA Laboratories, Somerset, UK). L-glutamine is an amino acid required for glycolysis while penicillin and streptomycin are antibiotics required to prevent bacterial contamination of cell cultures. The KGM supplement was made up of 10 ng/ml epidermal growth factor (EGF), 0.5 µg/ml hydrocortisone, 5 µg/ml insulin (bovine pancreas), $1.8x10^{-4}$ M adenine and $1x10^{-10}$ M cholera toxin (Sigma, Poole, UK). Cells were incubated at 37°c in 5% (v/v) CO_2. EGF is a growth factor that stimulates cell growth, differentiation and proliferation while hydrocortisone and insulin are steroid hormones. Adenine is an amino acid that forms adenosine which is a component of ATP. Cholera toxin increases intracellular cAMP levels in cells which promotes cell growth.

Cells were passaged at 70% confluence. Cells were washed with phosphate buffered saline (PBS) (PAA Laboratories, Somerset, UK) once and after aspirating, 1x Trypsin-EDTA (PAA Laboratories, Somerset, UK) was added. Cells were incubated at 37°c until they detached from the culture flask and an equal amount of serum containing media e.g. KGM media to Trypsin-EDTA was added to neutralise the enzyme reaction and prevent proteolysis.

Cells were counted using a haemocytometer. A coverslip was placed on the haemocytometer and 20 µl of cell suspension placed at the edge of the coverslip. A count was taken for all four 4x4 outer quadrants on the haemocytometer. An average number of cells of the four quadrants was taken and the total number of cells calculated. After centrifugation and aspiration of the supernatant, an appropriate amount of KGM media would be added to re-suspend the pellet before seeding of the cells.

2.2 Retroviral particle formation

All retroviral DNA constructs were transfected into amphotropic Phoenix packaging cells (developed in the Nolan lab, Stanford University, USA) to produce the retrovirus which was cultured in DMEM media (PAA Laboratories, Somerset, UK) supplemented with 10% (v/v) heat inactivated foetal bovine serum (FBS), 2 mM L-glutamine and 2% (v/v) penicillin streptomycin.

$1.5x10^6$ Phoenix cells were seeded in a 6 cm dish 24 hours before transfection. Fugene6 (Roche Applied Science, East Sussex, UK) was added to 100 µl serum and antibiotic free DMEM media in polypropylene flow cytometry tubes and incubated for 5 minutes. 8 µg of DNA construct was added to the mixture at a ratio of 1:2.5 of construct to Fugene6. After adding a further 100 µl of serum and antibiotic free DMEM media, the mixture was incubated at room temperature for 15 minutes. This was added to the Phoenix cells and incubated at 37°c, 5% (v/v) CO_2. The media was changed the following day and 1 µg/ml Puromycin (Sigma, Poole, UK) added with fresh serum containing DMEM media.

After selection with Puromycin, the cells were left to grow until 100% confluence at which point new DMEM media was added and the cells incubated at 32°c, 5% (v/v) CO_2. After 24 hours, the virus containing media was harvested and syringed through a 0.45 µm filter to remove virus producing cells (Thermo Fisher Nalgene, Loughborough, UK). The virus was then snap frozen in liquid nitrogen and stored at -80°c until required.

2.3 Retroviral transduction

Keratinocyte cell lines were retrovirally transduced with PTCH1 small hairpin RNA (shRNA) constructs 29A and 189A that target exons 3 and 24 respectively (a gift from Professor David Kelsell, Queen Mary University of London). A scramble control vector was used to generate a control cell line (a gift from Monika Cichon, Queen Mary University of London). All sequences were previously cloned into the pSUPERIOR.retro.puro vector (Oligoengine, Seattle, USA) which contains Puromycin resistance.

Scramble control non-targeting sequence:	GCGCGATATATAGAATACG
29A target sequence exon 3:	AAGGTGCTAATGTCCTGACCA
189A target sequence exon 24:	AAGGAAGGATGTAAAGTGGTA

A short loop sequence is incorporated between the sense and antisense target sequence then cloned into the pSUPERIOR.retro.puro vector downstream of the H1 promoter which ensures that the shRNA sequence is constitutively expressed. The hairpin structure is cleaved out of the vector as a small inhibitory RNA (siRNA) sequence and bound to an Argonaute protein which is part of the RNA-induced silencing complex (RISC). This complex will bind to the specific mRNA target sequence to degrade it thus silencing the target gene.

Keratinocytes were seeded in a 6 well plate and at 70% confluence they were ready for retroviral transduction. The media was aspirated and cells washed with PBS. Serum and antibiotic free DMEM media was mixed with 5 µg/ml of Polybrene (Millipore, Watford, UK) and added to the keratinocytes for 10 minutes. Polybrene is a positively charged molecule that binds to the cell to neutralise its surface allowing for stronger virus binding due to reduced charge repulsion (Davis et al., 2002). The retrovirus was then added to the cells and centrifuged in their 6 well plates at 3,000xg for 1 hour. Cells were washed once with PBS before adding KGM media. The retrovirally transduced cells were then selected with 1 µg/ml Puromycin in the following days and cultured normally thereafter.

2.4 Vector construction

2.4.1 EGFP-SMO-WT/M2

For the study an EGFP-SMO fusion protein was generated to be transfected into keratinocyte cells to help determine the localisation of SMO protein. Compared to SMO-WT (wild type), SMO-M2 contains a point mutation of Trp-535-Leu which is an activating mutation first identified in a BCC patient (Xie et al., 1998). The PRK-SMO (M2) vector used in the paper was utilised for generating an EGFP-SMO-WT/M2 vector.

SMO-WT/M2 was excised from PRK-SMO (M2) using XhoI and EcoRI restriction enzymes simultaneously (New England Biolabs, Hertfordshire, UK). 1 µg of PRK-SMO-WT/M2 was incubated with 1 µl of both XhoI and EcoRI (20,000 units/ml), 2 µl of Buffer 4 with H_2O to make a total reaction volume of 20 µl which was incubated overnight at 37°c. The following day, enzymes within the reaction mix were heat inactivated for 20 minutes at 65°c.

A 0.6% (w/v) agarose gel (Fisher Scientific, Leicestershire, UK) was prepared in 1x TAE solution (Appendix Table 8.1) and repeatedly boiled until the agarose crystals were fully dissolved. At this point, the agarose solution was cooled for 1 minute with cold tap water before GelRed

was added at 1 µl/ml (Biotium, CA, USA). The solution was then poured into a gel castor with a comb and left to solidify. The reaction mix was then loaded onto the gel (placed in gel tank, submerged in 1x TAE) along with DNA Hyperladder I and II (Bioline, London, UK). The gel is run at 90 V until the products of the reaction mix were appropriately separated.

2.4.2 Gel extraction of cloning products

Digested cloning products were purified from the 0.6% (w/v) agarose gel in 1x TAE using QIAquick Gel Extraction kit (Qiagen, Crawley, UK). The restriction cut product bands that were visible under UV light, were cut from the gel and transferred to a 1.5 ml tube. The excised gel was weighed and for every 100 mg, 300 µl of QG buffer was added and incubated at 50°c to dissolve the gel. Chaotropic salts within the QG buffer disrupt the hydrogen bonds of the extracted DNA and also create a hydrophobic environment which makes the silica membrane of the QIAquick spin column more suitable for DNA binding. A volume of isopropanol (1 µl/mg of gel) is added to the 1.5 ml tube which precipitates the DNA allowing it to better bind to the silica.

The samples were then transferred to a QIAquick spin column and centrifuged at 13,000 rpm for 1 minute which binds the DNA to the silica membrane of the column. The flow-through from the centrifugation process was discarded. The column was washed with 750 µl of Buffer PE and centrifuged again. The flow-through was again discarded and the column was dried by empty centrifuging for a further minute. The DNA was eluted from the column into a sterile 1.5 ml tube by loading 50 µl of Buffer EB into the column which was left to stand for 1 minute before centrifuging at 13,000 rpm for 1 minute. The DNA was then measured on the NanoDrop spectrophotometer and the DNA stored at -20°c.

2.4.3 SMO-WT/M2 ligation with EGFP-C2

Using the same methodology to excise SMO-WT/M2 from PRK-SMO-WT/M2, a small fragment from the multiple cloning site (MCS) of pEGFP-C2 (Clontech Laboratories, CA, USA) was removed using XhoI and EcoRI enzymes leaving sticky ends available for ligating SMO-WT/M2 (Figure 2.1). The pEGFP-C2 vector was selected so that SMO-WT/M2 would be inserted in-frame to ensure that SMO-WT/M2 was correctly expressed upon transfection into cells. Having isolated SMO-WT/M2 from the PRK-SMO-WT/M2 vector as well as pEGFP-C2, both were ligated together at a ratio calculated using the following equation:

$$\left[\frac{[x]\ \mu g\ pEGFP\text{-}C2 \times [y]\ kb\ SMO\text{-}WT/M2\ insert}{[z]\ kb\ EGFP\text{-}SMO\text{-}WT/M2\ total}\right] \times 3 = SMO\text{-}WT/M2\ insert\ (\mu g)$$

The ligation mix was made up of approximately a 3:1 ratio of SMO-WT/M2:pEGFP-C2, 1 µl of T4 DNA Ligase enzyme and 2 µl of 10x T4 DNA Ligase Buffer (New England Biolabs, Hertfordshire, UK). H_2O was added to make a total of 20 µl and the mix incubated at room temperature overnight.

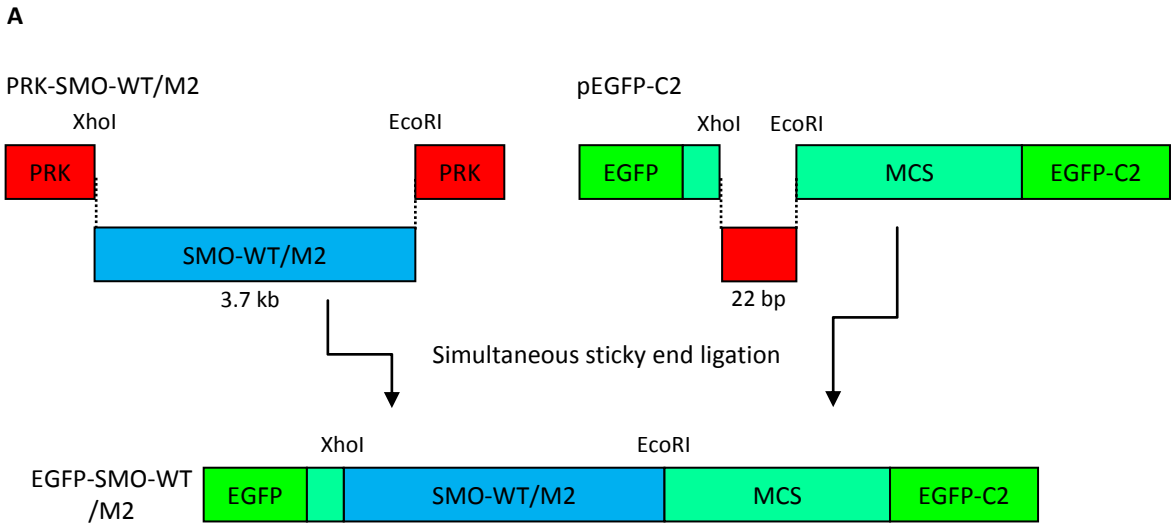

Figure 2.1: Strategy for cloning SMO-WT/M2 into EGFP-C2

2.4.4 Bacterial transformation

After ligation of SMO-WT/M2 into pEGFP-C2, the reaction mix was transformed using One Shot TOP10 competent *Escherichia coli* bacteria (Invitrogen, Paisley, UK). The purpose of this procedure is to amplify the DNA plasmid in large quantities. The competent bacteria originally stored at -80°c, were thawed on ice prior to transformation. Up to 100 ng of ligation mix was added to the bacteria and mixed by gently tapping which was then left on ice for 30 minutes. The bacteria mix was then heat shocked at 42°c for 30 seconds and placed back on ice immediately for 2 minutes. The heat shock process makes the bacterial lipid membrane permeable so that DNA can enter the bacteria. 250 µl of SOC media (Invitrogen, Paisley, UK) is added to the bacteria which is nutrient rich and encourages bacterial growth with better transformation. The bacteria mix was incubated at 37°c for 1 hour on a fast shaker.

100 µl of the bacteria mix was then streaked out on a Kanamycin resistant Luria-Bertani (LB) (Sigma, Poole, UK) agar plate as pEGFP-C2 is resistant to this antibiotic. The bacterial plate was inverted and incubated at 37°c overnight. As a negative control competent bacteria that were not transformed with any DNA were also plated out with the hope that no colonies appear as the bacteria would have not gained resistance to Kanamycin.

2.4.5 Miniprep of EGFP-SMO-WT/M2 plasmid

Successfully transformed bacteria were identifiable as bacterial colonies on the agar plates as pEGFP-C2 contains a Kanamycin resistance gene. However, this does not necessarily mean that the bacteria contains EGFP-SMO-WT/M2 DNA therefore, a number of colonies were selected for analysis. A small amount of the selected colony was isolated and transferred to 5 ml of pre-autoclaved LB broth (Sigma, Poole, UK) containing 50 µg/ml of Kanamycin (Sigma, Poole, UK) and left on a fast shaker at 37°c overnight.

The DNA plasmids were purified from the bacterial LB broth using the QIAprep Miniprep kit (Qiagen, Crawly, UK). The bacterial LB broth was centrifuged at 4000 rpm for 10 minutes whilst at 4°c. The resultant pellet was re-suspended in 250 µl of Buffer P1 which contains RNase A that digests unwanted RNA. 250 µl of Buffer P2 was then added and mixed by inverting five times. Buffer P2 contains SDS to lyse the cells and NaOH to create an alkaline condition that denatures genomic DNA. 350 µl of Buffer N3 was added immediately and again the solution inverted five times before being centrifuged at 4000 rpm for 10 minutes. After this, the supernatant was transferred to a QIAprep spin column and centrifuged for 1 minute. Buffer N3

is a neutralisation buffer which will cause all protein, debris and genomic DNA to precipitate as a salt. Buffer N3 also helps bind DNA to the silica particles within the QIAprep spin column.

The flow through was discarded from the QIAprep spin column as now the DNA was bound to the column filter. The spin column was centrifuged again for 30 seconds to remove any residual buffer. The top of the spin column was transferred to a clean 1.5 ml tube and the DNA eluted by adding 50 µl of Buffer EB onto the silica within the tube. The column was left to stand for 1 minute before being centrifuged for a minute. The plasmid was quantified on the NanoDrop spectrophotometer (NanoDrop Technologies, DE, USA) and stored at -20°c. Cloning products were validated by PCR and protein analysis.

2.4.6 Maxiprep of EGFP-SMO-WT/M2 plasmid

A small amount of the selected colony was isolated and transferred to 20 ml of pre-autoclaved LB broth containing 50 µg/ml of Kanamycin and incubated at 37°c for 8 hours whilst shaking. The 20 ml of bacterial LB media was then added to 200 ml of LB media containing 50 µg/ml of Kanamycin and left on a fast shaker at 37°c overnight.

The DNA plasmids were purified from the bacterial LB broth using the Qiagen Plasmid Purification Maxi kit (Qiagen, Crawly, UK). The bacterial LB broth was centrifuged (in 50 ml falcon tubes) at 4000 rpm for 10 minutes whilst at 4°c. The resultant pellet was re-suspended in 10 ml of Buffer P1. 10 ml of Buffer P2 was then added and incubated for 5 minutes at room temperature. 10 ml of Buffer P3 was added and the mix was left to incubate for 20 minutes at room temperature. This is a neutralisation buffer similar to Buffer N3 that precipitates unwanted debris into a salt. The mix was then centrifuged at 4000 rpm for 10 minutes at 4°c to remove the waste materials as the supernatant was collected and centrifuged again for increased purity.

The plasmid containing supernatant was then transferred to a pre-equilibrated Qia-Tip column. The DNA was retained in the column filter while the flow-through was removed in a conical flask. 30 ml of wash Buffer QC was added to the filter, twice. The Qia-Tip was then placed in a 50 ml falcon tube and the DNA was eluted using 15ml of Buffer QF which was subsequently precipitated with 10.5 ml of Isopropanol. The DNA was then centrifuged at 4000 rpm for 15 minutes at 4°c and the pellet washed with 5 ml of 70% ethanol before a second centrifugation. The pellet was then air dried before being re-suspended in 200 µl of Buffer EB. The plasmid was quantified on the NanoDrop and stored at -20°c.

2.5 RNA extraction

RNA was extracted from cells at 70% confluence or three days post seeding. The extraction was performed using an RNeasy Mini Kit (Qiagen, West Sussex, UK). After aspirating the PBS from the cells, 350 µl of RLT buffer (β-Mercaptoethanol added beforehand (10 µl for 1 ml of RLT buffer); Sigma, Poole, UK) was added which lyses the cells and also contains Guanidine Isothiocyanate, both of which deactivate RNase enzymes. The cell lysate was transferred and passed through a QIAshredder Mini Spin column by centrifugation at 13,000 rpm for 2 minutes which removes cell debris. The flow through solution was retained and transferred to the gDNA eliminator column and centrifuged for 1 minute which retains any genomic DNA in the filter. The flow through was then mixed with 600 µl of 70% ethanol and left to stand for 1 minute allowing the RNA to bind to the silica membrane when transferred into an RNeasy Mini Spin column. The RNA within the sample was collected by the column after centrifugation.

350 µl of RW1 wash buffer was added and the column was centrifuged in order to remove any remaining genomic DNA. The column was then washed with 700 µl RPE buffer and washed again with 500 µl RPE buffer. This removes any salts remaining from previous washes. The column was then transferred to a fresh 1.5 ml tube and RNA eluted by adding 25 µl of RNase free water and centrifuging. A second elution step with a further 25 µl was performed before quantifying the RNA. The RNA concentration was measured using the NanoDrop. A measurement of the absorbance values at 260 nm was recorded as this is the wavelength at which RNA absorbs light. RNA was stored at -80°c.

2.6 Complementary DNA (cDNA) synthesis

cDNA was synthesised from RNA obtained directly from the cells using the Superscript VILO cDNA synthesis kit (Invitrogen, Paisley, UK). Up to 2.5 µg of RNA was used per reaction. 4 µl of 5x VILO mix was added which contains random primers, $MgCl_2$ and deoxynucleotide triphosphates (dNTPs) all of which are optimised for PCR reactions. 2 µl of 10x Superscript mix is added and this consists of the reverse transcriptase enzyme to synthesise the cDNA and a recombinant ribonuclease inhibitor to prevent RNA degradation. The reaction mix is made up to a total of 20 µl with RNase free water and placed in a PCR thermocycler. The PCR machine was set for three holding steps the first being for 10 minutes at 25°c followed by 1 hour at 42°c and a final step for 5 minutes at 85°c. cDNA was quantified using the NanoDrop and then stored at-20°c.

2.7 Polymerase chain reaction (PCR)

PCR is a method used to amplify specific DNA sequences that are selected by specific primers. PCR can be used to detect messenger RNA (mRNA) by amplifying a section of its cDNA. To do this, oligonucleotide primer sequences (Sigma, Poole, UK) were designed around the region of interest.

Primer sequences were designed using the internet-based Primer3 program and were checked with the mRNA sequence of interest (Rozen and Skaletsky, 1998). In the case that multiple isoforms exist for the same gene, all isoforms were aligned together using the ClustalW alignment tool and primers were designed to overlap a region common to all the isoform sequences (Larkin et al., 2007). To check the specificity of the primers, both forward and reverse primer sequences were inputted into the NCBI Nucleotide BLAST search tool which searches the primer sequence against other genes (Altschul et al., 1990). This prevents the amplification of other genes that may have a similar sequence which would give a false positive result.

The ReddyMix PCR Mastermix kit (Fisher Scientific, Leicestershire, UK) was used for each PCR reaction. For each reaction, 200 ng of cDNA was added to 0.2 ml flat cap PCR tube (Qiagen, Crawly, UK). 12.5 µl of ReddyMix was added followed by 1 µl 25 mM $MgCl_2$, 2 µl of 1 µM primer (forward and reverse) and H_2O up to a final volume of 20 µl. For genes that have lower expression, the cDNA and/or primer concentration was increased. For a negative control, a reaction mix was made with cDNA substituted with an equal volume of H_2O. The PCR samples were then loaded onto the Tetrad PTC-225 Thermo Cycler (MJ Research, MA, USA) and the following program used:

Initialisation:	95°c	15 minutes	
Denaturation:	95°c	20 seconds	Cycling
Annealing:	*x*°c	20 seconds	
Extension:	72°c	25 seconds	
Repeat cycling steps 35 times			
Final extension:	72°c	10 minutes	

(*x*) denotes the optimised primer annealing temperature ranging from 57°c to 64°c, primer sequences and annealing temperatures are listed in the Appendix (Table 8.2). The initialisation step is required to heat activate the DNA polymerase enzymes contained in the ReddyMix.

Denaturation causes melting of the double stranded DNA so that annealing of the primer sequences to the single stranded DNA can occur as new hydrogen bonds are formed. As the DNA polymerase enzyme binds to the template, cDNA is synthesised using dNTPs within the ReddyMix. Multiple cycles are required to ensure that the full length of DNA is synthesised and to amplify as much of the DNA as possible. A final extension stage then ensures that any remaining single stranded DNA is synthesised. The reaction products were then loaded onto the gel (placed in gel tank, submerged in 1x TAE) along with DNA Hyperladder II. The gel was run at 90 V until the size of PCR product was determinable compared to the DNA ladder.

2.8 Quantitative polymerase chain reaction (qPCR)

This qPCR method was used to determine the comparative expression of mRNA levels between the cell types. The kit used for qPCR was Rotor-Gene SYBR green PCR kit (Qiagen, West Sussex, UK). SYBR Green is a dye that binds to double stranded DNA therefore, as the PCR product is amplified it can be detected and quantified by its fluorescence signal.

200 ng of cDNA was used per reaction with each sample analysed in triplicate. For each reaction, 12.5 µl of SYBR mix was added, 1 µl of 25 mM $MgCl_2$, 2 µl of 1 µM primer template and RNase free water up to a total of 20 µl. cDNA was omitted from negative control samples. The qPCR reactions were loaded into the Rotor-Gene Q (Qiagen, West Sussex, UK) and the following program was used:

Initialisation:	95°c	5 minutes	
Denaturation:	95°c	5 seconds	Cycling
Annealing:	*x*°c	5 seconds	
Extension:	60°c	10 seconds	

Repeat cycling steps 45 times followed by a melt stage.

A post-qPCR melting stage was performed to determine if a single PCR product was being amplified in which case, a single peak would be visible and also to make sure that there were no false positives caused by primer dimer formation. During the melt stage, the Rotor-Gene Q machine has an option to determine the optimal fluorescence gain level and this was always selected.

The relative mRNA expression values were calculated using the $x=2^{-\Delta\Delta Ct}$ formula where *x* represents the induction value and Ct represents the average threshold cycle of the triplicate

samples. ΔCt refers to the difference between the Ct values of the gene of interest and the housekeeping reference gene GAPDH. ΔΔCt represents the difference between the ΔCt value of the cDNA sample compared to the control sample e.g. NEB1-shPTCH1 ΔCt values normalised and compared to NEB1-shCON ΔCt values.

2.9 Small inhibitory RNA (siRNA) and plasmid DNA reverse transfection

siRNA sequences were pre-designed and transiently transfected into cells to silence SMO. The siRNA sequence binds to the Argonaute protein which then degrades the specific mRNA. Reverse transfection is a more efficient method of transfection than normal transfection. A variety of different transfection reagents were tested on the keratinocyte cell lines using siGLO Cyclophilin B (Fisher Scientific, Leicestershire, UK) as a positive control. Cyclophilin B binds to the cell nucleus which fluoresces red that can be observed under a microscope and it can also be used to ensure knockdown efficiency by qPCR.

Using various different transfection reagents, a siRNA concentration of 50 nM for 2 days was found to be most effective combined with Hiperfect (Qiagen, West Sussex, UK) transfection reagent. Hiperfect contains lipids that bind with the siRNA and allow its entry into the cell through the lipid bilayer. For DNA plasmid transfections, TransIT 2020 (Mirus Bio, WI, USA) was the most effective reagent which was optimised with EGFP-C2 at 1 µg.

Hiperfect or TransIT 2020 was added to serum and antibiotic free DMEM media in polypropylene flow cytometry tubes and left to incubate for 5 minutes. 50 nM of siRNA was added to the mixture at a ratio of 1:3 of siRNA or DNA to the transfection reagent and incubated at room temperature for 15 minutes. Serum and antibiotic free media was supplemented to the mixture, added to the culture dish or plates and incubated at 37°c, 5% (v/v) CO_2 for 30 minutes. During this time, NEB1 cells were trypsinised and counted. Cells were re-suspended in KGM media before being added to the siRNA or DNA treated culture dish or plates and incubated for 24 hours. The media was changed to KGM media after this period and harvested or fixed the next day.

2.10 Protein extraction and western blotting

Cells were grown to 70% confluence before being harvested. Cells were washed once with PBS before 220 µl of pre-heated protein lysis buffer (Appendix Table 8.1) was added ensuring that the entire culture surface was covered. Cells were scraped off the surface then transferred to a 1.5 ml tube before being heated at 95°c for 2 minutes. The lysate was then passed through a syringe and needle to reduce viscosity. 20 µl of the lysate was put into a 1.5 ml tube for quantification using the Bio-Rad DC Protein Assay kit (Bio-Rad, MA, USA). 2 µl of Solution S and 98 µl of Solution A were added to the 1.5 ml tube and mixed. 800 µl of Solution B was added to each tube and mixed at which point, the mix would change colour. The protein binds to the alkaline copper tartrate solution (Solution A and S) and as the Folin containing Solution B is added, the protein bound to copper reduces Folin. This reduction reaction generates a blue colour solution with a minimum and maximum absorbance of 405 nm and 750 nm respectively. A high protein concentration creates stronger blue colour intensity. The reagents were added and samples transferred to cuvettes. Using a spectrophotometer, the protein absorbance (*AU*) was measured at a wavelength of 655 nm. A standard curve was generated using the *AU* measurements obtained from known concentrations of bovine serum albumen (BSA, Sigma, Poole, UK) from which the following equation was formed:

$$\left[\frac{AU + 0.00091}{0.213}\right] \times 0.8 = \text{Concentration of protein } (\mu g/\mu l)$$

After quantifying the protein, 50 µl of 5x protein loading dye (Fisher Scientific, Leicestershire, UK) was added to the remaining 200 µl of sample and stored at -20°c.

Sodium dodecyl sulphate polyacrylamide gel electrophoresis (SDS-PAGE) was used to analyse the protein expression levels of the cells. A resolving gel was made consisting of distilled water, 30% (v/v) acrylamide gel, 1.5 M Tris (pH 8.8), 10% (w/v) SDS, 10% (w/v) ammonium persulphate (APS) and tetramethylethylenediamine (TEMED). The acrylamide gel forms cross links which creates pores by which the protein can be separated. The SDS negatively charges the protein so an electric current can be applied to separate the proteins. APS and TEMED are polymerisation agents that solidify the gel. A stacking gel was set on top of the resolving gel consisting of the same ingredients with 1 M Tris (pH 6.8) rather than 1.5 M Tris and with a higher concentration of acrylamide gel. A comb was set in the stacking gel so that protein samples could be loaded onto the gel.

Protein lysates were heated for 2 minutes at 95°c before 20 µg of protein was loaded into the gel. 10 µl of ColorPlus Prestained Protein Ladder (New England Biolabs, Hertfordshire, UK) was run alongside the samples. Gels were run in 1x running buffer (Appendix Table 8.1) for approximately 2 hours at 120 V. The electrical current creates a boundary that carries the protein through the stacking gel and into the resolving gel. The protein is condensed in a thin line before moving through the gel where the protein is separated by its molecular weight.

Once the samples had run, the protein from the gel was transferred onto nitrocellulose paper (GE Healthcare, Buckinghamshire, UK) by electroblotting. SDS coats the sample protein to give it a negative charge and also breaks the tertiary structure but leaves the secondary structure intact. Gels were transferred using a Hoeffer transfer tank in pre-cooled 1x transfer buffer (Appendix Table 8.1) for 2 hours at 350 mA. The transfer cassette is orientated so that the protein moves towards the membrane at the positive anode. Methanol within the transfer buffer helps the transfer of smaller proteins to the membrane. Once transfer was complete, the membrane was washed in TBST or PBST buffer (Appendix Table 8.1) depending on the primary antibody to be probed with, before 1 hour of blocking at room temperature in 5% (w/v) milk powder dissolved in T/PBST.

Membranes were then incubated for 16 hours at 4°c in the specific primary antibody diluted to 1:1000 in T/PBST. The membranes were then washed three times in T/PBST for 5 minutes before 1½ hour incubation with a horseradish peroxidise (HRP) conjugated secondary antibody diluted to 1:1000 in T/PBST, at room temperature. Membranes were given three washes in T/PBST for 5 minutes. An ECL western blot detection system kit (GE Healthcare, Buckinghamshire, UK) was used on the blot which binds to the HRP to produce a chemiluminescent signal that was recorded onto ECL Hyperfilm (GE Healthcare, Buckinghamshire, UK) when exposed to the membrane in a darkroom. The exposure time of the film to the membrane varied depending on the level of protein present and the primary antibody used. Western blot membranes were probed for α-Tubulin as a protein loading control.

Membranes were stripped of the primary antibodies (Appendix Table 8.3) in order to re-probe the same membrane for other proteins. A stripping buffer (Appendix Table 8.1) was added to the membrane and incubated at 55°c for 30 minutes. Membranes were then washed three times before being blocked again in 5% (w/v) milk and re-probed or stored in T/PBST at 4°c.

2.11 Immunocytochemistry

Immunocytochemistry staining was used to determine the sub-cellular localisation of proteins. Cells were initially seeded in 12 well plates on top of 18 mm diameter glass cover slips (VWR International Ltd, Leicestershire, UK) at a density of 15,000 cells per well and allowed to grow for three days. The cells were washed twice with PBS before being fixed with 4% (w/v) paraformaldehyde for 15 minutes. Cells were then washed with PBS three times and permeablised in 0.1% (w/v) Triton X-100 (Sigma, Poole, UK) for 10 minutes. The cells were blocked in 3% (w/v) BSA (Fisher Scientific, Leicestershire, UK) for 30 minutes followed by the addition of the primary antibody (Appendix Table 8.3) diluted 1:1000 in 3% (w/v) BSA for 1 hour.

Following three PBS washes for 5 minutes each, a fluorescence dye labelled secondary antibody diluted to 1:800 in PBS was added and incubated for 1 hour while being protected by light. Alexa 488 and Alexa 568 secondary antibodies (Invitrogen, Paisley, UK) have green and red fluorescence spectra respectively. After three PBS washes, the nuclei of the cells were stained with 0.1 μg/ml of DAPI for 5 minutes before a final wash in PBS.

Coverslips were mounted onto microscope slides using Vectashield fluorescence mounting medium (Vector Laboratories Ltd, Peterborough, UK) and stored at 4°c away from light. The slides were viewed and images taken on the Zeiss LSM 510 Meta Confocal Microscope. For the negative control, cells were stained with DAPI and the secondary antibodies, without any primary antibodies. All secondary antibodies were negative (Figure 2.2).

Images taken by the confocal microscope were quantified using Image J software (Collins, 2007). Images were edited to only show the fluorescence channel of the protein of interest and then converted to greyscale. Cells were selected and analysed based on the intensity of pixels taking into account the size of the cell. The relative density was then calculated which indicates the intensity of staining.

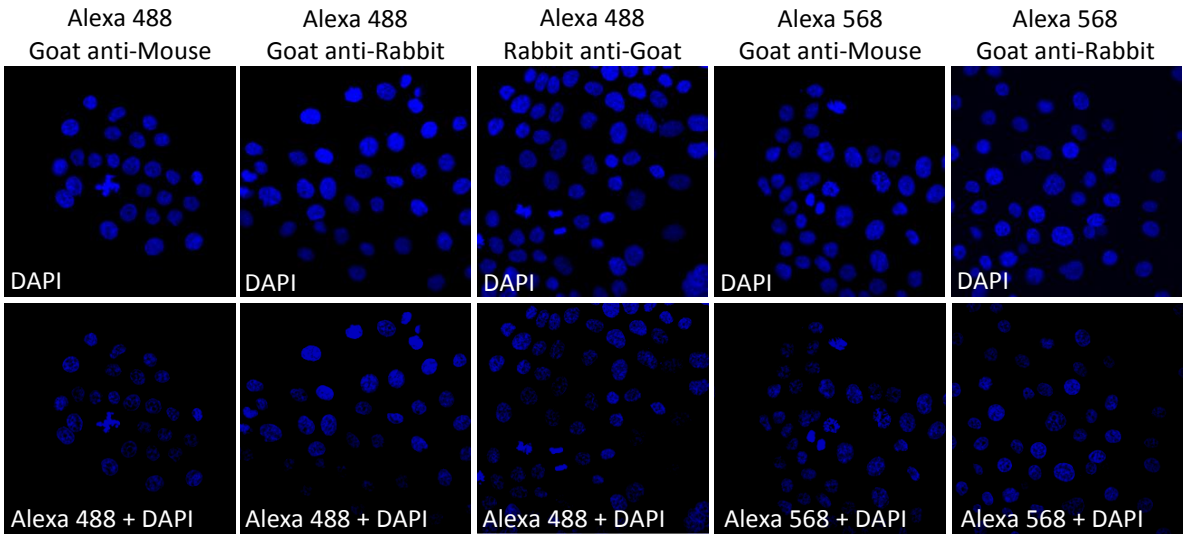

Figure 2.2: Negative controls for secondary immunofluorescence antibodies

2.12 Alamar blue viability/proliferation assay

The Alamar blue assay (AbD Serotec, Kidlington, UK) was used to measure keratinocyte cell proliferation. The Alamar blue solution contains Resazurin that will produce the fluorescent red dye Resorufin under redox reaction conditions. The intensity level of the red fluorescence indicates the proliferation of the cells. Cells were seeded in a 6 well plate and left to settle for 24 hours. The following day, 10% (v/v) of Alamar blue was added to the culture media. The old media was removed and the Alamar blue in media was added to the cells that were then incubated at 37°c for 6 hours. 100 µl of media was added to a white 96 well plate, each sample in triplicate. The control used was the Alamar blue with media. The fluorescence intensity was measured with the excitation wavelength set at 530-560 nm and an emission of 590 nm using a Wallac plate reader (Perkin Elmer, MA, USA).

2.13 Gene expression microarray

Gene expression microarray profiling was performed on NEB1-shCON and NEB1-shPTCH1 cells lines using Human Gene 1.1 ST Array Strip from Affymetrix (Affymetrix, CA, USA). The array chip contains 28,000 genes probed with multiple oligonucleotide sequences and in total, 750,000 probes to determine the gene expression profile of each sample. Each sample was repeated in triplicate and the data normalised using the MetaCore pathway analysis software (GeneGo, CA, USA) performed by Dr Joanne Selway and Avijit Guha Roy from The University of Buckingham.

Three Affymetrix chips were used for each sample and the raw data was processed using the multi array average (RMA) method. RMA utilises quantile normalisation that will fit all the chips used from the experiment into the same distribution and also gives them the same mean (Irizarry et al., 2003). This allows for normalisation and background correction of the data which will provide an expression value for each gene. From this, differentially expressed genes (DEGs) can be separated based on P-values and fold change.

Probabilities of gene expression between the experimental and control group are generated using Wilcoxon's Signed Rank test where P-values are used to compare between different groups of genes. Turkey's Biweight method is then used to obtain log ratios which are then anti-logged to generate fold change values comparing the genes between samples (Gentleman et al., 2005). Genes with a P-value at or below 5% and a fold change greater than +/- 2 fold are considered as DEGs.

DEGs were analysed in MetaCore using its GeneGo database of cellular pathways and process networks. P-values represent the probability for a set of genes to appear on a network or process map to arise by chance. The smaller the P-value is, the less likely that the result has occurred by chance. The P-value also considers the number of genes from the experimental data versus the number of genes in the network map. The formula for calculating the P-value is:

$$\text{P Value} = \frac{R!\, n!\, (N-R)!\, (N-n)!}{N!} \sum_{i=\max(r,R+n-N)}^{\min(n,R)} \frac{1}{i!\, (R-i)!\, (n-i)!\, (N-R-n+i)!}$$

N = total number of nodes in MetaCore database

R = number of the network's objects corresponding to the genes in microarray data list

n = total number of nodes in each small network generated from the microarray data

r = number of nodes with data in each small network generated from the microarray data

Once the microarray DEGs were applied to the network and process maps, a Z-score was calculated for each sub-network. The Z-score ranks the sub-networks based on the number of DEG saturation on each map. A high Z-score shows that the network is highly saturated with DEGs from the microarray data. The formula for calculating the Z-score is:

$$\text{Z Score} = \frac{r - n\frac{R}{N}}{\sqrt{n\left(\frac{R}{N}\right)\left(1-\frac{R}{N}\right)\left(1-\frac{n-1}{N-1}\right)}}$$

N = total number of nodes in MetaCore database

R = number of the network's objects corresponding to the genes in microarray data list

n = total number of nodes in each small network generated from the microarray data

r = number of nodes with data in each small network generated from the microarray data

2.14 DAVID functional annotation tool

The database for annotation, visualisation and integrated discovery (DAVID) is a set of online bioinformatics tools that provides the means to highlight biological processes and functions from a given gene list (Huang et al., 2009). There are a number of annotation categories including protein-protein interactions, protein functional domains, disease associations, gene functional summaries and signalling pathways.

The functional annotation clustering tool was used in order to map the DEGs from the microarray analysis onto signalling pathway and process maps. This was to determine which pathways are affected by the suppression of PTCH1 and also which components of the pathways were differentially regulated. Also, the number of components that are highlighted on a map would help determine the extent by which certain pathways were affected. DAVID is able to map user defined gene lists onto well known KEGG (Kyoto encyclopaedia of genes and genomes) pathways to help interpret the data in a network context.

2.15 Matrigel based organotypic culture

The Matrigel organotypic culture provides a base for an artificial skin model. A dermis layer is created using Matrigel, collagen and fibroblasts. Keratinocytes are then seeded on top of the 'dermis' layer and cultured with an air liquid interface where the fibroblasts grow in culture media but not the keratinocytes. This to an extent mimics the skin *in vitro*.

One day prior to the experiment, Matrigel (BD Pharmingen, NJ, USA) was taken from -20°c storage and allowed to defrost overnight at 4°c while on ice. On the day of the experiment, a mix was made up of 350 µl of Matrigel, 350 µl of Rat tail Collagen type 1 (Millipore, Watford, UK), 100 µl KGM media, 100 µl of FBS per gel. At this point, the mix is acidic therefore 1 M NaOH was added drop by drop until the solution changes from yellow to pink. 500,000 primary dermal fibroblasts re-suspended in 100 µl were added to the mix and all components were gently mixed in a 50 ml falcon tube avoiding any bubble formation. 1 ml of the mix was dispensed into the well of a 24 well plate and left in the incubator at 37°c, 5% (v/v) CO_2 for 2 hours. Once the gel had set, 1 ml of KGM media was added to the top of the gel and incubated overnight.

The 1 ml of media was then removed from the gel and a 4.7 I.D x 8 mm cloning ring (Fisher Scientific, Leicestershire, UK) was pressed onto the gel within the well. This dislodges the gel from the walls of the well plate and provides an enclosed space to add 500,000 NEB1 cells re-suspended in 500 µl of KGM media. This ensures that the NEB1 cells settle and grow on the surface of the gel. The gel was incubated overnight at 37°c, 5% (v/v) CO_2.

Stainless steel wire gauze that was sculpted to provide a raised platform was placed within a 6 well plate. A single Cyclopore 0.4 µm polycarbonate membrane with a 13 mm diameter (Whatman, Kent, UK) was placed on top of the gauze. The ring was removed from the gel and placed directly on the membrane. 4.5 ml of KGM media was added to the well ensuring that

there were no bubbles underneath the gauze and that the media did not drown the gel. This allows the dermis part of the gel to receive media from the bottom while the NEB1 cells on the top do not. The organotypic model was incubated for 28 days or more with weekly media changes. At the end of the experiment, gels were either snap frozen of embedded in wax for histological sectioning.

2.16 Statistical analyses

All experiments were performed in triplicate. The standard deviation was calculated for experiments such as qPCR and Alamar blue proliferation assays. Standard deviation is a measure of the spread of data from the mean value. The following equation was used to measure the standard deviation:

$$\text{Standard deviation} = \sqrt{\frac{\Sigma(x - \bar{x})^2}{(\text{n} - 1)}}$$

x = score

$\bar{x}$ = mean

n = number of values

Σ = sum of values

The student's T-test was used to determine if control and experimental sample data significantly differ from each other for example, if the increase or decrease of protein expression from ImageJ analysis was significant or not. The student's T-test was calculated with the following equation:

$$t = \frac{\bar{x}_1 - \bar{x}_2}{\sqrt{\frac{s_1^2}{N_1} + \frac{s_2^2}{N_2}}}$$

$\bar{x}_1$ = mean of the first data set

$\bar{x}_2$ = mean of the second data set

s_1^2 = standard deviation of the first data set

s_2^2 = standard deviation of the second data set

N_1 = number of elements in the first data set

N_2 = number of elements in the second data set

Chapter 3

In vitro modelling of Basal cell carcinoma

Chapter 3 Introduction

BCC genetics and the involvement of HH signalling have primarily been studied in $PTCH^{+/-}$ mice that are then UV irradiated to initiate tumourigenesis and the formation of BCC-like tumours (Donovan, 2009; Daya-Grosjean and Couve´-Privat, 2005; Mancuso et al., 2004). Similarly, manipulation of HH components such as GLI1 and GLI2 have demonstrated that tumours can develop while there are inconsistencies where one study has shown that the over-expression of SMO-M2 in the IFE leads to BCC formation while others show no tumour growth (Youssef et al., 2010; Grachtchouk et al., 2003). The HH pathway is known to interact with a number of major signalling pathways and UV irradiation may have non-specific effects. Mouse models do suggest that HH may play a role in BCC biology however it is unclear why different types of tumours develop when manipulating HH components.

Regarding the HH signalling pathway, BCC is associated with the loss of function of *PTCH1* which leads to the downstream expression of GLI1 and GLI2 via SMO signalling. A study of NIH-3T3 cells where mutant SMO is over-expressed revealed that HH signalling could not be repressed by Cyclopamine (Taipale et al., 2000). It is not known why a large number of BCC patients do not respond to SMO inhibitors and this brings into question how important HH signalling is in BCC biology (Van Hoff et al., 2009; Göppner et al., 2010). Furthermore, studies by Dr Neill's group have shown that GLI1 is not highly expressed in a number of BCCs by immunohistochemistry (unpublished data). To understand more an *in vitro* model of BCC was developed by the suppression of PTCH1 using shRNA and the HH signalling pathway characterised.

3.1 Creation and characterisation of human keratinocyte cell lines with stable PTCH1 suppression

3.1.1 PTCH1 suppression in NEB1, N/Tert and HaCaT cell lines

The human immortalised cell lines NEB1, N/Tert and HaCaT were chosen for this study as they are widely used in skin research and retain the ability to differentiate (Morley et al., 2003; Dickson et al., 2000; Boukamp et al., 1988). In addition, the levels of PTCH1 and the downstream HH signalling component GLI1 were analysed by qPCR to confirm that these cells were suitable for targeted PTCH1 suppression (Figure 3.1). PTCH1 was readily detected in all cells and compared to NEB1 cells, both N/Tert and HaCaT parental cell lines displayed higher levels of PTCH1 mRNA and lower levels of GLI1 mRNA.

Parental NEB1, N/Tert and HaCaT cell lines were retrovirally transduced with a construct containing a non-targeting scrambled control (shCON) as well as two constructs targeting exons 3 (termed 29A) and 24 (termed 189A) of the PTCH1 gene respectively (Figure 3.2). After drug selection with Puromycin, clonal cell lines were derived by single cell seeding from the heterogeneous populations of NEB1-29A, NEB1-189A, N/Tert-29A and N/Tert-189A cells. HaCaT-29A and HaCaT-189A clonal lines were not generated due to time constraints.

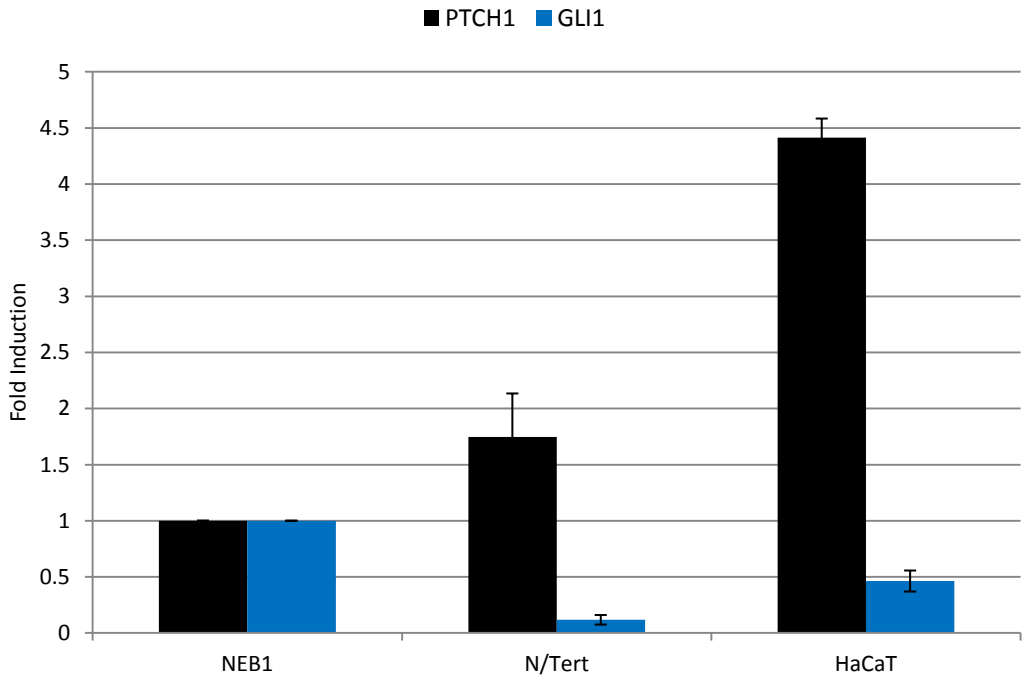

Figure 3.1: qPCR analysis for PTCH1 and GLI1 fold induction in N/Tert and HaCaT, relative to NEB1 cells

Error bars represent mean ± standard deviation.

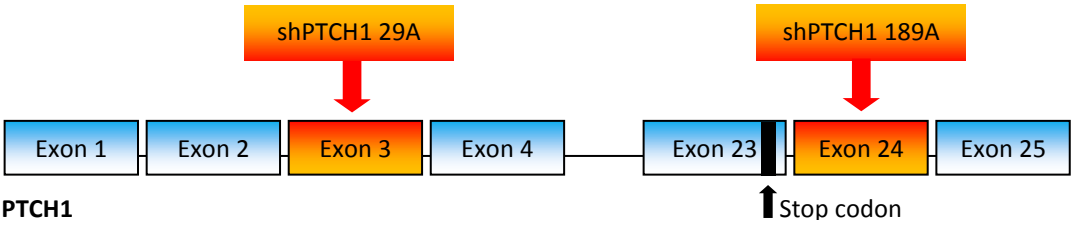

Figure 3.2: PTCH1 shRNA exon targets

A number of clonal cell lines were derived from 29A and 189A heterogeneous populations based on their compact, BCC-like morphology and the level of PTCH1 suppression was assessed by qPCR (Figure 3.3). Of the three keratinocytes cell lines, NEB1-189A-β1 cells showed the strongest suppression of PTCH1 which correlated with an increase of GLI1 and therefore, most of the studies were conducted on this particular clonal cell line. NEB1-189A-β1 will now be referred to as NEB1-shPTCH1. Of the N/Tert clones, N/Tert-29A-β1 showed the lowest levels of PTCH1 and highest GLI1 induction. For consistency with NEB1-shPTCH1 (NEB1-189A-β1) cells, N/tert-189A-β2 showed the strongest induction of GLI1 of the N/Tert-189A clones and will be referred to as N/Tert-shPTCH1 cells. The majority of the studies performed utilised 189A shPTCH1 clones but where 29A shPTCH1 clones were employed these will be clearly labelled. Interestingly, despite the suppression of PTCH1 there was no induction of GLI1 in certain clones such as NEB1-29A-β2, NEB1-29A-β3 and N/tert-29A-β2.

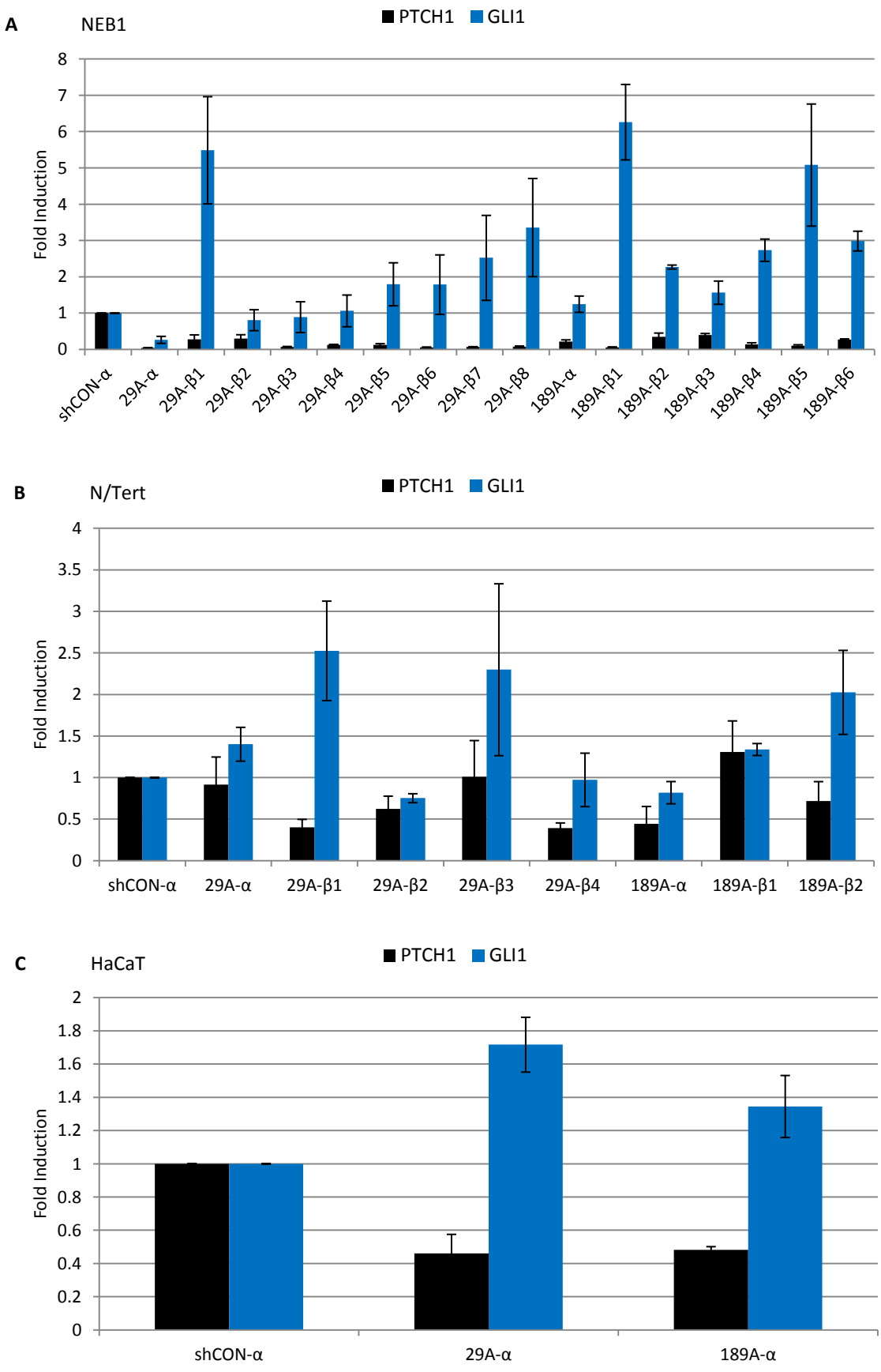

Figure 3.3: qPCR for PTCH1 and GLI1 in shPTCH1 clonal cell lines

PTCH1 and GLI1 mRNA expression levels in [**A**] NEB1-shPTCH1, [**B**] N/Tert-shPTCH1 clonal lines and heterogeneous populations of [**C**] HaCaT-shPTCH1 cells. Error bars represent mean ± standard deviation.

Morphologically, NEB1-shPTCH1 cells displayed a more compact cobblestone-like colony formation compared to NEB1-shCON cells and parental NEB1 cells. A similar more compact morphology was observed in N/Tert-shPTCH1 cells but as HaCaT cells are inherently compact, there was no visible difference between the control cell line and HaCaT-shPTCH1 cells (Figure 3.4).

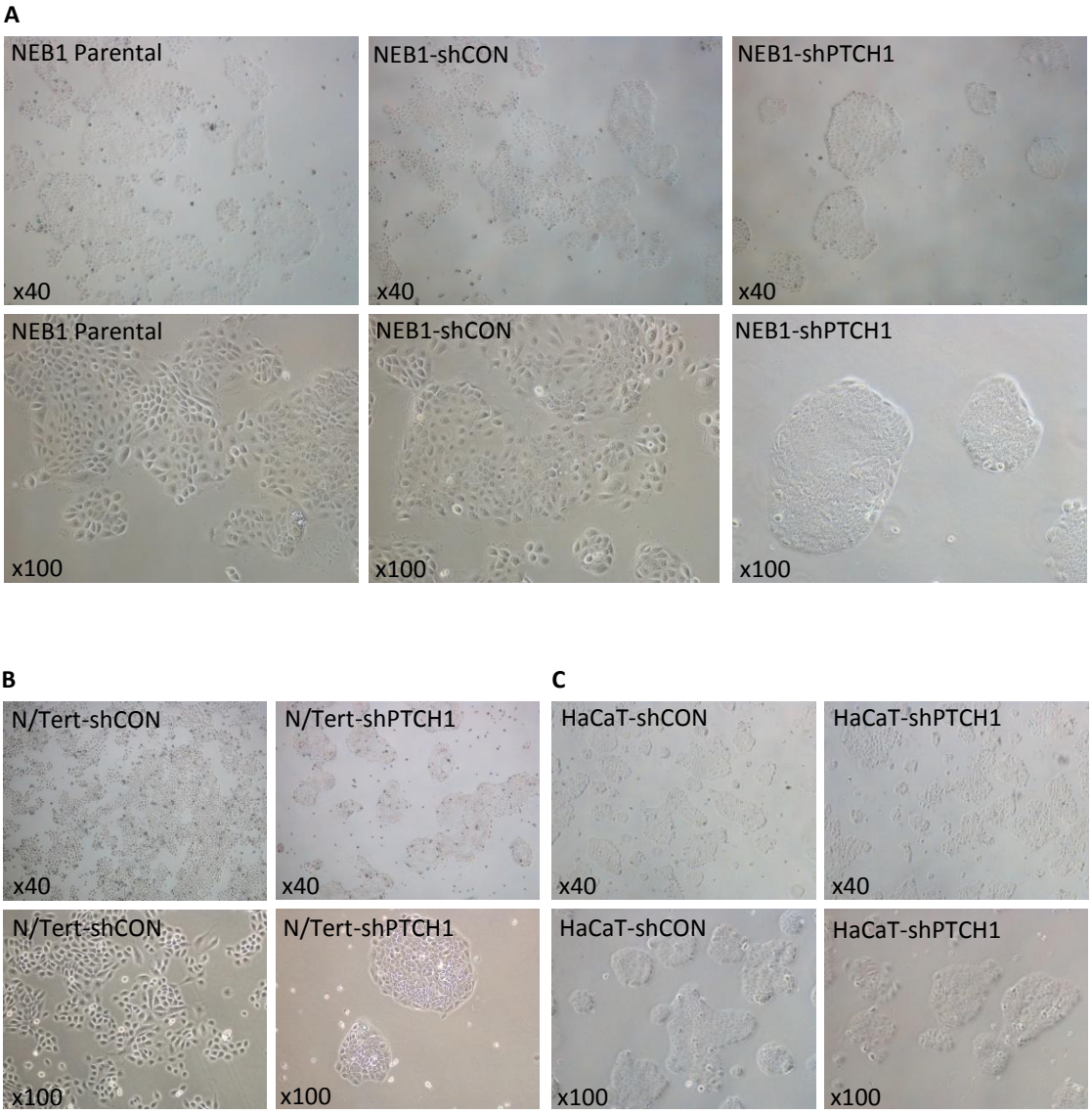

Figure 3.4: PTCH1 suppression induces a highly compact morphology in human keratinocytes

Upon the suppression of PTCH1 in [**A**] NEB1, [**B**] N/Tert and [**C**] HaCaT cells, NEB1 and N/Tert cells display a compact cobblestone-like morphology. No such differences were observed in HaCaT cells as HaCaT-shCON cells grow as tight colonies.

To confirm that the increase of GLI1 is specifically due to reduced PTCH1 activity in NEB1-shPTCH1 cells, a rescue experiment was performed by ectopically expressing the PTCH1B isoform and analysing GLI1 expression. As the PTCH1B vector only contains the coding sequence (i.e. START to STOP codons) its mRNA is not subject to degradation by the PTCH1 shRNA as the hairpin targets a region that is downstream of the STOP codon in exon 24. Ectopic PTCH1B suppressed GLI1 to basal levels thus confirming that the increase of the latter is due to reduced PTCH1 function in NEB1-shPTCH1 cells (Figure 3.5).

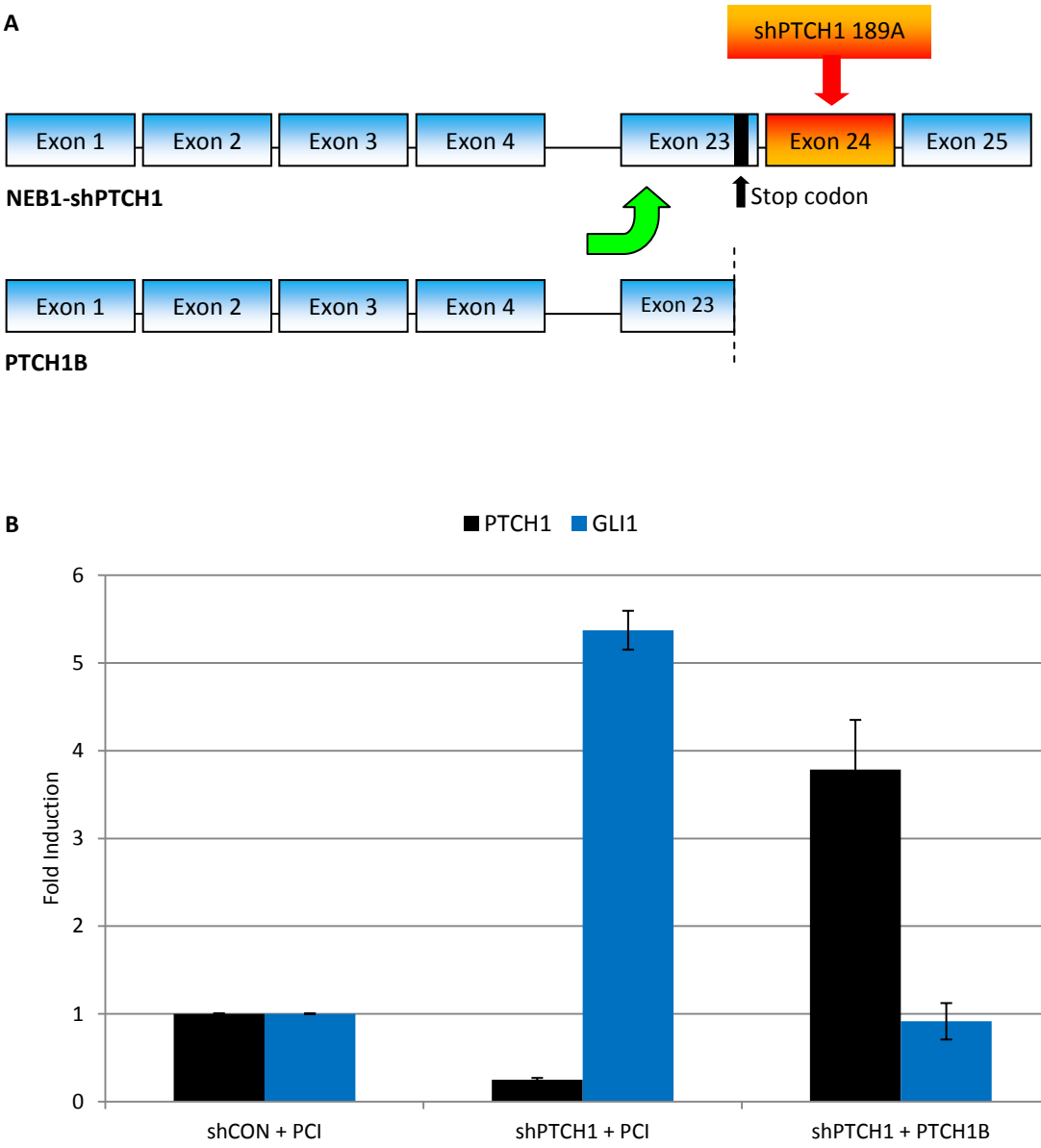

Figure 3.5: PTCH1B rescue experiment

[**A**] The PTCH1B construct does not contain PTCH1 exon 24 which is targeted by the 189A shRNA vector. [**B**] qPCR for GLI1 in NEB1-shPTCH1 cells transfected with 1 µg PTCH1B, control cells were transfected with 1 µg PCI empty vector and 0.5 µg CFP as a normalisation control. Error bars represent mean ± standard deviation.

Having established that GLI1 expression is increased in NEB1-shPTCH1 cells and that the increase is mediated through reduced PTCH1 function, GLI1 activity was measured using a GLI luciferase reporter assay. Unfortunately, a useful reading was unobtainable as the NEB1 cells were resistant to the lysis buffers provided in the Promega Dual Luciferase Reporter assay kit. Attempts to manually syringe, scrape, sonicate and freeze-thaw NEB1 cells were unsuccessful and did not provide enough protein for the assay. In addition, buffers known to lyse NEB1 cells were also ineffective as they impaired luciferase activity. Therefore, as opposed to measuring luciferase enzyme activity, luciferase mRNA expression was analysed by qPCR. NEB1 cells were transfected with 1 µg of 6xGLI-BS-Firefly reporter construct with 0.5 µg of GFP as a transfection control. qPCR targeting luciferase revealed a 3-fold increase in luciferase mRNA in NEB1-shPTCH1 cells compared to the control (Figure 3.6).

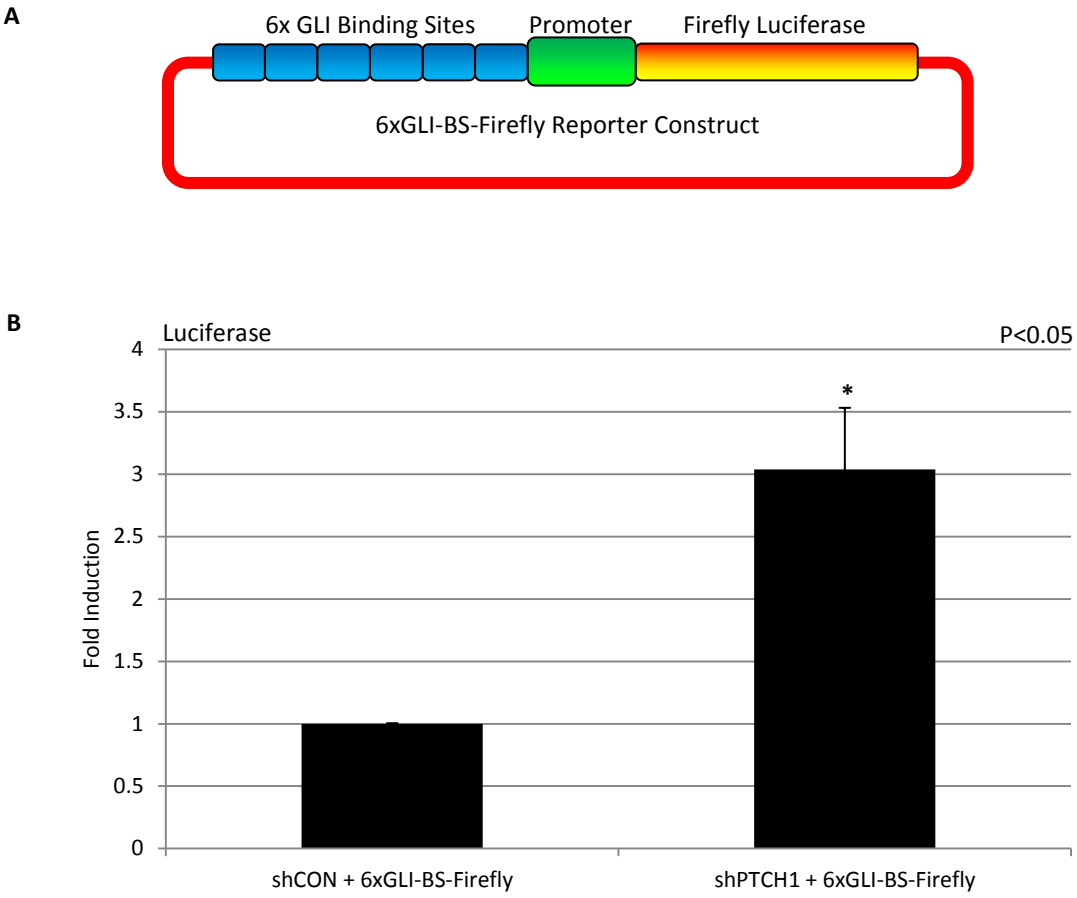

Figure 3.6: Analysis of GLI1 reporter activity

[**A**] Diagram of 6xGLI-BS-Firefly reporter construct and [**B**] qPCR for Luciferase in NEB1-shPTCH1 cells transfected with 6xGLI-BS-Firefly reporter construct. Error bars represent mean ± standard deviation, student's t-test shows a significant difference with 95% confidence (P<0.05).

3.2 Characterisation of NEB1-shPTCH1 cells

3.2.1 Characterisation of Hedgehog signalling components in NEB1-shPTCH1 cells

Having established that PTCH1 is strongly suppressed in NEB1-shPTCH1 cells, further characterisation at the protein level by immunocytochemistry confirmed a reduction of PTCH1 protein which was quantified by Image J software (Figure 3.7). The commercial (Santa Cruz) PTCH1-C20 antibody is specific to the C-terminus of the protein and this gave a distinct signal in the nucleus of NEB1-shCON cells which was reduced in NEB1-shPTCH1 cells thus helping confirm antibody specificity. PTCH1 is generally considered to be a transmembrane protein however, a recent study showed that the protein is cleaved and that the C-terminus resides in the nucleus where it can regulate GLI1 (Kagawa et al., 2011).

A

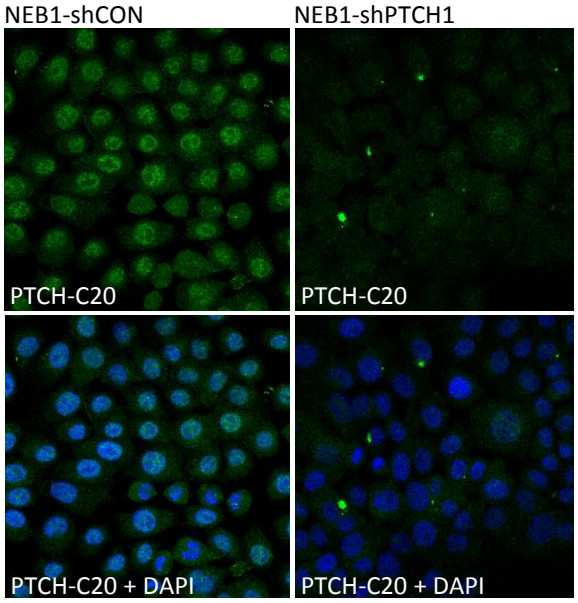

B

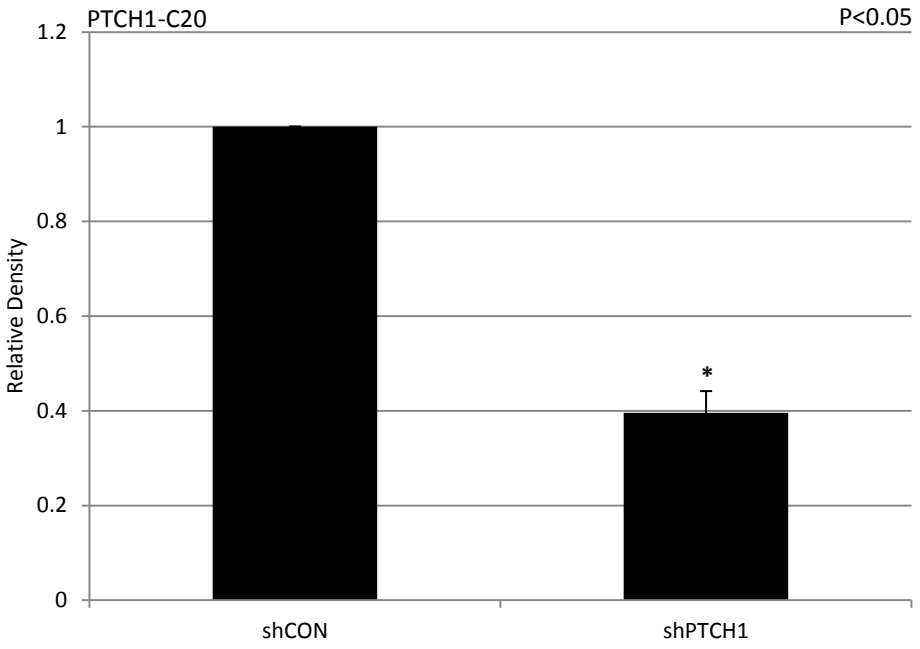

Figure 3.7: Immunofluorescent analysis of PTCH1 protein expression

[**A**] NEB1-shCON and NEB1-shPTCH1 cells stained for C-terminal PTCH1-C20. [**B**] Image J quantification for PTCH1 staining. Error bars represent mean ± standard deviation, student's t-test shows a significant difference with 95% confidence ($p<0.05$).

Consistent with the results of qPCR analysis (Figure 3.3 A), GLI1 protein was also found to be increased in NEB1-shPTCH1 cells. Two different antibodies were used with GLI1-C18 detecting cytoplasmic and nuclear protein and GLI1-H300 detecting mainly nuclear protein (Figure 3.8). The reason for this is unclear but other studies in the laboratory have shown that both antibodies detect ectopic GLI1 by Western blot analysis of keratinocyte protein lysates. Interestingly, GLI2 which positively regulates GLI1 and is thought to be required for its elevated levels in BCC (Regl et al., 2002), showed a slight decrease in mRNA levels (Figure 3.9). Suppression of PTCH1 and increased GLI1 protein expression was also confirmed in N/Tert-shPTCH1 cells (data not shown).

Other components of the HH signalling pathway were also investigated in NEB1-shPTCH1 cells. SHH was found to be decreased at the protein and mRNA level and IHH at the mRNA level (n.b. no antibody was available for IHH immunocytochemistry). SMO mRNA was also increased two fold in NEB1-shPTCH1 cells (Figure 3.10).

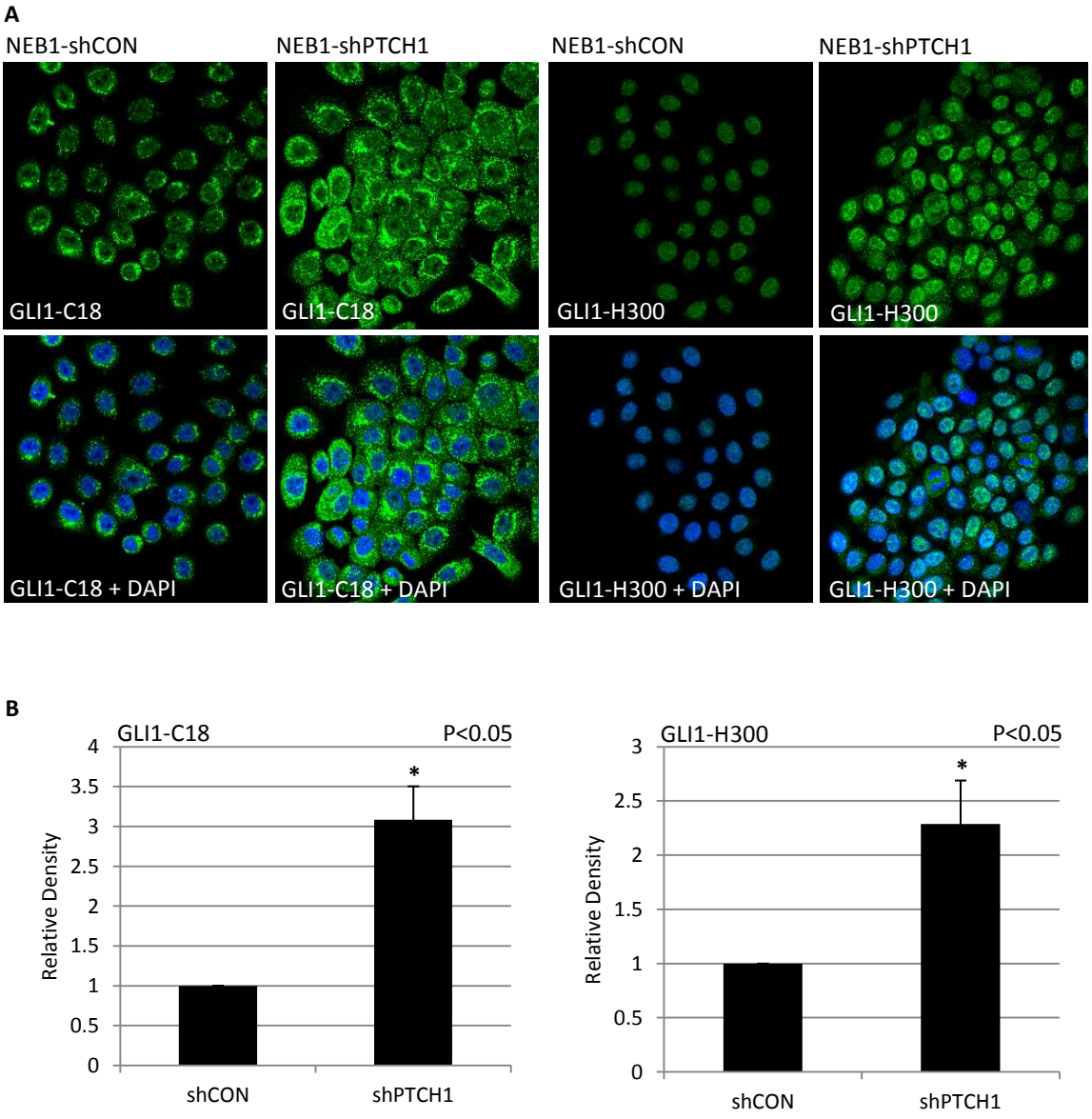

Figure 3.8: Immunofluorescent analysis of GLI1 protein expression

[**A**] NEB1-shPTCH1 cells stained for cytoplasmic GLI1-C18 and nuclear GLI1-H300. [**B**] Image J quantification for GLI1 staining. Error bars represent mean ± standard deviation, student's t-test shows a significant difference with 95% confidence (P<0.05).

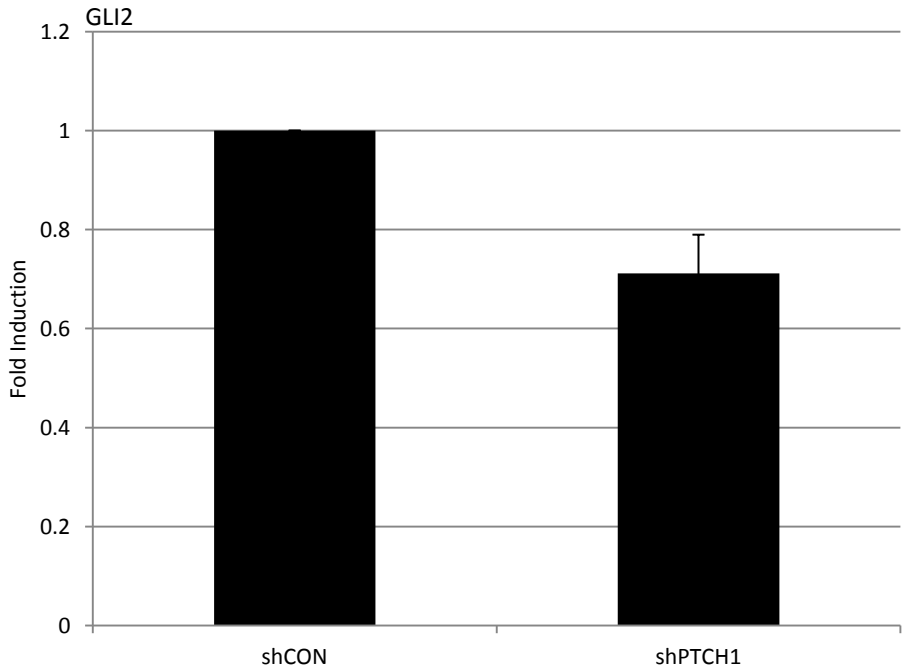

Figure 3.9: GLI2 mRNA expression in NEB1-shPTCH1 cells

Error bars represent mean ± standard deviation.

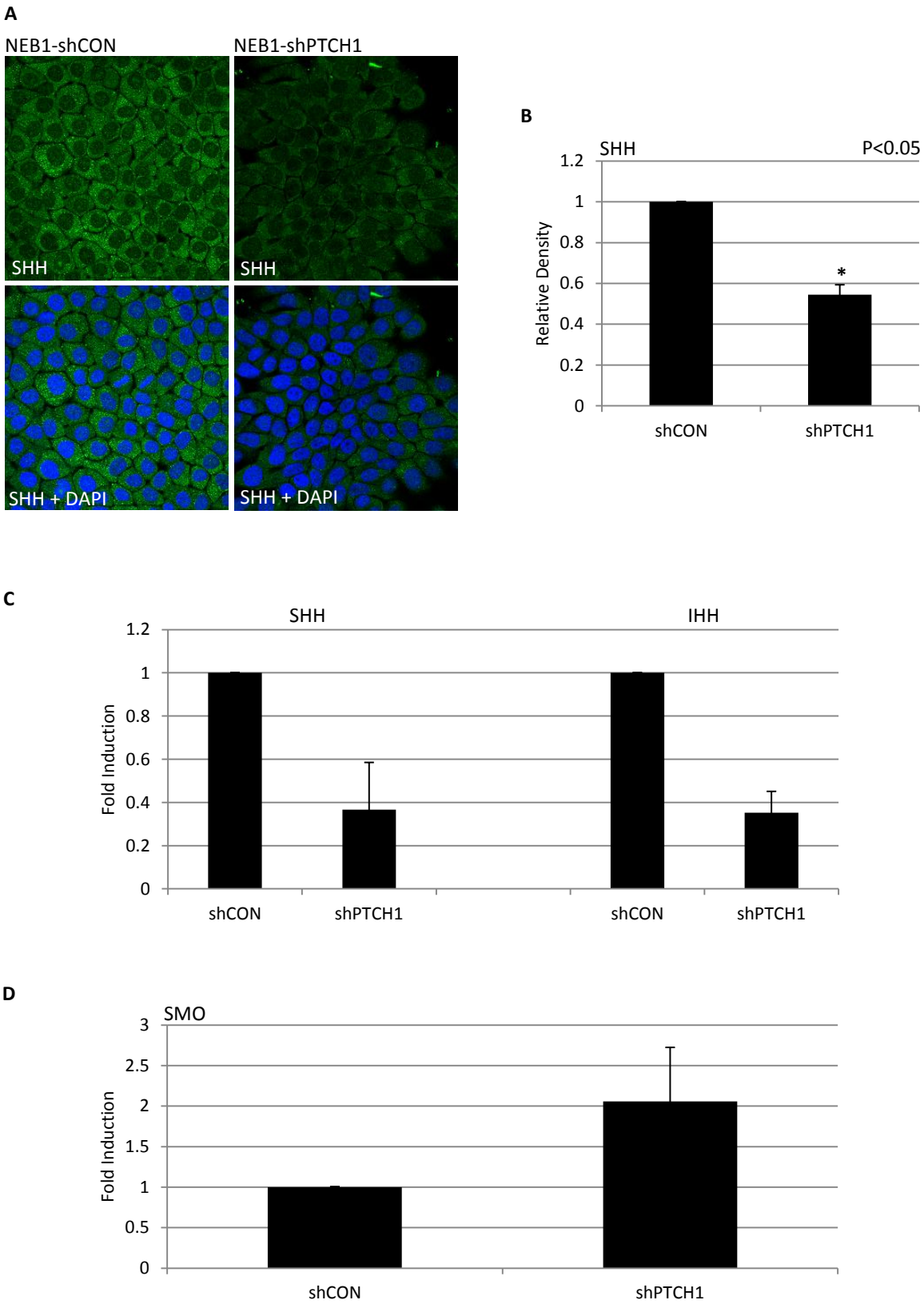

Figure 3.10: Analysis of HH signalling components in NEB1-shPTCH1 cells

[**A**] Immunofluorescent staining for SHH in NEB1 cells [**B**] quantified using Image J, student's t-test showing a significant difference with 95% confidence (P<0.05). [**C**] qPCR for SHH, IHH and [**D**] SMO. Error bars represent mean ± standard deviation.

3.2.2 Non-canonical GLI1 signalling in NEB1-shPTCH1 cells

To determine if the increase of GLI1 expression in NEB1-shPTCH1 cells is mediated through SMO (i.e. canonical HH signalling), NEB1-shPTCH1 cells were exposed to the SMO antagonist Cyclopamine-KAAD (Appendix Table 8.4). As shown by qPCR and IF, over a period of 24 hours GLI1 expression was strongly suppressed in NEB1-shCON cells whereas it was not significantly altered in NEB1-shPTCH1 cells (Figure 3.11).

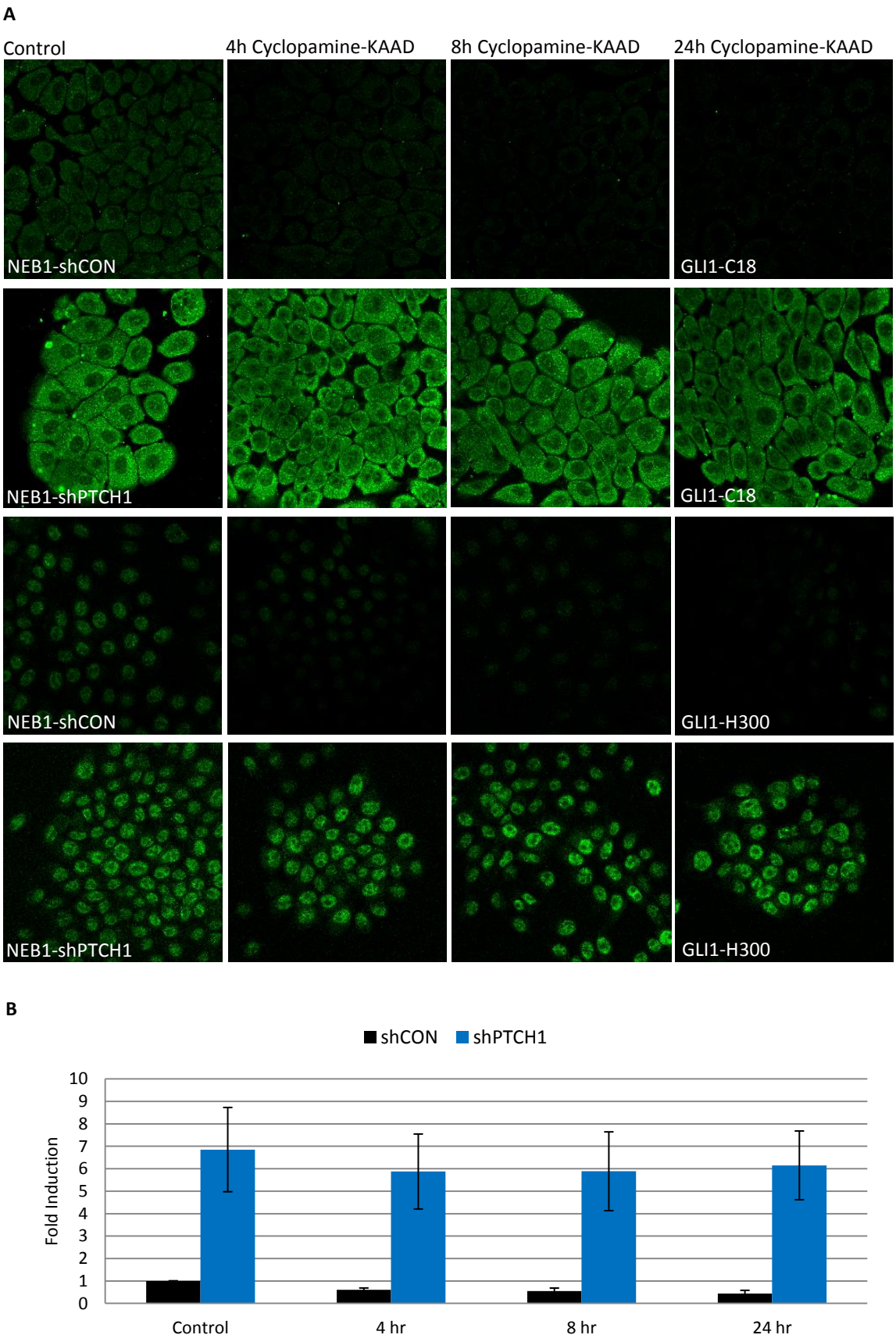

Figure 3.11: GLI1 expression is not influenced by SMO pharmacological inhibition in NEB1-shPTCH1 cells [**A**] Immunofluorescent staining for GLI1-C18 and GLI1-H300 in NEB1 cells treated with 100 nM Cyclopamine-KAAD for up to 24 hours and [**B**] qPCR for GLI1. Error bars represent mean ± standard deviation.

NEB1 cells were treated with a second SMO inhibitor SANT1 which also had no effect upon GLI1 expression in NEB1-shPTCH1 cells (Figure 3.12). Indeed, GLI1 expression remained constant after prolonged exposure to Cyclopamine-KAAD or SANT1 (96 hours) (Figure 3.13 A and B). Finally, when cells were exposed to a higher concentration of Cyclopamine-KAAD (1 μM), GLI1 expression was fully suppressed in NEB1-shCON cells but not in NEB1-shPTCH1 cells (Figure 3.13 C).

To confirm that the results presented were not specific to the NEB1-shPTCH1 clone 189A-β1, other NEB1-shPTCH1 clones were treated with Cyclopamine-KAAD and analysed for GLI1 expression. As for NEB1-shPTCH1 clone 189A-β1, the expression of GLI1 was not significantly suppressed by either drug in clone 189A-β5 (targeting the same exon, 24) or clone 29A-β1 (targeting exon 3) (Figure 3.14).

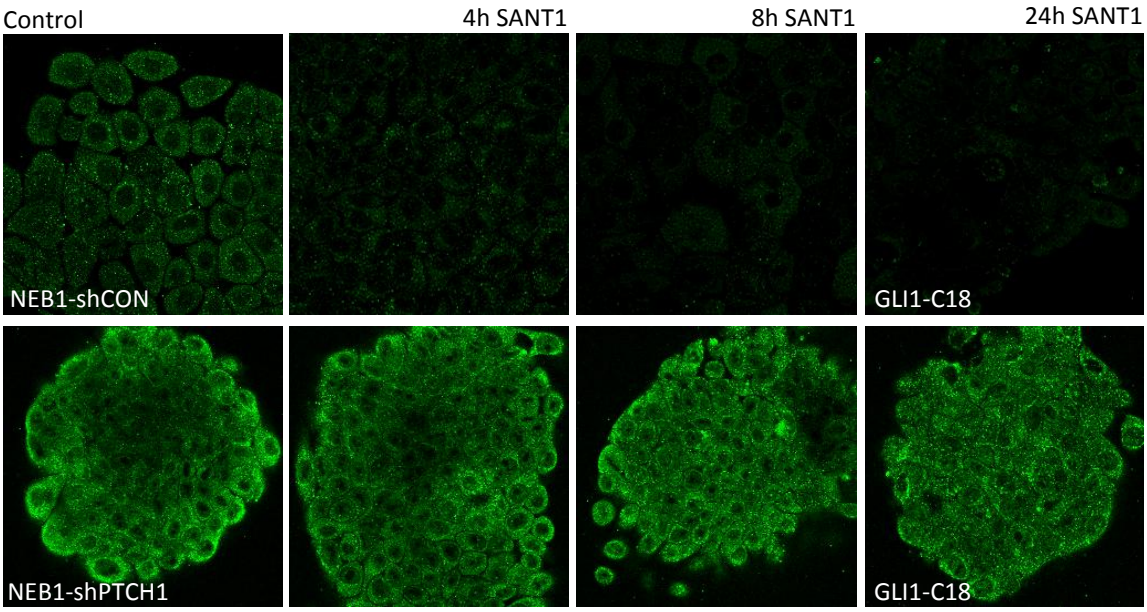

Figure 3.12: Immunofluorescent staining for GLI1 (C18) in NEB1-shPTCH1 cells treated with the SMO inhibitor SANT1 at 100 nM

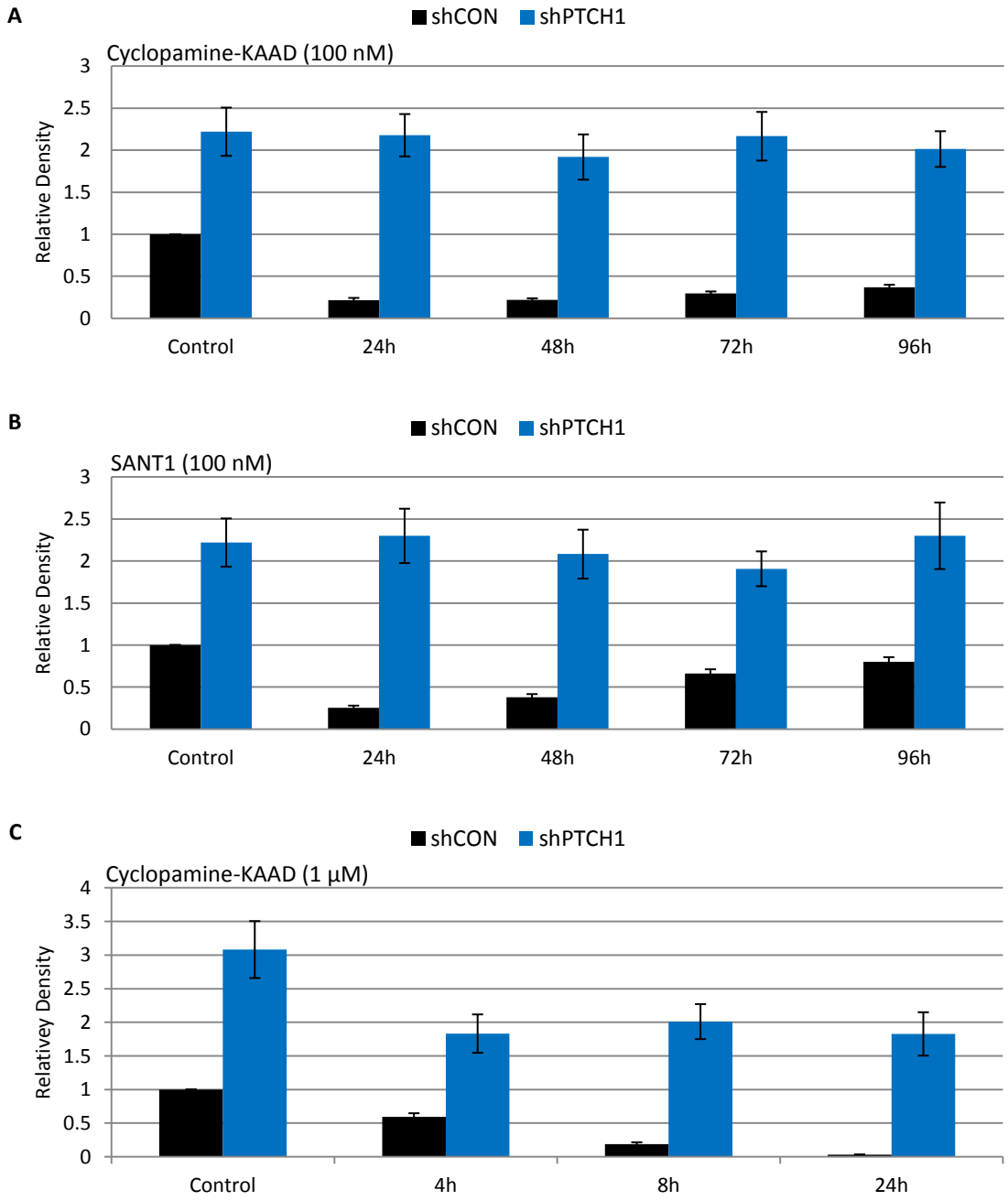

Figure 3.13: Image J analysis of GLI1-C18 staining in NEB1 cells treated with SMO inhibitors

[**A**] Quantification of GLI1-C18 staining in NEB1 cells with prolonged exposure (96 hours) to Cyclopamine-KAAD at 100 nM and [**B**] SANT1 at 100 nM. [**C**] Image J analysis of NEB1 cells treated with Cyclopamine-KAAD at 1 µM. Error bars represent mean ± standard deviation.

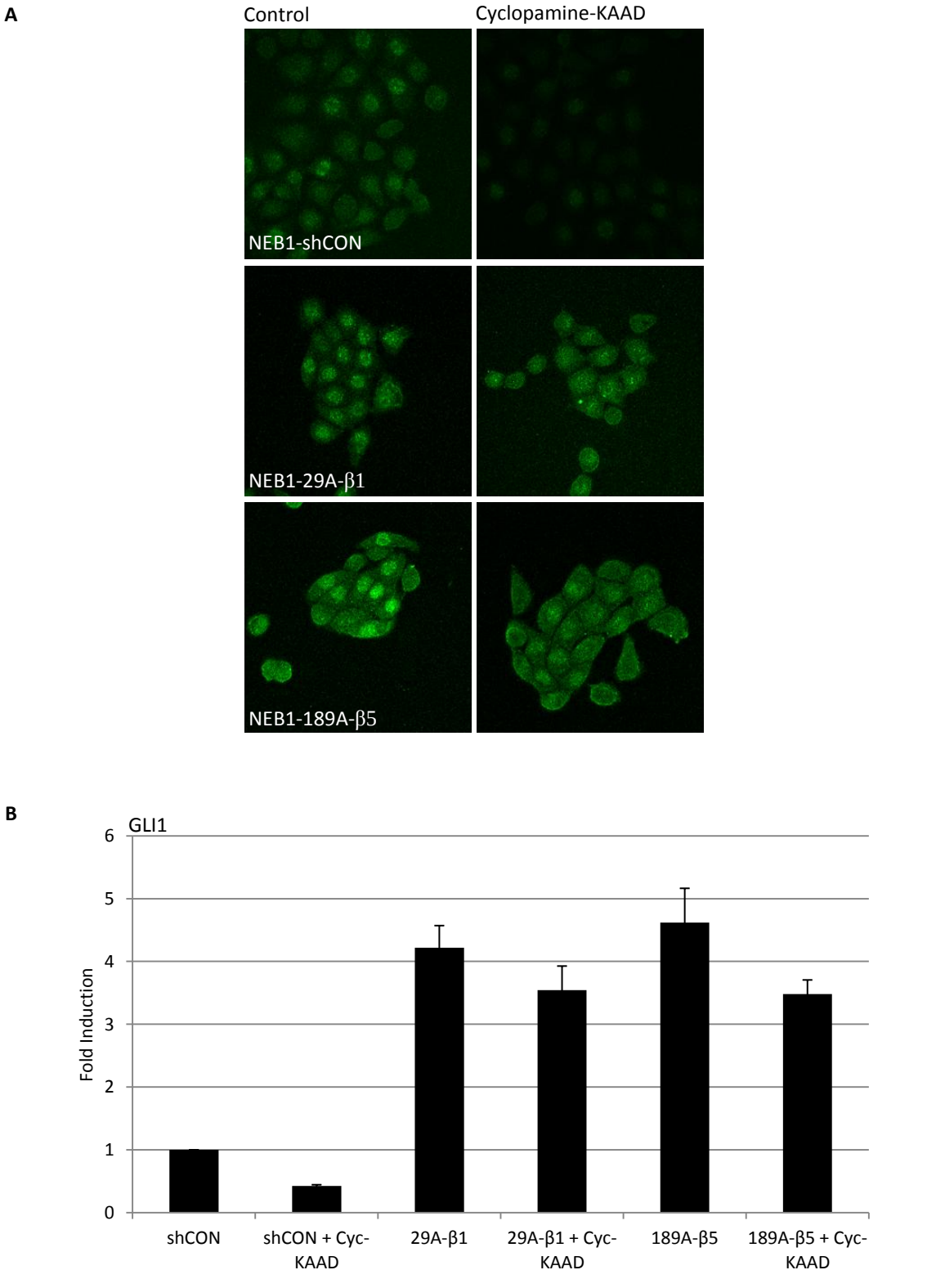

Figure 3.14: GLI1 expression is maintained in other clonal shPTCH1 cells exposed to Cyclopamine-KAAD [**A**] Immunocytochemistry for GLI1-H300 and [**B**] qPCR in NEB1 cells treated with 100 nM Cyclopamine-KAAD for 24 hours. Error bars represent mean ± standard deviation.

Subsequently, to validate the findings obtained with NEB1-shPTCH1 cells in another keratinocyte cell line, N/Tert-shPTCH1 cells were exposed to both SMO inhibitors. Again, GLI1 expression was suppressed in the control cell line (N/Tert-shCON) but remained constant in N/Tert-shPTCH1 cells (Figure 3.15).

In summary, all keratinocyte shPTCH1 cell lines that were treated with the SMO inhibitors retained a higher GLI1 expression level (compared to shCON cells) which suggests that PTCH1 regulates GLI1 via a SMO-independent mechanism.

NEB1 cells exposed to SMO inhibitors were analysed for GLI2 mRNA levels which were lower in NEB1-shPTCH1 cells compared to NEB1-shCON. GLI2 mRNA expression in both cell lines were suppressed by Cyclopamine-KAAD which suggests that GLI2 signalling occurs via canonical HH signalling (Figure 3.16).

Taken together, these data suggest that there is a canonical SMO-GLI1/GLI2 signalling axis in shCON cells and a canonical SMO-GLI2 signalling axis in shPTCH1 cells, but they also indicate the presence of a non-canonical PTCH1-GLI1 signalling axis that is independent of SMO activity in shPTCH1 cells (Figure 3.17).

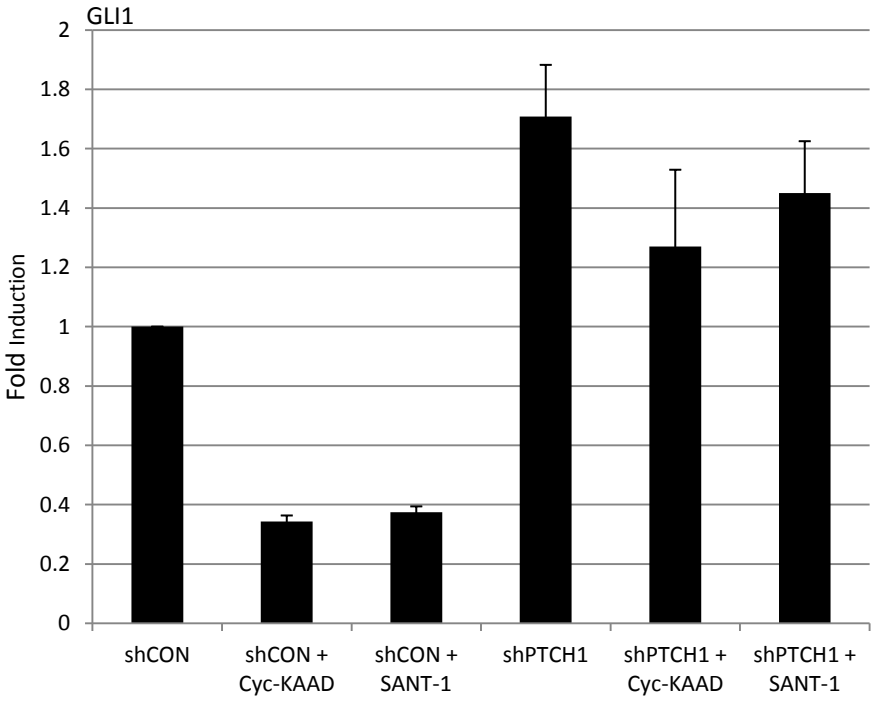

Figure 3.15: N/Tert-shPTCH1 cells treated with SMO inhibitors

qPCR for GLI1 in N/Tert cells treated with 100 nM Cyclopamine-KAAD and SANT1 for 24 hours. Error bars represent mean ± standard deviation.

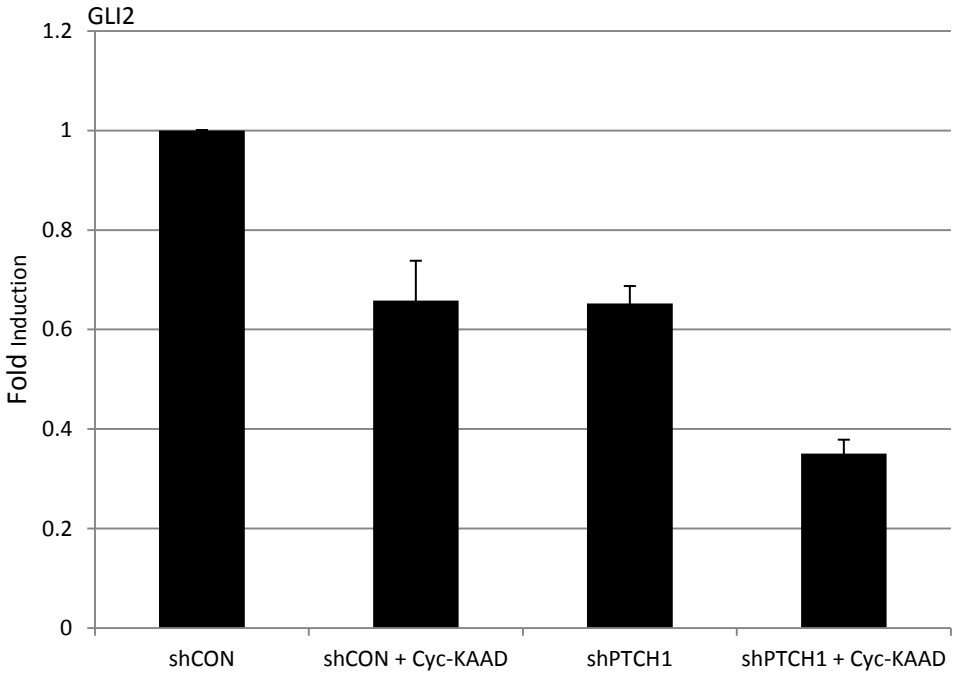

Figure 3.16: GLI2 mRNA expression in NEB1-shPTCH1 cells treated with SMO inhibitors

Error bars represent mean ± standard deviation.

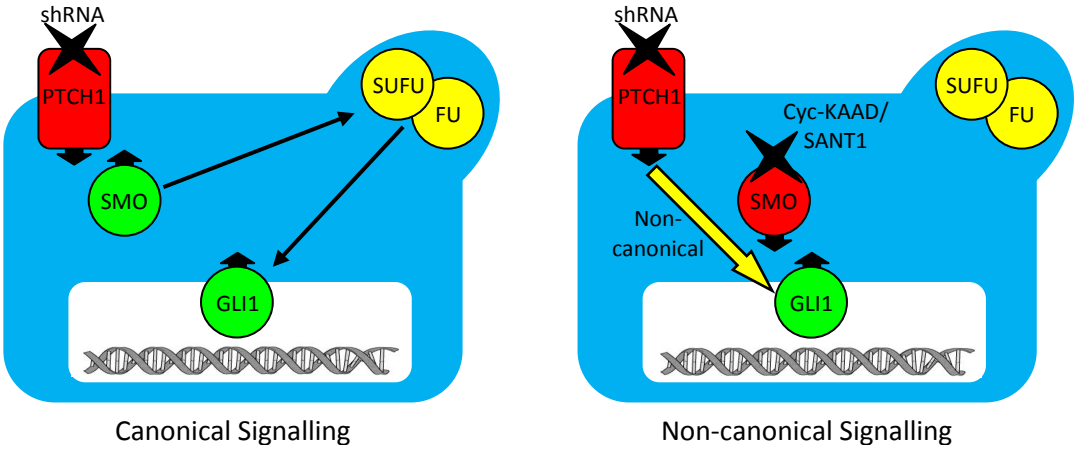

Figure 3.17: Schematic diagram depicting a novel non-canonical PTCH1-GLI signalling pathway in shPTCH1 cells (right panel)

3.3 The role of SMO in NEB1-shPTCH1 cells

3.3.1 Analysis of SMO siRNA treatment upon GLI1 expression in NEB1-shPTCH1 cells

As noted above, *SMO* mRNA was increased in NEB1-shPTCH1 cells (Figure 3.10 D) and this correlates with the fact that *SMO* mRNA levels are known to be elevated in BCC (Xie et al., 1998). SMO protein levels were shown to be increased in NEB1-shPTCH1 cells by immunofluorescent labelling (Figure 3.18). In addition, SMO was observed to be distinctly more nuclear with two commercial antibodies (Santa Cruz N19 and C17) although whether this reflects an increase of protein levels and/or increase of nuclear localisation is unclear. In addition, a third commercial antibody (Abcam ab72130) gave a stronger nuclear/peri-nuclear signal in NEB1-shPTCH1 cells.

To determine if the increase of GLI1 expression is fully independent of SMO, siRNA targeting was employed to suppress SMO mRNA in NEB1-shPTCH1 cells. A decrease of SMO mRNA and protein levels was confirmed by qPCR and immunocytochemistry respectively (Figures 3.19 and 3.20). With regards to GLI1, both mRNA and protein levels were suppressed upon SMO knockdown which indicates that, although GLI1 levels are unresponsive to SMO inhibitors in NEB1-shPTCH1 cells, they are not fully independent of SMO protein function (Figures 3.19).

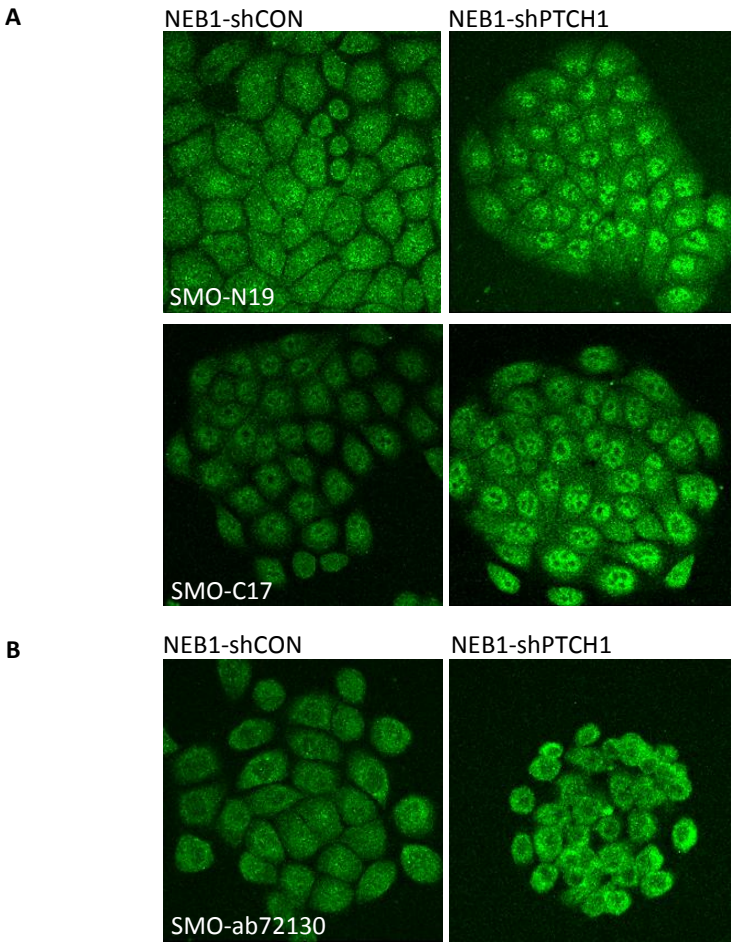

Figure 3.18: SMO expression in NEB1 cells

[**A**] Immunofluorescence staining with SMO (N19, C17) reveals increased nuclear localisation in NEB1-shPTCH1 cells and [**B**] peri-nuclear staining with SMO-ab72130.

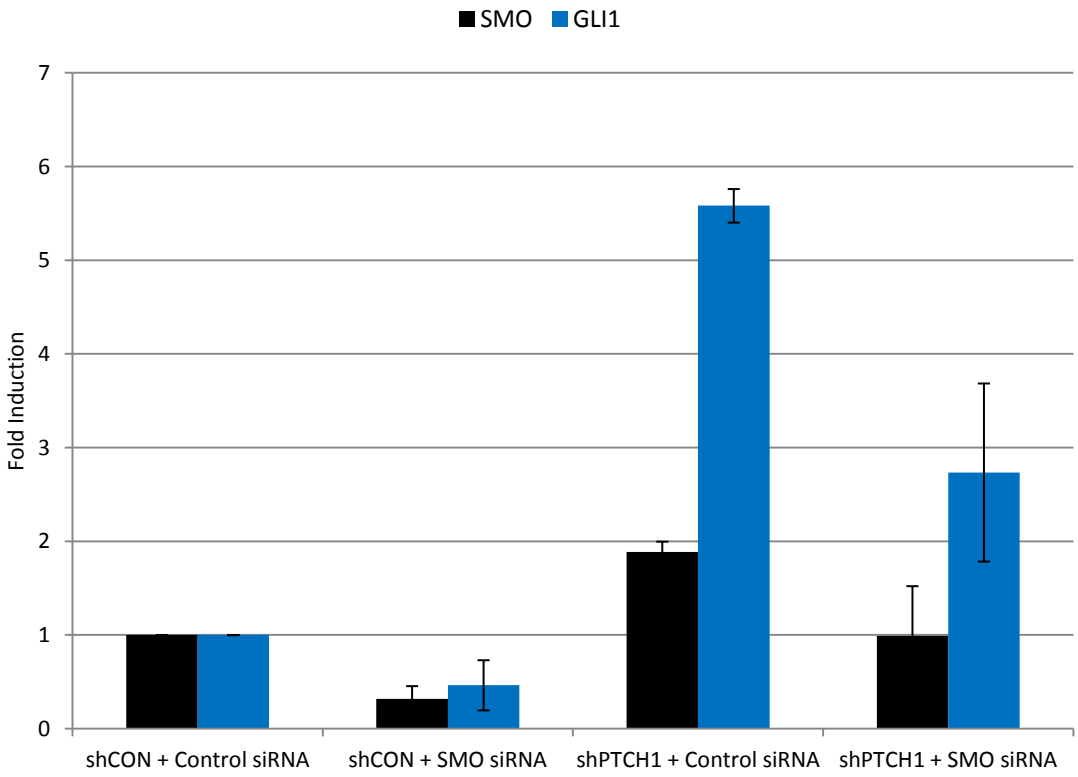

Figure 3.19: SMO and GLI1 mRNA expression in NEB1 cells treated with SMO siRNA

Error bars represent mean ± standard deviation.

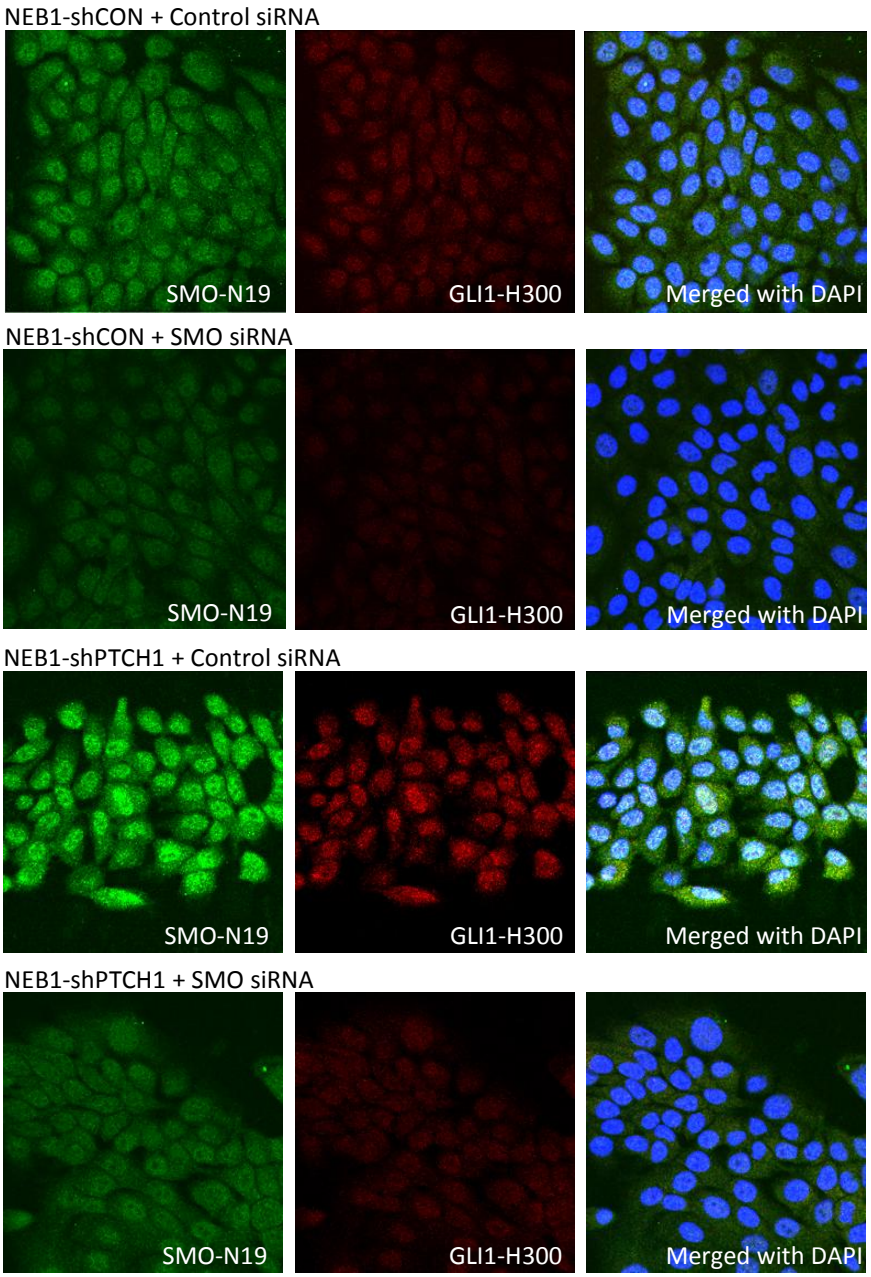

Figure 3.20: SMO and GLI1 protein expression in NEB1 cells treated with SMO siRNA

3.3.2 Analysis of EGFP-SMO-WT/M2 in NEB1 cells

One reason for the lack of response to anti-SMO inhibitors in shPTCH1 cells may be that upon PTCH1 suppression, SMO translocates to the nucleus/peri-nucleus region where Cyclopamine-KAAD and SANT1 are unable to inhibit SMO effectively. To investigate the subcellular localisation of SMO and its potential effect upon GLI1 expression, EGFP-SMO-WT (wild type) and EGFP-SMO-M2 (constitutively active mutant) fusion constructs were created for expression in NEB1-shCON and NEB1-shPTCH1 cells. I was unable to PCR amplify the predicted full length SMO coding sequence from NEB1 or N/Tert keratinocytes so the SMO-WT/M2 coding sequences were sub-cloned from vectors obtained from the de Sauvage laboratory (Genentech, CA, USA). It was discovered that these constructs lack the N-terminal signal peptide (residues 1-31) that would be predicted to target the protein to its correct subcellular localisation; however, the plasmids were previously used to show that even without the N-terminus SMO-M2 is oncogenic in soft agar assays and that it activates GLI1 in rat embryonic fibroblast REF52 cells (Xie et al., 1998).

To confirm that the plasmids were functional, HEK293 cells were initially transfected with the EGFP-SMO-WT/M2 constructs and protein lysates were analysed by Western blot. A band of the correct size was present in both samples (Figure 3.21 B) and it was noted that the EGFP-SMO-M2 band was considerably stronger than EGFP-SMO which may account for its enhanced tumourigenic potential.

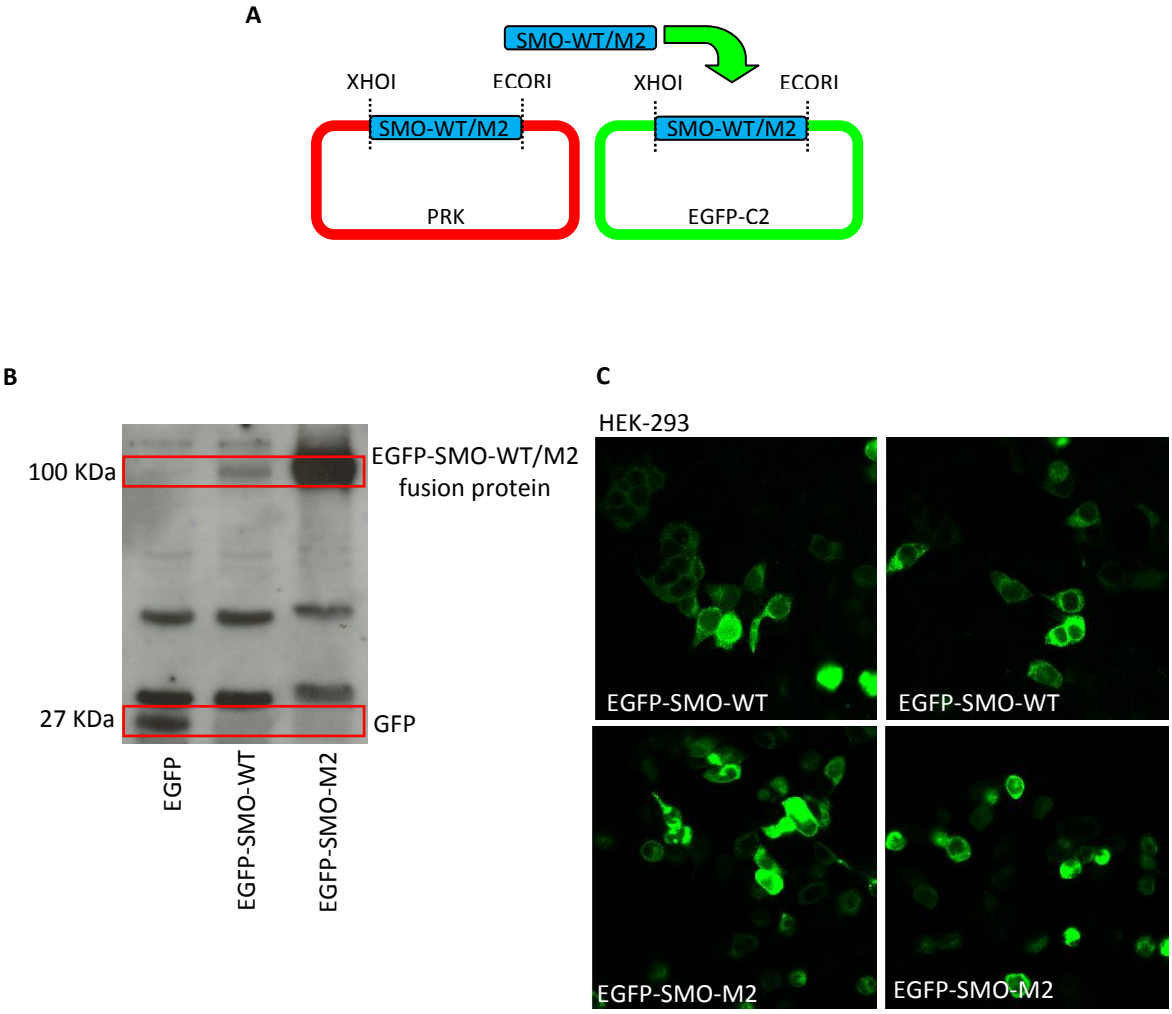

Figure 3.21: EGFP-SMO-WT/M2 expression in HEK-293 cells

(**A**) EGFP-SMO-WT and EGFP-SMO-M2 fusion proteins were generated by excising SMO from PRK-SMO and then ligating into pEGFP-C2, (**B**) validated by PCR for SMO and GFP. (**C**) Western blot for GFP in HEK-293 cells transfected with EGFP-SMO-WT and EGFP-SMO-M2. (**D**) HEK-293 cells transfected with EGFP-SMO-WT and EGFP-SMO-M2.

Subsequently, NEB1-shCON and NEB1-shPTCH1 cells were transfected the EGFP-SMO-WT/M2 constructs: keratinocytes are difficult to transfect but using a reverse transfection method that I adapted from siRNA protocols, the transfection efficiency was increased to approximately 20% of cells.

Confocal microscopy revealed that EGFP-SMO-WT was predominantly cytoplasmic in both NEB1-shCON and NEB1-shPTCH1 cells: small areas of nuclear fluorescence were observed in NEB1-shPTCH1 cells (Figure 3.22) but these did not correlate with the uniform nuclear localisation of endogenous SMO observed by immunocytochemistry (Figure 3.18 A). Peri-nuclear fluorescence was observed in NEB1-shCON and NEB1-shPTCH1 cells which correlated with the staining pattern using the anti-SMO Abcam antibody (Figure 3.18 B). The pattern of EGFP-SMO-M2 expression was similar to that of EGFP-SMO-WT in both NEB1-shCON and NEB1-shPTCH1 cells (Figure 3.23).

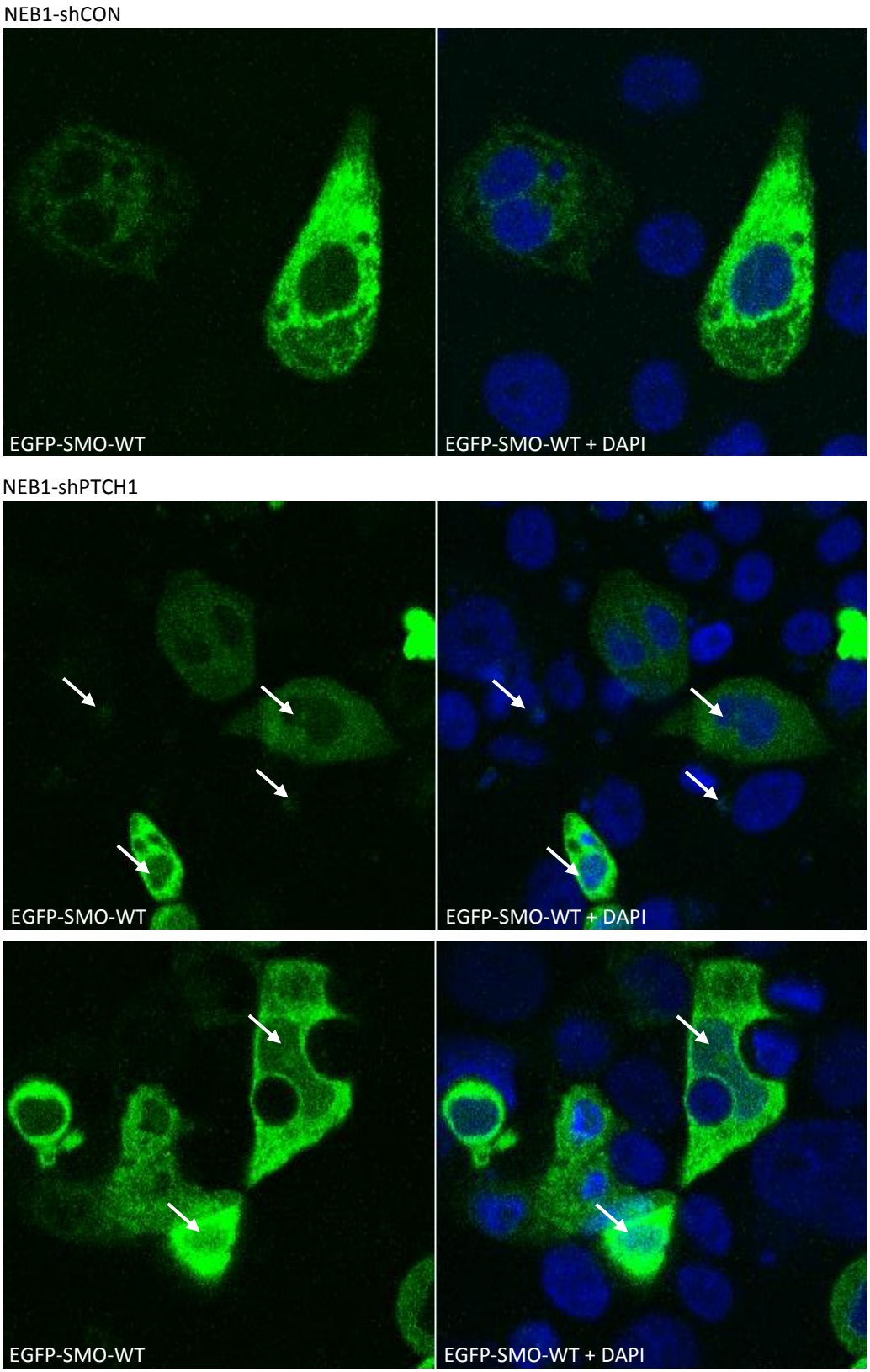

Figure 3.22: NEB1 cells transfected with EGFP-SMO-WT

White arrows show nuclear localised EGFP-SMO in NEB1-shPTCH1 cells.

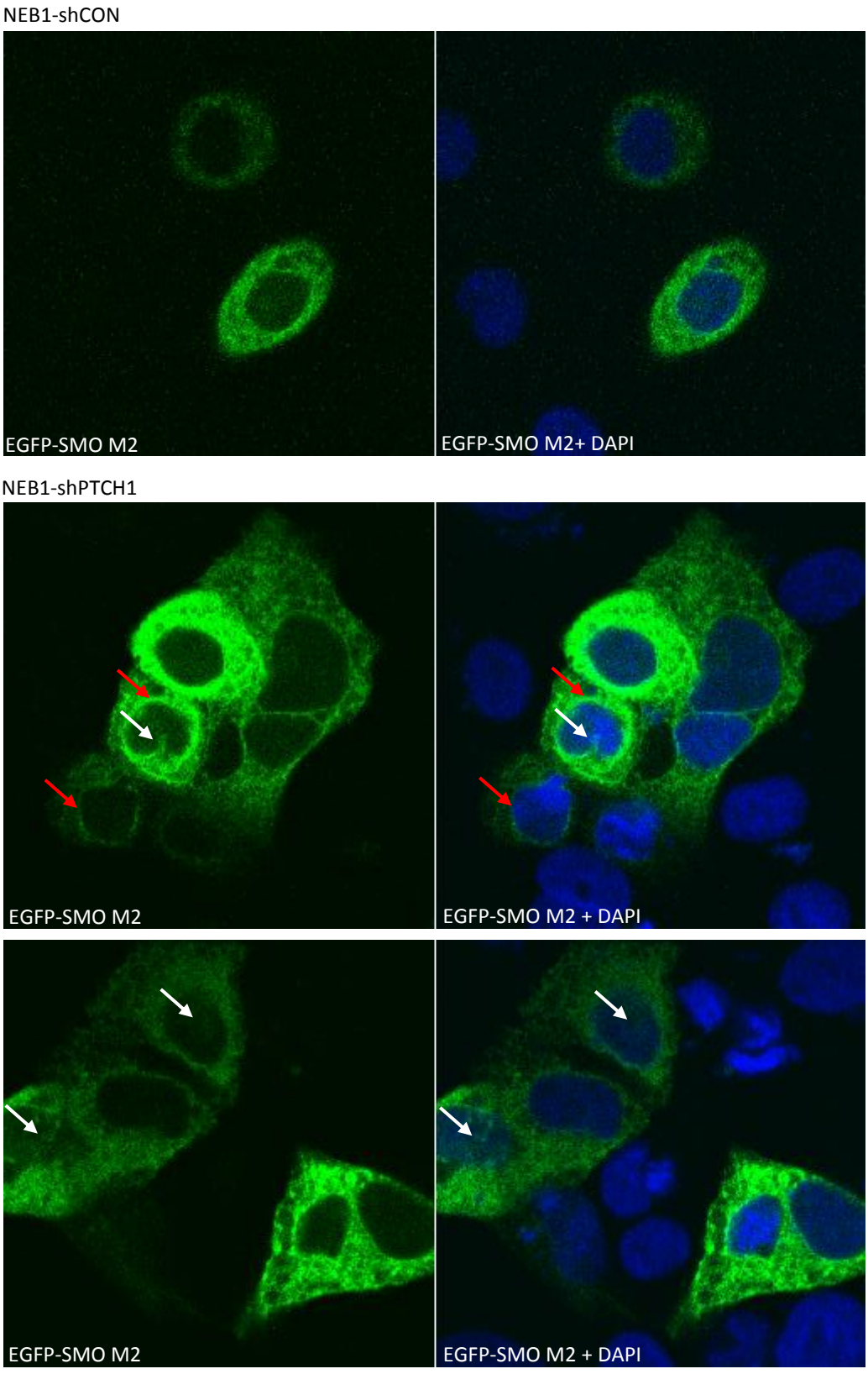

Figure 3.23: NEB1 cells transfected with EGFP-SMO-M2

White arrows show nuclear localised EGFP-SMO-M2 in NEB1-shPTCH1 cells and red arrows highlight peri-nuclear expression.

3.3.3 EGFP-SMO-WT/M2 activates GLI1 in NEB1 cells

Although a distinct increase of nuclear EGFP-SMO-WT/M2 was not observed in NEB1-shPTCH1 cells, I sought to determine if either construct is capable of activating GLI1 expression and if this is increased upon PTCH1 suppression. A modest but reproducible increase of GLI1 was observed in both NEB1-shCON and NEB1-shPTCH1 cells with EGFP-SMO-WT and a more potent increase was observed with EGFP-SMO-M2 (Figure 3.24). Surprisingly, the fold-increase of GLI1 was higher for EGFP-SMO-M2 in NEB1-shCON cells (~10 fold) compared to NEB1-shPTCH1 cells (~4 fold) despite comparable transfection efficiencies as determined by co-transfection with a CFP vector.

In summary, these data demonstrate that EGFP-SMO (WT and M2) induces GLI1 expression but they do not support the notion that the increase of GLI1 observed in NEB1-shPTCH1 cells is mediated by an increase of nuclear SMO.

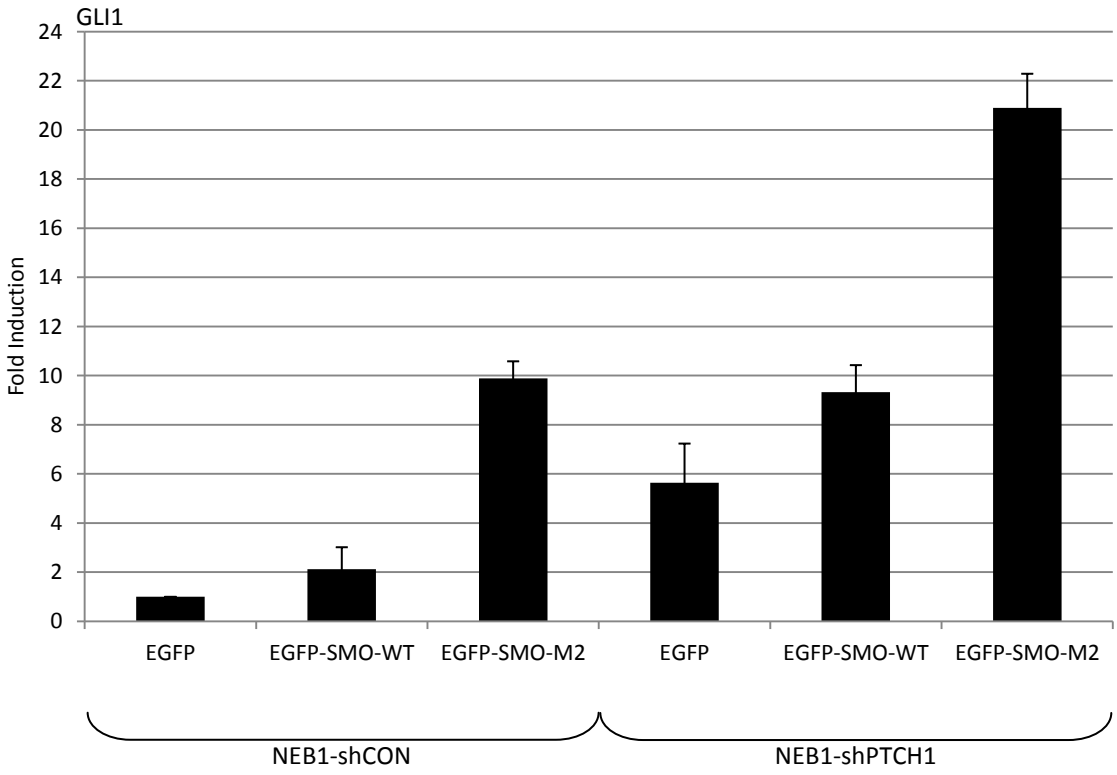

Figure 3.24: GLI1 mRNA expression in NEB1 cells transfected with EGFP-SMO-WT/M2

Error bars represent mean ± standard deviation.

3.4 Functional studies of NEB1-shPTCH1 cells

As well as investigating the HH signalling pathway, the *in vitro* BCC model was established to investigate specifically the effects of PTCH1 suppression upon certain aspects of keratinocyte biology including proliferation, invasion and anchorage-independent growth.

With regards to proliferation rate, there was a slight but consistent decrease in NEB1-shPTCH1 cells (29A and 189A) compared to the control (Figure 3.25). The Alamar blue proliferation assay measures redox reactions that occur in the mitochondria therefore, the assay better represents cell viability rather than proliferation. A more appropriate experiment would have been to measure the population doublings of the cells.

Despite a lower proliferation rate as seen by the Alamar blue assay, NEB1-shPTCH1 cells were hyper-proliferative when seeded onto a Matrigel based organotypic culture system although there was no evidence of invasion into the artificial dermis characteristic of superficial BCC or compact colony formation characteristic of nodular BCC (Figure 3.26). The organotypic culture is an artificial model of the dermis mimicking the skin allowing for the culture of keratinocytes under these conditions.

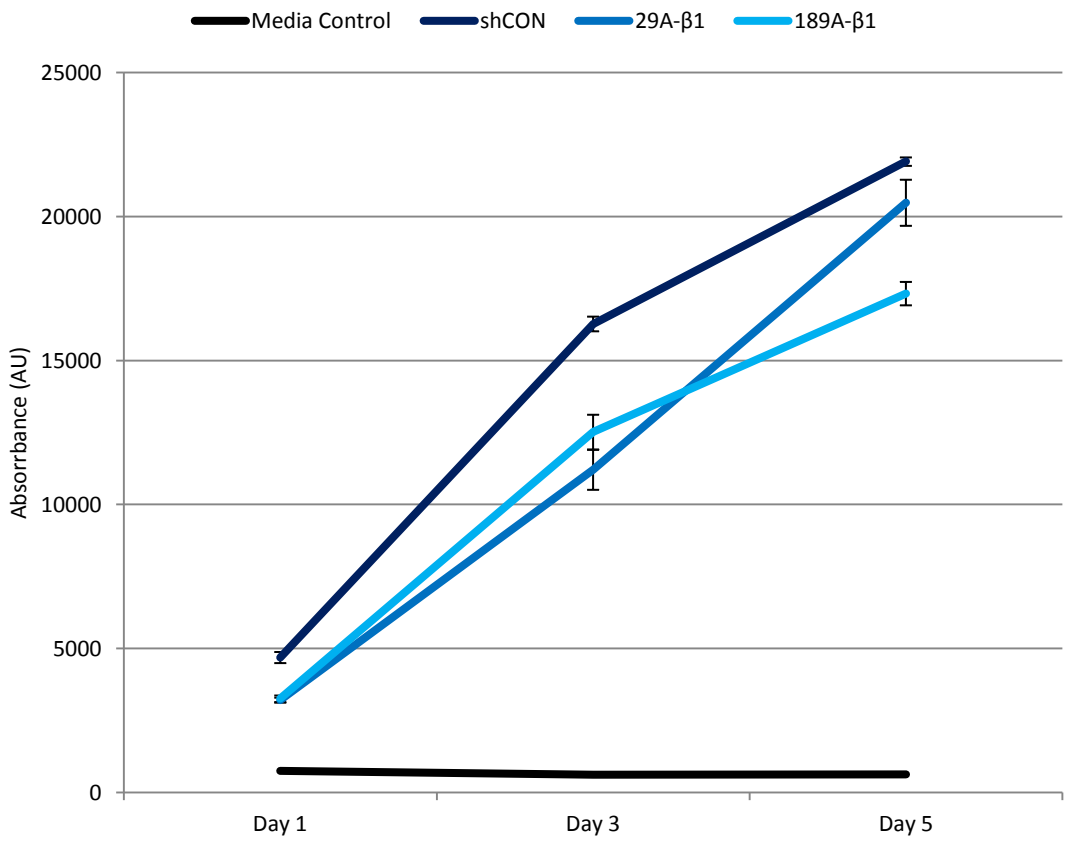

Figure 3.25: Alamar blue proliferation assay of NEB1 cells

Error bars represent mean ± standard deviation.

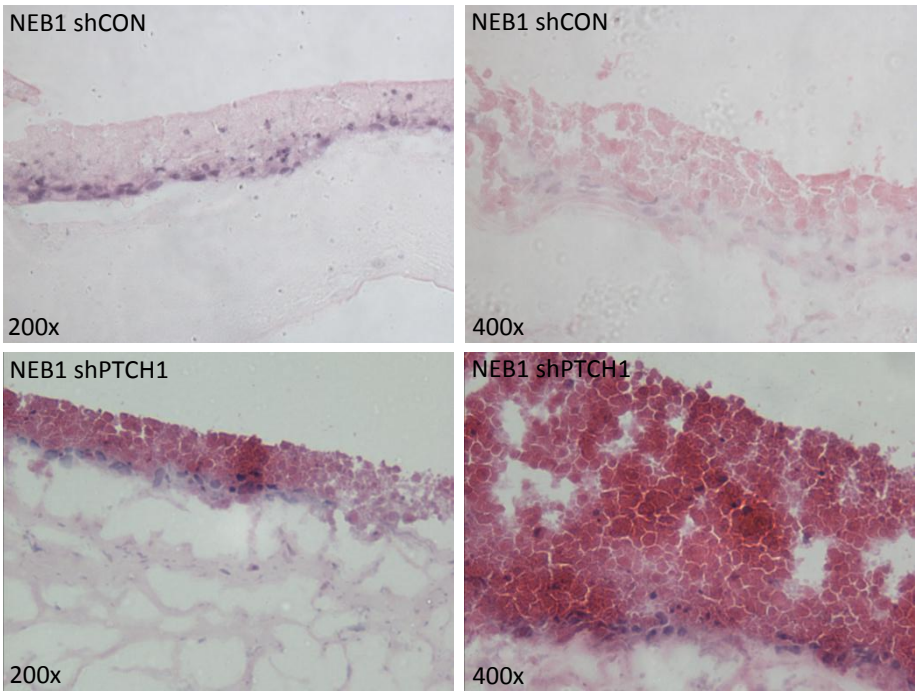

Figure 3.26: Organotypic skin model of NEB1 cells

3.5 Discussion

This project has adopted a novel approach to investigating the role of *PTCH1* in BCC biology by using RNAi to suppress the PTCH1 gene product in human keratinocytes. Modelling BCC by suppressing PTCH1 function is superior to ectopically expressing GLI1 because this is a better representation of the *in vivo* situation i.e. *PTCH1* mutations have been found in numerous tumours whereas the increase of GLI1 in BCCs is less convincing. Indeed, one of the initial studies from our department showed that GLI1 was expressed at higher levels in the ORS of the hair follicle compared to the adjacent nodular tumour islands (Ghali et al., 1999). In addition, because of the feedback loop ectopic GLI1 leads to strong increase of endogenous PTCH1 levels with a subsequent increase of wild-type protein function as a cellular response to try and limit HH signalling.

Clonal cell lines were derived from heterogenous populations and some of these cultured as more compact colonies than parental or control cells; this is a characteristic of nodular tumour islands and helped validate the clonal lines as a viable model of human BCC. In addition, the clonal lines proliferated slowly and BCCs are characterised by their slow growth. It has previously been shown that the retroviral transduction of N/Tert cells with an EGFP-GLI1 fusion protein promotes tight colony formation (Neill et al., 2008). This suggests that the increase of GLI1 in shPTCH1 cells could cause this phenotypic change; however the level of GLI1 protein resulting from ectopic expression is considerably higher than that induced upon PTCH1 suppression and it is possible that additional factors regulate compact colony formation. This is supported by the fact that some clonal lines did not display an increase of GLI1 but were more compact than control shCON cells. Indeed, recent research in our laboratory (Dr Neill and Professor Philpott, unpublished data) has shown by immunohistochemistry that despite their similar histology, the expression of GLI1 varies considerably between nodular tumours from different patients which further supports the idea that GLI1-independent factors contribute to the compact phenotype as well as to tumour formation itself. However, the clonal cell lines NEB1-29A-β1 and NEB1-189A-β1 also displayed increased levels of GLI1. The induction of GLI1 via PTCH1 suppression was confirmed by the fact that the increase of endogenous GLI1 was suppressed upon ectopic expression of the PTCH1B isoform which is not targeted by the PTCH1 shRNA construct (Figure 3.5).

Investigation of PTCH1 protein using an antibody that is specific for the C-terminal (PTCH1-C20) in NEB1 cells revealed nuclear expression of PTCH1 in NEB1-shCON cells and a reduction in NEB1-shPTCH1 cells (Figure 3.7). This has been reported previously along with N-terminal

PTCH1 expressed in the cytoplasm (Kagawa et al., 2011). PTCH1 is known to be a transmembrane protein that is localised to the cell membrane therefore its presence in the nucleus is surprising. It is unclear whether the full PTCH1 protein also resides in the nucleus or if this is a product of cleavage. This may be linked to SMO which was also found in the nucleus of NEB1-shPTCH1 cells (Figure 3.18). With PTCH1, SMO and GLI1 found in the nucleus, HH signalling may occur in the nucleus rather than at the cell membrane or in cilia. There is no mention in the literature of SMO being localised in the nucleus however, C-terminal PTCH1 has been shown to enter the nucleus and PTCH1 staining of Sertoli cells (cells that sustain the testis) revealed nuclear localisation (Kagawa et al., 2011; Kogerman et al., 2002). One study has also shown that PTCH1 is localised in the nucleus of sporadic nodular BCCs which suggests a role for PTCH1 signalling directly to SMO or GLI1 in the nucleus (Unden et al., 1997).

This study has led to the discovery of a potentially novel mode of GLI1 signalling. Pharmacological inhibition of SMO in NEB1-shPTCH1 and N/Tert-shPTCH1 cells failed to reduce GLI1 expression compared to shCON cells where both GLI1 protein and mRNA levels were strongly reduced (Figures 3.11, 3.12 and 3.15). This shows that signalling of GLI1 in shCON cells is mediated through a canonical HH pathway whereby SMO activates GLI1. In NEB1-shPTCH1 and N/Tert-shPTCH1 cells, inhibition of SMO did not suppress GLI1 expression which was also observed with different NEB1-shPTCH1 clones (Figures 3.14 and 3.15).

The formation of BCC is thought to be dependent upon increased GLI1 expression and as such, novel compounds targeting SMO are being used in the clinic. The fact that GLI1 expression is not suppressed upon exposure to SMO pharmacological inhibitors in NEB1-shPTCH1 and N/Tert-shPTCH1 cells is interesting and it is worth noting that no studies have convincingly shown that GLI1 expression is actually reduced in BCCs using clinical compounds such as GDC-0449. Various SMO inhibitors have been described including GDC-0449 however, many patients do not respond to these treatments and the levels of GLI1 have not been reported in non-responding tumours (Van Hoff et al., 2009). Indeed, having demonstrated that GLI1 is not suppressed by Cyclopamine-KAAD or SANT1 in shPTCH1 cells, the effects of anti-SMO inhibitors upon GLI1 expression in BCCs requires further evaluation.

This mode of non-canonical GLI1 signalling may occur through other pathways such as TGF-β which has been shown to induce GLI1 and GLI2 expression in keratinocytes. It has also been reported that GLI2 is a direct transcriptional target of the SMAD pathway downstream of TGF-β. TGF-β is able to induce GLI1 expression in a GLI2-dependent mode which could not be suppressed by Cyclopamine (Dennler et al., 2007). Also, pharmacological inhibition of TGF-β

has also been shown to suppress GLI2 expression in cancer cells that are resistant to Cyclopamine (Dennler et al., 2009).

The finding that GLI1 expression is not reduced in NEB1-shPTCH1 cells upon treatment with SMO inhibitors suggests that GLI1 signalling is independent of SMO however siRNA inhibition of SMO reveals that GLI1 expression is in fact repressed (Figures 3.19 and 3.20). The mode of signalling may in fact be a novel form of canonical signalling whereby the suppression of PTCH1 allows SMO to activate GLI1 in a different way i.e. without cilia or directly at the nucleus. It is worth noting that GLI2 expression was not increased in NEB1-shPTCH1 cells compared to NEB1-shCON cells therefore, TGF-β expression in these cells requires characterisation.

If TGF-β and downstream SMAD components are over-expressed in NEB1-shPTCH1, this still does not explain why GLI2 expression is not increased in these cells. The findings that GLI1 can be over-expressed in NEB1-shPTCH1 cells and not induce GLI2 expression suggests that GLI1 and GLI2 can signal independently of each other. TGF-β activation has been shown to be required for SMO-mediated BCC development (Fan et al., 2010) however, the finding that TGF-β inhibition suppresses GLI2 in Cyclopamine resistant cancer cells (Dennler et al., 2009) suggests that TGF-β may be driving the non-canonical HH pathway seen in NEB1-shPTCH1 cells.

The idea that HH signalling can occur non-canonically has been explored and is not entirely a new concept. GLI1 was over expressed in NIH-3T3 cells and the increase of activity was confirmed with a GLI1 reporter construct. Treatment of the cells with Cyclopamine did not repress GLI1 reporter activity which only returned to basal levels when the cells were transfected with PTCH (3:1 ratio of PTCH:GLI1) (Rahnama et al., 2006). This shows that GLI1 is controlled by PTCH but signals independently of SMO. Also, if the HH pathway was linear i.e. PTCH1 signals through to GLI1 without the influence of any other pathway, a lower amount of PTCH would need to be transfected into NIH-3T3 cells to suppress GLI1. Since three times the amount of PTCH to GLI1 is required, GLI1 may be expressed thorough other non-conventional modes.

As NEB1 cells display nuclear expression of PTCH1, SMO and GLI1 then potentially, if SMO signals to GLI1 in the nucleus this may explain why pharmacological SMO inhibitors did not reduce GLI1 levels in NEB1-shPTCH1 cells. SMO could potentially enter the nucleus to activate GLI1 in a mode where SMO can function despite the presence of a SMO inhibitor. Analysis of the SMO protein sequence reveals a bipartite N-terminal nuclear localisation sequence (NLS)

which provides evidence that SMO has the capacity to localise to the nucleus (Appendix Figure 8.1).

EGFP-SMO-WT/M2 clones were generated to determine if SMO is present in the nucleus however, the PRK-SMO sequence that was used to make the clone lacks the signal peptide which may affect the localisation of the protein. Transfection of NEB1-shCON cells with EGFP-SMO-WT shows cytoplasmic expression of the protein while in NEB1-shPTCH1 cells there is some evidence of nuclear localisation as well as nuclear material positive for EGFP-SMO-WT (Figure 3.21). Expression of EGFP-SMO-M2 in NEB1-shPTCH1 cells also shows some nuclear localisation however, a peri-nuclear pattern is more evident (Figure 3.22).

It is still unclear whether SMO localises and functions within the nucleus and this may be due to limited transfection efficiency and perhaps, EGFP-SMO-WT/M2 should be stably expressed in NEB1 cells to better determine the localisation. A problem with the reverse transfection method is that NEB1-shPTCH1 cells are not given the time to settle and form tight colonies. This may affect the expression of GLI1 and also the treatment of cells with the transfection reagent did alter the behaviour of the cells. Over expression of EGFP-SMO-WT/M2 in NEB1 cells induced GLI1 mRNA and protein levels although there was a significantly greater induction caused by EGFP-SMO-M2 (Figure 3.24). Expression of EGFP-SMO-WT/M2 in HEK-293 cells shows much stronger expression of EGFP-SMO-M2 suggesting that the mutant form of SMO is more stable than the wild type which may account for its tumourigenic potential (Figure 3.21). SMO-M2 mutations have been found in BCCs and expression of the more stable SMO-M2 could lead to constitutive activation of HH that gives rise to BCC development (Xie et al., 1998). To determine if nuclear SMO is the cause for GLI1 over expression in NEB1-shPTCH1 cells, the NLS of EGFP-SMO-WT/M2 could be altered via site directed mutagenesis. NEB1 cells would then be analysed for the protein localisation of EGFP-SMO-WT/M2 as well as by qPCR for GLI1 to conclude whether or not GLI1 expression is reduced in NEB1 cells. Creating stable EGFP-SMO-WT/M2 expressing NEB1-shCON and NEB1-shPTCH1 cell lines would help determine where SMO-WT and SMO-M2 are localised in the cells and how the proteins behave when there are elevated levels of GLI1 i.e. in NEB1-shPTCH1.

By comparing NEB1-shCON to NEB1-shPTCH1 cells, there is evidence that HH signalling may occur in the nucleus as opposed to the cell membrane or cilia. NEB1-shCON cells have nuclear PTCH1 and cytoplasmic SMO and GLI1. It is possible that PTCH1 may be suppressing HH signalling possibly by preventing SMO entering the nucleus although PTCH1 regulates SMO at the cell membrane to limit HH signalling. Although it has been reported that N-terminal PTCH1

is localised in the cytoplasm while C-terminal PTCH1 is present in the nucleus (Kagawa et al., 2011) it is possible that full length PTCH1 is active at the cell membrane as well as the nuclear membrane. Immunocytochemistry for SMO-ab72130 reveals a peri-nuclear expression pattern in NEB1-shCON cells so PTCH1 may prevent SMO from entering the nucleus and activating GLI1. In contrast, NEB1-shPTCH1 cells have reduced nuclear PTCH1 allowing for SMO to migrate to and enter the nucleus and constitutively activate GLI1 which is also more nuclear. This would explain why there is greater SMO protein expression in and around the nucleus in NEB1-shPTCH1 compared to NEB1-shCON cells (Figure 3.18). It is not known how SMO inhibitors would act upon nuclear proteins i.e. is drug efficacy different if proteins are localised in certain parts of the cell. It should be stated that further experiments are required to be certain of the sub-cellular localisation of SMO by fractionation methods.

BCC tumours that do not have mutated PTCH1, may still have increased HH signalling as a result of SMO activating mutations which negates the repressive function of PTCH1 on the pathway (Xie et al., 1998). However, a study has shown that SMO-M2 over expressing mice do not develop BCCs but instead, follicular Hamartomas emerge (Grachtchouk et al., 2003) although others have shown that BCCs develop on the ears and tail of mice transgenically expressing SMO-M2 (Wang et al., 2011). From the literature it is unclear whether SMO-M2 mutation is sufficient for the development of BCC although there is a significant increase in GLI1 mRNA expression in transfected NEB1 cells. A study where NIH-3T3 cells were induced with SMO-WT and SMO-M2 to stimulate HH signalling reveals that the addition of Cyclopamine can suppress the pathway in cells induced with SMO-WT but not SMO-M2 (Taipale et al., 2000). This raises questions to the nature of the SMO-M2 mutation for example, does the mutation prevent Cyclopamine from binding to the protein or not.

Based on the findings that NEB1-shPTCH1 cells do not respond to SMO inhibitors, it may be possible that SMO-M2 operates non-canonically as opposed to SMO-WT. The involvement of cilia may also be a factor that has not yet been investigated. The HH pathway is mediated through cilia and upon SHH activation, SMO localises at the primary cilium (Corbit et al., 2005). In NEB1-shPTCH1 cells, SHH is not required as the HH pathway is constitutively active so SMO may be signalling independently of cilia however, this depends on whether SHH mediates canonical signalling through cilia in NEB1 cells. NEB1 cells should be analysed for cilia as there is the possibility that they are not present in the cells.

With reduced PTCH1 in shPTCH1 cells, SMO and the other downstream targets are constitutively active however this does not explain why SMO inhibitors do not decrease GLI1

expression. It is likely that the SMO inhibitors do bind to SMO in NEB1-shPTCH1 cells however SMO could be acting in a different way to signal to GLI1 that is not affected by inhibitors. It is unknown exactly where the SMO antagonists bind regarding proteomics but this would help determine the active region of SMO in NEB1-shCON cells. This raises questions as to the effectiveness of SMO inhibitors to treat BCCs which may be determined by the method by which the tumour was initiated i.e. through PTCH1 mutations, SMO activation or UV associated DNA damage for example.

Of the mouse models of BCC that exist mice that develop normally before PTCH1 is conditionally knocked down, display BCC formation (Adolphe et al., 2006). The mice and skin develop for 32 days before treatment with Retinoic acid which triggers the conditional knock down of *PTCH1* in the mice. Histological sections are examined 4 weeks after the treatment. A criticism of this model is that BCCs occur in Gorlin's patients after the loss of heterozygosity of PTCH1 (Gailani et al., 1996) therefore, even the presence of one functioning PTCH1 allele may prevent BCC formation. $PTCH^{+/-}$ mice have been shown to develop tumours that resemble BCCs upon UV irradiation (Donovan, 2009; Daya-Grosjean and Couve´-Privat, 2005). Another study has shown that $PTCH^{+/-}$ mice develop tumours that are similar to Trichoblastomas and UV irradiation of these mice increased the number of tumours and altered their appearance to be more similar to nodular BCCs (Mancuso et al., 2004). These studies suggest that BCCs do not form if at least one PTCH1 allele is functional and that a separate event such as a UV induced mutation is required to initiate tumour formation.

Although the loss of PTCH1 in mice results in the formation of BCCs, other mouse studies where components of the HH pathway can lead to BCC formation while others do not. Further upstream of PTCH1, mice that have over expressed SHH ligand develop BCCs (Oro et al., 1997). At the end of the signalling cascade, mice over expressing GLI1 develop tumours resembling BCCs (Nilsson et al., 2000) compared to mice over expressing an activated mutant form of GLI2 which developed multiple BCCs (Sheng et al., 2002; Grachtchouk et al., 2000). An interesting observation is that GLI2 mRNA is suppressed by SMO inhibitors in both NEB1-shCON and NEB1-shPTCH1 cells (Figure 3.9). This suggests that GLI2 is mediated through SMO in NEB1-shPTCH1 cells unlike GLI1 so GLI2 may only signal canonically. GLI1 and GLI2 are part of a positive feedback loop (Regl et al., 2002) and it is unusual that in NEB1-shPTCH1 cells GLI2 is not induced in contrast to GLI1. An active mutant form of GLI2 has been shown to directly activate GLI1 while GLI1 can only activate GLI2 indirectly. It may be that GLI2 does not signal in the same non-canonical mode that GLI1 signals. It is difficult to draw conclusions over the involvement of GLI2 in BCC formation as mice were over expressing an active mutant of GLI2

and not the wild type protein which is much less transcriptionally active (Roessler et al., 2005; Sheng et al., 2002; Grachtchouk et al., 2000). Also, studies of mice over expressing SMO-M2 show that follicular Hamartomas develop rather than BCCs even though this is a known mutation found in BCCs (Grachtchouk et al., 2003). The mouse studies show that the HH pathway alone may not be responsible for BCC formation as it would be expected that GLI1 over expression would cause the illness. If the HH pathway were linear, the disruption of each component would result in the formation of the same tumour however this is not the case suggesting the HH pathway is not linear and that there is the possibility of non-canonical signalling where GLI1 and GLI2 can signal independently of other components such as SMO.

Regarding NEB1-shPTCH1 cells as a model of BCC, shRNA does not fully suppress PTCH1 meaning that there is a certain level of PTCH1 functionality. This may provide an explanation as to why Matrigel based organotypic culture of NEB1-shPTCH1 cells (Figure 3.26) did not result in BCC formation as there may need to be a certain level of PTCH1 suppression to initiate tumour formation despite the presence of a non-canonical mode of HH signalling in NEB1-shPTCH1 cells. However, there was evidence of hyperproliferation of the epidermal layer and as NEB1-shPTCH1 cells have heavily suppressed PTCH1, a separate event may need to occur before BCCs develop. This may be through UV irradiation as seen in mouse studies or via other pathways that are linked to HH signalling.

However not all BCCs display a loss of PTCH expression and in fact, human nodular BCCs showed over expressed PTCH and SMO mRNA expression especially in areas where the tumour was advancing, superficial BCCs showed an absence of PTCH and SMO mRNA expression. It is possible that in these tumours, PTCH and SMO play a role in more aggressive BCCs (Tojo et al. 1999). A study utilising $PTCH^{+/-}$ mice found that the wild type allele was being expressed as well as the mutated form which was shown to be capable of pathway inhibition (Uhmann et al., 2005). Another study comparing $PTCH^{+/-}$ and $PTCH^{-/-}$ mouse embryonic fibroblasts showed that mutated PTCH is as stably expressed as the wild type PTCH and that both $PTCH^{+/-}$ and $PTCH^{-/-}$ mouse fibroblasts show similar induction of SMO and GLI2 but $PTCH^{-/-}$ cells have increased levels of GLI1 (Bailey et al., 2002). The study shows that a slight reduction of PTCH activity has the potential to initiate certain disease phenotypes. Another anomaly was reported in $PTCH^{+/-}$ mice where GLI1 expression was strongly expressed in medulloblastoma despite the presence of PTCH (Wetmore et al., 2000). These studies highlight that GLI1 can be over expressed even though PTCH1 is present which should supposedly suppress the HH pathway. Also, BCCs can form with active PTCH and GLI1 which suggests that GLI1 signalling may occur via other modes as PTCH should suppress GLI1.

The study has shown that GLI1 is expressed in NEB1-shPTCH1 cells via a non-canonical mode of signalling. Treatment of NEB1-shPTCH1 cells with SMO inhibitors failed to reduce GLI1 expression suggesting that GLI1 signals independently of SMO however, GLI1 is repressed by SMO siRNA. This shows that NEB1-shPTCH1 cells are unresponsive to SMO inhibitors which have clinical implications for BCCs that may have arisen due to loss of function mutations to PTCH1. A potential reason for this is that SMO may enter the nucleus to directly influence GLI1 expression or there is an unknown factor that is inducing GLI1 linked to loss of PTCH1 function (Figure 3.27).

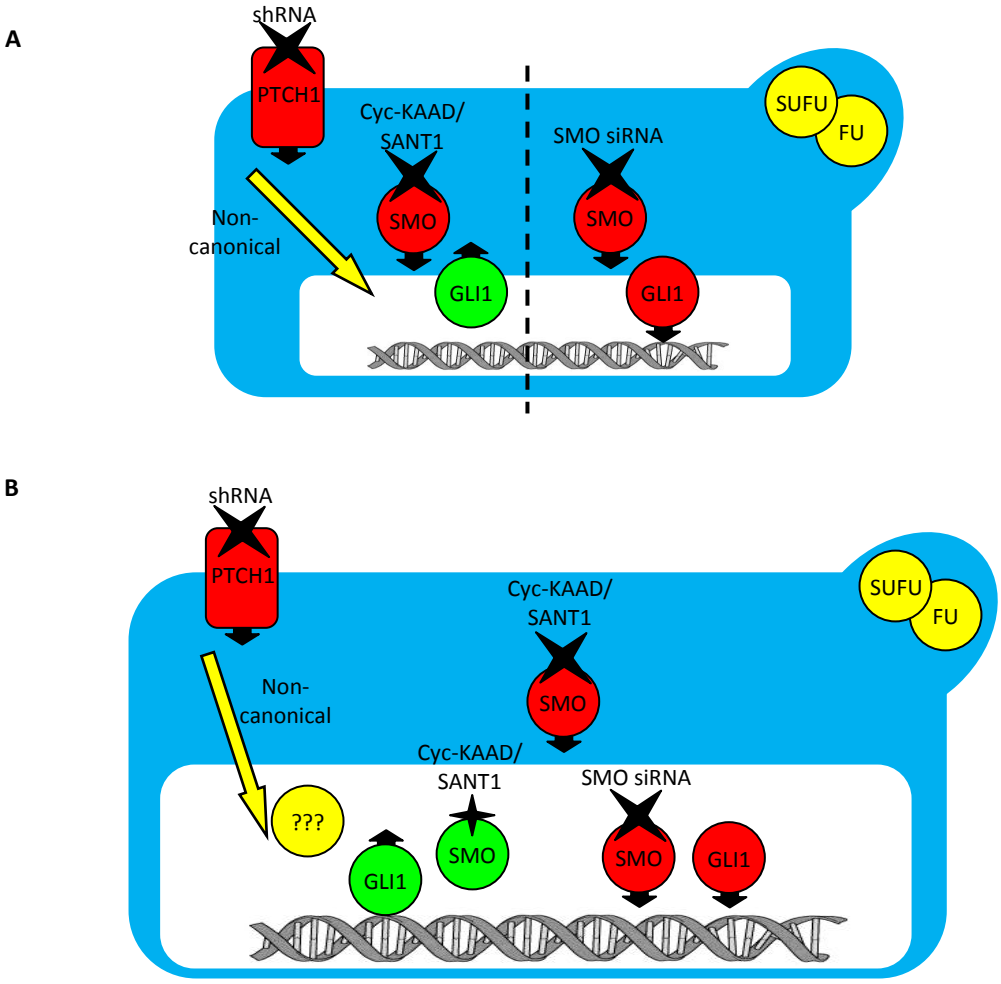

Figure 3.27: Non-canonical HH signalling in NEB1-shPTCH1 cells

[**A**] NEB1-shPTCH1 cells are unresponsive to SMO inhibitors however GLI1 is suppressed by SMO siRNA.

[**B**] GLI1 may be induced by nuclear SMO or another undiscovered factor.

Chapter 4

Identification of novel pathways regulated by PTCH1 in human keratinocytes

Chapter 4 Introduction

Characterisation of NEB1-shPTCH1 cells as an *in vitro* model of BCC in chapter 3 revealed a potentially novel non-canonical mode of HH signalling. It was confirmed that the suppression of PTCH1 in NEB1-shPTCH1 cells leads to the over-expression of GLI1 as well as promoting a nodular BCC-like morphology of NEB1-shPTCH1 cells. NEB1-shPTCH1 cells were also shown to be unresponsive to pharmacological SMO inhibition as GLI1 levels were not reduced. However, GLI1 may not be fully independent of SMO as SMO siRNA did suppress GLI1 in NEB1-shPTCH1 cells. This could be related to the finding that SMO is localised in the nucleus of NEB1-shPTCH1 cells or via another signalling pathway. As such, gene expression microarray profiling of NEB1-shPTCH1 cells was performed to determine which other pathways may be affected by the suppression of PTCH1 which may in turn be involved with BCC biology.

The fact that NEB1-shPTCH1 cells were unresponsive to SMO inhibitors has clinical implications as studies have shown that many BCC patients did not respond to SMO antagonists such as GDC-0449 (Van Hoff et al., 2009). Performing a microarray analysis on NEB1-shPTCH1 cells treated with Cyclopamine-KAAD will therefore help determine which pathways are differentially regulated and potentially, pathways that may signal via a non-canonical HH mode.

4.1 Gene expression profiling of NEB1-shPTCH1 cells

As stated previously, one of the reasons for suppressing PTCH1 expression in human keratinocytes was to identify novel mechanisms that are regulated by this tumour suppressor protein and that may be important in BCC biology. Therefore, cDNA microarray profiling was employed to compare NEB1-shCON with NEB1-shPTCH1 keratinocytes. In addition, to help determine if any novel genes or pathways are mediated through canonical Hedgehog signalling, NEB1-shPTCH1 cells exposed to KAAD-Cyclopamine were included in the array: this also stems from the fact that GLI1 levels were insensitive to SMO pharmacological inhibition in NEB1-shPTCH1 cells, although this may have been because SMO has nuclear signalling capability which is insensitive to the anti-SMO compounds used in this study.

Gene expression microarray profiling was performed on NEB1-shCON, NEB1-shPTCH1 and NEB1-shPTCH1 cells treated with 100 nM Cyclopamine-KAAD using the Human Gene 1.1 ST Array Strip from Affymetrix containing 28,000 genes. A threshold value of 2 fold change was set to identify differentially expressed genes (DEGs) between samples. When comparing NEB1-

shPTCH1 to NEB1-shCON cells, the DEGs represented 6% of all transcripts whereas the DEGs represented 8% of all transcripts when comparing NEB1-shCON to NEB1-shPTCH1 + Cyclopamine-KAAD (Figure 4.1). A full list of DEGs can be found in the Appendix (Tables 8.5-8.8). The efficacy of Cyclopamine-KAAD had been previously validated (Figures 3.11 B and 3.14 B).

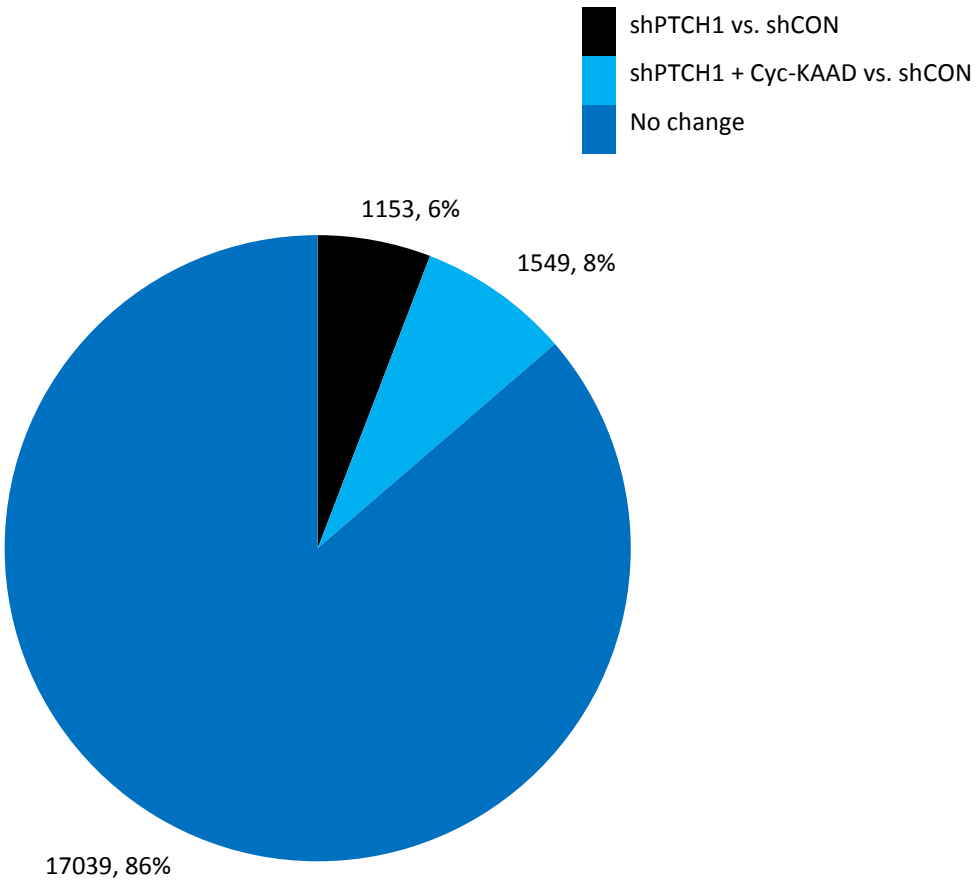

Figure 4.1: Pie chart showing number of DEGs identified when comparing NEB1-shPTCH1 vs NEB1-shCON and NEB1-shPTCH1 + Cyclopamine-KAAD vs. NEB1-shCON as a percentage of all transcripts analysed

NEB1-shPTCH1 and NEB1-shPTCH1 + Cyclopamine-KAAD were compared to each other from which 478 DEGs were identified. Of these genes, 70% did not return to basal levels in the presence of Cyclopamine-KAAD (Figure 4.2). Comparison of the DEG expression values between NEB1-shPTCH1 and NEB1-shPTCH1 + Cyclopamine-KAAD samples did not show much difference in expression (Table 4.1). This raises the question as to which pathways or processes are affected by Cyclopamine-KAAD in NEB1-shPTCH1 cells or if non-canonical HH signalling can compensate for the inhibition of canonical HH signalling.

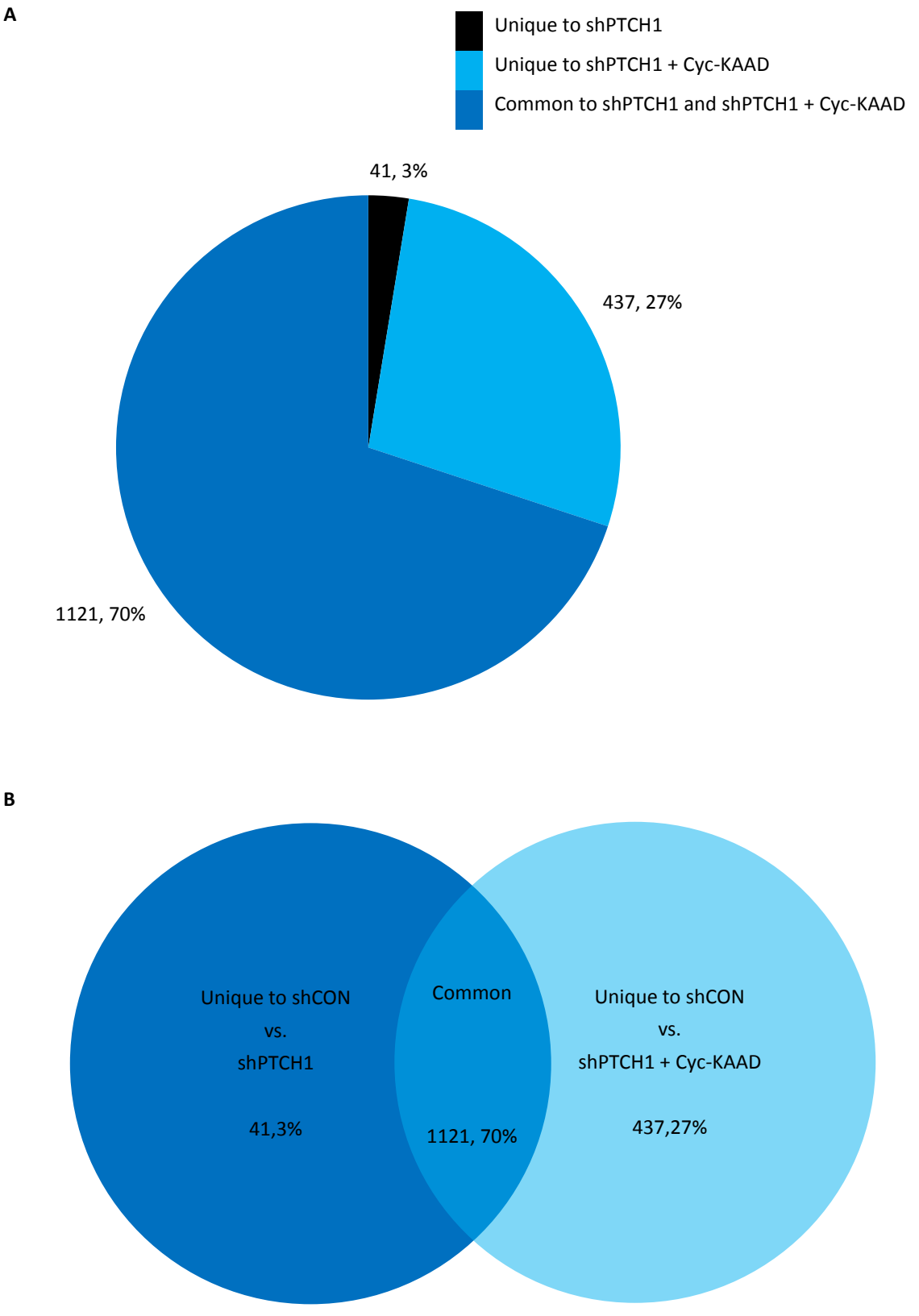

Figure 4.2: DEGs identified when comparing NEB1-shPTCH1 and NEB1-shPTCH1 + Cyclopamine-KAAD [**A**] Pie chart and [**B**] Venn diagram of DEGs unique to and independent of NEB1-shPTCH1 and NEB1-shPTCH1 + Cyclopamine-KAAD.

A

Gene (Top 20)	Expression vs. shCON		Gene (Bottom 20)	Expression vs. shCON		Gene expression
	shPTCH1	shPTCH1 + Cyc-KAAD		shPTCH1	shPTCH1 + Cyc-KAAD	
MMP7	9.4698	4.9019	TCF7L1	-2.9485	-3.2716	6.56 - 8.21
SCGB1A1	9.1472	6.0769	SPRR1A	-3.0105	-3.4343	4.92 - 6.56
CXCL10	8.2059	3.8459	WDR17	-3.0175	-2.4623	3.28 - 4.92
PTGIS	7.0453	4.9474	ANKFN1	-3.0667	-2.8415	1.64 - 3.28
ANKRD1	6.4681	1.4241	KRT15	-3.1023	-4.4795	0.00 - 1.64
THY1	6.3496	7.2267	SERPINB13	-3.2266	-4.2575	-1.64 - 0.00
NNMT	5.4516	5.1814	SH3BGRL	-3.2415	-3.3636	-3.28 - -1.64
SRPX	5.0397	4.8793	AGR2	-3.3173	-5.8835	-4.92 - -3.28
ESX1	4.9818	4.9019	SPRR3	-3.3250	-4.7568	-6.56 - -4.92
CXCL11	4.8906	2.5198	ZNF165	-3.4661	-5.3641	-8.21 - -6.56
ADAM19	4.8456	5.1456	EPB41L4A	-3.4661	-3.5472	
IL7R	4.8456	4.2281	SCD5	-3.4882	-3.2490	
GPRC5B	4.7349	4.1892	AMOT	-3.6553	-3.4343	
FAM20C	4.5315	4.1315	SULT1E1	-3.7149	-5.2174	
SAA1	4.4076	3.5064	KRT4	-3.8106	-4.7240	
LAPTM5	4.2477	4.0652	MCOLN3	-3.8282	-3.6893	
MMP2	4.1315	3.8637	H2AFY2	-3.9267	-3.8548	
LIFR	3.9908	4.8232	PNLIPRP3	-4.3269	-6.0769	
CYP24A1	3.8548	3.8018	CNTN1	-4.3469	-4.4795	
CFB	3.8194	2.6329	MUC15	-4.3772	-3.7235	
ALDH2	3.7842	3.9908	KLHL13	-4.5525	-4.5842	
MCAM	3.7581	4.3369	LASS3	-5.8159	-5.7491	
APOBEC3G	3.6050	2.4284	ARHGEF9	-8.6538	-7.9815	
VIM	3.5718	3.4027	C9orf125	-8.7341	-8.0000	
SLCO2A1	3.5718	3.7494	FBN2	-10.1965	-10.0329	

B

Gene	Expression vs. shCON		Gene expression
	shPTCH1	shPTCH1 + Cyc-KAAD	
CXCL11	4.8906	2.5198	6.56 - 8.21
MMP2	4.1315	3.8637	4.92 - 6.56
TGFB2	3.2868	3.3173	3.28 - 4.92
SNAI1	2.4005	2.3241	1.64 - 3.28
TNC	2.3565	2.0562	0.00 - 1.64
MMP9	2.1987	2.3187	-1.64 - 0.00
NES	1.9498	2.1189	-3.28 - -1.64
LCN2	1.7411	-1.1019	-4.92 - -3.28
FOSL1	1.6434	1.6974	-6.56 - -4.92
CDKN1A	1.4573	1.3226	-8.21 - -6.56
TP53	1.2628	1.2002	
IGFBP2	-2.6759	-2.9828	

Table 4.1: Comparison of DEGs when comparing NEB1-shPTCH1 and NEB1-shPTCH1 + Cyc-KAAD to NEB1-shCON expression

[**A**] Table of top and bottom 20 genes that were differentially expressed. [**B**] Table of selected genes of interest related to BCC and cancer biology.

A number of interesting targets were selected from the microarray and validated by qPCR using primer sequences as the microarray uses a number of probe sequences per gene, generic PCR probes were designed that take into account of all potential isoforms (Figure 4.3). The genes of interest are involved in BCC and tumour biology and will be discussed later such as MMP-9, CXCL11, SNAI1, THY1 and VIM (Discussion). Results from qPCR mimic the trend from the microarray data with the exception of KRT15 being slightly increased and MMP-9 in Cyclopamine-KAAD treated cells being significantly increased by qPCR. In general qPCR is more sensitive than the microarray.

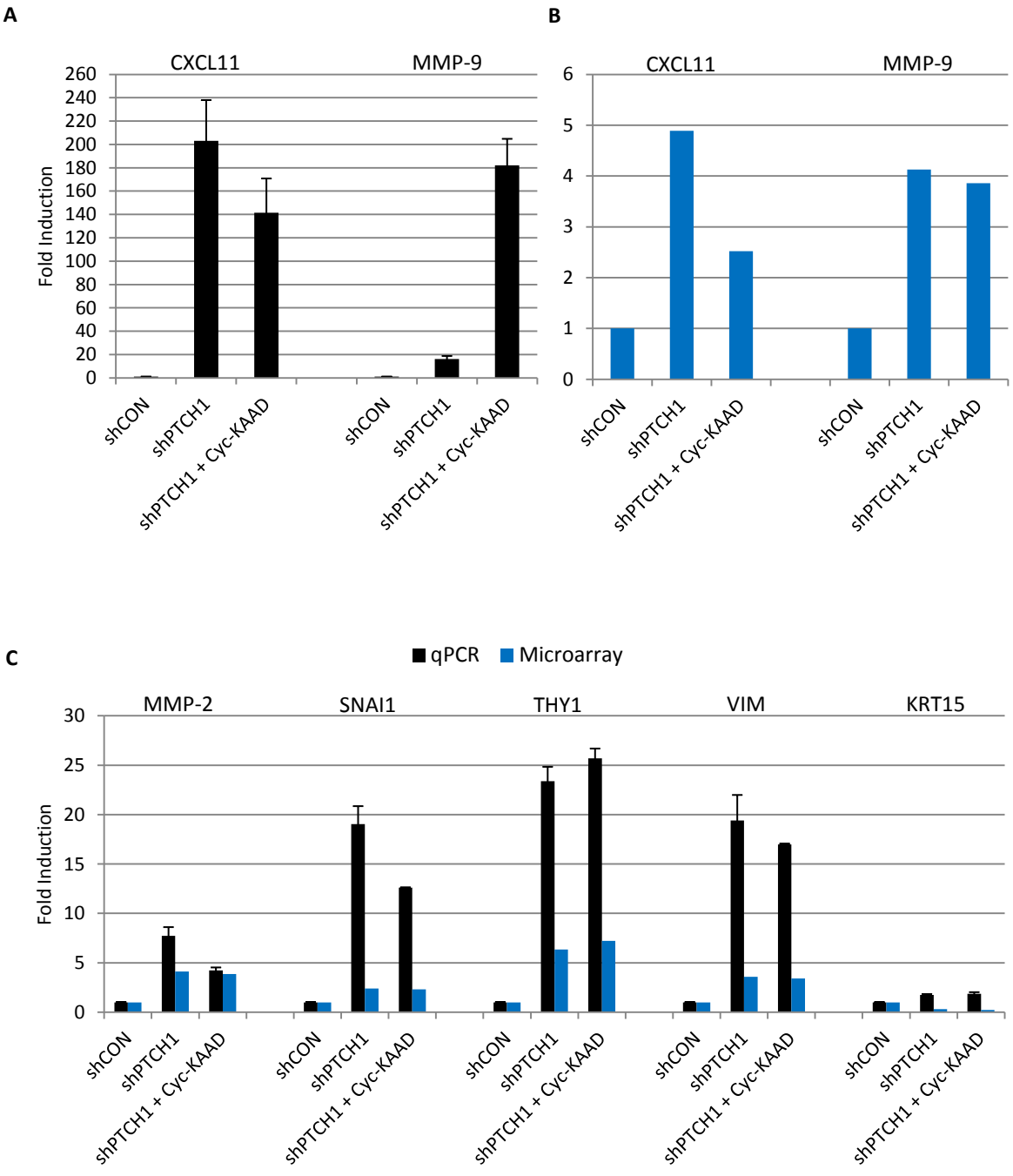

Figure 4.3: qPCR validation of microarray target genes

Comparison of CXCL11 and MMP-9 expression by [**A**] qPCR and [**B**] microarray analysis. [**C**] Comparison of other DEGs identified by microarray analysis with qPCR. Error bars represent mean ± standard deviation.

4.2 Functional grouping of differentially expressed genes

A list of the DEGs (478) unique to PTCH1 were then analysed via the internet based DAVID bioinformatics resource (Huang et al., 2009). DAVID is a gene annotation tool that highlights biological processes and functions from list of DEGs. The software was used to overlay the list of DEGs onto known signalling pathways from the KEGG database. This gave an indication of whether there were interesting clusters of genes to investigate further as opposed to single genes that may be affected by the suppression of PTCH1. As such, a number of interesting signalling pathways were retrieved from the analysis including pathways in cancer, MAPK, TGF-β and Toll-like receptor (TLR) pathways (Figures 4.4 to 4.7).

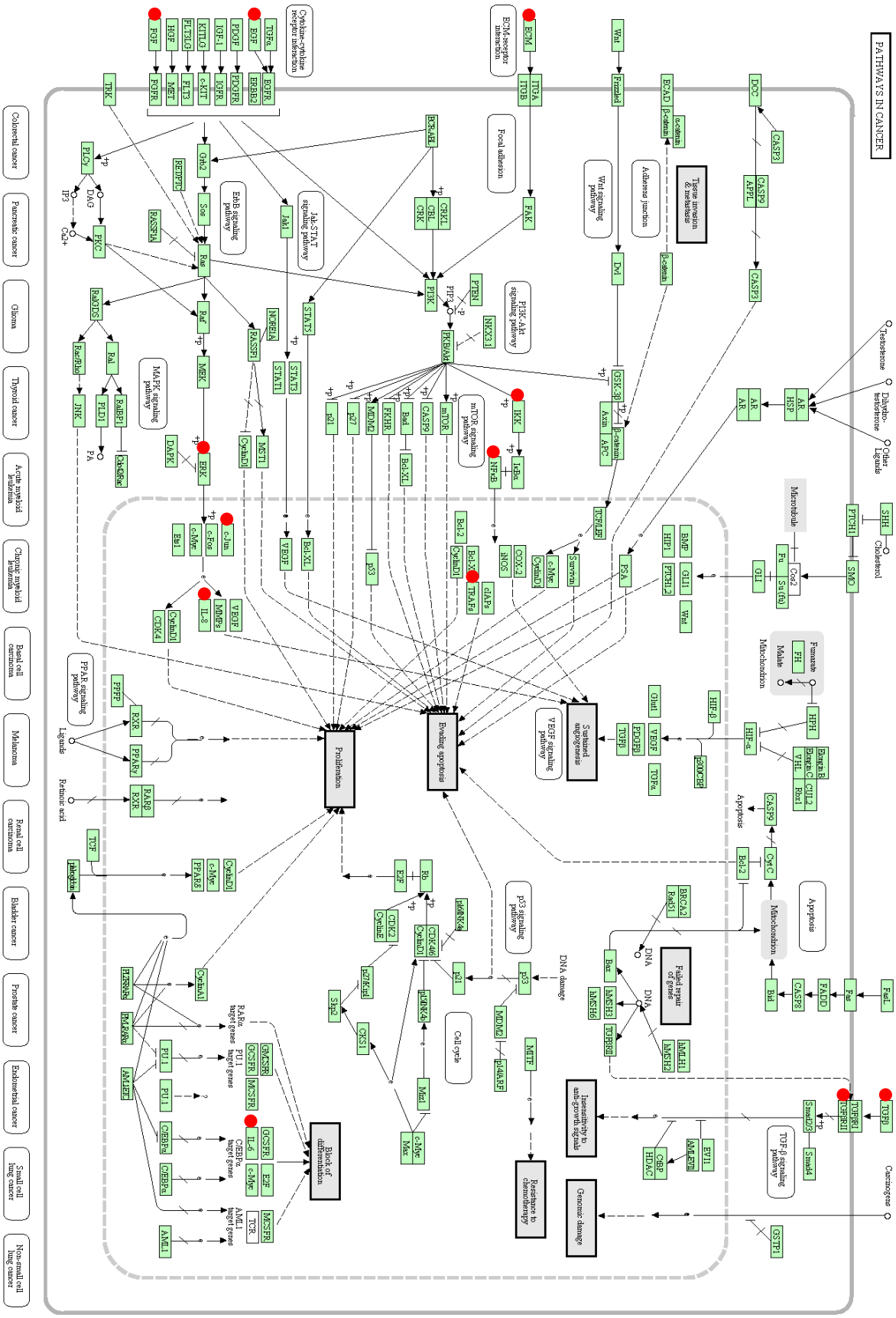

Figure 4.4: Pathways in cancer map of DEGs unique to PTCH1 from DAVID analysis

● Upregulated and ● downregulated DEGs and differentially expressed pathways.

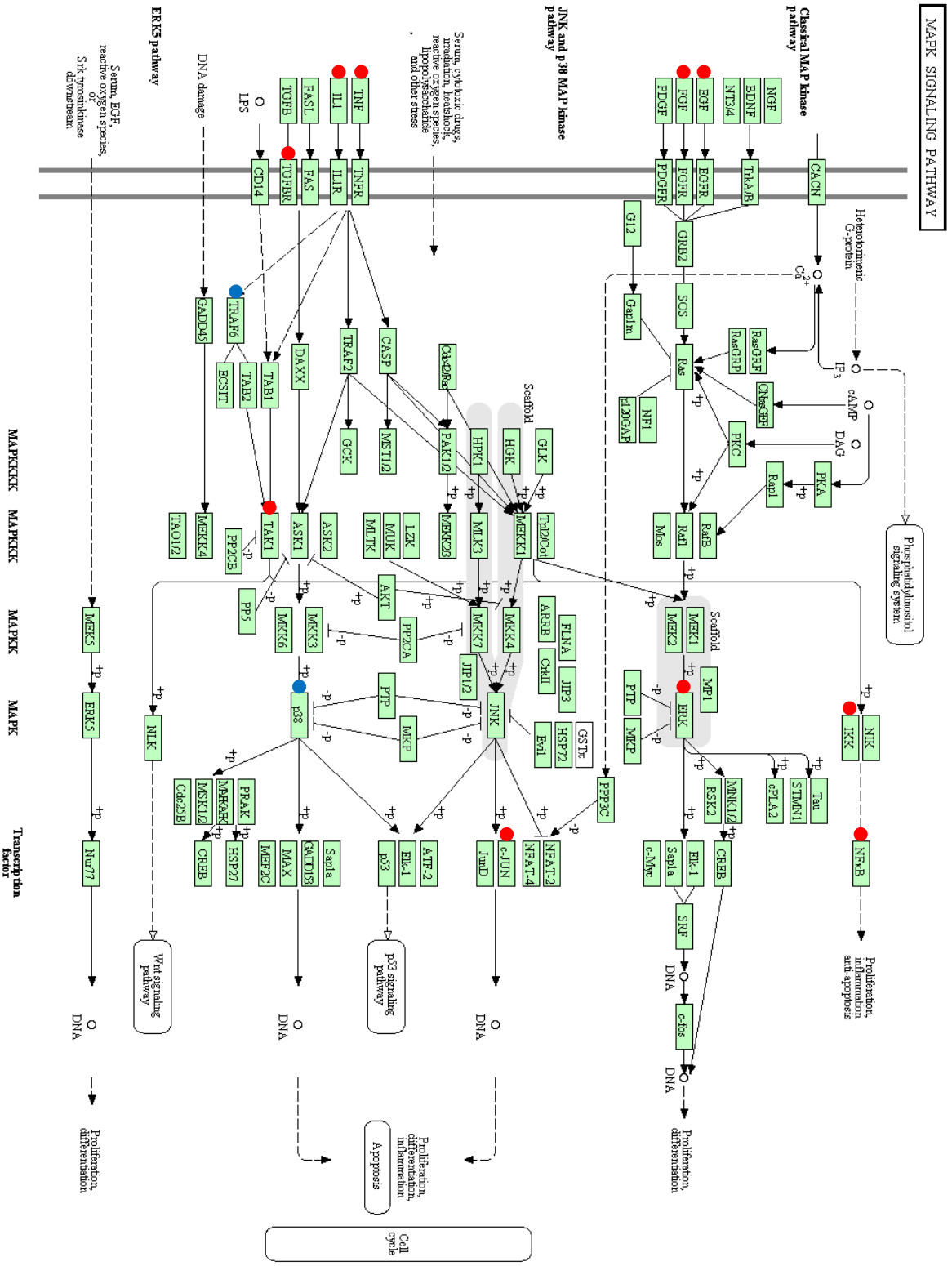

Figure 4.5: MAPK signalling pathway map of DEGs unique to PTCH1 from DAVID analysis

● Upregulated and ● downregulated DEGs and differentially expressed pathways.

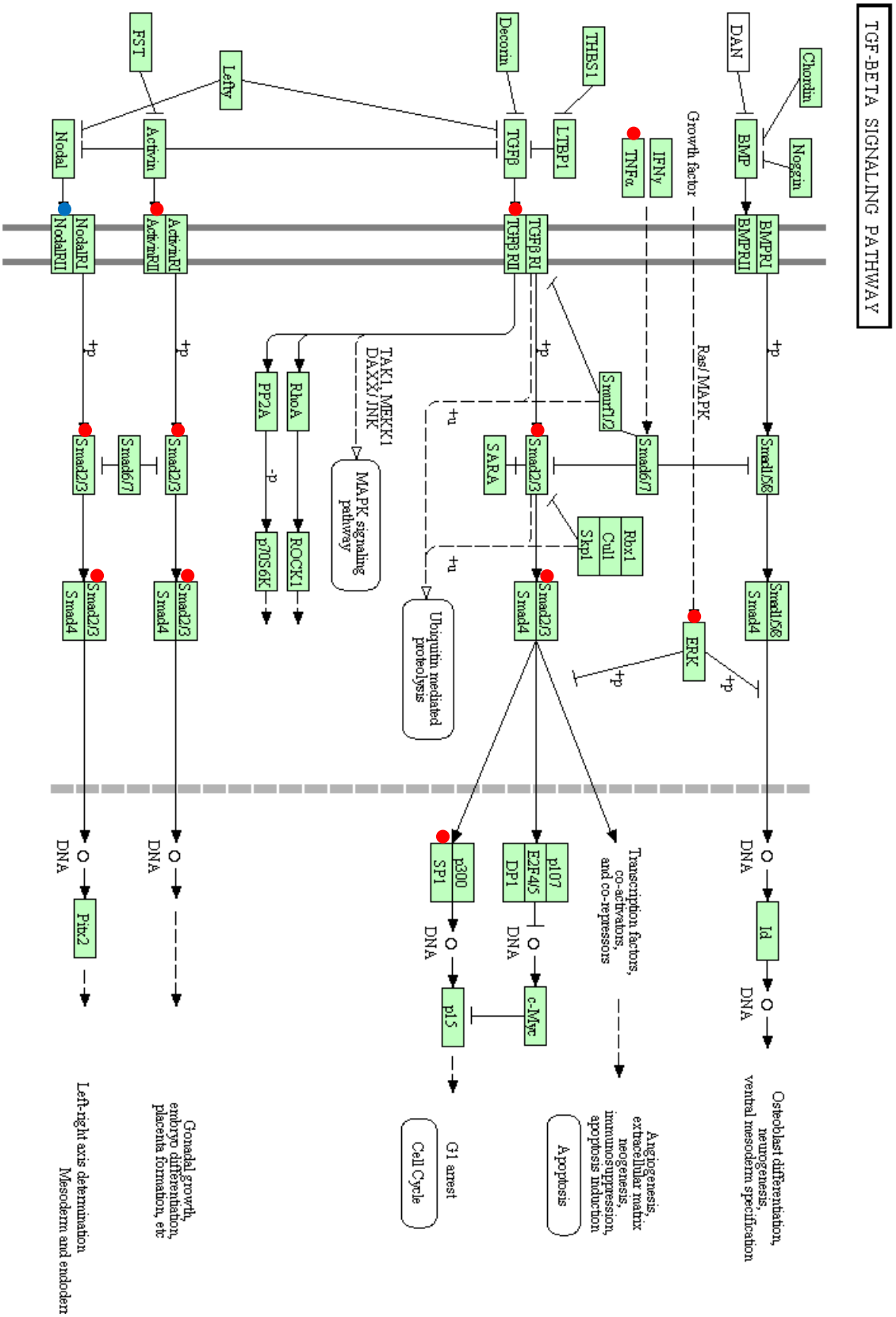

Figure 4.6: TGF-β signalling pathway map of DEGs unique to PTCH1 from DAVID analysis ● Upregulated and ● downregulated DEGs and differentially expressed pathways.

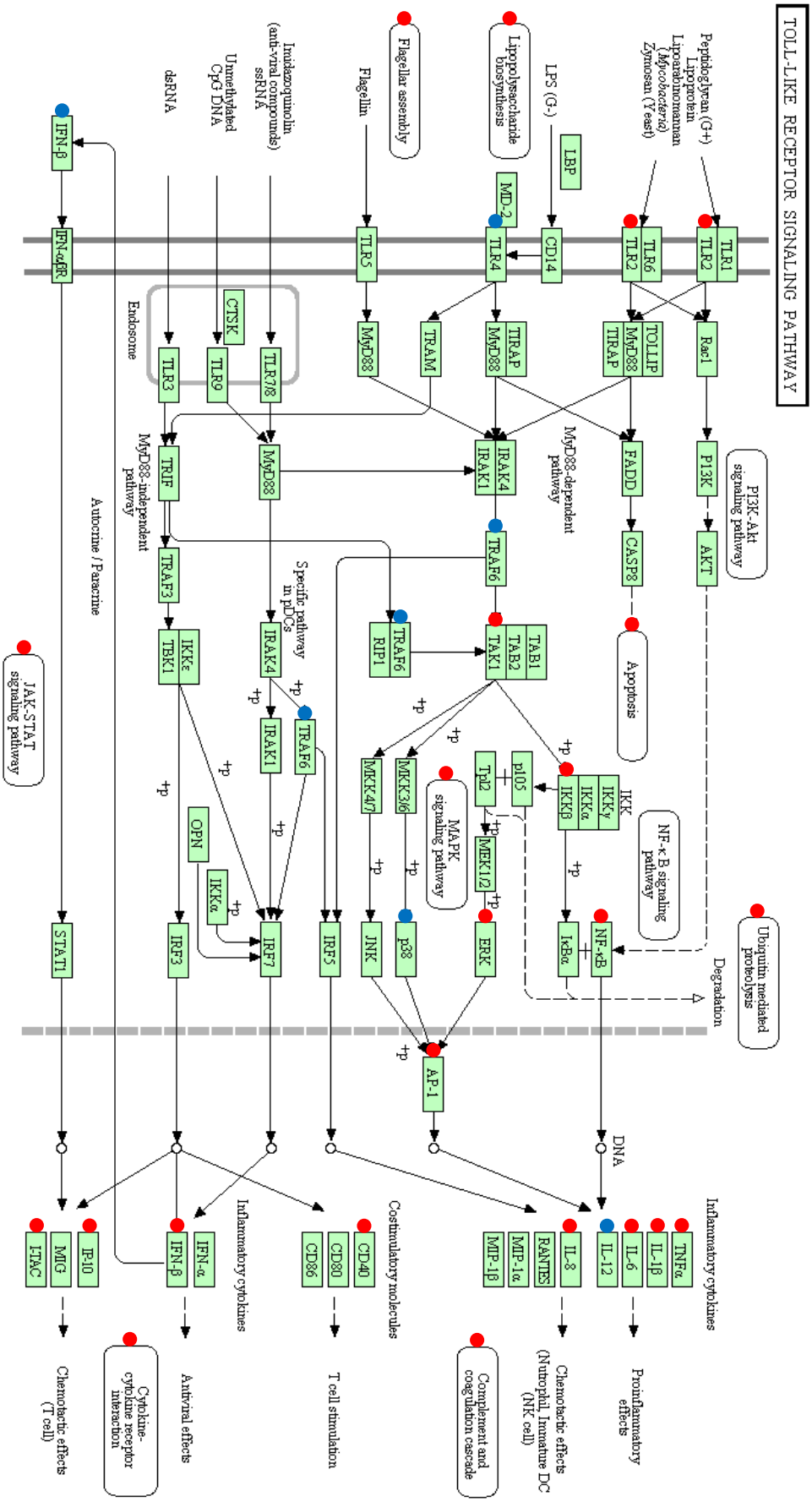

Figure 4.7: TLR signalling pathway map of DEGs unique to PTCH1 from DAVID analysis

● Upregulated and ● downregulated DEGs and differentially expressed pathways.

4.3 Novel pathways downstream of PTCH1 that may be linked to Basal cell carcinoma formation

Using the data generated from the microarray, a more detailed analysis was performed using MetaCore software in order to identify networks in NEB1-shPTCH1 cells that may help understand how suppression of PTCH1 could promote BCC biology, these networks may be SMO dependent or SMO independent. Utilising the MetaCore software database, network maps were generated based on pathways that contain the DEGs (Figure 4.8 (legend), Figure 4.9 and 4.10). The data set consisted of the 6% (1153) of DEGs and networks were generated based on gene associations that have been reported in scientific literature. DAVID analysis simply overlays the relevant genes onto a signalling pathway map whereas with MetaCore analysis, genes that are associated with other genes are clustered together. Network map 1 (Figure 4.9) highlights two distinct clusters one of which consists of MAPK, ERK and JUN while the other cluster consists of caspases. Network map 2 (Figure 4.10) shows a number of interesting clusters such as NF-kB, IL-8, EGFR and Fatty acid binding protein (FABP).

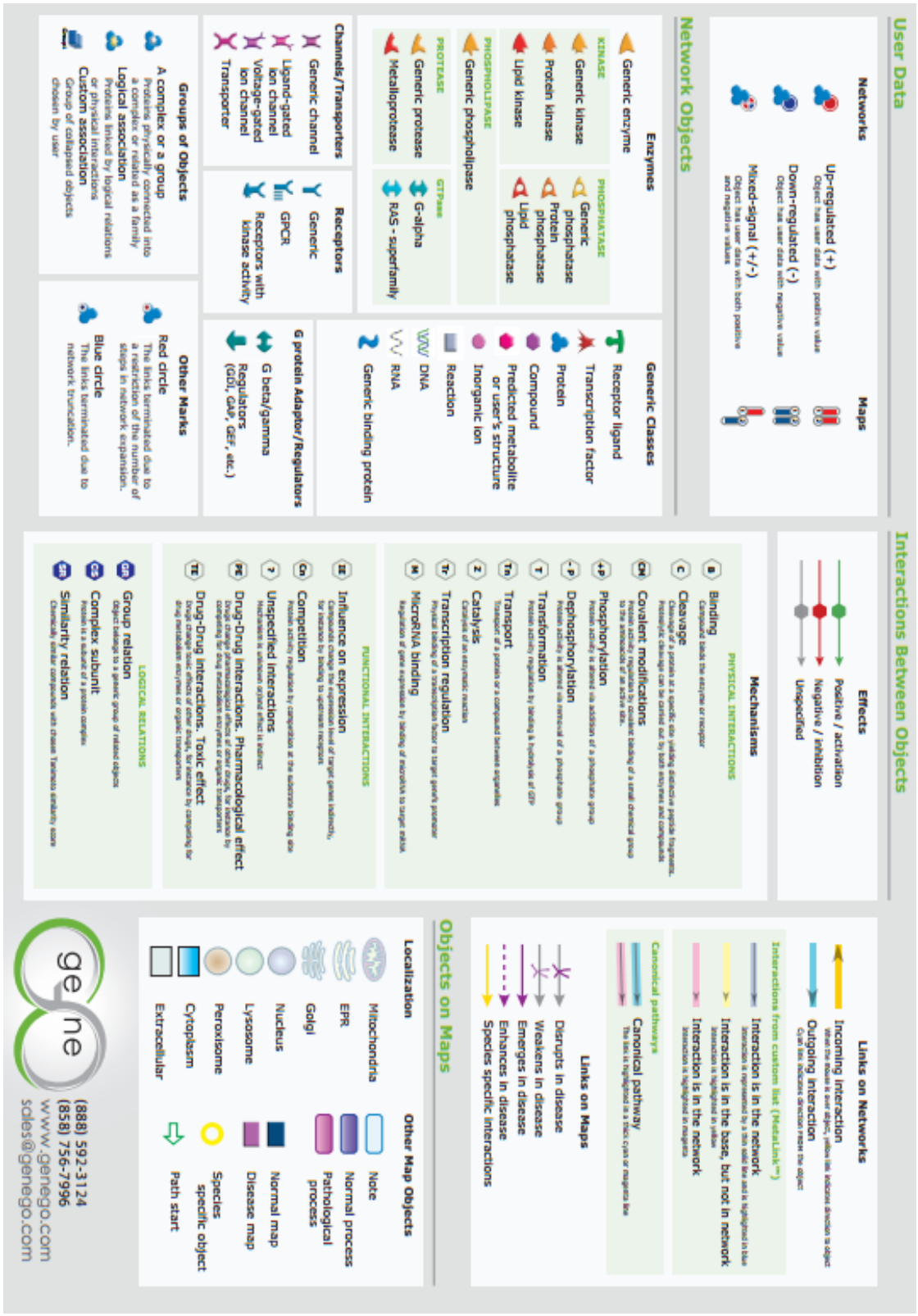

Figure 4.8: MetaCore network map legend

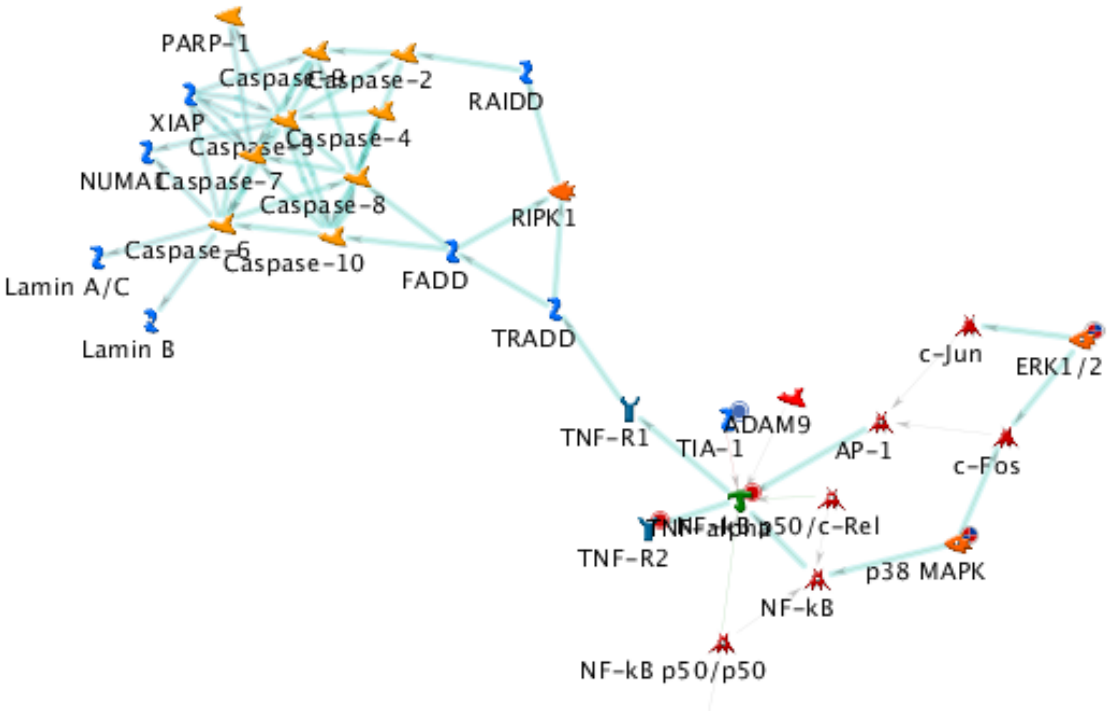

Figure 4.9: Network map 1 of DEGs unique for NEB1-shPTCH1 compared to NEB1-shCON

There are two main clusters of genes shown in this network map one of which contains a number of caspases which are involved in apoptosis. The second cluster contains MAPK and ERK as well as various transcription factors.

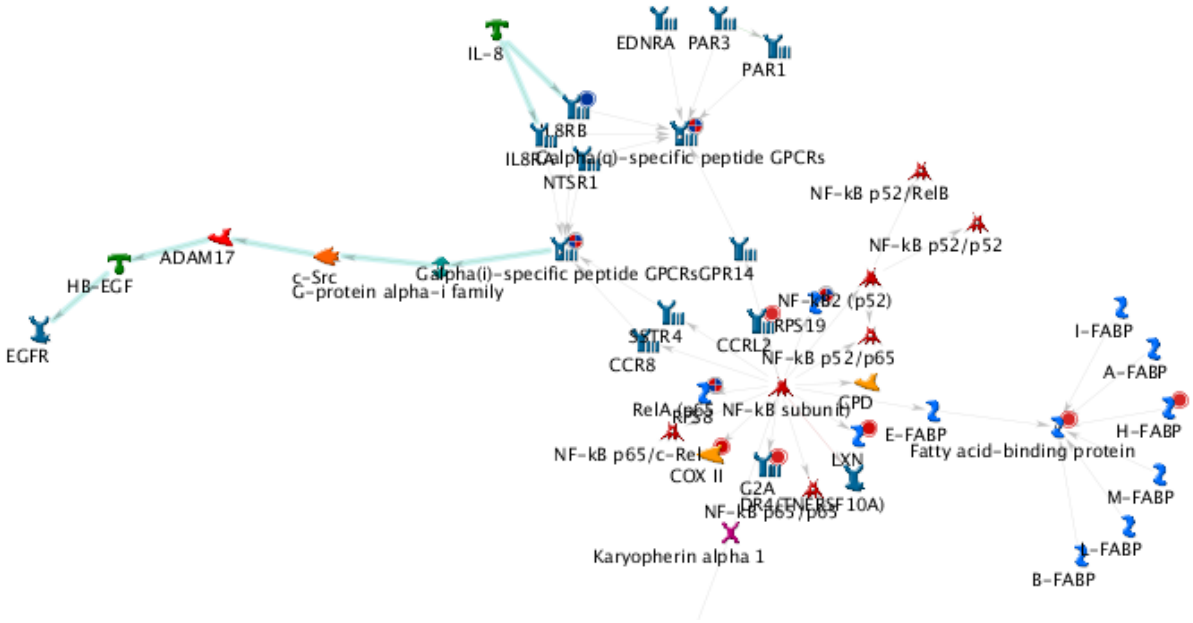

Figure 4.10: Network map 2 of DEGs unique for NEB1-shPTCH1 compared to NEB1-shCON

This network map shows a number of fatty acid binding proteins (FABP). The other main focal point is NF-kB that has a number of genes clustered around which suggests that the suppression PTCH1 may have had a significant effect on the pathway.

Having compared NEB1-shPTCH1 cells to NEB1-shCON cells, NEB1-shPTCH1 + Cyclopamine-KAAD cells were also compared to NEB1-shCON cells to determine which pathways or genes that are differentially regulated in NEB1-shPTCH1 return to basal levels i.e. pathways activated through the canonical HH pathway should return to basal levels upon the treatment Cyclopamine-KAAD.

This data set consisted of the 8% (1549) of DEGs when comparing NEB1-shPTCH1 + Cyclopamine-KAAD cells to NEB1-shCON cells. MetaCore generated network map 3 (Figure 4.11) shows ERK as well as MEK, FOS and JUN. The other major pathway that was exposed was the p53 pathway and components such as p21 and Cyclin D1. Network map 4 (Figure 4.12) highlights MMP-2, EGFR and structural cytoskeletal components such as actin, collagen IV and fibronectin.

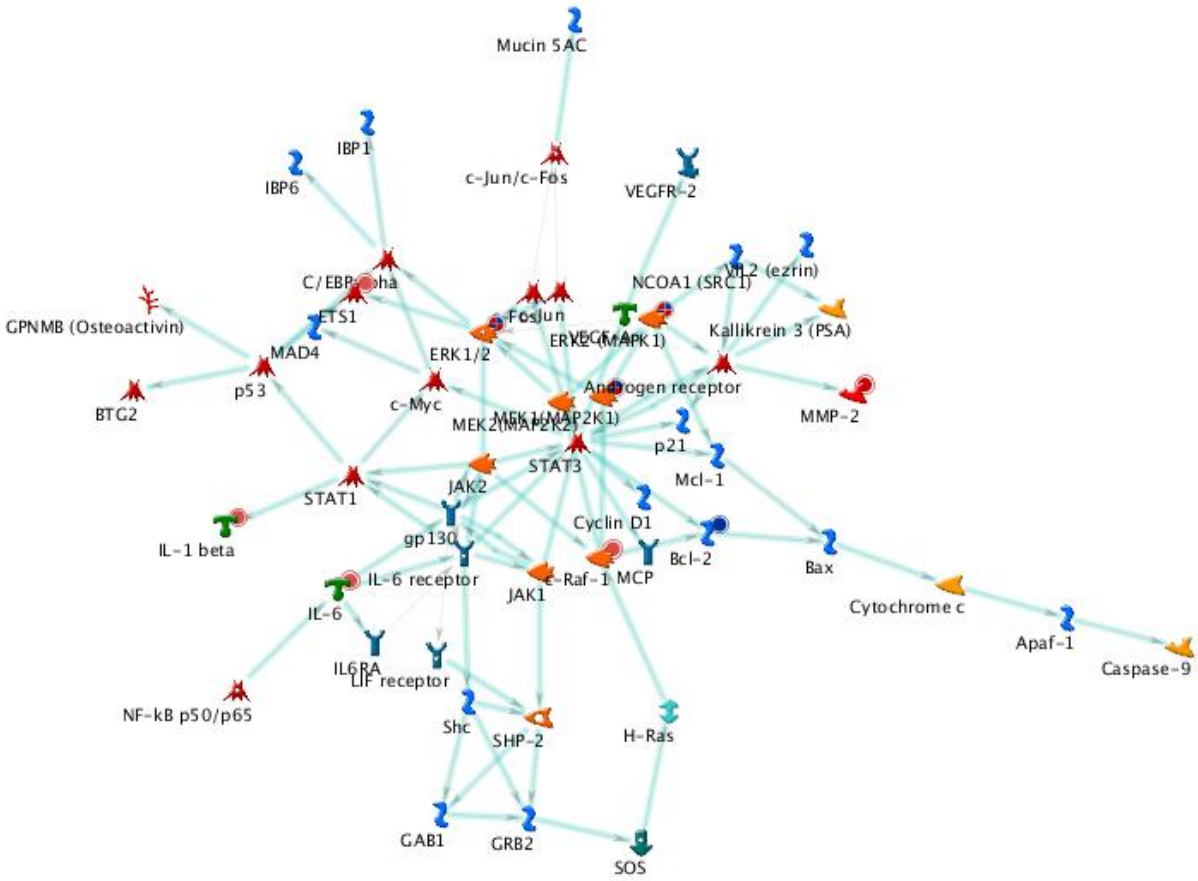

Figure 4.11: Network map 3 of DEGs unique for NEB1-shPTCH1 + Cyc-KAAD compared to NEB1-shCON MEK genes are central to this network map as they are associated with various different pathways (JAK, STAT and ERK) and downstream transcription factors including FOS and JUN. Interestingly there are a number of cancer biology related genes that are more loosely clustered around MEK such as NF-kB, p53 and p21.

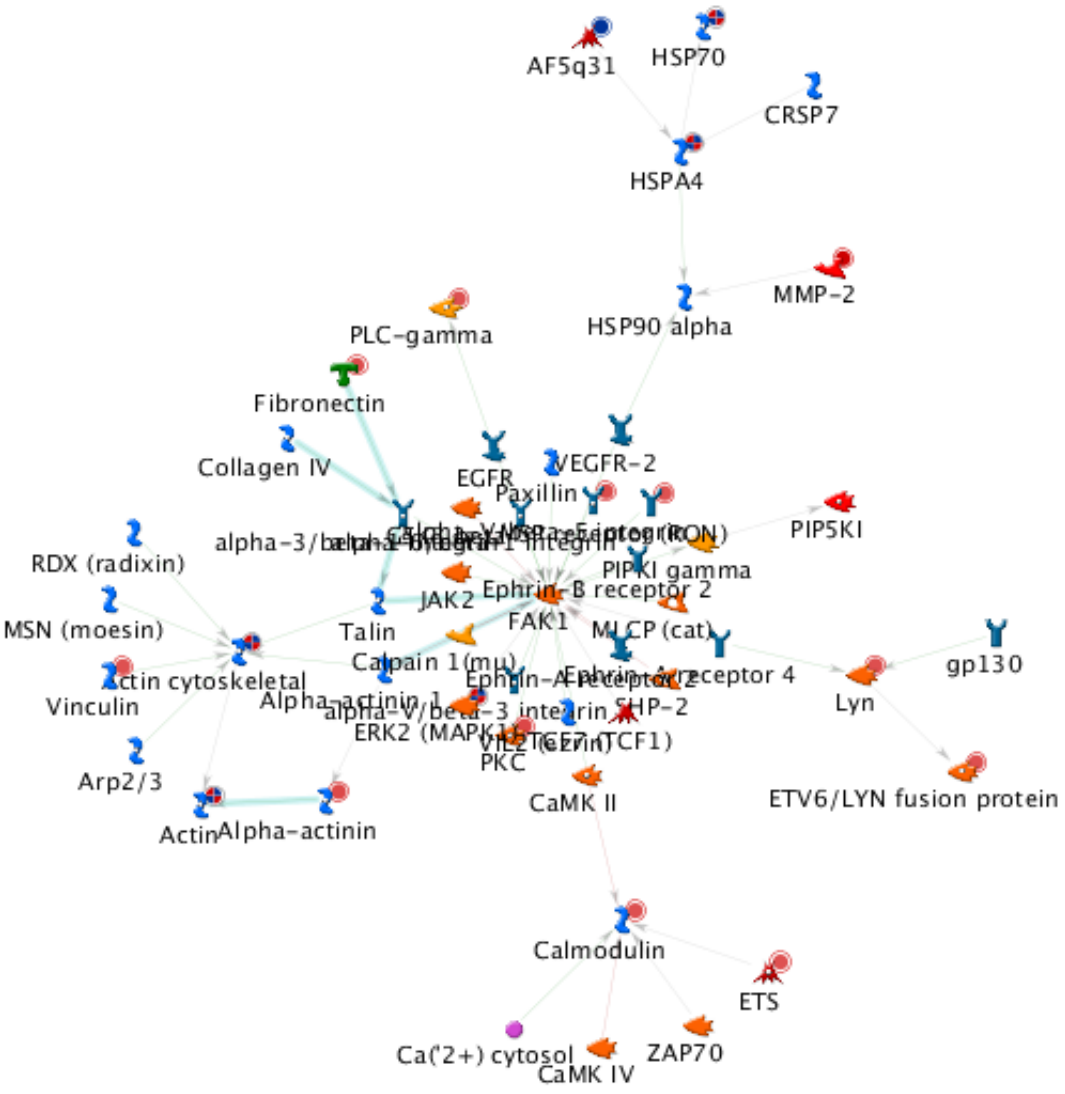

Figure 4.12: Network map 4 of DEGs unique for NEB1-shPTCH1 + Cyc-KAAD compared to NEB1-shCON This network map consists of EGFR which could account for MEK/ERK expression as seen in Figure 4.11. Cytoskeletal components including actin, collagen IV, vinculin and fibronectin were clustered together which may account for the change in morphology of NEB1-shPTCH1 cells.

The DEGs unique to PTCH1 including unique genes which are affected by Cyclopamine-KAAD (478) were then analysed. MetaCore analysis was performed and network pathways were generated which also take into account the cellular localisation of the DEGs. This gives a better account of the pathways a receptor ligand may follow to activate a transcription factor for example.

Network map 5 (Figure 4.13) shows a number of canonical pathway links between JNK, MEK, ERK, JUN, NF-kB and interleukin pathways. Network map 6 (Figure 4.14) highlights SMAD components while network map 7 (Figure 4.15) links EGF, FGF and VEGF with MEK, ERK, AKT pathways.

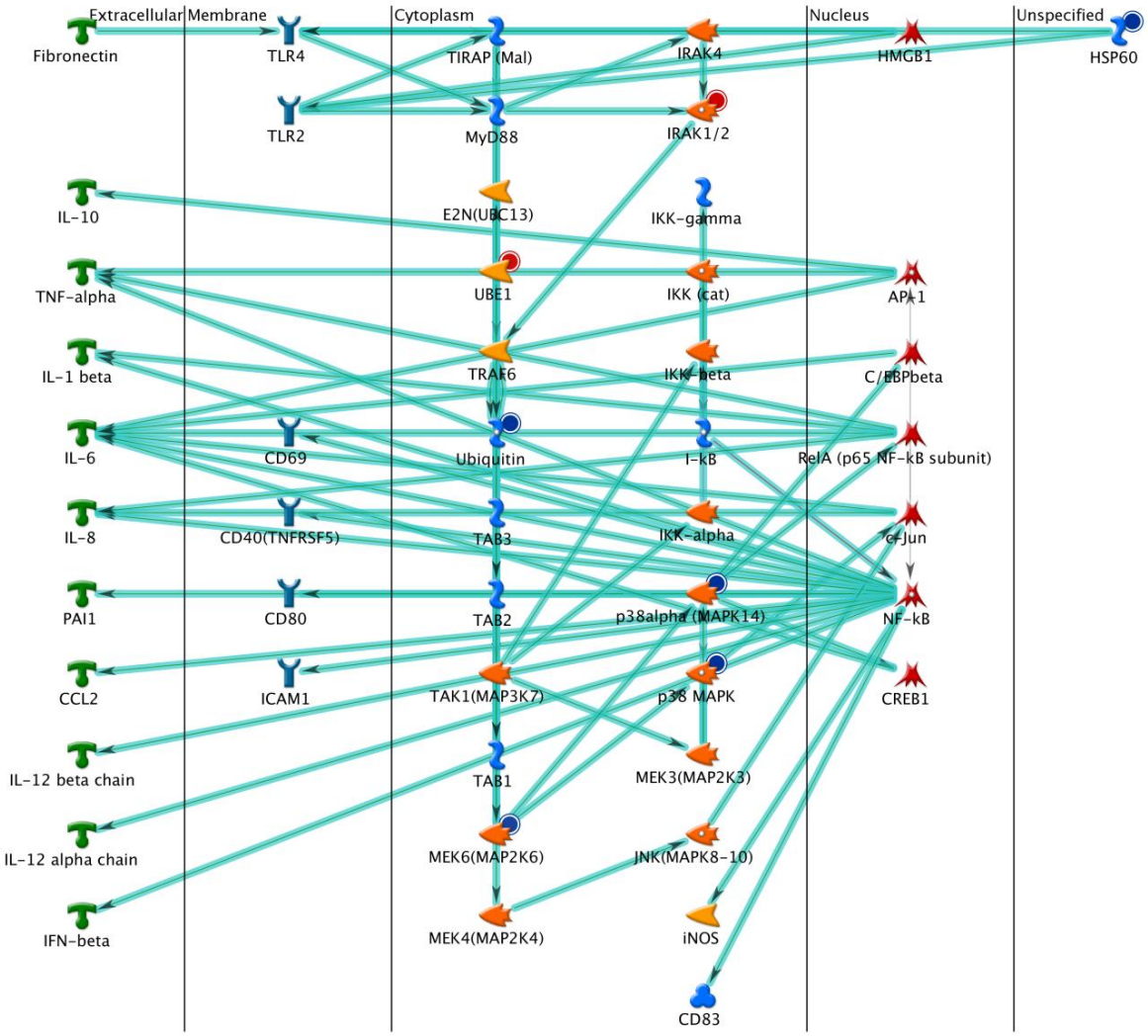

Figure 4.13: Network map 5 of DEGs unique to PTCH1

The network map shows that NF-kB is associated with a number of ligands and receptors. Also, MEK, JNK and p38 were shown to signal to c-JUN.

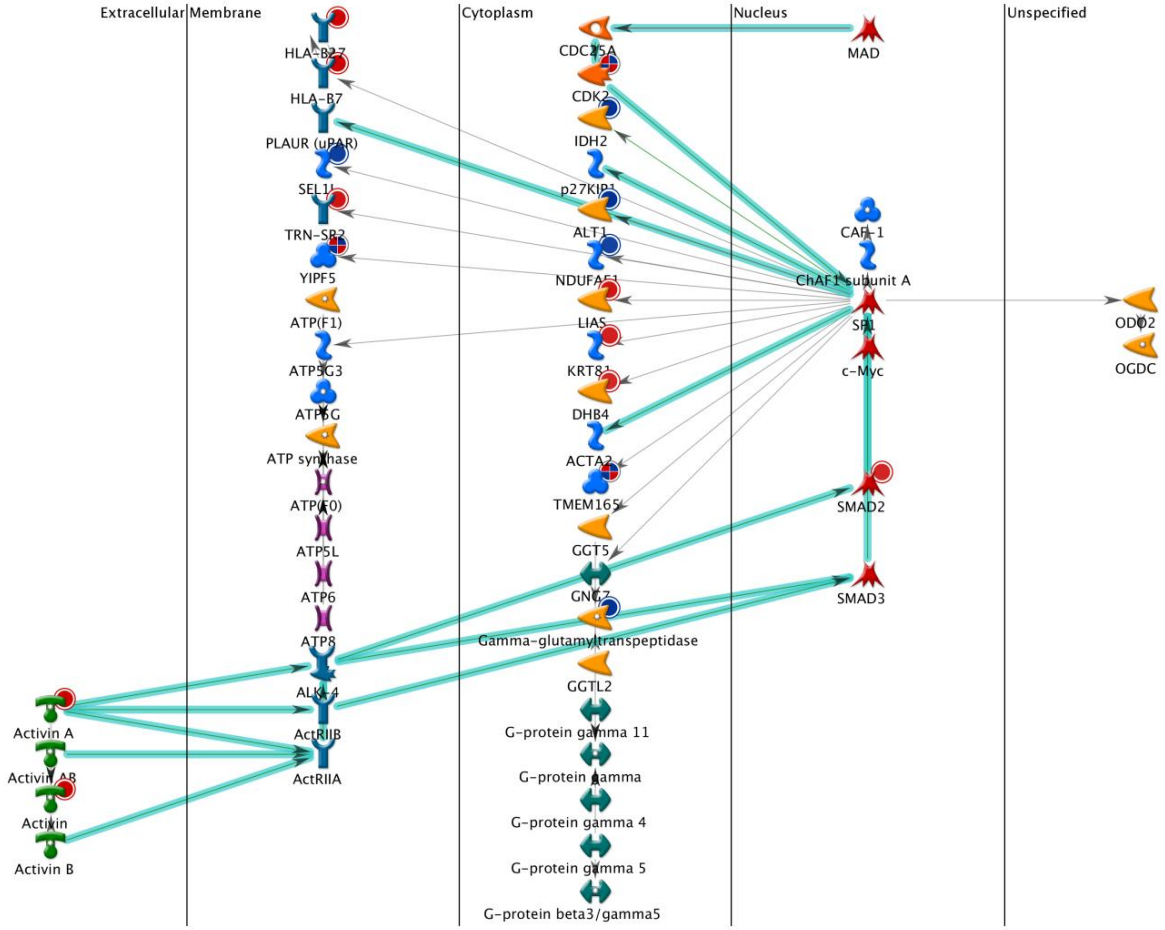

Figure 4.14: Network map 6 of DEGs unique to PTCH1

The network map highlights the signalling to SMAD2 and SMAD3 which may then interact with c-Myc.

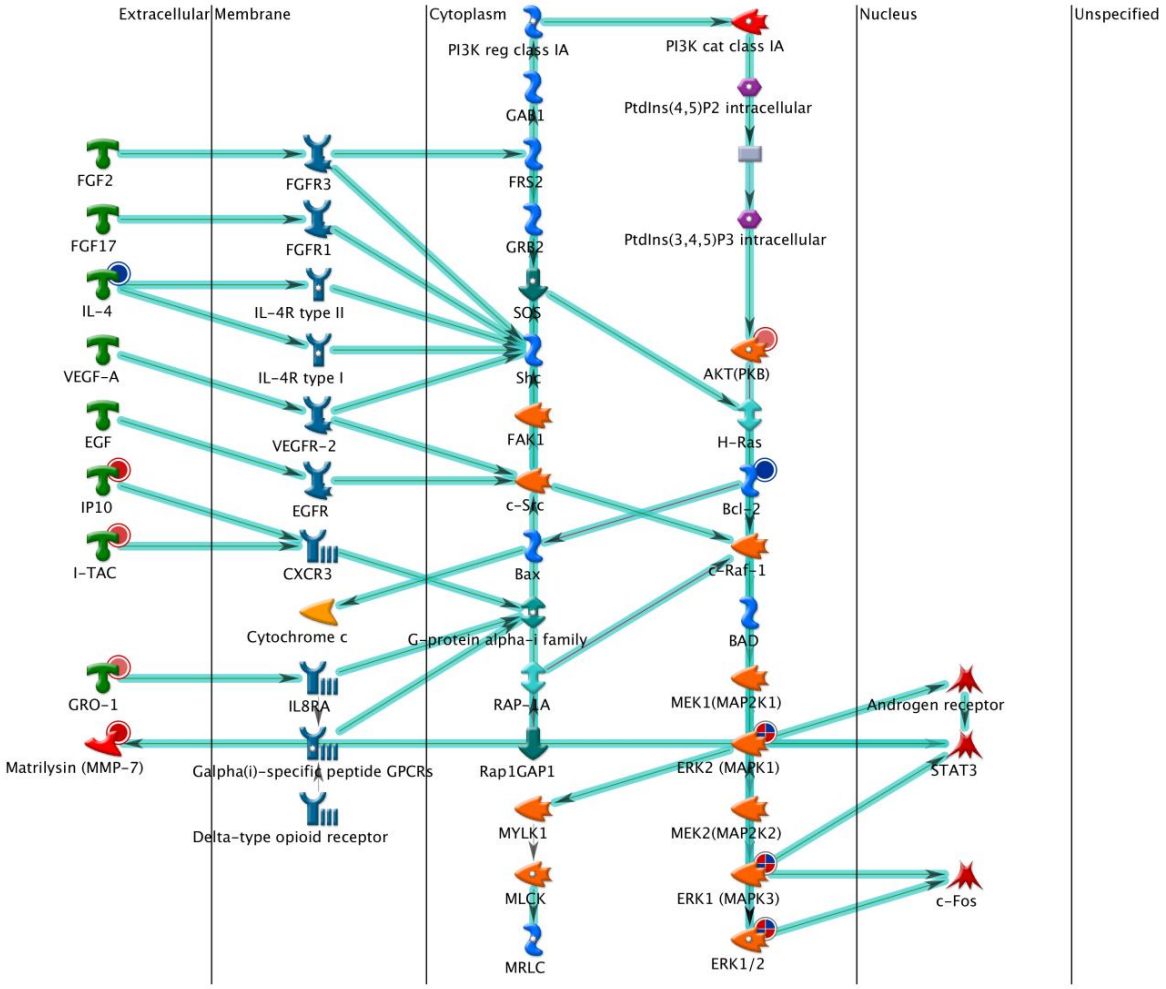

Figure 4.15: Network map 7 of DEGs unique to PTCH1

MEK and ERK signalling is the main feature of this network map and are shown to be associated with Androgen receptor, STAT3 and c-FOS transcription factors and stimulated by EGF, FGF and VEGF ligands and receptors. EGFR downstream targets ERK, MEK, PI3K and AKT appear on the map.

4.4 Discussion

Microarray analysis has revealed a number of interesting pathways and components that may help to better define BCC biology based on the assumption that suppression of PTCH1 plays a significant role in NEB1 cells. Surprisingly, the suppression of PTCH1 in NEB1 cells did not affect 86% of the genes which is interesting as the HH pathway is a major signalling pathway (Figure 4.1). 6% of genes were differentially regulated when comparing NEB1-shPTCH1 with NEB1-shCON cells from which MetaCore network maps were generated.

Microarray data analysis highlights the EGFR signalling pathway in a number of network maps as well as downstream targets such as JNK, MEK and ERK (Figures 4.5, 4.9, 4.10, 4.13 and 4.15). This is interesting as studies have shown that EGFR modulates GLI target genes in N/Tert cells through MEK/ERK pathways (Kasper et al., 2006). HH and EGFR synergy can induce oncogenic transformation via EGFR activation of RAS/RAF/MEK/ERK as well as JUN which was also shown in the array (Schnidar et al., 2009). Downstream of ERK, FOSL1 expression was increased in NEB1-shPTCH1 cells (Table 4.1). FOSL1 forms dimers with JUN pathway proteins to form the AP-1 transcription factor which has been implicated in carcinogenesis (Young and Colburn, 2006).

EGFR and MEK/ERK pathways have also been shown to induce GLI1 and GLI2 expression which may account for GLI1 not being suppressed by SMO inhibitors in NEB1-shPTCH1 cells. Although there is a link between EGFR and GLI1 expression, staining of BCCs reveals that pERK is absent in the majority of tumours (Neill et al., 2008). As such, the EGFR signalling pathway was investigated in further detail and will be discussed later (Chapter 5). Conversely, SHH expression is known to increase EGFR, JNK and Raf phosphorylation which leads to increased MMP-9 expression that is implicated in cell invasion and tumour aggression (Rebecca et al., 2005; Tai et al., 2008). These studies suggest that HH and EGFR pathways may together contribute to tumour invasion through the activation of MMP-9 (Rebecca et al., 2005).

With evidence that the downstream target ERK is differentially regulated in NEB1-shPTCH1 cells, downstream targets such as CXCL11 were highlighted in the microarray and studies have shown that CXCL11 mRNA levels are increased in BCC tissue (Lo et al., 2010). Also, CXCL11 expression increases during skin inflammation therefore there may be a link with stress response pathways and components like caspase (Flier et al., 2001).

Another major signalling pathway to appear in the microarray was the NF-kB pathway (nuclear factor kappa-light-chain-enhancer of activated B cell) (Figures 4.10 and 4.13). NF-kB signalling is involved in inflammatory and innate immune responses and there is evidence that suggests that the pathway is important for tumour development. NF-kB itself is a transcription factor that controls immune factors, proliferation and prevent apoptosis (Karin et al., 2002). The inhibitor of kB kinase complex (IKK) is stimulated by a number of factors including interleukin-1 (IL-1) or the CD40 ligand. IkB proteins that are bound to NF-kB heterodimers are phosphorylated leading to nuclear localisation and transcription of target genes (Karin et al., 2002). Interleukins make up a large group of cytokines with IL-1β, IL-6, IL-8, IL-10, IL-12α and IL-12β highlighted by network analysis (Figure 4.14). IL-1, IL-6, IL-8 and IL-12 are reported to activate or signal through NF-kB whereas IL-10 is thought to inhibit signalling (Parik et al., 2000; Libermann and Baltimore, 1990; Elliott et al., 2001; Weinstock et al., 2003; Wang et al., 1995).

The NF-kB pathway is shown to be involved in skin cancers however there is little known in relation to BCC biology (Sur et al., 2008). In melanoma, NF-kB is up-regulated to deregulate gene transcription and that active NF-kB is able to switch between pro and anti-apoptotic functions in these tumours (Ueda and Richmond, 2006). The NF-kB pathway is known to overlap with a number of different pathways and the IKK promoter contains a p53 binding site that inhibits transcription therefore the loss of p53 results in IKK up-regulation (Gu et al., 2004). This suggests that the loss of or mutational inactivation of p53 leads to activation of the NF-kB pathway. Activation of EGFR has also been reported to stimulate NF-kB signalling and gene transcription. Inhibition of NF-kB reduces activity of certain EGF induced genes such as Cyclin D1 (Haussler et al., 2005).

A study of pancreatic cancer reveals a positive correlation of NF-kB and SHH expression and that inhibition of NF-kB also does suppress SHH (Nakashima et al., 2006). SHH was shown to be induced by IL-1β and TNF-α acting upon NF-kB leading to the hypothesis that pancreatic cancer cell proliferation is accelerated by activation of both HH and NF-kB signalling. This was confirmed by others and further to this, the SHH promoter region was found to contain a NF-kB binding site (Kasperczyk et al., 2009). Silencing of SHH prevented NF-kB stimulated proliferation also, NF-kB inhibition lead to decreased proliferation that could be rescued with the addition of SHH. NF-kB could contribute to GLI1 over expression in NEB1-shPTCH1 cells however SHH expression was decreased in the cells as the HH pathway is constitutively active. NF-kB may be responding to try and suppress the effects but this requires further study.

The p53 signalling pathway and downstream components such as p21 and Cyclin D1 were identified which have been strongly implicated in BCC formation although this is through UV irradiation (Figure 4.11). Regarding NEB1-shPTCH1 cells, these were not UV irradiated however the suppression of PTCH1 could be perceived as a form of cellular stress. This is because the HH pathway is constitutively active resulting in constant GLI1 expression therefore to prevent tumours from forming it is likely that the p53 or other pathways may become active. This may be an attempt to initiate apoptosis which could be examined in NEB1-shPTCH1 cells in future studies. Mouse models utilising $PTCH^{+/-}$ mice show that after UV irradiation, the mice develop nodular and infiltrative BCCs (Mancuso et al., 2004). As UV irradiation is a common initiator of BCC tumour formation, NEB1-shPTCH1 could be UV irradiated and then investigated further. This could be the event which is required for NEB1-shPTCH1 cells to develop tumours in organotypic culture for example. As there is no UV related damage in NEB1-shPTCH1 cells, it would be better to focus on EGFR signalling and downstream components as it is more relevant to our current BCC model although the p53 pathway is an important pathway to explore in the future.

A number of caspases were identified and clustered together in a network pathway (Figure 4.9). There are two main ways in which cells are targeted and disposed of, necrosis and apoptosis. Necrosis can be triggered when the targeted cell plasma membrane is ruptured so that an inflammatory response is generated (Brown, 2008). The second method is apoptosis. This is thought of as a cleaner form of cell death where DNA is fragmented forming apoptotic bodies that are phagocytosed by macrophages (Lauberet al., 2004). This results in cell death without an inflammatory response. In mammalian cells, apoptosis may occur via three modes which are the extrinsic, the intrinsic and the Granzyme B pathways (Ghavami et al., 2009). The extrinsic pathway is triggered by the ligation of cell death receptors (e.g. tumour necrosis factors, TNF) and involves the activation of caspase-8. The intrinsic pathway is initiated by cellular stress with subsequent activation of caspase-9 and this route involves the mitochondria as well as anti-apoptotic factors such as Bcl-2. Regarding BCCs, the intrinsic pathway is more relevant as UV exposure is a factor that is known to cause BCC formation. The role of UV-induced caspase-9 is known to be cell specific and shown to be active and play an important role in UV-induced apoptosis in human keratinocytes (Sitailo et al., 2002). Caspase-9 is an initiator of apoptosis and it was shown that in HaCaT cells with two mutant p53 alleles, UV-induced apoptosis was inhibited. Therefore mutations of caspases have the potential to prevent apoptosis of potential tumour cells. Along with the p53 pathway, caspase expression could be characterised in NEB1-shPTCH1 cell for future experiments.

As the EGFR pathway is shown to be differentially regulated, it is possible that the PI3K/AKT pathway is active as caspases are negatively regulated to inhibit apoptosis (Cardone et al., 1998; Brunet et al., 1999). AKT has also been shown to activate IKK (Li and Stark, 2002). Studies show that AKT is important for HH signalling as AKT positively regulates HH signalling implying that both pathways work in tandem and are required for embryonic development (Riobo et al., 2006 A). In BCC biology there is conflicting data regarding pAKT levels and activity in tumours however this may depend on the tumour environment as factors such as the expression of caspases for example.

Structural proteins were clustered together in a network map (Figure 4.12). Fibronectin binds cell surfaces and interact with other structural proteins including collagen, actin and heparin. Fibronectin is involved in processes including cell adhesion, migration, cell shape maintenance and wound healing. Histological studies of BCC reveal that fibronectin is strongly expressed in the stroma and concentrated around tumour islands. Fibronectin mRNA was localised in the stromal cells as well as in the central areas of the tumour islands (Peltonen et al., 1988). This suggests that the tumour cells regulate fibronectin expression in the stroma and may also explain why BCCs are rarely metastatic and locally destructive. Another study has compared actin expression between stromal tissue and tumour islands of BCC. Actin was expressed in the tumour islands in both aggressive and non-aggressive BCC however, strong expression was found in the stroma of the more aggressive BCCs (Adegboyega et al., 2010). Other studies have shown similar results where actin was present in the infiltrative component of 13/13 nodular BCCs as well as in 8/13 showing stromal staining. There was no actin present in the stroma on non-infiltrative nodular BCCs (Law et al., 2003). These studies suggest that actin expression may contribute in tumour invasiveness and aggression. Collagen IV consists of a number of collagen chain subunits that are bound together to give the fibres structural stability. Histological studies of Collagen IV show the protein to be expressed around the tumour islands and in the surrounding skin. Defects were found in the α1 subunit and the protein was absent in invasive tumours (Marasa et al., 2008; Quatresooz et al., 2003).

NEB1-shPTCH1 cells display a tight colony formation which implies that in two-dimensional culture, these structural proteins may be expressed to maintain this morphology (Figure 3.4). Based on studies that show stromal fibronectin, actin and collagen IV, the expression of these may differ depending on tumour progression. There are a number of features that NEB1-shPTCH1 cells possess suggesting that they may have tumourigenic potential but another factor to consider is that a tumour mass usually forms in order to establish the tumour before invasion. Once the tumour mass stabilises it is then viable to invade and spread at which point

the expression of fibronectin for example may change. To understand more about this, NEB1-shPTCH1 cells could be cultured with fibroblasts and then the expression of fibronectin, actin and collagen IV analysed by immunocytochemistry. Although NEB1-shPTCH1 cells did not show tumourigenic potential in organotypic cultures, the cells may signal to the fibroblasts within the dermis component of the culture. If actin is expressed in NEB1-shPTCH1 cells and increased in fibroblasts this would suggest that NEB1-shPTCH1 cells have the potential to invade based on previous studies of BCC (Law et al., 2003).

MMP-2 and MMP-9 are known to degrade collagen IV proteins which are associated with tumour invasion in a number of cancers. Malignant SCCs and melanoma tissue has been shown to express increased levels of MMP-2 mRNA (Orimoto et al., 2008). While MMP-2 protein expression was shown to be mostly absent in BCCs, MMP-9 protein was strongly expressed in aggressive tumours (Karahan et al., 2011). The significantly increased mRNA expression of MMP-2 (~8 fold) and MMP-9 (~16 fold) in NEB1-shPTCH1 cells (Figure 4.3) would imply that the cells have the potential to migrate however, morphologically NEB1-shPTCH1 cells form tight colonies and are slow growing (Figure 3.4 and 3.26). A histological study of BCC reveals the absence of MMP-2 protein in all BCC subtypes whereas MMP-9 is strongly expressed with increased intensity in correlation to tumour aggressiveness (Karahan et al., 2011). A more interesting observation was the substantial increase of MMP-9 mRNA expression (~182 fold) upon NEB1-shPTCH1 cell treatment with Cyclopamine-KAAD (Figure 4.3 A). For future experiments, migration or scratch assays could be performed to investigate the effect of Cyclopamine-KAAD in NEB1-shPTCH1 cells. When cells were treated with SMO inhibitors, I did not observe any change in morphology however it would be interesting to determine if collagen IV expression is reduced and if this is the case, there could be other factors that are preventing the cells from migrating.

Tenascin C (TNC) is an ECM glycoprotein identified from the microarray (Table 4.1) that has the capacity to bind with fibronectin. TNC is reported to have anti-adhesive properties related to binding with fibronectin preventing its functionality (Latijnhouwers et al., 2000). Fibroblasts extracted from healthy skin in Gorlin's patients ($PTCH^{+/-}$) were analysed for BCC components and TNC was one of the components that was over expressed (Valin et al., 2009). Furthermore, studies of TNC in skin tumours revealed TNC mRNA expression in BCC, SCC and melanoma tumour masses (Tuominen et al., 1997). A study of endometrial carcinoma (tumours that arise from the lining of the uterus) showed strong expression of TNC particularly in the most aggressive and invasive tumours (Doi et al., 1996). Strong levels of TNC were associated with reduced levels of oestrogen receptor and increased levels of TGF-β1 which supports the idea

that TNC is associated with tumour cell motility, invasion and further proliferation. Interestingly, TGF-β2 was shown to be increased in NEB1-shPTCH1 cells and other components of the pathway differentially expressed (Table 4.1 B and Figure 4.6).

FABPs are responsible the shuttling of lipids, solubilising fatty acids and transporting them. Epidermal-FABP (E-FABP) is exclusive to keratinocytes and was shown in the microarray (Figure 4.10). E-FABP expression is elevated in the keratinocytes of healing wounds (Kusakari et al., 2006). E-FABP expression is thought to be expressed in relation to keratinocyte differentiation and it has been shown that E-FABP is negative in BCCs and SCCs (Masouye et al., 1996).

DAVID gene annotation software was used to map the DEGs that were unique to PTCH1 onto network maps i.e. genes that are differentially expressed due to the suppression of PTCH1 and that did not return to basal levels upon Cyclopamine-KAAD treatment. This was to uncover potential genes and pathways that may induce GLI1 expression in NEB1-shPTCH1 cells accounting for the lack of response to SMO inhibitors. A number of the DEGs were highlighted in a map summarises pathways involved in cancer (Figure 4.4). A number of MAPK pathways were identified from the microarray which will be discussed in Chapter 5 (Figure 4.5).

A major pathway to emerge from the data is the TGF-β signalling pathway (Figure 4.6) which has been linked to the HH pathway (Cretnik et al., 2009). TGF-β has been reported to induce both GLI1 and GLI2 expression in keratinocytes and increased GLI expression was maintained in the presence of the SMO inhibitor Cyclopamine. This suggests that both GLI proteins can function independently of SMO (Dennler et al., 2007). TGF-β and SMAD pathway component mRNA is reported to be elevated in BCC (Gambichler et al., 2007). The TGF-β signalling pathway controls differentiation and proliferation among other functions and acts with the TGF-α cytokine to induce cell transformation as well as initiate apoptosis (Schuster and Krieglstein, 2002). SMAD and TAK1 are components of the TGF-β pathway and were highlighted in the microarray. It is possible that GLI1 over-expression in NEB1-shPTCH1 cells is mediated through the TGF-β pathway. It is also worth noting that TGF-β may be involved in regulating apoptosis as a number of caspases were differentially regulated.

A number of TLRs were clustered together from the microarray (Figure 4.7). TLRs make up a family of receptors that are important for host defence from infection. There is also evidence that TLRs are important for tissue homeostasis maintenance and the regulation of inflammatory responses. Downstream of TLR, TRAF6 phosphorylates TAK1 which ultimately leads to NF-kB and MAPK pathways activation (Kawai and Akira, 2006). As well as TRAF6 and

TAK1, TLR2 and TLR4 were also shown in the pathway map. TLR expression is reported to be increased in tumours and polymorphisms of TLR2 and TLR4 have been associated with increased risk and tumour progression (El-Omar et al., 2008). TLR gene expression could be used to detect melanoma and antagonists of TLRs can inhibit melanoma cell migration (So and Ouchi, 2010). In BCCs Imiquimod creams are used as a treatment which acts via TLR-7 activation. It is not clear exactly how the cream works however IL-1, IL-6, IL-12 and TNF-α cytokines are thought to play a role. This method has been shown to be successful for the treatment of superficial BCCs (Stockfleth et al., 2003). NEB1-shPTCH1 cells may cause the expression of TLRs in response to stress in similar fashion to the p53 pathway however the overlap of NF-kB signalling may be a factor which responds to HH signalling.

Other interesting genes that emerged from the microarray include SNAI1, THY1, Vimentin (VIM) and KRT15 (Table 4.1 and Figure 4.3 B). SNAI1 is a target gene for HH signalling which promotes epithelial to mesenchymal transition (EMT) where cells lose the expression of genes such as E-cadherin thus allowing for cells to migrate or invade in the case of tumour cells (Katoh and Katoh, 2009). SNAI1 has also been reported to co-express with GLI1 in hair follicles and skin tumours. The over-expression of SNAI1 in RK3E rat kidney cell lines also induced GLI1. Conversely, the over expression of GLI1 in basal mouse keratinocytes induced SNAI1 expression and cell proliferation in the IFE (Li et al., 2006). THY1 also known as CD90 is thought to affect intra-cellular signalling and modulate adhesion and migration. By comparing THY1 positive to THY1 negative fibroblasts, it was discovered that THY1 regulates RHO GTPase which is important for cytoskeletal organisation and cellular adhesion. THY1 or CD90 is a cancer stem cell marker (Barker et al., 2004).

VIM is a member of the intermediate filament family along with microtubules and actin. VIM is responsible for maintaining cell shape, integrity of the cytoplasm and stabilising cytoskeletal interactions. During normal conditions, cells express keratins and are generally stable but as VIM is expressed, this drives EMT (Gilles et al., 1996). VIM expression in prostate cancer and SCC has been shown to correlate with tumour invasiveness (Singh et al., 2003; Tomson et al., 1996). In contrast, the decrease of keratins is thought to be associated with tumour progression such as KRT19 in SCC and KRT15 in psoriasis (Crowe et al., 1999; Waseem et al., 1999). Suppression of VIM in SCC derived cells reduced proliferation, migration and invasion and also re-expressed KRT13, KRT14 and KRT15 (Paccione et al., 2008). These cells also showed significantly reduced tumourigenic potential as they were approximately 70% smaller than control SCC cells. Regarding BCC, tumours have been shown to originate from hair follicle stem cells that express KRT15 as seen in $PTCH1^{+/-}$ mice upon X-ray irradiation (Wang et al., 2011).

qPCR validation of the microarray for SNAI1, THY1 and VIM show that the expression of these DEGs are increased in NEB1-shPTCH1 cells (Figure 4.3 B). KRT15 expression is significantly reduced by qPCR whereas it is slightly increased from the microarray so this requires further validation. The stem cell marker nestin (NES) was also highlighted as a DEG and this is an intermediate filament protein (Table 4.1). NES is expressed in dividing cells of the central nervous system (CNS) among other tissues such as the bulge region of hair follicles (Hoffman, 2007). NES is over-expressed in various tumours including prostate, breast and melanoma (Kleeberger et al., 2007; Li et al., 2007; Brychtova et al., 2007).

Neutrophil gelatinase associated lipocalin (LCN2) is a soluble protein that carries small molecules to cells, specifically dimerising with MMP-9 (Kjeldsen et al., 1993). LCN2 that is detectable in serum is known to be increased on psoriatic patients and in general, an indicator of increased inflammation (Kamata et al., 2012). Normal skin expresses LCN2 and it is induced in skin disorders such as psoriasis and SCC while BCCs however were negative for LCN2 expression (Mallbris et al., 2002). This suggests that LCN2 is over-expressed in NEB1-shPTCH1 cells is the result of inflammation which correlates with the stress response pathways identified by microarray analysis. In endometrial cancer, increased LCN2 expression correlated with aggressiveness and a greater chance of reoccurrence (Mannelqvist et al., 2012). In a study of breast cancer LCN2 was reported to induce EMT as well as angiogenesis via VEGF signalling (Yang et al., 2012). LCN2 was also shown to regulate the HIF-1α transcription factor thorough ERK. Elevated LCN2 in NEB1-shPTCH1 cells may be signalling through ERK to increase certain downstream targets and this requires further exploration as LCN2 is a marker for aggressiveness in tumours.

Insulin-like growth factor binding protein 2 (IGFBP2) is a regulator of the IGF pathway that is pro-survival and anti-apoptotic. IGFBP2 which was identified in the microarray with a -2.2759 fold reduction in NEB1-shPTCH1 cells compared to NEB1-shCON cells (Table 4.1). Interestingly, a study of human and mouse BCC showed increased IGFBP2 expression after the loss of PTCH1 expression (Villani et al., 2010). Furthermore, mice that over express SHH display increased expression of IGFBP2 in hair follicle cells (Harris et al., 2010). These studies suggest that IGFBP2 expression is important in the hair follicle and that BCCs that arise from hair follicles may express IGFBP2 for that reason. NEB1-shPTCH1 cells are keratinocytes and if they have the capacity to develop into BCCs, this may not be associated with increased IGFBP2 expression. Another reason may be that IGFBP2 increases after the tumour initiation in NEB1-shPTCH1 cells. These studies also suggest that perhaps it would be better to model BCC by suppressing

PTCH1 in ORS or cells from the bulge region. It would be interesting to compare the differences between hair follicle cells and keratinocytes.

The behaviour of NEB1-shPTCH1 cells in two-dimensional culture suggests that genes such as SNAI1 and VIM expression would be reduced as the cells form tight colonies. These genes suggest that NEB1-shPTCH1 cells are capable of EMT and could be aggressive and invasive. If indeed KRT15 is reduced in NEB1-shPTCH1 cells, this would correlate with VIM expression. For this reason, NEB1-shPTCH1 cells should be further characterised in organotypic cultures as certain areas may have localised expression of the protein i.e. in areas of hyperproliferation for example.

The data obtained from the microarray analysis provides a number of genes that are related to BCC biology and tumourigenesis as well as pathways that may account for non-canonical modes of GLI1 expression. A number of pathways represent ways by which NEB1-shPTCH1 cells could overcome the effects of SMO inhibitors one of which is the ERK signalling pathway.

Chapter 5

EGFR signalling in NEB1-shPTCH1 cells

Chapter 5 Introduction

Microarray analysis of NEB1-shPTCH1 cells revealed that a number of major signalling pathways are affected by the suppression of PTCH1. One significant pathway that was highlighted was the MEK/ERK pathway downstream of EGFR signalling. It has been shown that EGFR signalling modulates the expression of GLI1 in N/Tert keratinocytes and that a number of genes could be induced synergistically by GLI1 and EGF treatment. Furthermore, the GLI1 target genes were modulated by EGFR signalling via MEK/ERK pathways (Kasper et al., 2006). Other studies have demonstrated that GLI1 and GLI2 expression is induced by EGFR mediated MEK/ERK signalling and that mouse BCCs treated with EGFR and GLI inhibitors reduced tumour growth (Schnidar et al., 2009).

In contrast, the Neill group has previously shown that the over expression of GLI1 in N/Tert cells reduces EGFR expression and that ERK activity is also repressed. Furthermore, pERK protein was not expressed in 13/14 BCC tumours whereas it was expressed in the epidermis indicating that the loss of pERK may be important for tumour formation (Neill et al. 2008). These contradictions in the literature warrant further investigation to determine if MEK/ERK signalling is a viable therapeutic target for BCC treatment. As such, NEB1-shPTCH1 cells were analysed for the expression of EGFR signalling and downstream MEK/ERK components.

5.1 Analysis of EGFR pathway activity in shPTCH1 cells

MetaCore analysis of the DNA microarray indicated that ERK signalling was more active in NEB1-shPTCH1 cells compared to the control (Figures 4.3, 4.5 and 4.13). Our research group has previously shown that ectopic GLI1 suppresses EGFR expression and ERK activity in N/Tert keratinocytes and that the active phosphorylated form of ERK (pERK) is predominantly absent in human BCC (Neill et al., 2008). In contrast, others have shown that EGFR signalling (via MEK/ERK/JUN) is strong in mouse BCC cell lines and that co-targeting EGFR and HH signalling has an additive effect in suppressing the growth of these cells (Schnidar et al., 2009). Therefore, the extent of EGFR/MEK/ERK signalling was investigated in NEB1-shPTCH1 cells.

EGFR expression was shown to be reduced at the mRNA level and also by western blotting (Figure 5.1 A and B). Downstream of EGFR, pMEK and pERK protein levels were also reduced in NEB1-shPTCH1 cells compared to NEB1-shCON cells (Figure 5.1 C). To confirm if MEK/ERK signalling expression was reduced in NEB1-shPTCH1 cell, the expression of several target genes known to be activated by MEK/ERK signalling including FOS, JUN and MYC were investigated by qPCR in NEB1 and N/Tert cells (Figure 5.2 and 5.3). The expression of all these genes was increased in NEB1-shPTCH1 cells (189A) and this was additionally confirmed in NEB1-29A cells. Similar results were obtained from N/Tert-shPTCH1 cells although the fold inductions were not as high as those in NEB1-shPTCH1 cells.

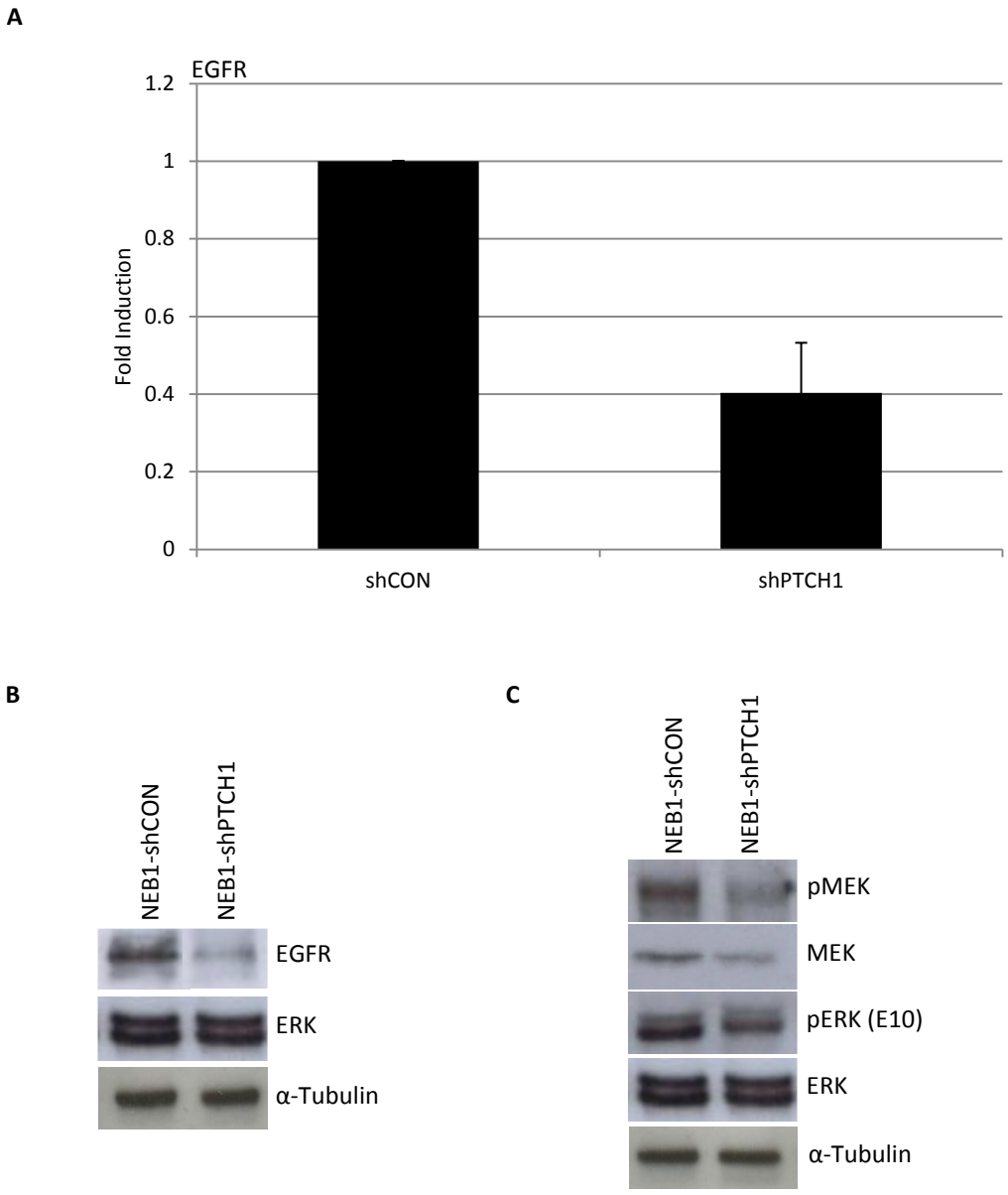

Figure 5.1: EGFR pathway expression in NEB1 cells

EGFR analysis by [A] qPCR and [B] western blotting.

EGFR protein analysis of NEB1-shCON and NEB1-shPTCH1 cells by [**A**] Immunocytochemistry and [**B**] western blot in NEB1 cells. [**C**] Western blot for EGFR downstream targets pERK (E10), pMEK, MEK, ERK with α-Tubulin loading control.

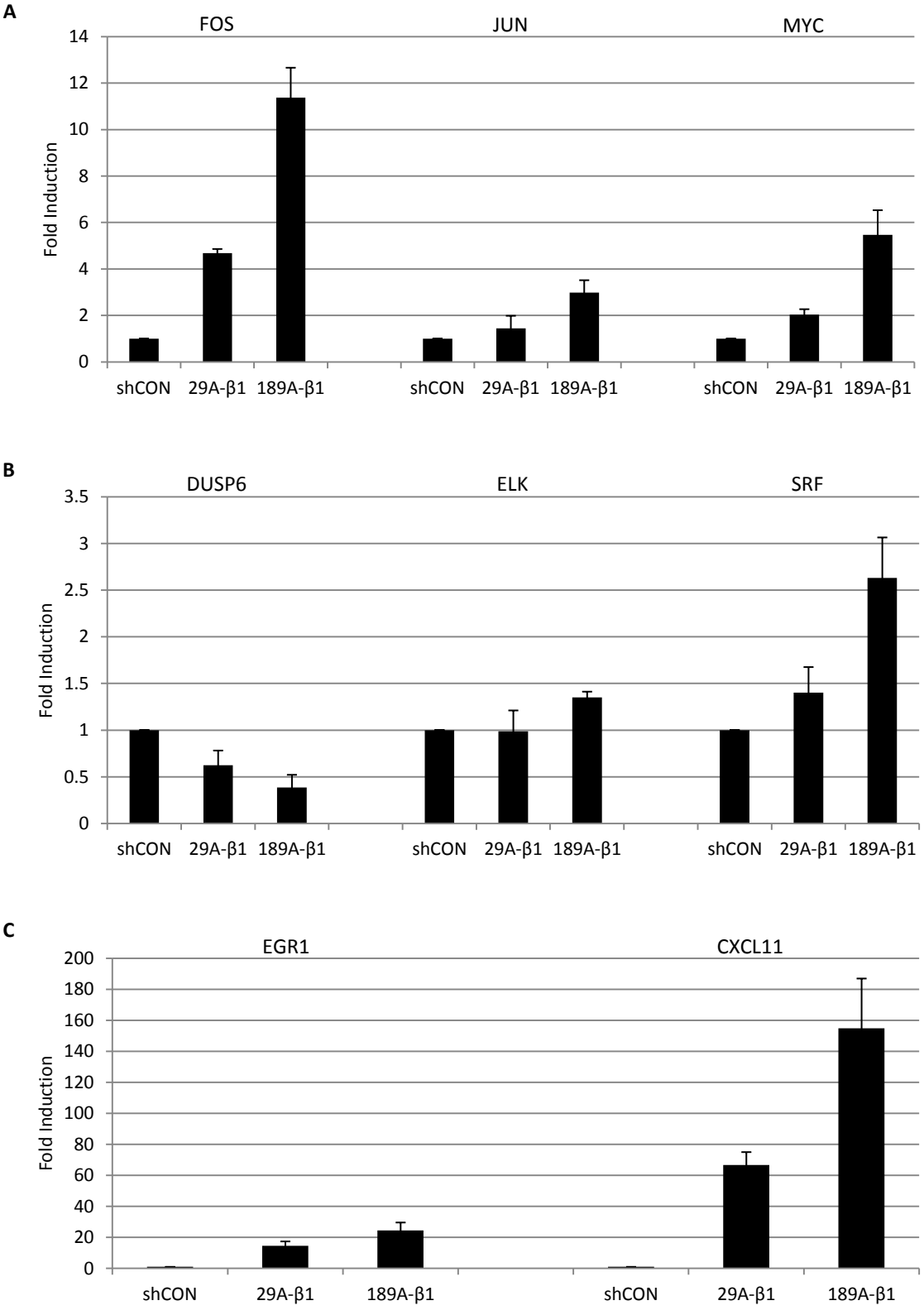

Figure 5.2: qPCR for ERK target genes in NEB1 cells

[**A**] FOS, JUN, MYC, [**B**] DUSP6, ELK, SRF, [**C**] EGR1 and CXCL11 mRNA expression in NEB1 cells.

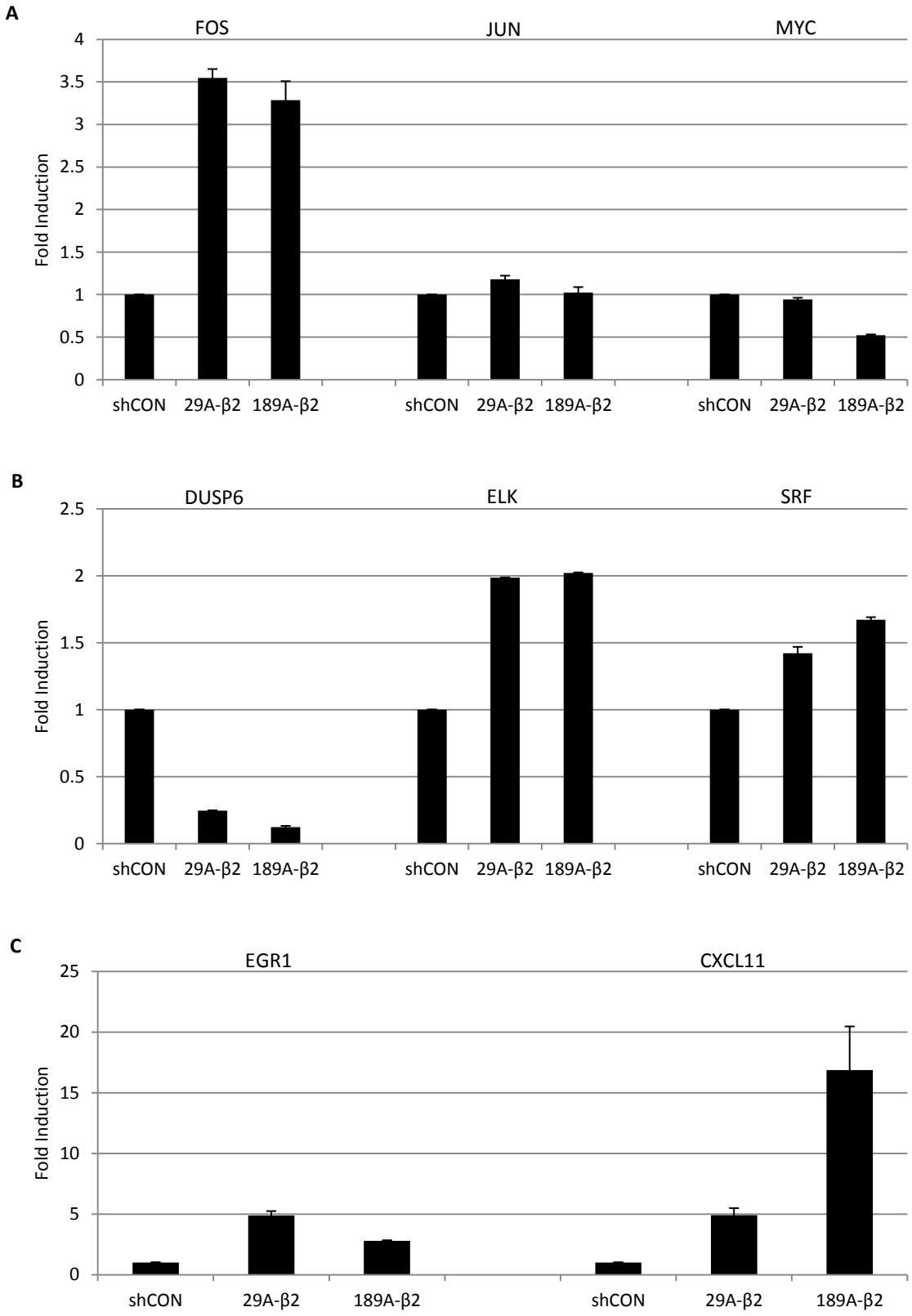

Figure 5.3: qPCR for ERK target genes in N/Tert cells

[**A**] FOS, JUN, MYC, [**B**] DUSP6, ELK, SRF, [**C**] EGR1 and CXCL11 mRNA expression in N/Tert cells.

At the mRNA level, there is evidence that the ERK signalling pathway is active however western blotting revealed that protein levels of MEK, pMEK and pERK were decreased in NEB1-shPTCH1 cells compared to NEB1-shCON cells. This correlates with the finding that EGFR protein expression was reduced in NEB1-shPTCH1 cells however it does not explain why ERK target genes would be increased. Intriguingly, immunocytochemical analysis of pEGFR revealed an increase of nuclear localisation in NEB1-shPTCH1 cells (Figure 5.4 A). The reason for this is unclear but it could account for reduced MEK/ERK signalling due to weaker signals emanating from the outer cell membrane. Nuclear EGFR translocation is induced in cultured cells exposed to DNA damaging agents (including UVB irradiation) where it is linked with DNA repair and suppression of the apoptotic response (Xu et al., 2009).

Further analysis by immunocytochemistry revealed that pERK was more localised in the nucleus in NEB1-shPTCH1 cells which could account for the increase of the pERK target genes (Figure 5.4 B). Also, immunocytochemical analysis of pMEK localisation was inconclusive although there was some evidence of nuclear pMEK in NEB1-shPTCH1 cells that was not observed in NEB1-shCON cells (Figure 5.4 C).

Nuclear EGFR has signalling capability and has been shown to activate expression of the target genes COX2, iNOS and STAT3 (Wang et al., 2010). However, no increase of any known nuclear EGFR target gene was observed in NEB1-shPTCH1 cells and this was not pursued further (Figure 5.5).

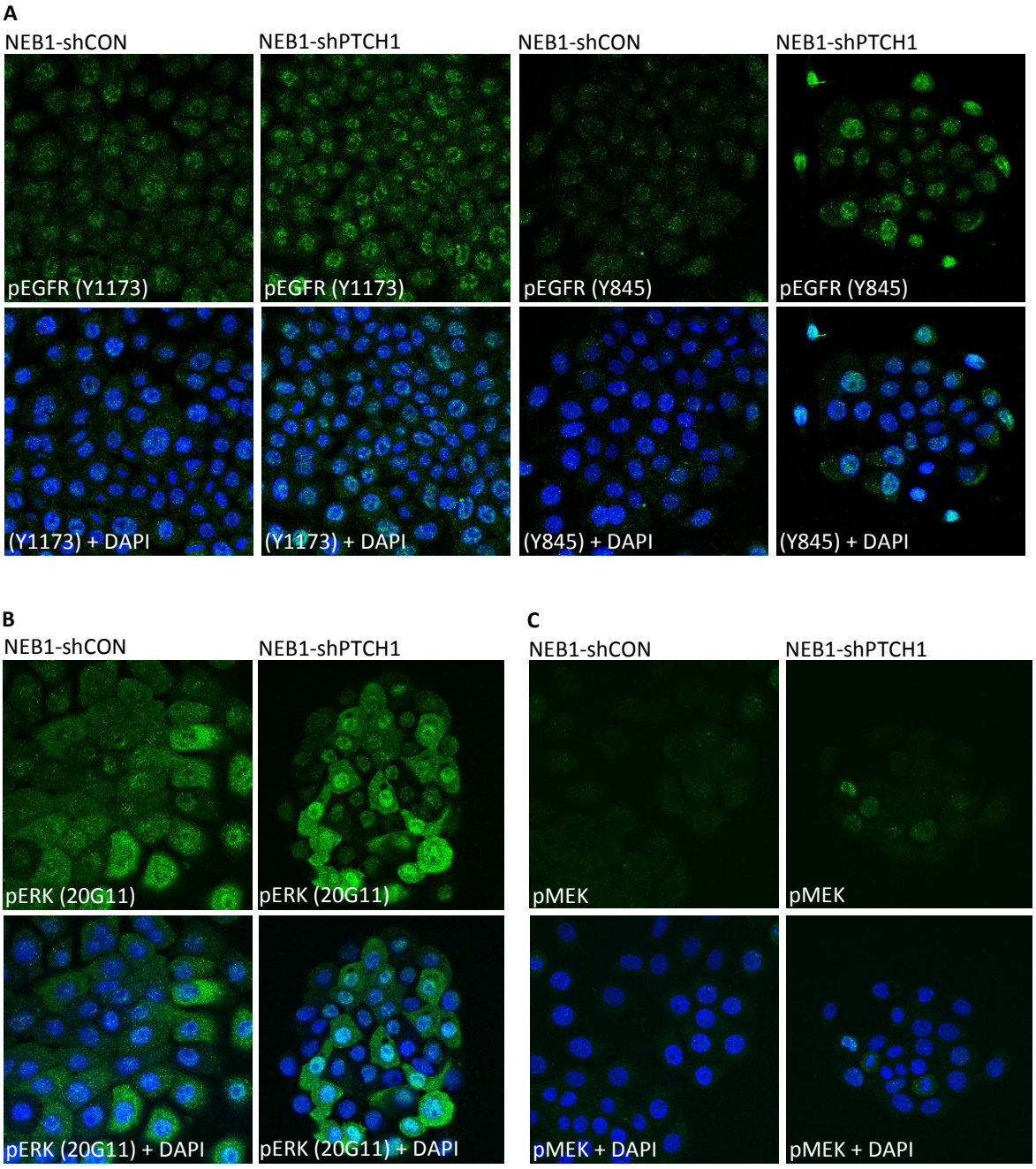

Figure 5.4: pEGFR, pERK and pMEK protein expression in NEB1 cells

Immunofluorescence staining of [**A**] pEGFR (Y1173 and Y845), [**B**] pERK (20G11) and [**C**] pMEK in NEB1-shCON and NEB1-shPTCH1 cells.

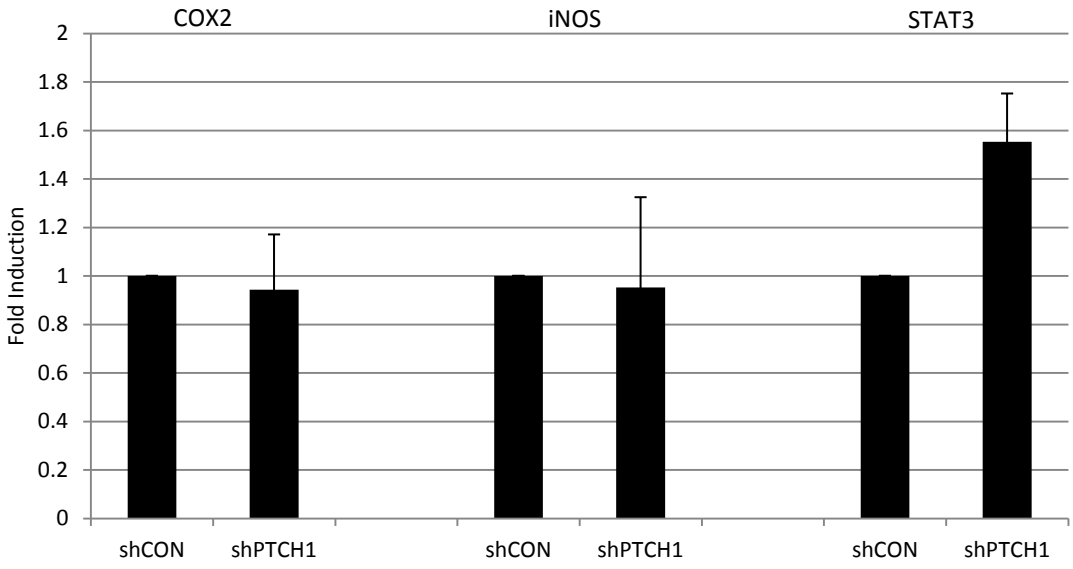

Figure 5.5: qPCR for EGFR target genes in NEB1 cells

5.2 EGFR signalling and control of GLI expression in shPTCH1 cells

Several studies have shown that GLI1 transcriptional activity is increased by MEK/ERK signalling and it has also been shown that GLI1 expression is actually induced by MEK/ERK signalling (Schnidar et al., 2009). To determine if MEK/ERK signalling regulates the increase of GLI1 in NEB1-shPTCH1 cells, cultures were exposed to the MEK inhibitor U0126 as well as the EGFR inhibitor AG1478. The expression of GLI1 returned to basal levels in the presence of both U0126 and AG1478 indicating that the increase of GLI1 is mediated by EGFR/MEK/ERK signalling (Figure 5.6). Intriguingly, inhibition of EGFR, led to an increase of GLI2 mRNA levels which raises concerns about the use of anti-EGFR compounds for the treatment of BCC and possibly other tumours.

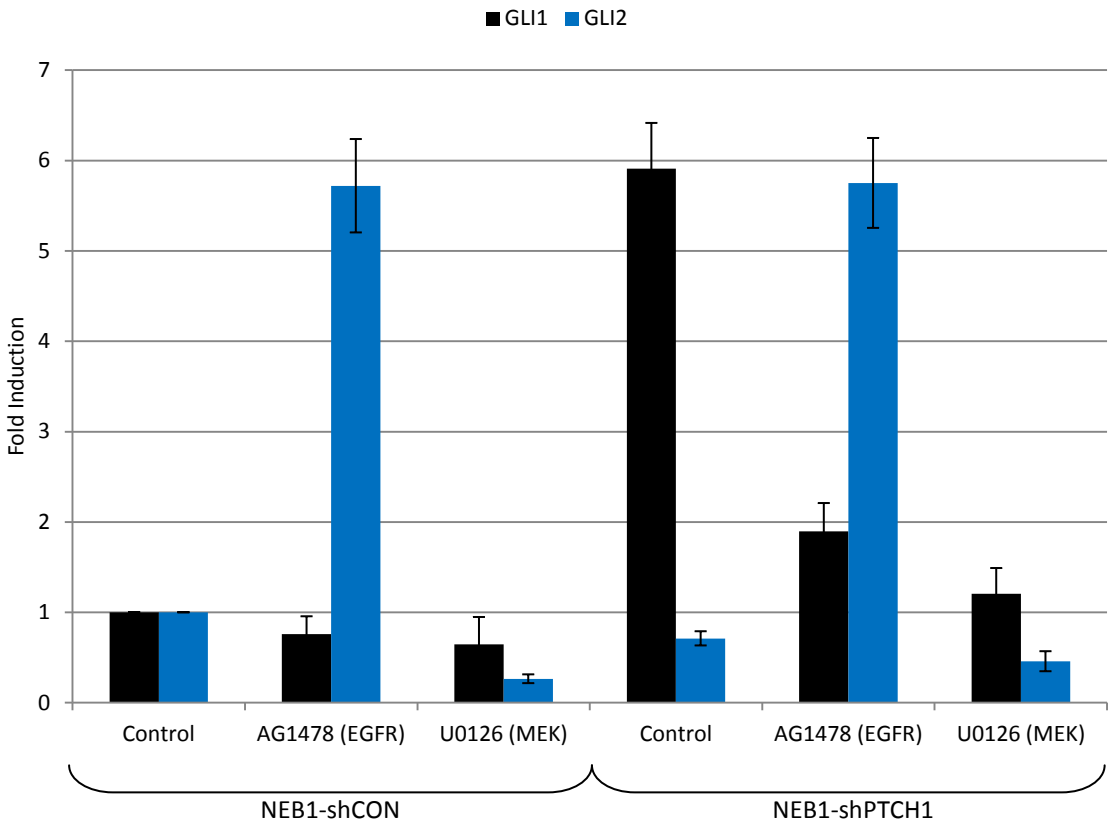

Figure 5.6: NEB1 cells treated with EGFR and MEK inhibitors

NEB1 cells were treated with AG1478 (1μM) or U0126 (10μM) for 24 hours. Error bars represent mean ± standard deviation.

5.3 Discussion

The EGFR signalling pathway and its downstream targets are altered in NEB1-shPTCH1 cells due to the suppression of PTCH1. The Neill group has previously shown that EGFR signalling influences GLI1 target genes in human keratinocytes and that strong GLI1 activity negatively regulates EGFR/ERK signalling (Neill et al., 2008). The previous study involved over expressing GLI1 in N/Tert keratinocytes using an EGFP-GLI1 fusion protein whereas this study utilised NEB1-shPTCH1 cells with a modest increase of GLI1 levels however there was a reduction in EGFR mRNA expression in NEB1-shPTCH1 cells compared to NEB1-shCON cells (Figure 5.1). Interestingly, analysis of pEGFR (Y1173 and Y845) showed increased nuclear expression in NEB1-shPTCH1 cells compared to NEB1-shCON cells (Figure 5.5 A). Phosphorylation of Y845 has been implicated in maintaining activation of EGFR (Hubbard et al., 1994) while Y1173 phosphorylation has been linked to ERK activation (Hsu et al., 2011). Despite a decrease in EGFR protein and mRNA expression in NEB1-shPTCH1 cells, downstream ERK and its target genes are more active.

Western blot analysis of EGFR downstream targets pERK and pMEK showed that there was reduced expression in NEB1-shPTCH1 cells compared to NEB1-shCON cells (Figure 5.4). Similar to pEGFR expression, there was increased nuclear staining for pERK and pMEK in NEB1-shPTCH1 cells compared to NEB1-shCON cells (Figure 5.5 B and C). Again, this suggests that pERK and pMEK are more active in NEB1-shPTCH1 due to nuclear protein localisation. However, without a MEK/ERK reporter construct, it would be difficult to determine if ERK is more active in the cells. NEB1 cells were difficult to lyse as discussed earlier when attempting to perform a Luciferase assay therefore ERK target genes were analysed (Figures 5.2 and 5.3).

Based on the data obtained from the microarray that suggests EGFR signalling is differentially regulated, ERK target genes were analysed by qPCR in both NEB1 and N/Tert cells. Downstream targets of ERK were increased in NEB1-shPTCH1 cells compared to NEB1-shCON cells (Figure 5.2) and also a similar trend was seen in N/Tert cells although not in all ERK targets (Figure 5.3). As ERK is phosphorylated and translocates to the nucleus, it acts upon FOS, JUN, MYC and ELK transcription factors (Kerkhoff and Rapp, 1998). FOS and SRF are known to bind to each other to regulate DNA binding activity (Prywes et al., 1988). Also, activated ERK has been shown to induce phosphorylation of ELK (Cruzalequi et al., 1999). EGR1 expression in PC3 prostate cell lines has been shown to be mediated through the EGF induced ERK signalling pathway (Gregg and Fraizer, 2011). CXCL11 is part of the CXC chemokine family and binds to the CXC Receptor 3 (CXCR3) that is involved in T-cell recruitment and skin immune response

(Lo et al., 2010). A study has shown that inhibition of the ERK pathway results in the suppression of CXCL11 (Hosokawa et al., 2010). This along with the nuclear expression of pEGFR that may lead to increased expression of pERK and pMEK supports the idea that ERK signalling is more active in NEB1-shPTCH1 cells compared to NEB1-shCON cells.

One potential explanation for increased nuclear pERK is the suppression of DUSP6. DUSP6 dephosphorylates pERK to inhibit pathway activity therefore, a decrease in DUSP6 mRNA expression correlates to the fact that there is increased nuclear pERK in NEB1-shPTCH1 cells but this is contradicted by lower levels of pERK protein shown by western blotting. Indeed, $DUSP6^{-/-}$ mice display increased levels of ERK signalling and a feature of this is reduced apoptosis (Maillet et al., 2008). Another reason for the changes in EGFR signalling could be a stress response due to the suppression of PTCH1 that results in GLI1 activation. Nuclear EGFR translocation is known to be induced in human keratinocytes exposed to UV irradiation and functionally, nuclear EGFR is associated with transcription, proliferation and DNA repair (Wang et al., 2010). Suppression of PTCH1 in NEB1-shPTCH1 cells could induce a similar stress response whereby there is an increase in nuclear pEGFR expression.

As mentioned earlier, the EGFR and HH signalling pathways are likely to be linked and that the over expression of GLI1 leads to differential expression of EGFR components in keratinocyte cell lines. The tight colony formation observed in NEB1-shPTCH1 cells was also observed when GLI1 was over expressed in N/Tert keratinocyes (Neill et al., 2008). In contrast, studies have shown that the EGFR and HH pathways are synergistically linked as demonstrated in N/Tert keratinocytes where 19 genes were found to be induced synergistically by GLI1 and EGF treatment also; GLI1 target genes were shown to be modulated by EGFR signalling through MEK/ERK pathways (Kasper et al., 2006). This is further supported by the study of mouse BCC cell lines ASZ001 and BSZ2 ($Ptch^{-/-}$) as well as CSZ1 ($p53^{-/-}$). These cell lines express higher levels of EGFR mRNA compared to keratinocytes. By inhibiting both EGFR with gefitinib and GLI signalling with GANT61 there is a reduction of BCC growth which suggests that both are a good target for BCC therapy (Schnidar et al., 2009). Conversely, this suggests that the dysregulation of both pathways may give rise to BCC formation or development.

The study also demonstrated that EGFR/MEK/ERK pathways increase GLI1 and GLI2 expression (Schnidar et al., 2009) In agreement with this, the expression of GLI1 was reduced in NEB1-shCON and NEB1-shPTCH1 cells that were treated with the EGFR inhibitor AG1478 and both GLI1 and GLI2 were suppressed with the MEK inhibitor U0126 (Figure 5.6). However, inhibition

of EGFR, led to an increase of GLI2 mRNA levels which suggests that EGFR and HH signalling do not act in synergy with regards to control of GLI2 in human keratinocytes.

This data also shows that the inhibition of MEK/ERK effectively suppresses both GLI1 (canonical as well as non-canonical GLI1 that is not suppressed by SMO inhibitors) and GLI2 in NEB1-shPTCH1 cells which could be a good therapeutic target. In NIH-3T3 cell, MEK and ERK were able to stimulate GLI reporter activity and when MEK/ERK combined with either GLI1 or GLI2, there was a much greater induction of GLI reporter activity (Riobo et al., 2006 B). Based on this and the data generated that shows activation of ERK signalling, GLI1 induction in NEB1-shPTCH1 cells may be mediated through ERK rather than the canonical HH pathway. The question then arises as to whether the loss of PTCH1 leads to MEK/ERK mediated GLI expression in a signalling mode that may not require SMO. This would explain why NEB1-shPTCH1 cells do not respond to SMO inhibitors to a certain extent but not why SMO siRNA represses GLI1. One study has shown that $SMO^{-/-}$ breast cells that are treated with SHH ligand can activate ERK also, SHH was able to activate ERK in the presence of Cyclopamine (Chang et al., 2010). This implies that SHH can activate ERK independently of SMO and this may be mimicked in NEB1-shPTCH1 cells whereby reduced PTCH1 leads to increased GLI1 levels through increased ERK activity independently of SMO.

Treatment of NEB1 cells with EGFR inhibitor increased GLI2 expression despite GLI1 expression being reduced (Figure 5.6). This is interesting as GLI1 and GLI2 are part of a feedback loop therefore if GLI1 is suppressed then GLI2 should also be suppressed (Regl et al., 2002). The induction of GLI2 may occur to compensate for the suppression of GLI1. Also, the data suggests that GLI1 and GLI2 can be expressed independently of each other i.e. GLI2 expression does not depend on GLI1 expression. To use such inhibitors for therapy may therefore induce GLI2 which in turn could facilitate BCC growth. A study where the targeting of both the EGFR and HH pathways reduced mouse BCC growth (Schnidar et al., 2009) could therefore be interpreted as the EGFR inhibitor reducing GLI1 and the HH inhibitor repressing GLI2. If the MEK/ERK cascade is disrupted by the EGFR inhibitor, it is likely that both GLI1 and GLI2 are reduced.

Despite demonstrating that the ERK pathway is more active in NEB1 and N/Tert cells due to the suppression of PTCH1, this does not correlate in BCC tissue. Immunohistological studies of pERK and pAKT in BCC tissue show that neither protein is active in BCC (Neill et al., 2008; Hafner et al., 2012). Dr. Dimalee Herath (Neill Group) has done extensive analysis of EGFR signalling in BCCs and confirmed that pERK is not expressed in non-aggressive human BCCs.

Interestingly, Dr. Herath has also shown that human BCCs express pMEK so why it does not phosphorylate its principal target ERK (the un-phosphorylated protein is expressed in the tumours) is surprising and under further investigation. Moreover, Dr. Herath has also shown that pERK is not expressed in mouse BCCs whereas pMEK is abundant (unpublished data).

The expression of pEGFR, pERK and pMEK was examined in 15 non-invasive and 14 invasive human BCCs. All phospho-proteins were expressed in normal and tumour associated epidermis (nuclear/cytoplasmic) but whereas pEGFR and pMEK were also present in all tumours (albeit at varying levels and with no apparent correlation), pERK was consistently absent in non-invasive BCCs; pERK staining was slightly higher in invasive tumour islands but the main feature of these samples was that pERK was often localised to the stroma. pERK (but not pMEK) was dramatically absent compared to the epidermis. Conversely, pERK (but not pMEK) was expressed in the stromal cells of a more aggressive BCC-like variant which correlates with the presence of stromal pERK in invasive human BCC (unpublished data).

As pEGFR was localised in the nucleus in nodular BCCs and in NEB1-shPTCH1 cells, it is possible that this could account for the global reduction of pERK due to reduced EGFR activity at the cell membrane. Analysis of the EGFR signalling in human tumours reveals that the canonical pathway is not fully active in BCC and that further work is required to determine if and how components of the pathway warrant therapeutic attention. Indeed, whether or not loss of ERK activity is important for tumour formation also requires further investigation including how this affects GLI transcriptional activity.

Also, a major risk factor for BCC is UV radiation therefore NEB1 cells would have to be UV irradiated and analysed for changes to HH and EGFR components as a number of studies that employ $PTCH^{+/-}$ mice irradiate the mice in order to initiate BCC formation. This would provide a better understanding of whether a secondary event is required in NEB1-shPTCH1 cells to initiate BCC formation as these cells showed no sign of invasion in organotypic culture (Figure 3.26). Currently, ERK signalling is active in NEB1-shPTCH1 cells and the induction of downstream targets such as CXCL11 indicate that the cells have the potential to develop BCCs although how CXCL11 can be over expressed in BCCs in the absence of pERK is a mystery. It is possible that a secondary event such as a mutation may be required that represses ERK which could then lead to BCC formation.

Chapter 6

Discussion and conclusion

Chapter 6 Discussion and conclusion

6.1 Overview

This study has employed RNAi technology to suppress PTCH1 expression in immortalised human keratinocytes with the aim of identifying novel genes and mechanisms that may contribute to BCC biology. Current thinking predicts that the loss of PTCH1 function leads to activation of the canonical HH signalling pathway which is critically dependent upon the G protein-coupled receptor SMOOTHENED. However, although anti-SMO inhibitors can effectively suppress the formation of BCC-like tumours in pre-clinical mouse models and they have also demonstrated good results in clinical trials, many tumours only partially or do not respond to these drugs. One explanation for the lack of patient response to anti-SMO compounds is that although PTCH1 mutations are the most common genetic aberration in BCC, such mutations have not been identified in all BCCs and therefore the formation of these tumours may be PTCH1-independent (and by association independent of SMO and canonical HH signalling). However, in tumours that arise from mutational inactivation of PTCH1, an alternative explanation for the lack of response to anti-SMO compounds is that there are SMO-independent signalling mechanisms that contribute to tumour formation and progression. Therefore, to help identify these potential mechanisms, this study employed RNAi technology to suppress PTCH1 in immortalised human keratinocytes combined with gene expression profiling. In addition, this novel approach was also used to investigate the effect of PTCH1 suppression upon canonical HH signalling and control of the GLI transcription factors.

The validity of suppressing PTCH1 to create an *in vitro* model of BCC was first supported by the observation that in two-dimensional culture some clonal NEB1-shPTCH1 cell lines cultured as more compact colonies compared to parental or control cells, a morphology similar to that of nodular BCC. A similar phenotype was observed in N/Tert-shPTCH1 cells but no such difference was found in HaCaT-shPTCH1 cells. Microarray analysis of NEB1-shPTCH1 cells did reveal a number of interesting genes related to cell morphology, migration and invasion. The over expression of GLI1 in N/Tert cells results in tight colony formation with actin and E-cadherin expressed at the cell membrane to ensure that the cells bind closely with each other (Neill et al., 2008). It is difficult to determine which form of BCC NEB1-shPTCH1 cells are modelling but the morphology of the cells would suggest that they are more like nodular BCC in two-dimensional culture and superficial in organotypic culture.

The study of structural protein expression should be examined on a larger scale i.e. the BCC tumours and surrounding stromal tissue. As a result, NEB1-shPTCH1 cells should be cultured with fibroblasts and examined in the context of NEB1-shPTCH1 cells signalling to the surrounding fibroblasts. MMP-2 and MMP-9 are associated with tumour invasion and degrade collagen IV that keeps cells attached to each other. MMP-2 was shown to be absent in BCCs while MMP-9 was strongly expressed in aggressive BCCs as determined by immunohistochemistry (Karahan et al., 2011). In areas where the tumour may become invasive i.e. the periphery of the tumour mass, it is more likely that MMP-9 will be expressed here so that the cells can migrate more easily into the surrounding tissue. Once the cells have migrated and new tumour masses are formed, the expression of MMP-9 may become reduced. If MMP-9 is more active in NEB1-shPTCH1 cells, the stromal cells (co-cultured fibroblasts) may exhibit a reduction of collagen IV. Other structural components revealed through microarray analysis could also be analysed in this capacity, for example, fibronectin and actin that have been shown to be found in BCC tumour islands and stromal cells (Peltonen et al., 1988; Adegboyega et al., 2010). It is possible that in two-dimensional culture NEB1-shPTCH1 cells express certain structural proteins to maintain phenotype as it is characteristic of tumours to firstly establish itself as a cellular mass. The addition of fibroblasts as the stromal component in a co-culture system may alter the expression of these structural proteins.

Mouse models of BCC have demonstrated that the manipulation of the HH signalling pathway does not always result in BCC tumour formation therefore NEB1-shPTCH1 cells were generated as an alternative model using human keratinocytes. Similar to $PTCH^{+/-}$ mouse models where BCCs are induced after UV irradiation, NEB1-shPTCH1 cells should be UV irradiated. It is worth noting that many studies that utilise $PTCH^{+/-}$ mice did not always develop actual BCCs after UV treatment but tumours that only resemble BCCs (Donovan, 2009; Daya-Grosjean and Couve´-Privat, 2005; Mancuso et al., 2004). Based on this, NEB1-shPTCH1 cells should be UV irradiated and then analysed further by making Matrigel based organotypic cultures. This would allow us to compare the differences between the cells post UV irradiation.

NEB1-shPTCH1 and NEB1-shCON cells that were compared by microarray analysis identified the p53 signalling pathway as being differentially regulated. UV irradiation of NEB1-shPTCH1 cells may lead to the formation of BCCs as studies have shown that tumours arise from UV induced p53 loss of function mutations (Mancuso et al., 2004; D'Errico et al., 1997; Denef et al., 2000; Zhang et al., 2001). A study of $PTCH^{+/-}$ $p53^{-/-}$ mice showed increased BCC carcinogenesis however this may be attributed to the over expression of SMO because there was no BCC formation in the ears or tail where SMO was absent (Wang et al., 2011). This

implies that there is a specific set of mutations that are required for the formation of BCC that may follow the suppression of PTCH1 with a p53 loss of function mutation for example. Indeed, this provides evidence for how BCCs develop however as mentioned earlier, UV irradiation of $PTCH^{+/-}$ mice does not necessarily lead to BCC formation. The specific effects of UV irradiation with regards to other signalling pathways needs to be better defined as well as the involvement with HH signalling as $PTCH^{+/-}$ $p53^{-/-}$ mice developed BCCs where SMO was expressed (Wang et al., 2011). This could be achieved by treating NEB1-shPTCH1 cells with p53 inhibitors and analysing the HH pathway components for changes however, UV irradiation should also be performed as this would take into account the other stress responses and the adaptations that the cells may undertake if there is any permanent damage.

As opposed to $PTCH^{+/-}$ mouse models that have to be UV irradiated before tumours develop, an inducible PTCH1 knockout mouse system has shown that BCC-like tumours develop in mice (Adolphe et al., 2006). The knockout of PTCH1 occurs in the basal cell population which may be the critical factor that causes these tumours to form. Based on these subtle differences in mouse models, there are variations in the tumours that develop. This is something to consider regarding NEB1-shPTCH1 cells as a model of BCC as I have mentioned earlier - tumours may develop after UV irradiation but it would be difficult to protect the cells from non-specific effects. Another approach to this could be to suppress PTCH1 in other cell types such as those specific to hair follicles. It has been proposed that BCCs arise from ORS cells (Crowson, 2006; Owens and Watt, 2003) therefore it may be better to isolate ORS cells then suppress PTCH1 in these cells. It can be argued that ORS cells and basal cell keratinocytes are similar because ORS cells are a continuation of the IFE and stem cells may be an important factor. The basal layer is consistent of approximately 10% of stem cells that gives rise to TA cells that differentiate to either the IFE, sebaceous gland or hair follicle (Li and Neaves, 2006; Watt et al., 2006). ORS cells surround the bulge region that contains a niche for epithelial stem cells (Cotsarelis et al., 1990). Compared to basal layer stem cells, bulge region stem cells differentiate into eight types of cell including the IFE, ORS, hair fibre and GE (Liu et al., 2003). Also, it is understood that the main source of stem cells that give rise to keratinocytes are from the hair follicle as opposed to the basal layer therefore, bulge region stem cells or DP could be isolated and PTCH1 suppressed in these cells (Cotsarelis et al., 1990). As NEB1-shPTCH1 may not develop into BCCs solely from the suppression of PTCH1, further mutations may be required and stem cells that reside in the DP or bulge region for long periods may accumulate a number of mutations or changes over time that may be required for BCCs to develop. Furthermore, bulge region stem cells are pre-programmed to be more invasive through the dermis than keratinocytes which

potentially makes the cells more tumourigeneic if stem cells were to be used as a model (Perez-Losanda and Balmain, 2003).

Based on mouse studies where different components of the HH pathway are manipulated, different forms of tumour develop which demonstrates that there may be a set of specific requirements for actual BCCs to develop. GLI1 over expressing mice were able to develop BCC-like tumours (Nilsson et al., 2000) while the expression of an activated mutant form of GLI2 resulted in multiple BCC formation (Sheng et al., 2002; Grachtchouk et al., 2000). Controlled targeted expression of GLI2 in hair follicle stem cells and the IFE showed that nodular BCCs arise from hair follicle stem cells while superficial BCCs arise from IFE (Grachtchouk et al., 2011). It would therefore be interesting to compare how the loss of PTCH1 expression affects hair follicle stem cells as opposed to keratinocytes and if BCCs arise from different cell types.

$SUFU^{+/-}$ mice have been shown to develop Gorlin-type characteristics and fibroblasts derived from $SUFU^{-/-}$ mice showed increased levels of GLI1 mediated HH signalling (Svard et al., 2006). Further upstream of SUFU, SMO activating mutations have been reported in BCCs however, mice that carry the SMO-M2 mutation develop hamartomas (Xie et al., 1998; Grachtchouk et al., 2003). One explanation for hamartomas developing instead of BCCs was that the induction of HH signalling was not strong enough as demonstrated in a GLI2 over expressing mouse model where HH signalling induction was much greater in comparison, thus leading to BCC formation (Grachtchouk et al., 2003). Another study has shown that SMO-M2 mice develop BCCs but here it was shown that the tumours originate from undifferentiated basal layer stem cells (Youssef et al., 2010). The stem cell capacity of the cells may be the crucial factor that determines whether tumours form or not in BCCs that do not arise from UV irradiation therefore a population of stem cells from the hair follicle may be a better model to suppress PTCH1.

6.2 Non-canonical Hedgehog signalling in BCC

As shown in Chapter 3, NEB1-shPTCH1 cells are unresponsive to pharmacological SMO inhibitors although GLI1 may be mediated through SMO as demonstrated by SMO siRNA which was able to partially suppress GLI1. One hypothesis for this is that SMO translocates to the nucleus where it regulates GLI1 which was based upon the discovery that SMO is localised in the nucleus of NEB1-shPTCH1 cells. With the transfection of EGFP-SMO-WT fusion protein into NEB1-shPTCH1 cells, there was some evidence of nuclear SMO localisation although this was not convincing. The transfection of EGFP-SMO-WT/M2 in NEB1 cells also induced GLI1 mRNA

expression. To better understand about this non-canonical mode of HH signalling, NEB1-shCON cells could be transfected with EGFP-SMO-WT/M2 which would induce GLI1 expression then the cells treated with Cyclopamine-KAAD to see if HH signalling could be suppressed. If SMO-WT/M2 induced HH signalling can be repressed by Cyclopamine-KAAD, it would imply that GLI1 expression is mediated through SMO signalling. It is possible that Cyclopamine-KAAD binds to SMO-M2 but the protein is able to activate the signalling cascade via another mode.

Also, the cells could be treated with SHH upon transfection of EGFP-SMO-WT and EGFP-SMO-M2 to establish whether SMO localisation is altered upon stimulation of the pathway. Although PTCH1 is strongly suppressed in NEB1-shPTCH1 cells, there is still some expression of PTCH1 therefore it would be interesting to see if SHH can stimulate the pathway. If this is the case, the cells could be treated with SMO inhibitors to determine if any increase of GLI1 could be suppressed. Also, if cilia are not present in NEB1 cells we could determine other locations where HH signalling occurs i.e. nucleus mediated signalling.

An important observation from performing the microarray on NEB1-shPTCH1 cells was that a large number of DEGs are insensitive to the presence of the SMO inhibitor Cyclopamine-KAAD. As for GLI1, whether or not their expression is truly SMO-independent would require qPCR analysis in cells transfected with SMO siRNA. A comparison of NEB1-shPTCH1 cells treated with Cyclopamine-KAAD and NEB1-shPTCH1 cells treated with SMO siRNA would clarify which signalling pathways are SMO dependent as well as those that are affected if the cells are resistant to SMO inhibitors. In addition, analysis of these DEGs could be performed in NEB1 and N/Tert keratinocytes over expressing EGFP-SMO-WT and EGFP-SMO-M2 to help determine if they are SMO-dependent or SMO-independent.

One of the interesting and unexpected observations from my project was that the expression of *MMP-9* mRNA is strongly increased in the presence of anti-SMO inhibitors. The expression of MMP-9 protein was not investigated but if it is increased then it would be interesting to determine if MMP-9 is elevated in tumours exposed to anti-SMO inhibitors. As discussed above, MMP-9 is associated with tumour cell invasion and although there is no evidence that tumours spread in patients receiving anti-SMO inhibitors, it is a clinically undesirable aspect which warrants further investigation. However, the analysis of MMP-9 expression in tumours may be used as a marker of drug exposure in patients taking anti-SMO inhibitors even if their tumours do not respond favourably to these drugs.

In order to determine the correct treatment for BCC, it would be a better strategy to find the causative factor before administering treatment. An example of this was demonstrated in a study where an active mutant of SMO induced hamartoma development in mice via constitutively active HH signalling however, the addition of the Wnt antagonist Dkk1 resulted in the inhibition of hamartoma development (Yang et al., 2008). This suggests that inhibition of Wnt may serve as a viable therapeutic target for tumours initiated via mutant SMO expression.

Before therapies can be selected, a better understanding of the impact of PTCH1 suppression on other major signalling pathways such as the TGF-β pathway is required. Using NEB1-shPTCH1 cells, the expression levels of TGF-β would be established to confirm if there is an increase. If this is the case, a TGF-β inhibitor could be used to treat NEB1-shPTCH1 cells to see whether GLI1 levels are reduced. Reciprocally, NEB1-shCON and NEB1-shPTCH1 cells could then be treated with TGF-β to determine if GLI1 is induced as demonstrated in one study (Dennler et al., 2007). Microarray analysis revealed that the TGF-β pathway and SMAD genes were over expressed in NEB1-shPTCH1 cells and studies have also demonstrated that TGF-β and SMAD pathway components are over expressed in BCC (Gambichler et al., 2007). Furthermore, it would also be interesting to determine if TGF-β signalling could be suppressed by SMO inhibitors and if there are differences between NEB1-shCON and NEB1-shPTCH1 cells for example, could TGF-β signalling account for increased ERK signalling and how does the induction or suppression of the pathway affect ERK target genes. Both pharmacological SMO inhibitors as well as SMO siRNA could be used to try and suppress TGF-β expression so this may help determine if TGF-β is causing increased GLI1 expression despite SMO being inhibited.

6.3 Novel genes and pathways that may be important in BCC aetiology

The other major signalling pathway identified by gene expression profiling (Chapter 4) was MEK/ERK signalling which is possibly activated through EGFR signalling. EGFR at the mRNA and protein level was reduced in NEB1-shPTCH1 cells compared to NEB1-shCON cells however there was increased nuclear localisation of pEGFR. The results observed with NEB1-shPTCH1 cells support the previous findings of the Neill group whereby increased GLI1 activity in N/Tert cells negatively regulated EGFR expression and downstream signalling (Neill et al., 2008). However, Neill et al. (2008) did not investigate the expression of ERK target genes. Indeed, despite a global decrease of pERK expression in NEB1-shPTCH1 cells, they display an increase of nuclear pERK and an increase of target genes associated with ERK signalling. To investigate this further, a reporter construct for ERK could be transfected into NEB1-shPTCH1 cells to assess ERK activity providing that this is optimised and made viable for NEB1 cells. Also, if

NEB1-shPTCH1 cells are rescued with the PTCH1B isoform, it would help determine if the suppression of PTCH1 is involved in reducing EGFR expression and/or increased ERK target expression. Similarly, the transfection of NEB1-shCON cells with PTCH1B may increase EGFR expression and it would be interesting to determine how this would affect pERK subcellular localisation, total expression levels and activity.

Another factor to consider would be whether ERK mediated GLI1 expression signals via SMO or not. A study utilising $SMO^{-/-}$ breast cells treated with SHH ligand has been shown to activate ERK as well as in the presence of Cyclopamine (Chang et al., 2010). As demonstrated in this study, SHH was able to activate ERK independently of SMO and this may explain how GLI1 signals in NEB1-shPTCH1 cells. To confirm this, NEB1-shPTCH1 cells could be treated with SMO inhibitors and the expression of ERK target genes analysed. However, it should be mentioned that SMO suppression by siRNA did reduce GLI1 levels. Therefore GLI1 expression may be mediated via SMO in NEB1-shPTCH1 cells but the activation of ERK signalling (through the suppression of PTCH1) also activates GLI1. Indeed, pharmacological inhibition of EGFR (AG1478) and MEK (U0126) led to a decrease of GLI1 in both NEB1-shCON and NEB1-shPTCH1 cells. ERK target genes could therefore be analysed in NEB1-shCON cells treated with Cyclopamine-KAAD to confirm if ERK signalling is still active or not.

Interestingly, the expression of GLI2 was increased upon exposure to the EGFR inhibitor AG1478 whereas both GLI1 and GLI2 were suppressed by the MEK inhibitor U0126 in both NEB1-shCON and NEB1-shPTCH1 cells; this suggests that EGFR regulates GLI2 independently of MEK/ERK and it would be interesting to determine if there is a corresponding increase of GLI reporter activity in keratinocytes exposed to AG1478. Mouse studies have demonstrated that the induction of GLI2 can lead to the formation of BCCs (Sheng et al., 2002; Grachtchouk et al., 2000) therefore, if BCCs are treated with EGFR inhibitors this may in fact facilitate BCC development. It would be a better strategy to use MEK inhibitors to treat BCCs that may arise as the result of GLI1 or GLI2 over expression. MEK may control or signal to GLI specifically in the nucleus and not the cytoplasm which would explain the increased nuclear localisation of pERK and pMEK in NEB1-shPTCH1 cells.

Despite these observations in cultured keratinocytes, immunohistological staining of BCCs by Dr. Herath (Neill/Philpott Group) revealed that pERK is predominantly absent from tumours. Moreover this lack of pERK protein expression in BCC tissue has been reported in other studies (Neill et al., 2008; Hafner et al., 2012). Dr. Herath observed that pERK was present in the epidermis but lost in the tumour therefore it is possible that the loss of ERK expression may be

an important factor in BCC initiation. As such, NEB1-shPTCH1 cells could be grown in organotypic culture and then via an inducible knockout system, ERK could be suppressed. This would help determine whether loss of ERK expression as a second event after the suppression of PTCH1 could initiate BCC formation in the organotypic culture model. Another anomaly discovered by Dr. Herath was the positive expression of pMEK in the panel of BCCs so why its direct downstream target ERK is not phosphorylated is unexpected. Dr. Herath has also demonstrated that BCC-like tumours derived from X-ray irradiated PTCH1$^{+/-}$ mice do not express pERK whereas they do express pMEK and this is under investigation.

The Neill/Philpott group has shown that GLI1 expression in a panel of BCCs is highly variable with some tumours displaying strong GLI1 expression while GLI1 is absent in others (unpublished data). With pERK predominantly absent from BCCs and some tumours lacking GLI1, it is possible that GLI1 expression is mediated by pMEK independently of pERK. The panel of BCCs analysed by Dr. Herath should therefore also be analysed for GLI1. NEB1 cells could also be treated with GLI1 siRNA to determine how MEK/ERK expression is affected in particular, if pERK remains in the nucleus of NEB1-shPTCH1 cells.

An explanation for increased nuclear pERK in NEB1-shPTCH1 cells may be that DUSP6 expression was reduced which would prevent the dephosphorylation of pERK. As such, the panel of BCCs analysed by Dr. Herath could be stained for DUSP6 to determine if there is a correlation between pERK and DUSP6 protein expression as well as the protein localisation i.e. DUSP6 could be present in tumours but absent in the epidermis. This theory may apply if DUSP6 protein were to be localised in the nucleus of tumour cells.

It is also possible that EGFR signalling is altered in NEB1-shPTCH1 cells as a stress response as nuclear EGFR expression has been observed in human keratinocytes after UV irradiation (Wang et al., 2010). Furthermore, mouse BCC cell lines ASZ001 and BSZ2 (*Ptch*$^{-/-}$) as well as CSZ1 (*p53*$^{-/-}$) express higher levels of EGFR mRNA compared to normal keratinocytes (Schnidar et al., 2009). To address this, both NEB1-shCON and NEB1-shPTCH1 cells could be UV irradiated and EGFR components examined. In this case also the protein localisation of pEGFR and pERK could be examined as well as total protein levels. The differential expression of caspases in NEB1-shPTCH1 cells also suggests that the cells are responding to a form of cellular stress. This may be to initiate apoptosis however other anti-apoptotic factors may have an effect similar to a study where HaCaT cells with two mutant p53 alleles showed that UV-induced apoptosis was inhibited (Sitailo et al., 2002). Changes to the p53 signalling components caused by the suppression of PTCH1 in NEB1-shPTCH1 cells may contribute to differential expression of

caspases as shown by microarray profiling. This would need to be analysed further as to determine specifically which caspases are induced in NEB1-shPTCH1 cells.

Immune responses may also play a part in BCC formation as highlighted by the over expression of CXCL11 in NEB1-shPTCH1 cells which is involved in T-cell recruitment and is a skin immune response (Lo et al., 2010). CXCL11 has been shown to be an ERK target gene and has also been reported to be expressed at higher levels in BCCs (Hosokawa et al., 2010; Lo et al., 2010). The expression of CXCL10 and CXCL11 were also shown to be mediated through ERK (Hosokawa et al., 2010). The over expression of a number of caspases in NEB1-shPTCH1 cells may contribute to the induction of CXCL11 during skin inflammation (Flier et al., 2001).

Other inflammatory response pathways that appear in the microarray include NF-kB signalling. While there is little known regarding NF-kB signalling in BCC, the pathway is up regulated in melanoma (Ueda and Richmond, 2006). The stimulation of NF-kB signalling may be involved in preventing apoptosis which is a feature of tumours (Karin et al., 2002). A number of interleukins were also up regulated in NEB1-shPTCH1 cells which provide more evidence of an immune response to the suppression of PTCH1 in NEB1-shPTCH1 cells. Each of the interleukins should be further analysed by qPCR to determine specifically which cytokines are most active i.e. are the interleukins signal activators or repressors. The NF-kB pathway has also been reported to interact with p53, EGFR and HH signalling pathways (Gu et al., 2004; Haussler et al., 2005; Nakashima et al., 2006). As such, NEB1-shCON and NEB1-shPTCH1 cells could be treated with inhibitors of p53, EGFR, NF-kB and the HH pathway to determine how components of each of these pathways may interact with each other and similarly, each of the pathways could be stimulated as well. Depending on the findings, inhibitors could also be combined with the purpose of finding ways to suppress GLI1 in NEB1-shPTCH1 cells for example. From a therapeutic perspective once the cause of the tumour is identified then a suitable inhibitor combination could be administered. Further characterisation of the tumour may be of benefit for example, to know if ERK signalling is active in which case a MEK/ERK inhibitor may not be useful.

Toll-like receptors (TLRs) that are involved in tissue homeostasis maintenance and regulating inflammatory responses were shown to the differentially expressed in NEB1-shPTCH1 cells. Downstream of TLR activation, MAPK and NF-kB pathways were active in NEB1-shPTCH cells and this link between these pathways has been described in the literature (Kawai and Akira, 2006). The therapeutic potential of the pathway has been identified in studies where TLR associated Imiquimod cream has been used to successfully treat superficial BCCs (Stockfleth et

al., 2003). It is possible that NEB1-shPTCH1 cells exhibit increased TLR mediated signalling as a stress response which could subsequently affect the p53, MAPK and NF-kB pathways. It is not known which pathway could be the main initiator of this multi-pathway cascade if this is indeed occurring but with the use of inhibitors with NEB1-shPTCH1 cells, this could be determined. By identifying the main pathway that is altered by suppressing PTCH1, inhibition of this pathway may then reduce the expression of a number of inter-connected signalling pathways which could be a very specific mode of targeted therapy. A good example of this would be the use of MEK/ERK inhibitor to suppress GLI1 and GLI2 in NEB1-shPTCH1 cells although a profile of the tumour would need to be generated first.

Microarray analysis also revealed the induction of SNAI1 (HH target gene) and VIM in NEB1-shPTCH1 cells compared to NEB1-shCON cells. SNAI1 and VIM are both indicators of EMT and the over expression of these genes implies that NEB1-shPTCH1 cells have tumourigenic potential (Katoh and Katoh, 2009; Tomson et al., 1996). However, the tight cobblestone morphology of NEB1-shPTCH1 cells suggests that the cells may not migrate which further justifies the co-culture of these cells with fibroblasts. It is possible that NEB1-shPTCH1 cells may become invasive in the presence of fibroblasts so the staining of NEB1-shPTCH1 colonies with VIM or E-cadherin may reveal a specific staining pattern i.e. if NEB1-shPTCH1 cells have the potential to invade then E-cadherin expression may be less pronounced in the cells surrounding the colony (Katoh and Katoh, 2009). It is possible that a certain level of expression for VIM for example has to be exceeded before EMT initiates and this may occur upon UV irradiation of NEB1-shPTCH1 cells. VIM expression has been shown to correlate with tumour invasiveness therefore, once BCC formation is initiated then perhaps VIM expression is further induced depending on the classification of tumour (Singh et al., 2003; Tomson et al., 1996). The inhibition of VIM in SCC derived cells reduced proliferation, migration and invasion which may have implications for treating infiltrative BCCs however this does not address how non-infiltrative BCCs develop (Paccione et al., 2008). Furthermore, it is not yet established which type of BCCs NEB1-shPTCH1 cells most closely resemble and this requires further investigation.

LCN2 which is an indicator of increased inflammation (Kamata et al., 2012) was also shown to be induced in NEB1-shPTCH1 cells. LCN2 has been shown to be over expressed in SCCs but negative in BCCs (Mallbris et al., 2002). It may be that the loss of LCN2 expression in NEB1-shPTCH1 cells could be an indicator of BCC formation. LCN2 may also be involved in the process leading up to tumour initiation as studies have demonstrated that increased LCN2 expression correlated with aggressiveness as well as inducing EMT and angiogenesis in human breast cancer (Mannelqvist et al., 2012; Yang et al., 2012). As such, LCN2 should be analysed in

NEB1-shPTCH1 cells under normal conditions and then under stress i.e. after UV irradiation as well as in co-culture with fibroblasts. With increased UV mediated stress, there may be an induction of EMT markers like SNAI1 and VIM as mentioned earlier. There may be a certain mutation that is required or a change that occurs which would suppress LCN2 expression in BCCs once tumours have formed. A specific threshold may need to be exceeded at which point LCN2 expression is not required, similar to what may occur with ERK signalling. Another anomaly is the decreased expression of IGFBP2 in NEB1-shPTCH1 cells as studies have shown that the loss of PTCH1 expression in human and mouse BCCs leads to increased IGFBP2 levels (Villani et al., 2010). Furthermore, mice over expressing SHH displayed increased IGFBP2 in hair follicle cells (Harris et al., 2010). It is possible that IGFBP2 plays an important role in hair follicle biology possibly in the stem cell component or in cells that have the potential to develop into BCCs. Similarly, expression of IGFBP2 may be induced after tumour formation.

6.4 Conclusion

This study has identified a number of caveats with regards to how the loss of PTCH1 function and by association canonical Hedgehog signalling is thought to promote BCC formation. In particular, the data presented reveal that:

1) PTCH1 (or at least the C-terminal half) is expressed in the nucleus of human keratinocytes whereas it is generally considered to be a 12-span transmembrane receptor protein (this supports the results of a recent study which showed that the C-terminal half of PTCH1 is nuclear and controls GLI1 expression in C3H10T1/2 cells (Kagawa et al. 2011).

2) PTCH1 suppression leads to an increase of nuclear/perinuclear SMO (although SMO is considered a transmembrane receptor, the presence of a strong N-terminal bipartite nuclear localisation signal indicates that nuclear signalling is possible and is currently under investigation in the Neill group).

3) The effects of PTCH1 suppression upon the transcriptome - including the increase of GLI1 levels - are largely insensitive to the presence SMO pharmacological inhibitors.

Following on from point 3, the chemokines CXCL10 and CXCL11 were increased in shPTCH1 keratinocytes; these genes were recently shown to be increased in human BCC with functional activity that supports tumourigenesis (Lo et al., 2010) but they did not return to basal levels in the presence of SMO inhibitors. This *in vitro* model also identified a number of BCC and

tumour related characteristics i.e. nodular BCC-like morphology and expression of LCN2, SNAI1, and VIM as well as major signalling pathways such as NF-kB, TGF-β and MEK/ERK pathways that can be attributed to active HH signalling. These studies help support the validity of shPTCH1 keratinocytes as a model of BCC and show that this model may be used to identify novel SMO-independent genes and signalling mechanisms involved in the aetiology of this common tumour form.

Chapter 7

References

Chapter 7 References

ADEGBOYEGA, P. A., RODRIGUEZ, S., MCLARTY, J. 2010. Stromal expression of actin is a marker of aggressiveness in basal cell carcinoma. *Hum Pathol*. 41(8):1128-37.

ADOLPHE, C., HETHERINGTON, R., ELLIS, T., WAINWRIGHT, B. 2006. Patched1 functions as a gatekeeper by promoting cell cycle progression. *Cancer Res*. 2006:66(4);2081-8.

AGAR, N., YOUNG, A. R. Melanogenesis: a photoprotective response to DNA damage? 2005. *Mutat Res*. 571(1-2):121-32.

ALCEDO, J., AYZENZON, M., VON OHLEN, T., NOLL, M., HOOPER, J. E. 1996. The Drosophila smoothened gene encodes a seven-pass membrane protein, a putative receptor for the hedgehog signal. *Cell*. 86(2):221-32.

ALESSI, E., VENEGONI, L., FANONI, D., BERTI, E. 2008. Cytokeratin profile in basal cell carcinoma. *Am J Dermatopathol*. 30(3):249-55.

ALLEN, B. L., SONG, J. Y., IZZI, L., ALTHAUS, I. W., KANG, J. S., CHARRON, F., KRAUSS, R. S., MCMAHON, A. P. 2011. Overlapping roles and collective requirement for the coreceptors GAS1, CDO, and BOC in SHH pathway function. *Dev Cell*. 20, 775-787.

ALTSCHUL, S.F., GISH, W., MILLER, W., MYERS, E.W., LIPMAN, D.J. 1990. Basic local alignment search tool. *J Mol Biol.* 215:403-410.

ANG, K. K., BERKEY, B. A., TU, X., ZHANG, H. Z., KATZ, R., HAMMOND, E. H., FU, K. K., MILAS, L. 2002. Impact of epidermal growth factor receptor expression on survival and pattern of relapse in patients with advanced head and neck carcinoma. *Cancer Res*. 62:7350–7356.

ANGERS, S., MOON, R. T. 2009. Proximal events in Wnt signal transduction. *Nat Rev Mol Cell Biol*. 10, 468-77.

ATHAR, M., LI, C., TANG, X., CHI, S., ZHANG, X., KIM, A. L., TYRING, S. K., KOPELOVICH, L., HEBERT, J., EPSTEIN, E. H. JR, BICKERS, D. R., XIE, J. 2004. Inhibition of smoothened signaling prevents ultraviolet B-induced basal cell carcinomas through regulation of Fas expression and apoptosis. *Cancer Res*. 64(20):7545-52.

BAILEY, E. C., MILENKOVIC, L., SCOTT, M. P., COLLAWN, J. F., JOHNSON, R. L. 2002. Several PATCHED1 missense mutations display activity in patched1-deficient fibroblasts. *J Biol Chem*. 277(37):33632-40.

BARKER, T. H., GRENETT, H. E., MACEWEN, M. W., TILDEN, S. G., FULLER, G. M., SETTLEMAN, J., WOODS, A., MURPHY-ULLRICH, J., HAGOOD, J. S. 2004. Thy-1 regulates fibroblast focal adhesions, cytoskeletal organization and migration through modulation of p190 RhoGAP and Rho GTPase activity. *Exp Cell Res*. 295(2):488-96.

BEACHY, P. A., HYMOWITZ, S. G., LAZARUS, R. A., LEAHY, D. J., SIEBOLD, C. 2010. Interactions between Hedgehog proteins and their binding partners come into view. *Genes Dev*. 24, 2001-2012.

BEACHY, P. A., KARHADKAR, S. S., BERMAN, D. M. 2004. Tissue repair and stem cell renewal in carcinogenesis. *Nature*. 432:324-31.

BEALES, P. L., ELCIOGLU, N., WOOLF, A. S., PARKER, D., FLINTER, F. A. 1999. New criteria for improved diagnosis of Bardet-Biedl syndrome: results of a population survey. *J Med Genet*. 36:437–446.

BEHRENS, J., VON KRIES, J. P., KUHL, M., BRUHN, L., WEDLICH, D., GROSSCHEDL, R., BIRCHMEIER, W. 1996. Functional interaction of beta-catenin with the transcription factor LEF-1. *Nature*. 382, 638-642.

BERBARI, N. F., O'CONNOR, A. K., HAYCRAFT, C. J., YODER, B. K. 2009. The primary cilium as complex signaling center. *Curr Biol*. 19(13):R526-35.

BERGMANN, C., FLIEGAUF, M., BRÜCHLE, N. O., FRANK, V., OLBRICH, H., KIRSCHNER, J., SCHERMER, B., SCHMEDDING, I., KISPERT, A., KRÄNZLIN, B., NÜRNBERG, G., BECKER, C., GRIMM, T., GIRSCHICK, G., LYNCH, S. A., KELEHAN, P., SENDEREK, J., NEUHAUS, T. J., STALLMACH, T., ZENTGRAF, H., NÜRNBERG, P., GRETZ, N., LO, C., LIENKAMP, S., SCHÄFER, T., WALZ, G., BENZING, T., ZERRES, K., OMRAN, H. 2008. Loss of nephrocystin-3 function can cause embryonic lethality, Meckel-Gruber-like syndrome, *situs inversus*, and renal-hepatic-pancreatic dysplasia. *Am J Hum Genet*. 82(4):959-70.

BIGELOW, R. L., JEN, E. Y., DELEHEDDE, M., CHARI, N. S., MCDONNELL, T. J. 2005. Sonic Hedgehog Induces Epidermal Growth Factor Dependent Matrix Infiltration in HaCaT Keratinocytes. *J Invest Dermatol*. 124(2):457-65.

BISHOP, C. L., BERGIN, A. M., FESSART, D., BORGDORFF, V., HATZIMASOURA, E., GARBE, J. C., STAMPFER, M. R., KOH, J., BEACH, D. H. 2010. Primary cilium-dependent and -independent Hedgehog signaling inhibits p16(INK4A). *Mol Cell*. 40(4):533-47.

BLANPAIN, C., FUCHS, E. 2006. Epidermal stem cells of the skin. *Annu Rev Cell Dev Biol*. 22:339-73.

BONNER, J. A., HARARI, P. M., GIRALT, J., AZARNIA, N., SHIN, D. M., COHEN, R. B., JONES, C. U., SUR, R., RABEN, D., JASSEM, J., OVE, R., KIES, M. S., BASELGA, J., YOUSSOUFIAN, H., AMELLAL, N., ROWINSKY, E. K., ANG, K. K. 2006. Radiotherapy plus cetuximab for squamous-cell carcinoma of the head and neck. *N Engl J Med*. 354:567–578

BOTCHKAREV, V. A., SHAROV, A. A. 2004. BMP signaling in the control of skin development and hair follicle growth. *Differentiation*. 72(9-10): 512-26.

BOUKAMP, P. 2005. Non-melanoma skin cancer: what drives tumor development and progression? *Carcinogenesis*. 26(10):1657-67.

BOUKAMP, P., PETRUSSEVSKA, R. T., BREITKREUTZ. D., HORNUNG, J., MARKHAM, A., FUSENIG, N. E. 1988. Normal kertinization in a spontaneously immortalized aneuploid human keratinocyte cell line. *J Cell Biol*. 106(3):761-71.

BOX, N. F., DUFFY, D. L., CHEN, W., STARK, M., MARTIN, N. G., STURM, R. A., HAYWARD, N. K. 2001. MC1R Genotype modifies risk of mealnoma in families segregating CDKN2A mutations. *Am J Hum Genet.* 69:765-773.

BRAMBILLA, E., GAZADAR, A. 2009. Pathogenesis of lung cancer signalling pathways: roadmap for therapies. *Eur Respir J*. 33(6):1485-97.

BRAMEIER, M., KRINGS, A., MACCALLUM, R. M. 2007. NucPred—predicting nuclear localization of proteins. *Bioinformatics*. 23(9):1159-60.

BROWN, G. D. 2008. Sensing necrosis with Mincle. *Nat Immunol.* 9(10):1099-100.

BRUNET, A., BONNI, A., ZIGMOND, M. J., LIN, M. Z., JUO, P., HU, L. S., ANDERSON, M. J., ARDEN, K. C., BLENIS, J., GREENBERG, M. E. 1999. Akt promotes cell survival by phosphorylating and inhibiting a Forkhead transcription factor. *Cell*. 96(6):857-68.

BRYCHTOVA, S., FIURASKOVA, M., HLOBILKOVÁ, A., BRYCHTA, T., HIRNAK, J. 2007. Nestin expression in cutaneous melanomas and melanocytic nevi. *J Cutan Pathol.* 34:370–375.

CADIGAN, K. M., NUSSE, R. 1997. Wnt signaling: a common theme in animal development. *Genes Dev.* 11(24):3286-305.

CARDONE, M. H., ROY, N., STENNICKE, H. R., SALVESEN, G. S., FRANKE, T. F., STANBRIDGE, E., FRISCH, S., REED, J. C. 1998. Regulation of cell death protease caspase-9 by phosphorylation. *Science*. 282(5392):1318-21.

CARPENTER, D., STONE, D. M., BRUSH, J., RYAN, A., ARMANINI, M., FRANTZ, G., ROSENTHAL, A., DE SAUVAGE, F. J. 1998. Characterization of two patched receptors for the vertebrate hedgehog protein family. *Proc Natl Acad Sci U S A*. 95(23):13630-4.

CARSTEA, E. D., MORRIS, J. A., COLEMAN, K. G., LOFTUS, S. K., ZHANG, D., CUMMINGS, C., GU, J., ROSENFELD, M. A., PAVAN, W. J., KRIZMAN, D. B., NAGLE, J., POLYMEROPOULOS, M. H., STURLEY, S. L., IOANNOU, Y. A., HIGGINS, M. E., COMLY, M., COONEY, A., BROWN, A., KANESKI, C. R., BLANCHETTE-MACKIE, E. J., DWYER, N. K., NEUFELD, E. B., CHANG, T. Y., LISCUM, L., STRAUSS, J. F. 3RD, OHNO, K., ZEIGLER, M., CARMI, R., SOKOL, J., MARKIE, D., O'NEILL, R. R., VAN DIGGELEN, O. P., ELLEDER, M., PATTERSON, M. C., BRADY, R. O., VANIER, M. T., PENTCHEV, P. G., TAGLE, D. A. 1997. Niemann-Pick C1 disease gene: homology to mediators of cholesterolhomeostasis. *Science*. 11;277(5323):228-31.

CASTELLINO, R. C., DURDEN, D. L. 2007. Mechanisms of disease: the PI3K-Akt-PTEN signaling node-an intercept point for the control of angiogenesis in brain tumors. *Nat Clin Pract Neurol.* 3(12):682-93.

CHANG, A. E., KARNELL, L. H., MENCK, H. R. 1998. The National Cancer Data Base report on cutaneous and non cutaneous melanoma: a summary of 84,836 cases from the past decade. The American College of Surgeons Commission on Cancer and the American Cancer Society. *Cancer*. 83(8):1664-78.

CHANG, D. T., LOPEZ, A., VON KESSLER, D. P., CHIANG, C., SAMANDL, B. K., ZHAO, R., SELDIN, M. F., FALLON, J. F., BEACHY, P. A. 1994. Products, genetic linkage and limb patterning activity of a murine hedgehog gene. *Development*. 120:3339–3353.

CHANG, H., LI, Q., MORAES, R. C., LEWIS, M. T., HAMEL, P. A. 2010. Activation of Erk by sonic hedgehog independent of canonical hedgehog signalling. *Int J Biochem Cell Biol*. 42(9):1462-71.

CHEN, Y., SASAI, N., MA, G., YUE, T., JIA, J., BRISCOE, J., JIANG, J. 2011. Sonic Hedgehog dependent phosphorylation by CK1alpha and GRK2 is required for ciliary accumulation and activation of smoothened. *PLoS Biol.* 9, e1001083.

CHIANG, C., LITINGTUNG, Y., LEE, E., YOUNG, K. E., CORDEN, J. L., WESTPHAL, H., BEACHY, P. A. 1996. Cyclopia and defective axial patterning in mice lacking Sonic hedgehog gene function. *Nature*. 383(6599):407-13.

CHIEN, A. J., CONRAD, W. H., MOON, R. T. 2009. A Wnt survival guide: from flies to human disease. *J Invest Dermatol*. 129(7):1614-27.

COLLINS, T. J. 2007. ImageJ for microscopy. *Biotechniques*. 43(1 Suppl):25-30.

CORBIT, K. C., AANSTAD, P., SINGLA, V., NORMAN, A. R., STAINIER, D. Y., REITER, J. F. 2005. Vertebrate Smoothened functions at the primary cilium. *Nature*. 437(7061):1018-21.

CORBIT, K. C., SHYER, A. E., DOWDLE, W. E., GAULDEN, J., SINGLA, V., CHEN, M. H., CHUANG, P. T., REITER, J. F. 2008. Kif3a constrains beta-catenin-dependent Wnt signalling through dual ciliary and non-ciliary mechanisms. *Nat Cell Biol*. 10(1):70-6.

COTSARELIS, G., SUN, T. T., LAVKER, R. M. 1990. Label-retaining cells reside in the bulge area of pilosebaceous unit: implications for follicular stem cells, hair cycle, and skin carcinogenesis. *Cell*. 61(7): 1329-37.

COUVÉ-PRIVAT, S., LE BRET, M., TRAIFFORT, E., QUEILLE, S., COULOMBE, J., BOUADJAR, B., AVRIL, M. F., RUAT, M., SARASIN, A., DAYA-GROSJEAN, L. 2004. Functional analysis of novel sonic hedgehog gene mutations identified in basal cell carcinomas from xeroderma pigmentosum patients. *Cancer Res*. 64(10):3559-65.

CRETNIK, M., POJE, G., MUSANI, V., KRUSLIN, B., OZRETIC, P., TOMAS, D., SITUM, M., LEVANAT, S. 2009. Involvement of p16 and PTCH in pathogenesis of melanoma and basal cell carcinoma. *Int J Oncol*. 2009:34; 1045-1050.

CREUZET, S., SCHULER, B., COULY, G., LE DOUARIN, N. M. 2004. Reciprocal relationships between Fgf8 and neural crest cells in facial and forebrain development. *Proc Natl Acad Sci U S A*. 101(14):4843-7.

CROWE, D. L., MILO, G. E., SHULER, C. F. 1999. Keratin 19 downregulation by oral squamous cell carcinoma lines increases invasive potential. *J Dent Res.* 78:1256–63.

CROWSON, A. N. 2006. Basal cell carcinoma: biology, morphology and clinical implications. *Mod Pathol*. 19 Suppl 2:S127-47.

CRUZALEGUI, F. H., CANO, E., TREISMAN, R. 1999. ERK activation induces phosphorylation of Elk-1 at multiple S/T-P motifs to high stoichiometry. *Oncogene*. 18(56):7948-57.

CURRIE, P. D., INGHAM, P. W. 1996. Induction of a specific muscle cell type by a hedgehog-like protein in zebrafish. *Nature*. 382:452–455.

D'ERRICO, M., CALCAGNILE, M. S., CORONA, R., FUCCI, M., ANNESSI, G., BALIVA, G., TOSTI, E., PASQUINI, P., DOGLIOTTI, E. 1997. p53 Mutations and Chromosome Instability in Basal Cell Carcinomas Developed at an Early or Late Age. *CanRes*. 57; 747-752.

DAHMANE, N., LEE, J., ROBINS, P., HELLER, P., RUIZ I ALTABA, A. 1997. Activation of the transcription factor Gli1 and the Sonic hedgehog signalling pathway in skin tumours. *Nature*. 389, 876-81.

DAHMANE, N., SÁNCHEZ, P., GITTON, Y., PALMA, V., SUN, T., BEYNA, M., WEINER, H., RUIZ I ALTABA, A. 2001. The Sonic Hedgehog-Gli pathway regulates dorsal brain growth and tumorigenesis. *Development*. 128(24):5201-12.

DAVIS, H. E., MORGAN, J. R., YARMUSH, M. L. 2002. Polybrene increases retrovirus gene transfer efficiency by enhancing receptor-independent virus absorption on target cell membranes. *Biophys Chem*. 19;97(2-3):159-72.

DAYA-GROSJEAN, L., COUVE´-PRIVAT, S. 2005. Sonic hedgehog signalling in basal cell carcinomas. *Cancer let*. 225(2) 181-192.

DENEF, N., NEUBUSER, D., PEREZ, L., COHEN, S. M. 2000. Hedgehog induces opposite changes in turnover and subcellular localization of patched and smoothened. *Cell*. 102:521–31.

DENNLER, S., ANDRÉ, J., ALEXAKI, I., LI, A., MAGNALDO, T., TEN DIJKE, P., WANG, X. J., VERRECCHIA, F., MAUVIEL, A. 2007. Induction of sonic hedgehog mediators by transforming growth factor-beta: Smad3-dependent activation of Gli2 and Gli1 expression in vitro and in vivo. *Cancer Res*. 67(14):6981-6.

DENNLER, S., ANDRE, J., VERRECCHIA, F., MAUVIEL, A. 2009. Cloning of the human GLI2 promoter: transcriptional activation by transforming growth factor-beta via SMAD3/beta-catenin cooperation. *J Biol Chem*. 284(46):31523-31.

DEPLEWSKI, D., ROSENFIELD, R. L. 2000. Role of hormones in pilosebaceous unit development. *Endocr Rev*. 21(4): 363-92.

DESSAUD, E., MCMAHON, A. P., BRISCOE, J. 2008. Pattern formation in the vertebrate neural tube: a sonic hedgehog morphogen-regulated transcriptional network. *Development*. 135:2489-503.

DICKER, T., SILLER, G., SAUNDERS, N. 2002. Molecular and cellular biology of basal cell carcinoma. *Australas J Dermatol.* 43(4):241-6.

DICKSON, M. A., HAHN, W. C., INO, Y., RONFARD, V., WU, J. Y., WEINBERG, R. A., LOUIS D. N., LI, F. P., RHEINWALD, J. G. 2000. Human keratinocytes that express hTERT and also bypass a p16(INK4a)-enforced mechanism that limits life span become immortal yet retain normal growth and differentiation characteristics. *Mol Cell Biol*. 20(4):1436-47.

DOI, D., ARAKI, T., ASANO, G. 1996. Immunohistochemical localization of tenascin, estrogen receptor and transforming growth factor-beta 1 in human endometrial carcinoma. *Gynecol Obstet Invest.* 41(1):61-6.

DONOVAN, J. 2009. Review of the Hair Follicle Origin Hypothesis for Basal Cell Carcinoma. *Dermatol Surg.* 35(9):1311-23

DOWNING, D. T., STRANIERI, A. M., STRAUSS, J. S. 1982. The effect of accumulated lipids on measurements of sebum secretion in human skin. *J Invest Dermatol*. 79(4): 226-8.

DUMAN-SCHEEL, M., WENG, L., XIN, S., DU, W. 2002. Hedgehog regulates cell growth and proliferation by inducing Cyclin D and Cyclin E. *Nature*. 417(6886):299-304.

ECKERT, R. L., CRISH, J. F., ROBINSON, N. A. 1997. The epidermal keratinocyte as a model for the study of gene regulation and cell differentiation. *Physiol Rev*. 77(2):397-424.

ECHELARD, Y., EPSTEIN, D. J., ST-JACQUES, B., SHEN, L., MOHLER, J., MCMAHON, J. A., MCMAHON, A. P. 1993. Sonic hedgehog, a member of a family of putative signaling molecules, is implicated in the regulation of CNS polarity. *Cell*. 75:1417–1430.

EGGENSCHWILER, J. T., ESPINOZA, E., ANDERSON, K. V. 2001. Rab23 is an essential negative regulator of the mouse Sonic hedgehog signalling pathway. *Nature*. 412(6843):194-8.

EKKER, S. C., UNGAR, A. R., GREENSTEIN, P., VON KESSLER, D. P., PORTER, J. A., MOON, R. T., BEACHY, P. A. 1995. Patterning activities of vertebrate hedgehog proteins in the developing eye and brain. *Curr Biol*. 5:944–955.

EL-OMAR, E. M., NG, M. T., HOLD, G. L. 2008. Polymorphisms in Toll-like receptor genes and the risk of cancer. *Oncogene*. 27(2):244-52.

ELIEZRI, Y. D., SILVERSTEIN, S. J., NUOVO, G. J. 1990. Occurrence of human papillomavirus type 16 DNA in cutaneous squamous and basal cell neoplasms. *J Am Acad Dermatol*. 23(5 Pt 1):836-42.

ELLIOTT, C. L., ALLPORT, V. C., LOUDON, J. A., WU, G. D., BENNETT, P. R. 2001. Nuclear factor-kappa B is essential for up-regulation of interleukin 8 expression in human amnion and cervicalepithelial cells. *Mol Hum Reprod.* 7(8):787-90.

ELLIS, R. A., MONTAGNA, W., FANGER, H. 1958. Histology and cytochemistry of human skin. XIV. The blood supply of the cutaneous glands. *J Invest Dermatol*. 30(3): 137-45.

ELWOOD, J. M., GALLAGHER, R. P., HILL, G. B., PEARSON, J. C. 1985. Cutaneous melanoma in relation to intermittent and constant sun exposure-the Western Canada Melanoma Study. *Int J Cancer.* 35(4):427-33.

ENDOH-YAMAGAMI, S., EVANGELISTA, M., WILSON, D., WEN, X., THEUNISSEN, J. W., PHAMLUONG, K., DAVIS, M., SCALES, S. J., SOLLOWAY, M. J., DE SAUVAGE, F. J., PETERSON, A. S. 2009. The mammalian Cos2 homolog Kif7 plays an essential role in modulating Hh signal transduction during development. *Curr Biol.* 19, 1320-1326.

EVANS, D. G., HOWARD, E., GIBLIN, C., CLANCY, T., SPENCER, H., HUSON, S. M., LALLOO, F. 2010. Birthe incidence and prevalence of tumor-prone syndromes: estimates from a UK family genetic register service. *Am J Med Genet A.* 152A(2):327-32.

FAN, Q., HE, M., SHENG, T., ZHANG, X., SINHA, M., LUXON, B., XHAO, X., XIE, J. 2010. Requirement of TGFbeta signalling for SMO-mediated carcinogenesis. *J Biol Chem*. 285(47):36570-6.

FAN, L., PEPICELLI, C. V., DIBBLE, C. C., CATBAGAN, W., ZARYCKI, J. L., LACIAK, R., GIPP, J., SHAW, A., LAMM, M. L., MUNOZ, A., LIPINSKI, R., THRASHER, J. B., BUSHMAN, W. 2004. Hedgehog signalling promotes prostate xenograft tumor growth. *Endocrinology*. 145, 3961-70.

FARAGE, M. A., MILLER, K. W., MAIBACH, H. I. 2010. Textbook of aging skin. Springer.

FEARS, T. R., SCOTTO, J. 1983. Estimating increases in skin cancer morbidity due to increases in ultraviolet radiation exposure. *Cancer Invest*. 1:119-26.

FERRANTE, M. I., ZULLO, A., BARRA, A., BIMONTE, S., MESSADDEQ, N., STUDER, M., DOLLÉ, P., FRANCO, B. 2006. Oral-facial-digital type I protein is required for primary cilia formation and left-right axis specification. *Nat Genet.* 38(1):112-7.

FREEDBERG, I. M., EISEN, A. Z., WOLFF, K., AUSTEN, K. F., GOLDSMITH, L. A., KATZ, S. I. 2003. Fitzpatrick's Dermatology in General Medicine, 6th ed. New York: McGraw-Hill.

FREINKEL, R. K., WOODLEY, D. 2001. The biology of the skin. New York: Parthenon Pub.

FUCHS, E. 1990. Epidermal differentiation: the bare essentials. *J Cell Biol*. 111(6 Pt 2):2807-14.

FUCHS, E. 2007. Scratching the surface of skin development. *Nature*. 445(7130):834-42.

GAILANI, M. R., BALE, A. E. 1997. Developmental genes and cancer: role of patched in basal cell carcinoma of the skin. *J Natl Cancer Inst*. 89(15):1103-9.

GAILANI, M. R., STÅHLE-BÄCKDAHL, M., LEFFELL, D. J., GLYNN, M., ZAPHIROPOULOS, P. G., PRESSMAN, C., UNDÉN, A. B., DEAN, M., BRASH, D. E., BALE, A. E., TOFTGÅRD, R. 1996. The role of the human homologue of Drosophila patched in sporadic basal cell carcinomas. *Nat Genet*. 14(1):78-81.

GAMBICHLER, T., SKRYGAN, M., KACZMARCZYK, J. M., HYUN, J., TOMI, N. S., SOMMER, A., BECHARA, F. G., BOMS, S., BROCKMEYER, N. H., ALTMEYER, P., KREUTER, A. 2007. Increased expression of TGF-beta/Smad proteins in basal cell carcinoma. *Eur J Med Res*. 12(10):509-14.

GAO, Z. H., SEELING, J. M., HILL, V., YOCHUM, A., VIRSHUP, D. M. 2002. Casein kinase I phosphorylates and destabilizes the beta-catenin degradation complex. *Proc Natl Acad Sci U S A*. 99(3):1182-7.

GARIBYAN, L., FISHER, D. E. 2010. How sunlight causes melanoma. *Curr Oncol Rep*. 12:319-326.

GENTLEMAN, R., CAREY, V., HUBER, W., IRIZARRY, R., DUDOIT, S. 2005. Bioinformatics and Computational Biology Solutions Using R and Bioconductor. New York:Springer.

GERDES, J. M., DAVIS, E. E.,KATSANIS, N. 2009. The vertebrate primary cilium in development, homeostasis, and disease. *Cell*. 137: 32–45.

GERDES, J. M., LIU, Y., ZAGHLOUL, N. A., LEITCH, C. C., LAWSON, S. S., KATO, M., BEACHY, P. A., BEALES, P. L., DEMARTINO, G. N., FISHER, S., BADANO, J. L., KATSANIS, N. 2007. Disruption of the basal body compromises proteasomal function and perturbs intracellular Wnt response. *Nat Genet*. 39(11):1350-60.

GHALI, L., WONG, S. T., GREEN, J., TIDMAN, N., QUINN, A. G. 1999. Gli1 protein is expressed in basal cell carcinomas, outer root sheath keratinocytes and a subpopulation of mesenchymal cells in normal human skin. *J Invest Dermatol.* 113(4):595-9.

GHAVAMI, S., HASHEMI, M., ANDE, S. R., YEGANEH, B., XIAO, W., ESHRAGHI, M., BUS, C. J., KADKHODA, K., WIECHEC, E., HALAYKO, A. J, LOS, M. 2009. Apoptosis and cancer: mutations within caspase genes. *J Med Genet.* 46(8):497-510.

GILLES, C., POLETTE, M., PIETTE, J., DELVIGNE, A. C., THOMPSON, E. W., FOIDART, J. M., BIREMBAUT, P. 1996. Vimentin expression in cervical carcinomas: association with invasive and migratory potential. *J Pathol.* 180:175–80.

GOLDSMITH, L. A. 2005. Physiology, biochemistry, and molecular biology of the skin. 2nd ed. New York: Oxford University Press.

GOODRICH, L. V., JOHNSON, R. L., MILENKOVIC, L., MCMAHON, J. A., SCOTT, M. P. 1996. Conservation of the hedgehog/patched signaling pathway from flies to mice: induction of a mouse patched gene by Hedgehog. *Genes Dev*. 10(3):301-12.

GÖPPNER, D., LEVERKUS, M. 2011. Basal cell carcinoma: from the molecular understanding of the pathogenesis to targeted therapy of progressive disease. *J Skin Cancer.* 2011:650258.

GORLIN, R. J., GOLTZ, R. W. 1960. Multiple nevoid basal-cell epithelioma, jaw cysts and bifid rib. A syndrome. *N Engl J Med*. 262:908–912.

GRACHTCHOUK, V., GRACHTCHOUK, M., LOWE, L., JOHNSON, T., WEI, L., WANG, A., DE SAUVAGE, F., DLUGOSZ, A. A. 2003. The magnitude of hedgehog signaling activity defines skin tumor phenotype. *EMBO J*. 22(11):2741-51.

GRACHTCHOUK, M., MO, R., YU, S., ZHANG, X., SASAKI, H., HUI, C. C., DLUGOSZ, A. A. 2000. Basal cell carcinomas in mice overexpressing Gli2 in skin. *Nat Genet.* 24(3):216-7.

GRACHTCHOUK, M., PERO, J., YANG, S. H., ERMILOV, A. N., MICHAEL, L. E., WANG, A., WILBERT, D., PATEL, R. M., FERRIS, J., DIENER, J., ALLEN, M., LIM, S., SYU, L. J., VERHAEGEN, M., DLUGOSZ, A. A. 2011. Basal cell carcinomas in mice arise from hair follicle stem cells and multiple epithelial progenitor populations. *J Clin Invest.* 121(5):1768-81.

GRANDO, S. A., SCHOFIELD, O. M., SKUBITZ, A. P., KIST, D. A., ZELICKSON, B. D., ZACHARY, C. B. 1996. Nodular basal cell carcinoma in vivo vs in vitro. Establishment of pure cell cultures, cytomorphologic characteristics, ultrastructure, immunophenotype, biosynthetic activities, and generation of antisera. *Arch Dermatol.* 132(10):1185-93.

GREGG, J., FRAIZER, G. 2011. Transcriptional regulation of EGR1 by EGF and the ERK Signaling Pathway in Prostate Cancer Cells. *Genes Cancer*. 2(9):900-9.

GROSSMAN, D., LEFFELL, D. J. 1997. The molecular basis of nonmelanoma skin cancer: new understanding. *Arch Dermatol.* 133:1263-70.

GRINDLEY, J. C., BELLUSCI, S., PERKINS, D., HOGAN, B. L. 1997. Evidence for the involvement of the Gli gene family in embryonic mouse lung development. *Dev Biol*. 188(2):337-48.

GU, L., ZHU, N., FINDLEY, H. W., WOODS, W. G., ZHOU, M. 2004. Identification and characterization of the IKKalpha promoter: positive and negative regulation by ETS-1 and p53, respectively. *J Biol Chem.* 279, 52141–52149.

HAFNER, C., HOUBEN, R., BAEURLE, A., RITTER, C., SCHRAMA, D., LANDTHALER, M., BECKER, J. C. 2012. Activation of the PI3K/AKT pathway in Merkel cell carcinoma. *PLoS One*. 7(2):e31255.

HAFNER, C., LANDTHALER, M., VOGT, T. 2010. Activation of the PI3K/AKT signalling pathway in non-melanoma skin cancer is not mediated by oncogenic PIK3CA and AKT1 hotspot mutations. *Exp Dermatol.* 19(8):e222-7.

HAHN, H., WICKING, C., ZAPHIROPOULOUS, P. G., GAILANI, M. R., SHANLEY, S., CHIDAMBARAM, A., VORECHOVSKY, I., HOLMBERG, E., UNDEN, A. B., GILLIES, S., NEGUS, K., SMYTH, I., PRESSMAN, C., LEFFELL, D. J., GERRARD, B., GOLDSTEIN, A. M., DEAN, M., TOFTGARD, R., CHENEVIX-TRENCH, G., WAINWRIGHT, B., BALE, A. E. 1996. Mutations of the human homolog of Drosophila patched in the nevoid basal cell carcinoma syndrome. *Cell*. 85(6):841-51.

HANSSON, J. 2010. Familial cutaneous melanoma. *Adv Exp Med Biol*. 685:134-145.

HARDCASTLE, Z., MO, R., HUI, C. C., SHARPE, P. T. 1998. The Shh signalling pathway in tooth development: defects in Gli2 and Gli3 mutants. *Development*. 125(15):2803-11.

HARRIS, P. J., TAKEBE, N., IVY, S. P. 2010. Molecular conversations and the development of the hair follicle and basal cell carcinoma. *Cancer Prev Res (Phila).* 3(10):1217-21.

HAUSSLER, U., VON WICHERT, G., SCHMID, R. M., KELLER, F., SCHNEIDER, G. 2005. Epidermal growth factor activates nuclear factor-kappaB in human proximal tubule cells. *Am J Physiol Renal Physiol*. 289, F808–F815.

HAYCRAFT, C. J., BANIZS, B., AYDIN-SON, Y., ZHANG, Q., MICHAUD, E. J., YODER, B. K. 2005. Gli2 and Gli3 localize to cilia and require the intraflagellar transport protein polaris for processing and function. *PLoS Genet*. 1, e53.

HEGDE, G. V., PETERSON, K. J., EMANUEL, K., MITTAL, A. K., JOSHI, A. D., DICKINSON, J. D., KOLLESSERY, G. J., BOCIEK, R. G., BIERMAN, P., VOSE, J. M., WEISENBURGER, D. D., JOSHI, S. S. 2008. Hedgehog-induced survival of B-cell chronic lymphocytic leukemia cells in a stromal cell microenvironment: a potential new therapeutic target. *Mol Cancer Res*. 6, 1928-36.

HINO, S., TANJI, C., NAKAYAMA, K. I., KIKUCHI, A. 2005. Phosphorylation of beta-catenin by cyclic AMP-dependent protein kinase stabilizes beta-catenin through inhibition of its ubiquitination. *Mol Cell Biol*. 25(20):9063-72.

HOFFMAN, R. M. 2007. The potential of nestin-expressing hair follicle stem cells in regenerative medicine. *Expert Opin Biol Ther.* 7(3):289-91.

HOLMES, S. A., MALINOVSZKY, K., ROBERTS, D. L. 2000. Changing trends in non-melanoma skin cancer in South Wales, 1988-1998. *Br J Dermatol*. 143: 1224-9.

HOOPER, J. E., SCOTT, M. P. 2005. Communicating with Hedgehogs. *Nat Rev Mol Cell Biol*. 6:306-17.

HORNE, K. A., JAHODA, C. A., OLIVER, R. F. 1986. Whisker growth induced by implantation of cultured vibrissa dermal papilla cells in the adult rat. *J Embryol Exp Morphol*. 97: 111-24.

HOSOKAWA, Y., HOSOKAWA, I., OZAKI, K., NAKAE, H., MATSUO, T. 2010. TNFSF14 coordinately enhances CXCL10 and CXCL11 productions from IFN-gamma-stimulated human gingival fibroblasts. *Mol Immunol.* 47(4):666-70.

HUANG, D. W., SHERMAN, B. T., LEMPICKI, R. A. 2009. Systematic and integrative analysis of large gene lists using DAVID Bioinformatics Resources. *Nature Protoc*. 4(1):44-57.

HUANGFU, D., ANDERSON, K. V. 2006. Signaling from Smo to Ci/Gli: Conservation and divergence of Hedgehog pathways from Drosophila to vertebrates. *Development*. 133:3–14.

HUANGFU, D., LIU, A., RAKEMAN, A. S., MURCIA, N. S., NISWANDER, L., ANDERSON, K. V. 2003. Hedgehog signalling in the mouse requires intraflagellar transport proteins. *Nature*. 426, 83-7.

HUELSKEN, J., VOGEL, R., ERDMANN, B., COTSARELIS, G., BIRCHMEIER, W. 2001. beta-Catenin controls hair follicle morphogenesis and stem cell differentiation in the skin. *Cell*. 105(4): 533-45.

HUMKE, E. W., DORN, K. V., MILENKOVIC, L., SCOTT, M. P., ROHATGI, R. 2010. The output of Hedgehog signaling is controlled by the dynamic association between Suppressor of Fused and the Gli proteins. *Genes Dev*. 24, 670-682.

HYNES, N. E., LANE, H. A. 2005. ERBB receptors and cancer: the complexity of targeted inhibitors. *Nat Rev Cancer.* 5(5):341-54.

INGHAM, P. W., MCMAHON, A. P. 2001. Hedgehog signaling in animal development: Paradigms and principles. *Genes & Dev*. 15:3059–3087.

INOUE, Y., NIWA, N., MITO, T., OHUCHI, H., YOSHIOKA, H., NOJI, S. 2002. Expression patterns of hedgehog, wingless, and decapentaplegic during gut formation of Gryllus bimaculatus (cricket) Mech. *Dev*. 110:245–248.

IRIZARRY, R. A., BOLSTAD, B. M., COLLIN, F., COPE, L. M., HOBBS, B., SPEED, T. P. 2003. Summaries of Affymetrix GeneChip probe level data. *Nucleic Acids Res*. 31(4):e15.

ISEKI, S., ARAGA, A., OHUCHI, H., NOHNO, T., YOSHIOKA, H., HAYASHI, F., NOJI, S. 1996. Sonic hedgehog is expressed in epithelial cells during development of whisker, hair, and tooth. *Biochem Biophys Res Commun.* 218:688-93.

IZZI, L., LEVESQUE, M., MORIN, S., LANIEL, D., WILKES, B. C., MILLE, F., KRAUSS, R. S., MCMAHON, A. P., ALLEN, B. L., CHARRON, F. 2011. Boc and Gas1 each form distinct Shh receptor complexes with Ptch1 and are required for Shh-mediated cell proliferation. *Dev Cell*. 20, 788-801.

JAHODA, C. A. 1992. Induction of follicle formation and hair growth by vibrissa dermal papillae implanted into rat ear wounds: vibrissa-type fibres are specified. *Development*. 115(4):1103-9.

JAHODA, C. A., HORNE, K. A., MAUGER, A., BARD, S., SENGEL, P. 1992. Cellular and extracellular involvement in the regeneration of the rat lower vibrissa follicle. *Development*. 114(4):887-97.

JAHODA, C. A., OLIVER, R. F. 1984. Vibrissa dermal papilla cell aggregative behaviour in vivo and in vitro. *J Embryol Exp Morphol*. 79:211-24.

JAHODA, C. A., REYNOLDS, A. J. 2001. Hair follicle dermal sheath cells: unsung participants in wound healing. *Lancet*. 358(9291):1445-8.

JENSEN, C. G., POOLE, C. A., MCGLASHAN, S. R., MARKO, M., ISSA, Z. I., VUJCICH, K. V., BOWSER, S. S. 2004. Ultrastructural, tomographic and confocal imaging of the chondrocyte primary cilium in situ. *Cell Biol Int.* 28(2):101-10.

JEONG, H. S., PARK, K. C., KIM, D. S. 2012. PP2A and DUSP6 are involved in sphingosylphosphorylcholine-induced hypopigmentation. *Mol Cell Biochem*. 367(1-2):43-9.

JERANT, A. F., JOHNSON, J. T., SHERIDAN, C. D., CAFFREY, T. J. 2000. Early Detection and Treatment of Skin Cancer. *Am Fam Physician.* 62(2):357-68, 375-6, 381-2.

JIA, J., TONG, C., JIANG, J. 2003. Smoothened transduces Hedgehog signal by physically interacting with Costal2/Fused complex through its C-terminal tail. *Genes Dev.* 17, 2709-2720.

JOHNSON, R. L., ROTHMAN, A. L., XIE, J., GOODRICH, L. V., BARE, J. W., BONIFAS, J. M., QUINN, A. G., MYERS, R. M., COX, D. R., EPSTEIN, E. H. JR, SCOTT, M. P. 1996. Human homolog of patched, a candidate gene for the basal cell nevus syndrome. *Science*. 272(5268):1668-71.

JOHNSON, T. M., ROWE, D. E., NELSON, B. R., SWANSON, N. A. 1992. Squamous cell carcinoma of the skin (excluding lip and oral mucosa). *J Am Acad Dermatol*. 26:467-84

KAGAWA, H., SHINO, Y., KOBAYASHI, D., DEMIZU, S., SHIMADA, M., ARIGA, H., KAWAHARA, H. 2011. A novel signaling pathway mediated by the nuclear targeting of C-terminal fragments of mammalian Patched 1. *PLoS One*. 6(4):e18638.

KAMATA, M., TADA, Y., TATSUTA, A., KAWASHIMA, T., SHIBATA, S., MITSUI, H., ASANO, Y., SUGAYA, M., KADONO, T., KANDA, N., WATANABE, S., SATO, S. 2012. Serum lipocalin-2 levels are increased in patients with psoriasis. *Clin Exp Dermatol.* 37(3):296-9.

KANOH, M., AMOH, Y., SATO, Y., KATSUOKA, K. 2008. Expression of the hair stem cell-specific marker nestin in epidermal and follicular tumors. *Eur J Dermatol.* 18(5):518-23.

KARAHAN, N., BASPINAR, S., BOZKURT, K. K., CALOGLU, E., CIRIS, I. M., KAPUCUOGLU, N. 2011. Increased expression of COX-2 in recurrent basal cell carcinoma of the skin: a pilot study. *Indian J Pathol Microbiol*. 54(3):526-31.

KARHADKAR, S. S., BOVA, G. S., ABDALLAH, N., DHARA, S., GARDNER, D., MAITRA, A., ISAACS, J. T., BERMAN, D. M. & BEACHY, P. A. 2004. Hedgehog signalling in prostate regeneration, neoplasia and metastasis. *Nature*. 431, 707-12.

KARIN, M., CAO, Y., GRETEN, F. R., LI Z. W. 2002. NF-kappaB in cancer: from innocent bystander to major culprit. *Nat Rev Cancer*. 2(4):301-10.

KASPER, M., SCHNIDAR, H., NEILL, G. W., HANNEDER, M., KLINGLER, S., BLAAS, L., SCHMID, C., HAUSER-KRONBERGER, C., REGL, G., PHILPOTT, M. P., ABERGER, F. 2006. Selective modulation of Hedgehog/GLI target gene expression by epidermal growth factor signaling in human keratinocytes. *Mol Cell Biol*. 26(16):6283-98.

KASPERCZYK, H., BAUMANN, B., DEBATIN, K. M., FULDA, S. 2009. Characterization of sonic hedgehog as a novel NF-kappaB target gene that promotes NF-kappaB-mediated apoptosis resistance and tumor growth *in vivo*. *FASEB J*. 23(1):21-33.

KATOH, Y., KATOH, M. 2008. Hedgehog signaling, epithelial-to-mesenchymal transition and miRNA (review). *Int J Mol Med*. 22(3):271-5.

KATOH, Y., KATOH, M. 2009. Hedgehog target genes: mechanisms of carcinogenesis induced by aberrant hedgehog signaling activation. *Curr Mol Med*. 9(7):873-86.

KAWAI, T., AKIRA, S. 2006. TLR signaling. *Cell Death Differ*. 13(5):816-25.

KERKHOFF, E., RAPP, U. R. 1998. Cell cycle targets of Ras/Raf signalling. *Oncogene*. 17(11 Reviews):1457-62.

KIM, M. Y., PARK, H. J., BAEK, S. C., BYUN, D. G., HOUH, D. 2002. Mutations of the p53 and PTCH gene in basal cell carcinomas: UV mutation signature and strand bias. *J Dermatol Sci*. 29(1):1-9.

KISE, Y., MORINAKA, A., TEGLUND, S., MIKI, H. 2009. Sufu recruits GSK3beta for efficient processing of Gli3. *Biochem Biophys Res Commun.* 387, 569-574.

KJELDSEN, L., JOHNSEN, A. H., SENGELØV, H., BORREGAARD, N. 1993. Isolation and primary structure of NGAL, a novel protein associated with human neutrophil gelatinase. *J Biol Chem*. 268(14):10425-32.

KLEEBERGER, W., BOVA, G. S., NIELSEN, M. E., HERAWI, M., CHUANG, A. Y., EPSTEIN, J. I., BERMAN, D. M. 2007. Roles for the stem cell associated intermediate filament Nestin in prostate cancer migration and metastasis. *Cancer Res*. 67:9199–9206.

KOGERMAN, P., GRIMM, T., KOGERMAN, L., KRAUSE, D., UNDÉN, A. B., SANDSTEDT, B., TOFTGÅRD, R., ZAPHIROPOULOS, P. G. 1999. Mammalian suppressor-of-fused modulates nuclear-cytoplasmic shuttling of Gli-1. *Nat Cell Biol*. 1(5):312-9.

KOHTZ, J. D., LEE, H. Y., GAIANO, N., SEGAL, J., NG, E., LARSON, T., BAKER, D. P., GARBER, E. A., WILLIAMS, K. P., FISHELL, G. 2001. N-terminal fatty-acylation of sonic hedgehog enhances the induction of rodent ventral forebrain neurons. *Development*. 28(12):2351-63.

KOLI, K., HYYTIAINEN, M., RYYNANEN, M. J., KESKI-OJA, J. 2005. Sequential deposition of latent TGF-beta binding proteins (LTBPs) during formation of the extracellular matrix in human lung fibroblasts. *Exp Cell Res*. 310(2): 370-82.

KORE-EDA, S., HORIGUCHI, Y., UEDA, M., TODA, K., IMAMURA, S. 1998. Basal cell carcinoma cells resemble follicular matrix cells rather than follicular bulge cells: immunohistochemical and ultrastructural comparative studies. *Am J Dermatopathol*. 20(4):362-9.

KOVACS, J. J., HARA, M. R., DAVENPORT, C. L., KIM, J., LEFKOWITZ, R. J. 2009. Arrestin development: emerging roles for beta-arrestins in developmental signaling pathways. Dev Cell. 17(4):443-58.

KRAEMER, K. H., PATRONAS, N. J., SCHIFFMANN, R., BROOKS, B. P., TAMURA, D., DIGIOVANNA, J. J. 2007. Xeroderma pigmentosum, trichothiodystrophy and Cockayne syndrome: a complex genotype-phenotype relationship. *Neuroscience*. 145(4):1388–1396.

KRAHN, G., LEITER, U., KASKEL, P., UDART, M., UTIKAL, J., BEZOLD, G., PETER, RU. 2001. Coexpression patterns of EGFR, HER2, HER3 and HER4 in non-melanoma skin cancer. *Eur J Cancer*. 37:251–259.

KRATOCHWIL, K., DULL, M., FARINAS, I., GALCERAN, J., GROSSCHEDL, R. 1996. Lef1 expression is activated by BMP-4 and regulates inductive tissue interactions in tooth and hair development. *Genes Dev. 10*(11): 1382-94.

KRAUSS, S., CONCORDET, J. P., INGHAM, P. W. 1993. A functionally conserved homolog of the *Drosophila* segment polarity gene hh is expressed in tissues with polarizing activity in zebrafish embryos*. Cell.* 75*:*1431–1444*.*

KUMAR, R. 2003. BRAF Mutations in Metastatic Melanoma A Possible Association with Clinical Outcome. *Clin Canc Res*. 9:3362-3368.

KUSAKARI, Y., OGAWA, E., OWADA, Y., KITANAKA, N., WATANABE, H., KIMURA, M., TAGAMI, H., KONDO, H., AIBA, S., OKUYAMA, R. 2006. Decreased keratinocyte motility in skin wound on mice lacking the epidermal fatty acid binding protein gene. *Mol Cell Biochem.* 284(1-2):183-8.

KUWABARA, P. E., LEE, M. H., SCHEDL, T., JEFFERIS, G. S. 2000. A *C. Elegans* patched gene, ptc-1, functions in germ-like cytokinesis. *Genes & Dev.* 14*:*1933–1944*.*

LANDI, M. T., BAUER, J., PFEIFFER, R. M., ELDER, D. E., HULLEY, B., MINGHETTI, P., CALISTA, D., KANETSKY, P. A., PINKEL, D., BASTIAN, B. C. 2006. MC1R Germline Variants Confer Risk for BRAF-Mutant Melanoma. *Science*. 313:521-522.

LANSKE, B., KARAPLIS, A. C., LEE, K., LUZ, A., VORTKAMP, A., PIRRO, A., KARPERIEN, M., DEFIZE, L. H., HO, C., MULLIGAN, R. C., ABOU-SAMRA, A. B., JÜPPNER, H., SEGRE, G. V., KRONENBERG, H. M. 1996. PTH/PTHrP receptor in early development and Indian hedgehog-regulated bone growth. *Science*. 273(5275):663-6.

LARKIN, M. A., BLACKSHIELDS, G., BROWN, N. P., CHENNA, R., MCGETTIGAN, P. A., MCWILLIAM, H., VALENTIN, F., WALLACE, I. M., WILM, A., LOPEZ, R., THOMPSON, J. D., GIBSON, T. J., HIGGINS, D. G. 2007. ClustalW and ClustalX version 2. *Bioinformatics*. 23(21): 2947-2948.

LATIJNHOUWERS, M. A., DE JONGH, G. J., BERGERS, M., DE ROOIJ, M. J., SCHALKWIJK, J. 2000. Expression of tenascin-C splice variants by human skin cells. *Arch Dermatol Res.* 292(9):446-54.

LATINKIĆ, B. V., ZEREMSKI, M., LAU, L. F. 1996. Elk-1 can recruit SRF to form a ternary complex upon the serum response element. *Nucleic Acids Res*. 24(7):1345-51.

LAUBER, K., BLUMENTHAL, S. G., WAIBEL, M., WESSELBORG, S. 2004. Clearance of apoptotic cells: getting rid of the corpses. *Mol Cell*. 14(3):277-87.

LAUTH, M., BERGSTRÖM, A., SHIMOKAWA, T., TOFTGÅRD, R. 2007. Inhibition of GLI-mediated transcription and tumor cell growth by small-molecule antagonists. *Proc Natl Acad Sci U S A*. 104(20):8455-60.

LAUTH, M., TOFTGÅRD, R. 2007. Non-canonical activation of GLI transcription factors: implications for targeted anti-cancer therapy. *Cell Cycle*. 6(20):2458-63.

LAUTH, M., TOFTGÅRD, R. 2007. The Hedgehog pathway as a drug target in cancer therapy. *Curr Opin Investig Drugs.* 8(6):457-61.

LAW, A. M., OLIVERI, C. V., PACHECO-QUINTO, X., HORENSTEIN, M. G. 2003. Actin expression in purely nodular versus nodular-infiltrative basal cell carcinoma. *J Cutan Pathol.* 30(4):232-6.

LEE, J. H., GLEESON, J. G. 2010. The role of primary cilia in neuronal function. *Neurobiol Dis.* 38(2): 167–172.

LEE, J. D., KRAUS, P., GAIANO, N., NERY, S., KOHTZ, J., FISHELL, G., LOOMIS, C. A., TREISMAN, J. E. 2001. An acylatable residue of Hedgehog is differentially required in *Drosophila* and mouse limb development. *Dev Biol.* 233(1):122-36.

LEHMAN, T. A., MODALI, R., BOUKAMP, P., STANEK, J., BENNETT, W. P., WELSH, J. A., METCALF, R. A., STAMPFER, M. R., FUSENIG, N., ROGAN, E. M., HARRIS, C. C. 1993. p53 mutations in human immortalized epithelial cell lines. *Carcinogenesis*. 14(5):833-9.

LEIGH, I. M., PURKIS, P. E., MARKEY, A., COLLINS, P., NEILL, S., PROBY, C., GLOVER, M., LANE, E. B. 1993. Keratinocyte alterations in skin tumour development. *Recent Results Cancer Res*. 128:179-91.

LEWIS, P. M., DUNN, M. P., MCMAHON, J. A., LOGAN, M., MARTIN, J. F., ST-JACQUES, B., MCMAHON, A. P. 2001. Cholesterol modification of sonic hedgehog is required for long-range signaling activity and effective modulation of signaling by Ptc1. *Cell*. 105, 599-612.

LEWIS, D. A., YI, Q., TRAVERS, J. B., SPANDAU, D. F. 2008. UVB-induced senescence in human keratinocytes requires a functional insulin-like growth factor-1 receptor and p53. *Mol Biol Cell*. 19(4):1346-53.

LI, H., CHERUKURI, P., LI, N., COWLING, V., SPINELLA, M., COLE, M., GODWIN, A. K., WELLS, W., DIRENZO, J. 2007. Nestin is expressed in the basal/myoepithelial layer of the mammary gland and is a selective marker of basal epithelial breast tumors. *Cancer Res.* 67:501–510.

LI, X., DENG, W., NAIL, C. D., BAILEY, S. K., KRAUS, M. H., RUPPERT, J. M., LOBO-RUPPERT, S. M. 2006. Snail induction is an early response to Gli1 that determines the efficiency of epithelial transformation. *Oncogene*. 25(4):609-21.

LI, L., NEAVES, W. B. 2006. Normal stem cells and cancer stem cells: the niche matters. *Cancer Res*. 66(9):4553-7.

LI, C., SCOTT, D. A., HATCH, E., TIAN, X., MANSOUR, S. L. 2007. Dusp6 (Mkp3) is a negative feedback regulator of FGF-stimulated ERK signaling during mouse development. *Development*. 134(1):167-76.

LI, X., STARK, G. R. 2002. NFkappaB-dependent signaling pathways. *Exp Hematol.* 30(4):285-96.

LI, G., VEGA, R., NELMS, K., GEKAKIS, N., GOODNOW, C., MCNAMARA, P., WU, H., HONG, N. A., GLYNNE, R. 2007. A role for Alström syndrome protein, alms1, in kidney ciliogenesis and cellular quiescence. *PLoS Genet*. 3 (1): e8.

LIBERMANN, T. A., BALTIMORE, D. 1990. Activation of interleukin-6 gene expression through the NF-kappa B transcription factor. *Mol Cell Biol*. 10(5):2327-34.

LIEM, K. Z. F. JR, HE, M., OCBINA, P. J., ANDERSON, K. V. 2009. Mouse Kif7/Costal2 is a cilia-associated protein that regulates Sonic hedgehog signaling. *Proc Natl Acad Sci U S A*. 106, 13377-13382.

LIEM, K. F. JR, JESSELL, T. M., BRISCOE, J. 2000. Regulation of the neural patterning activity of sonic hedgehog by secreted BMP inhibitors expressed by notochord and somites. *Development*. 127(22):4855-66.

LIEM, K. F. JR, TREMML, G., ROELINK, H., JESSELL, T. M. 1995. Dorsal differentiation of neural plate cells induced by BMP-mediated signals from epidermal ectoderm. *Cell*. 82(6):969-79.

LIEN, M. H., SONDAK, V. K. 2001. Nonsurgical treatment options for Basal cell carcinoma. *J Skin Cancer*. 2011:571734.

LIN, H. Y., YANG, L. T. 2013. Differential response of epithelial stem cell populations in hair follicles to TGF-β signalling. *Dev Biol*. 373(2):394-406.

LING, L., NURCOMBE, V., COOL, S. M. 2009. Wnt signaling controls the fate of mesenchymal stem cells. *Gene*. 433(1-2):1-7.

LIU, Y., LYLE, S., YANG, Z., COTSARELIS, G. 2003. Keratin 15 promoter targets putative epithelial stem cells in the hair follicle bulge. *J Invest Dermatol.* 121(5):963-8.

LIU, X., RUBIN, J. S., KIMMEL, A. R. 2005. Rapid, Wnt-induced changes in GSK3beta associations that regulate beta-catenin stabilization are mediated by Galpha proteins. *Curr. Biol*. 15 (22): 1989–97.

LO, B. K., YU, M., ZLOTY, D., COWAN, B., SHAPIRO, J., MCELWEE, K. J. 2010. CXCR3/ligands are significantly involved in the tumorigenesis of basal cell carcinomas. *Am J Pathol*. 176(5):2435-46.

LODISH, H., BERK, A., ZIPURSKY, S. L., MATSUDARIA, P., BALTIMORE, D., DARNELL, J. 2000. Molecular Cell Biology, 4th ed. W. H. Freeman & Co.: New York.

LOVE, W. E., BERNHARD, J. D., BORDEAUX, J. S. 2009. Topical imiquimod or fluorouracil therapy for basal and squamous cell carcinoma: a systematic review. *Arch Dermatol*. 145(12):1431-8.

LU, C. J., DU, H., WU, J., JANSEN, D. A., JORDAN, K. L., XU, N., SIECK, G. C., QIAN, Q. 2008. Non-random distribution and sensory functions of primary cilia in vascular smooth muscle cells. *Kidney Blood Press Res.* 31(3):171-84.

LUM, L., BEACHY, P. A. 2004. The Hedgehog response network: sensors, switches, and routers. *Science*. 304(5678):1755-9.

MA, D. R., YANG, E. N., LEE, S. T. 2004. A review: the location, molecular characterisation and multipotency of hair follicle epidermal stem cells. *Ann Acad Med Singapore*. 33(6):784-8.

MADDOCKS, O. D., VOUSDEN, K. H. 2011. Metabolic regulation by p53. *J Mol Med (Berl).* 89(3):237-45.

MAEHAMA, T., DIXON, J. E. 1998. The tumor suppressor, PTEN/MMAC1, dephosphorylates the lipid second messenger, phosphatidylinositol 3,4,5-trisphosphate. *J Biol Chem*. 273(22):13375-8.

MAILLET, M., PURCELL, N. H., SARGENT, M. A., YORK, A. J., BUENO, O. F., MOLKENTIN, J. D. 2008.DUSP6 (MKP3) null mice show enhanced ERK1/2 phosphorylation at baseline and i ncreased myocyteproliferation in the heart affecting disease susceptibility. *J Biol Chem*. 283(45):31246-55.

MAKITIE, O., PUKKALA, E., TEPPO, L., KAITILA, I. 1999. Increased incidence of cancer in patients with cartilage-hair hypoplasia. *J Pediatr.* 134(3):315–318.

MALLBRIS, L., O'BRIEN, K. P., HULTHÉN, A., SANDSTEDT, B., COWLAND, J. B., BORREGAARD, N., STÅHLE-BÄCKDAHL, M. 2002. Neutrophil gelatinase-associated lipocalin is a marker for dysregulated keratinocyte differentiation in human skin. *Exp Dermatol.* 11(6):584-91.

MANCUSO, M., PAZZAGLIA, S., TANORI, M., HAHN, H., PAOLA, M., REBESSI, S., ATKINSON, M. J., MAJO, V. D., COVELLI, V., SARAN, A. 2004. Basal Cell Carcinoma and Its Development: Insights from Radiation-Induced Tumours in Ptch-1 Deficient Mice. *CanRes*. 64:934-941.

MANNELQVIST, M., STEFANSSON, I. M., WIK, E., KUSONMANO, K., RAEDER, M. B., OYAN, A. M., KALLAND, K. H., MOSES, M. A., SALVESEN, H. B., AKSLEN, L. A. 2012. Lipocalin 2 expression is associated with aggressive features of endometrial cancer. *BMC Cancer.* 12:169.

MARASÀ, L., MARASÀ, S. , SCIANCALEPORE, G. 2008. Collagen IV, laminin, fibronectin, vitronectin. Comparative study in basal cell carcinoma. Correlation between basement membrane molecules expression and invasive potential. *G Ital Dermatol Venereol.* 143(3):169-73.

MARICICH, S. M., WELLNITZ, S. A., NELSON, A. M., LESNIAK, D. R., GERLING, G. J., LUMPKIN, E. A., ZOGHBI, H. Y. 2009. Merkel cells are essential for light-touch responses. *Science*. 324(5934):1580-2.

MARIGO, V., DAVEY, R. A., ZUO, Y., CUNNINGHAM, J. M., TABIN, C. J. 1996. Biochemical evidence that patched is the Hedgehog receptor. *Nature*. 384(6605):176-9.

MARKS, R., STAPLES, M., GILES, G. 1993. Trends in non-melanocytic skin cancer treated in Australia: the second national survey. *Int J Cancer*. 53: 585-90.

MASOUYÉ, I., SAURAT, J. H., SIEGENTHALER, G. 1996. Epidermal fatty-acid-binding protein in psoriasis, basal and squamous cell carcinomas: an immunohistological study. *Dermatology*. 192(3):208-13.

MASSAGUE, J. 1998. TGF-beta signal transduction. *Annu Rev Biochem.* 67: 753-91.

MAUBEC, E., DUVILLARD, P., VELASCO, V., CRICKX, B., AVRIL, M. F. 2005. Immunohistochemical analysis of EGFR and HER-2 in patients with metastatic squamous cell carcinoma of the skin. *Anticancer Res*. 25:1205–1210.

MCGRATH, J. A., EADY, R. A., POPE, F. M. 2004. Rook's Textbook of Dermatology (Seventh Edition). Blackwell Publishing. Pages 3.8.

MCMAHON, A. P. 2000. More surprises in the Hedgehog signaling pathway. *Cell*. 100(2):185-8.

MERRILL, B. J., GAT, U., DASGUPTA, R., FUCHS, E. 2001. Tcf3 and Lef1 regulate lineage differentiation of multipotent stem cells in skin. *Genes Dev*. 15(13): 1688-705.

MICHAELSSON, G., OLSSON, E., WESTERMARK, P. 1981. The Rombo syndrome: a familial disorder with vermiculate atrophoderma, milia, hypotrichosis, trichoepitheliomas, basal cell carcinomas and peripheral vasodilation with cyanosis. *Acta Derm Venereol*. 61(6):497–503.

MILL, P., MO, R., FU, H., GRACHTCHOUK, M., KIM, P. C., DLUGOSZ, A. A., HUI, C. C. 2003. Sonic hedgehog-dependent activation of Gli2 is essential for embryonic hair follicle development. *Genes Dev*. 17(2):282-94.

MING, M., HE, Y. Y. 2009. PTEN: new insights into its regulation and function in skin cancer. *J Invest Dermatol*. 129(9):2109-12.

MIRSKY, R., PARMANTIER, E., MCMAHON, A. P., JESSEN, K. R. 1999. Schwann cell-derived desert hedgehog signals nerve sheath formation. *Ann N Y Acad Sci*. 883:196-202.

MIYAZONO, K. 1997. TGF-beta receptors and signal transduction. *Int J Hematol.* 65(2): 97-104.

MO, R., FREER, A. M., ZINYK, D. L., CRACKOWER, M. A., MICHAUD, J., HENG, H. H., CHIK, K. W., SHI, X. M., TSUI, L. C., CHENG, S. H., JOYNER, A. L., HUI, C. 1997. Specific and redundant functions of Gli2 and Gli3 zinc finger genes in skeletal patterning and development. *Development*. 124(1):113-23.

MONTAGNA, W., ELLIS, R. A. 1958. The Biology of Hair Growth. New York, Academic Press.

MORGAN, D., ELEY, L., SAYER, J., STRACHAN, T., YATES, L. M., CRAIGHEAD, A. S., GOODSHIP, J. A. 2002. Expression analyses and interaction with the anaphase promoting complex protein Apc2 suggest a role for inversin in primary cilia and involvement in the cell cycle. *Hum Mol Genet.* 11(26):3345-50.

MORGAN, B. A., ORKIN, R. W., NORAMLY, S., PEREZ, A. 1998. Stage-specific effects of sonic hedgehog expression in the epidermis. *Dev Biol*. 201(1): 1-12.

MORIN, P. J., SPARKS, A. B., KORINEK, V., BARKER, N., CLEVERS, H., VOGELSTEIN, B., KINZLER, K. W. 1997. Activation of beta-catenin-Tcf signaling in colon cancer by mutations in beta-catenin or APC. *Science*. 275(5307):1787-90.

MORLEY, S. M., D'ALESSANDRO, M., SEXTON, C., RUGG, E. L., NAVSARIA, H., SHEMANKO, C. S., HUBER, M., HOHL, D., HEAGERTY, A. I., LEIGH, I. M., LANE, E. B. 2003. Generation and characterization of epidermolysis bullosa simplex cell lines: scratch assays show faster migration with disruptive keratin mutations. *Br J Dermatol*. 149(1):46-58.

MÜLLER-RÖVER, S., HANDJISKI, B., VAN DER VEEN, C., EICHMÜLLER, S., FOITZIK, K., MCKAY, I. A., STENN, K. S., PAUS, R. 2001. A comprehensive guide for the accurate classification of murine hair follicles in distinct hair cycle stages. *J Invest Dermatol.* 117(1):3-15.

MULLOR, J. L., DAHMANE, N., SUN, T., RUIZ I ALTABA, A. 2001. Wnt signals are targets and mediators of Gli function. *Curr Biol.* 11(10):769-73.

MURONE, M., ROSENTHAL, A., DE SAUVAGE, F. J. 1999. Sonic hedgehog signaling by the patchedsmoothened receptor complex. *Curr Biol.* 9, 76-84.

NAGAO, K., TOYODA, M., TAKEUCHI-INOUE, K., FUJII, K., YAMADA, M., MIYASHITA, T. 2005. Identification and characterization of multiple isoforms of murine and human tumor suppressor, patched, having distinct first exons. *Genomics*. 85(4):462-71.

NAKASHIMA, H., NAKAMURA, M., YAMAGUCHI, H., YAMANAKA, N., AKIYOSHI, T., KOGA, K., YAMAGUCHI, K., TSUNEYOSHI, M., TANAKA, M., KATANO, M. 2006. Nuclear factor-kappaB contributes to hedgehog signaling pathway activation through sonic hedgehog induction in pancreatic cancer. *Cancer Res.* 66(14):7041-9.

NEILL, G. W., HARRISON, W. J., IKRAM, M. S., WILLIAMS, T. D., BIANCHI, L. S., NADENDLA, S. K., GREEN, J. L., GHALI, L., FRISCHAUF, A. M., O'TOOLE, E. A., ABERGER, F., PHILPOTT, M. P. 2008. GLI1 repression of ERK activity correlates with colony formation and impaired migration in human epidermal keratinocytes. *Carcinogenesis*. 29(4):738-46.

NEUGEBAUER, J. M., AMACK, J. D., PETERSON, A. G., BISGROVE, B. W., YOST, H. J. 2009. FGF signalling during embryo development regulates cilia length in diverse epithelia. *Nature*. 458(7238):651-4.

NICOLAS, M., WOLFER, A., RAJ, K., KUMMER, J. A., MILL, P., VAN NOORT, M., HUI, C. C., CLEVERS, H., DOTTO, G. P., RADTKE, F. 2003. Notch1 functions as a tumor suppressor in mouse skin. *Nat Genet*. 33(3):416-21.

NILSSON, M., UNDÈN, A. B., KRAUSE, D., MALMQWIST, U., RAZA, K., ZAPHIROPOULOS, P. G., TOFTGÅRD, R. 2000. Induction of basal cell carcinomas and trichoepitheliomas in mice overexpressing GLI-1. *Proc Natl Acad Sci U S A*. 97(7):3438-43.

NOLAN-STEVAUX, O., LAU, J., TRUITT, M. L., CHU, G. C., HEBROK, M., FERNANDEZ-ZAPICO, M. E., HANAHAN, D. 2009. GLI1 is regulated through Smoothened-independent mechanisms in neoplastic pancreatic ducts and mediates PDAC cell survival and transformation. *Genes Dev*. 23, 24-36.

NÜSSLEIN-VOLHARD, C., WIESCHAUS, E. 1980. Mutations affecting segment number and polarity in Drosophila. *Nature*. 287(5785):795-801.

ODA, K., MATSUOKA, Y., FUNAHASHI, A., KITANO, H. 2005. A comprehensive pathway map of epidermal growth factor receptor signaling. *Mol Syst Biol.* 1(1):2005.0010.

OLAYIOYE, M. A., NEVE, R. M., LANE, H. A., HYNES, N. E. 2000. The ErbB signaling network: receptor heterodimerization in development and cancer. *EMBO J*. 19(13):3159-67.

OLIVER, R. F. 1966. Regeneration of dermal papillae in rat vibrissae. *J Invest Dermatol.* 47(5):496-7.

OLIVER, R. F. 1967. The experimental induction of whisker growth in the hooded rat by implantation of dermal papillae. *J Embryol Exp Morphol.* 18(1): 43-51.

OLIVIER, M., HOLLSTEIN, M., HAINAUT, P. 2010. TP53 mutations in human cancers: origins, consequences, and clinical use. *Cold Spring Harb Perspect Biol.* 2(1):a001008.

O'REGAN, E. M., TONER, M. E., FINN, S. P., FAN, C. Y., RING, M., HAGMAR, B., TIMON, C., SMYTH, P., CAHILL, S., FLAVIN, R., SHEILS, O. M., O'LEARY, J. J. 2008. p16(INK4A) genetic and epigenetic profiles differ in relation to age and site in head and neck squamous cell carcinomas. *Hum Pathol.* 39:452–458.

ORIMOTO, A. M., NETO, C. F., PIMENTEL, E. R., SANCHES, J. A., SOTTO, M. N., AKAISHI, E., RUIZ, I. R. 2008. High numbers of skin cancers express MMP2 and several integrin genes. *J Cutan Pathol.* 35(3):285-91.

ORO, A. E., HIGGINS, K. M., HU, Z., BONIFAS, J. M., EPSTEIN, E. H. JR, SCOTT, M. P. 1997. Basal cell carcinomas in mice overexpressing sonic hedgehog. *Science*. 276(5313):817-21.

O'SHAUGHNESSY, R. F., AKGÜL, B., STOREY, A., PFISTER, H., HARWOOD, C. A., BYRNE, C. 2007. Cutaneous human papillomaviruses down-regulate AKT1, whereas AKT2 up-regulation and activation associates with tumors. *Cancer Res.* 67(17):8207-15.

OSHIMA, H., ROCHAT, A., KEDZIA, C., KOBAYASHI, K., BARRANDON, Y. 2001. Morphogenesis and renewal of hair follicles from adult multipotent stem cells. *Cell*. 104(2):233-45.

OWENS, D. M., WATT, F. M. 2003. Contribution of stem cells and differentiated cells to epidermal tumours. *Nat Rev Cancer*. 3(6):444-51.

PACCIONE, R. J., MIYAZAKI, H., PATEL, V., WASEEM, A., GUTKIND, J. S., ZEHNER, Z. E., YEUDALL, W. A. 2008. Keratin down-regulation in vimentin-positive cancer cells is reversible by vimentin RNA interference, which inhibits growth and motility. *Mol Cancer Ther.* 7(9):2894-903.

PALMA, V., RUIZ I ALTABA, A. 2004. Hedgehog-GLI signaling regulates the behavior of cells with stem cell properties in the developing neocortex. *Development*. 131(2):337-45.

PARIKH, A. A., MOON, M. R., PRITTS, T. A., FISCHER, J. E., SZABÓ, C., HASSELGREN, P. O., SALZMAN, A. L. 2000. IL-1beta induction of NF-kappaB activation in human intestinal epithelial cells is independent of oxyradical signaling. *Shock*. 13(1):8-13.

PARK, H. L., BAI, C., PLATT, K. A., MATISE, M. P., BEEGHLY, A., HUI, C. C., NAKASHIMA, M., JOYNER, A. L. 2000. Mouse Gli1 mutants are viable but have defects in SHH signaling in combination with a Gli2 mutation. *Development*. 127(8):1593-605.

PASCA DI MAGLIANO, M., HEBROK, M. 2003. Hedgehog signalling in cancer formation and maintenance. *Nat Rev* Cancer. 3(12):903-11.

PAUS, R., COTSARELIS, G. 1999. The biology of hair follicles. *N Engl J Med.* 341:491-7.

PAUS, R., FOITZIK, K., WELKER, P., BULFONE-PAUS, S., EICHMULLER, S. 1997. Transforming growth factor-beta receptor type I and type II expression during murine hair follicle development and cycling. *J Invest Dermatol*. 109(4): 518-26.

PEDERSEN, L. B., ROSENBAUM, J. L. 2008. Intraflagellar transport (IFT) role in ciliary assembly, resorption and signalling. *Curr Top Dev Biol.* 85:23-61.

PELTONEN, J., JAAKKOLA, S., LASK, G., VIRTANEN, I., UITTO, J. 1988. Fibronectin gene expression by epithelial tumor cells in basal cell carcinoma: an immunocytochemical and in situ hybridization study. *J Invest Dermatol.* 91(4):289-93.

PEREZ-LOSADA, J., BALMAIN, A. 2003. Stem-cell hierarchy in skin cancer. *Nat Rev Cancer.* 3(6):434-43.

PING, X. L., RATNER, D., ZHANG, H., WU, X. L., ZHANG, M. J., CHEN, F. F., SILVERS, D. N., PEACOCKE, M., TSOU, H. C. 2001. PTCH mutations in squamous cell carcinoma of the skin. *J Invest Dermatol.* 116(4):614-6.

PINZANI, M., MARRA, F. 2001. Cytokine receptors and signaling in hepatic stellate cells. *Semin Liver Dis.* 21(3):397-416.

PÖTZSCH, C., VOIGTLÄNDER, T., LÜBBERT, M. 2002. p53 Germline mutation in a patient with Li-Fraumeni Syndrome and three metachronous malignancies. *J Cancer Res Clin Oncol.* 128(8):456-60.

PRESTON, D. S., STERN, R. S. 1992. Nonmelanoma cancers of the skin. *N Engl J Med.* 327:1649-62.

PRYWES, R., DUTTA, A., CROMLISH, J. A., ROEDER, R. G. 1988. Phosphorylation of serum response factor, a factor that binds to the serum response element of the c-FOS enhancer. *Proc Natl Acad Sci U S A*. 85(19):7206-10.

QUATRESOOZ, P., MARTALO, O., PIÉRARD, G. E. 2003. Differential expression of alpha1 (IV) and alpha5 (IV) collagen chains in basal-cell carcinoma. *J Cutan Pathol.* 30(9):548-52.

RADY, P., SCINICARIELLO, F., WAGNER, R. F. JR, TYRING, S. K. 1992. p53 mutations in basal cell carcinomas. *Cancer Res.* 1;52(13):3804-6.

RAHNAMA, F., SHIMOKAWA, T., LAUTH, M., FINTA, C., KOGERMAN, P., TEGLUND, S., TOFTGÅRD, R., ZAPHIROPOULOS, P. G. 2006. Inhibition of GLI1 gene activation by Patched1. *Biochem J*. 394(Pt 1):19-26.

REDDY, S., ANDL, T., BAGASRA, A., LU, M. M., EPSTEIN, D. J., MORRISEY, E. E., MILLAR, S. E. 2001. Characterization of Wnt gene expression in developing and postnatal hair follicles and identification of Wnt5a as a target of Sonic hedgehog in hair follicle morphogenesis. *Mech Dev*. 107:69-82.

REGL, G., NEILL, G. W., EICHBERGER, T., KASPER, M., IKRAM, M. S., KOLLER, J., HINTNER, H., QUINN, A. G., FRISCHAUF, A. M., ABERGER, F. 2002. Human GLI2 and GLI1 are part of a positive feedback mechanism in Basal Cell Carcinoma. *Oncogene*. 21(36):5529-39.

REIFENBERGER, J., WOLTER, M., KNOBBE, C. B., KÖHLER, B., SCHÖNICKE, A., SCHARWÄCHTER, C., KUMAR, K., BLASCHKE, B., RUZICKA, T., REIFENBERGER, G. 2005. Somatic mutations in the PTCH, SMOH, SUFUH and TP53 genes in sporadic basal cell carcinomas. *Br J Dermatol.* 152(1):43-51.

REITER, J. F., BLACQUE, O. E., LEROUX, M. R. 2012. The base of the cilium: roles for transition fibres and the transition zone in ciliary formation, maintenance and compartmentalization. *EMBO Rep*. 13(7):608-18.

REYA, T., MORRISON, S. J., CLARKE, M. F., WEISSMAN, I. L. 2001. Stem cells, cancer, and cancer stem cells. *Nature*. 414(6859):105-11.

RIDDLE, R. D., JOHNSON, R. L., LAUFER, E., TABIN, C. 1993. Sonic hedgehog mediates the polarizing activity of the ZPA. *Cell.* 75:1401–1416.

RIOBO, N. A., HAINES, G. M., EMERSON, C. P. JR. 2006 B. Protein kinase C-delta and mitogen-activated protein/extracellular signal-regulated kinase-1 control GLI activation in hedgehog signaling. *Cancer Res*. 66, 839–845.

RIOBO, N. A., LU, K., AI, X., HAINES, G. M., EMERSON, C. P. JR. 2006A. Phosphoinositide 3-kinase and Akt are essential for Sonic Hedgehog signalling. *Proc Natl Acad Sci U S A*. 103(12):4505-10.

ROESSLER, E., ERMILOV, A. N., GRANGE, D. K., WANG, A., GRACHTCHOUK, M., DLUGOSZ, A. A., MUENKE, M. 2005. A previously unidentified amino-terminal domain regulates transcriptional activity of wild-type and disease-associated human GLI2. *Hum Mol Genet.* 14(15):2181-8.

ROHATGI, R., MILENKOVIC, L., SCOTT, M. P. 2007. Patched1 regulates hedgehog signaling at the primary cilium. *Science*. 317, 372-376.

ROSS, F. P., CHRISTIANO, A. M. 2006. Nothing but skin and bone. *J Clin Invest*. 116(5): 1140–1149.

ROSS, A. J., MAY-SIMERA, H., EICHERS, E. R., KAI, M., HILL, J., JAGGER, D. J., LEITCH, C. C., CHAPPLE, J. P., MUNRO, P. M., FISHER, S., TAN, P. L., PHILLIPS, H. M., LEROUX, M. R., HENDERSON, D. J.,MURDOCH, J. N., COPP, A. J., ELIOT, M. M., LUPSKI, J. R., KEMP, D. T., DOLLFUS, H., TADA, M., KATSANIS, N., FORGE, A., BEALES, P. L. 2005. Disruption of Bardet-Biedl syndrome ciliary proteins perturbs planar cell polarity in vertebrates. *Nat Genet.* 37(10):1135-40.

ROZEN, S., SKALETSKY, H. J., 1998. Primer3.

RUBIN, A. I., CHEN, E. H., RATNER, D. 2005. Basal-cell carcinoma. *N Engl J Med.* 353(21):2262-9.

RUBIN, L. L., DE SAUVAGE, F. J. 2006. Targeting the Hedgehog pathway in cancer. *Nat Rev Drug Discov*. 5:1026-33.

RUBINFELD, B., ROBBINS, P., EL-GAMIL, M., ALBERT, I., PORFIRI, E., POLAKIS, P. 1997. Stabilization of beta-catenin by genetic defects in melanoma cell lines. *Science*. 275(5307):1790-2.

RUIZ I ALTABA, A., NGUYÊN, V., PALMA, V. 2003. The emergent design of the neural tube: prepattern, SHH morphogen and GLI code. *Curr Opin Genet Dev.* 13(5):513-21.

RUIZ I ALTABA, A., PALMA, V., DAHMANE, N. 2002. Hedgehog-Gli signalling and the growth of the brain. *Nat Rev Neurosci*. 3(1):24-33.

RYAN, K. E., CHIANG, C. 2012. Hedgehog secretion and signal transduction in vertebrates. *J Biol Chem*. 287(22):17905-13.

SABURI, S., HESTER, I., FISCHER, E., PONTOGLIO, M., EREMINA, V., GESSLER, M., QUAGGIN, S. E., HARRISON, R., MOUNT, R., MCNEILL, H. 2008. Loss of Fat4 disrupts PCP signaling and oriented cell division and leads to cystic kidney disease. *Nat Genet.* 40(8):1010-5.

SALDANHA, G., FLETCHER, A., SLATER, D. N. 2003. Basal cell carcinoma: a dermatopathological and molecular biological update. *Br J Dermatol.* 148(2):195-202.

SALDANHA, G., GHURA, V., POTTER, L., FLETCHER, A. 2004. Nuclear beta-catenin in basal cell carcinoma correlates with increased proliferation. *Br J Dermatol.* 151(1):157-64.

SARAN, A. 2010. Basal cell carcinoma and the carcinogenic role of aberrant Hedgehog signaling. *Future Oncol*. 6(6):1003-14.

SCALES, S. J., DE SAUVAGE, F. J. 2009. Mechanisms of Hedgehog pathway activation in cancer and implications for therapy. *Trends Pharmacol Sci.* 30(6):303-12.

SCHIRREN, C. G., RÜTTEN, A., KAUDEWITZ, P., DIAZ, C., MCCLAIN, S., BURGDORF, W. H. 1997. Trichoblastoma and basal cell carcinoma are neoplasms with follicular differentiation sharing the same profile of cytokeratin intermediate filaments. *Am J Dermatopathol*. 19(4):341-50.

SCHNEIDER, L., CAMMER, M., LEHMAN, J., NIELSEN, S. K., GUERRA, C. F., VELAND, I. R., STOCK, C., HOFFMANN, E. K., YODER, B. K., SCHWAB, A., SATIR, P., CHRISTENSEN, S. T. 2010. Directional cell migration and chemotaxis in wound healing response to PDGF-AA are coordinated by the primary cilium in fibroblasts. *Cell Physiol Biochem*. 25(2-3):279-92.

SCHNEIDER, L., CLEMENT, C. A., TEILMANN, S. C., PAZOUR, G. J., HOFFMANN, E. K., SATIR, P., CHRISTENSEN, S. T. 2005. PDGFR-alpha signaling is regulated through the primary cilium in fibroblasts. *Curr Biol.* 15(20):1861-6.

SCHNIDAR, H., EBERL, M., KLINGLER, S., MANGELBERGER, D., KASPER, M., HAUSER-KRONBERGER, C., REGL, G., KROISMAYR, R., MORIGGL, R., SIBILIA, M., ABERGER, F. 2009. Epidermal growth factor receptor signaling synergizes with Hedgehog/GLI in oncogenic transformation via activation of the MEK/ERK/JUN pathway. *Cancer Res*. 69(4):1284-92.

SCHUSTER, N., KRIEGLSTEIN, K. 2002. Mechanisms of TGF-beta-mediated apoptosis. *Cell Tissue Res*. 307(1): 1-14.

SEIFERT, J. R., MLODZIK, M. 2007. Frizzled/PCP signalling: a conserved mechanism regulating cell polarity and directed motility. *Nat Rev Genet.* 8(2):126-38.

SEKULIC, A., MIGDEN, M. R., ORO, A. E., DIRIX, L., LEWIS, K. D., HAINSWORTH, J. D., SOLOMON, J. A., YOO, S., ARRON, S. T., FRIEDLANDER, P. A., MARMUR, E., RUDIN, C. M., CHANG, A. L., LOW, J. A.,MACKEY, H. M., YAUCH, R. L., GRAHAM, R. A., REDDY, J. C., HAUSCHILD, A. 2012. Efficacy and safety of vismodegib in advanced basal-cell carcinoma. *N Engl J Med*. 366(23):2171-9.

SHEA, C. R., MCNUTT, N. S., VOLKENANDT, M., LUGO, J., PRIOLEAU, P. G., ALBINO, A. P. 1992. Overexpression of p53 protein in basal cell carcinomas of human skin. *Am J Pathol*. 141(1): 25-29.

SHENG, H., GOICH, S., WANG, A., GRACHTCHOUK, M., LOWE, L., MO, R., LIN, K., DE SAUVAGE, F. J., SASAKI, H., HUI, C. C., DLUGOSZ, A. A. 2002. Dissecting the oncogenic potential of Gli2: deletion of an NH(2)-terminal fragment alters skin tumor phenotype. *Cancer Res*. 62(18):5308-16.

SHI, Q., LI, S., JIA, J., JIANG, J. 2011. The Hedgehog-induced Smoothened conformational switch assembles a signaling complex that activates Fused by promoting its dimerization and phosphorylation. *Development*. 138, 4219-4231.

SHIER, D., BUTLER, J., LEWIS, R. 1999. Hole's human anatomy and physiology, 7th Ed. Dubuque, IA; Wm. C. Brown Publishers.

SHIMIZU, T., IZUMI, H., OGA, A., FURUMOTO, H., MURAKAMI, T., OFUJI, R., MUTO, M., SASAKI, K. 2001. Epidermal growth factor receptor overexpression and genetic aberrations in metastatic squamous-cell carcinoma of the skin. *Dermatology*. 202:203–206.

SICKLICK, J. K., LI, Y. X., JAYARAMAN, A., KANNANGAI, R., QI, Y., VIVEKANANDAN, P., LUDLOW, J. W., OWZAR, K., CHEN, W., TORBENSON, M. S., DIEHL, A. M. 2006. Dysregulation of the Hedgehog pathway in human hepatocarcinogenesis. *Carcinogenesis*. 27, 748-57.

SIMONS, M., GLOY, J., GANNER, A., BULLERKOTTE, A., BASHKUROV, M., KRÖNIG, C., SCHERMER, B., BENZING, T., CABELLO, O. A., JENNY, A., MLODZIK, M., POLOK, B., DRIEVER, W., OBARA, T., WALZ, G. 2005. Inversin, the gene product mutated in nephronophthisis type II, functions as a molecular switch between Wnt signaling pathways. *Nat Genet.* 37(5):537-43.

SINGH, S., SADACHARAN, S., SU, S., BELLDEGRUN, A., PERSAD, S., SINGH, G. 2003. Overexpression of vimentin: role in the invasive phenotype in an androgen-independent model of prostate cancer. *Cancer Res.* 63:2306–11.

SITAILO, L. A., TIBUDAN, S. S., DENNING, M. F. 2002. Activation of caspase-9 is required for UV-induced apoptosis of human keratinocytes. *J Biol Chem*. 277(22):19346-52.

SLOMINSKI, A., PAUS, R., PLONKA, P., CHAKRABORTY, A., MAURER, M., PRUSKI, D., LUKIEWICZ, S. 1994. Melanogenesis during the anagen-catagen-telogen transformation of the murine hair cycle. *J Invest Dermatol.* 102(6): 862-9.

SMITH, F. J., IRVINE, A. D., TERRON-KWIATKOWSKI, A., SANDILANDS, A., CAMPBELL, L. E., ZHAO, Y., LIAO, H., EVANS, A. T., GOUDIE, D. R., LEWIS-JONES, S., ARSECULERATNE, G., MUNRO, C. S., SERGEANT, A., O'REGAN, G., BALE, S. J., COMPTON, J. G., DIGIOVANNA, J. J., PRESLAND, R. B., FLECKMAN, P., MCLEAN, W. H. 2006. Loss-of-function mutations in the gene encoding filaggrin cause ichthyosis vulgaris. *Nat Genet*. 38(3):337-42.

SMYTH, I., NARANG, M. A., EVANS, T., HEIMANN, C., NAKAMURA, Y., CHENEVIX-TRENCH, G., PIETSCH, T., WICKING, C., WAINWRIGHT, B. J. 1999. Isolation and characterization of human patched 2 (PTCH2), a putative tumour suppressor gene in basal cell carcinoma and medulloblastoma on chromosome 1p32. *Hum Mol Genet*. 8(2):291-7.

SO, E. Y., OUCHI, T. 2010. The application of Toll like receptors for cancer therapy. *Int J Biol Sci*. 6(7):675-81.

SOLETI, R., BENAMEUR, B., PORRO, C., PANARO, M. A., ANDRIANTSITOHAINA, R., MARTÍNEZ, M. A. 2009. Microparticles harboring Sonic Hedgehog promote angiogenesis through the upregulation of adhesion proteins and proangiogenic factors. *Carcinogenesis*. 30(4):580-588.

STECCA, B., MAS, C., CLEMENT, V., ZBINDEN, M., CORREA, R., PIGUET, V., BEERMANN, F., RUIZ I ALTABA, A. 2007. Melanomas require HEDGEHOG-GLI signalling regulated by interactions between GLI1 and the RAS-MEK/AKT path-ways. *Proc Natl Acad Sci USA*. 104, 5895–5900.

STECCA, B., RUIZ I ALTABA, A. 2005. Brain as a paradigm of organ growth: Hedgehog-Gli signaling in neural stem cells and brain tumors. *J Neurobiol.* 64(4):476-90.

STOCKFLETH, E., TREFZER, U., GARCIA-BARTELS, C., WEGNER, T., SCHMOOK, T., STERRY, W. 2003. The use of Toll-like receptor-7 agonist in the treatment of basal cell carcinoma: an overview. *Br J Dermatol.* 149 Suppl 66:53-6.

SUR, I., ULVMAR, M., TOFTGÅRD, R. 2008. The two-faced NF-kappaB in the skin. *Int Rev Immunol.* 27(4):205-23.

SVARD, J., HEBY-HENRICSON, K., PERSSON-LEK, M., ROZELL, B., LAUTH, M., BERGSTROM, A., ERICSON, J., TOFTGARD, R., TEGLUND, S. 2006. Genetic elimination of Suppressor of fused reveals an essential repressor function in the mammalian Hedgehog signaling pathway. *Dev Cell*. 10, 187-197.

TAI, K. Y., SHIEH, Y. S., LEE, C. S., SHIAH, S. G., WU, C. W. 2008. Axl promotes cell invasion by inducing MMP-9 activity through activation of NF-kappaB and Brg-1. *Oncogene*. 27(29):4044-55.

TAIPALE, J., BEACHY, P. A. 2001. The Hedgehog and Wnt signalling pathways in cancer. *Nature*. 411(6835):349-54.

TAIPALE, J., CHEN, J. K., COOPER, M. K., WANG, B., MANN, R. K., MILENKOVIC, L., SCOTT, M. P., BEACHY, P. A. 2000. Effects of oncogenic mutations in Smoothened and Patched can be reversed by cyclopamine. *Nature*. 406(6799):1005-9.

TAIPALE, J., COOPER, M. K., MAITI, T., BEACHY, P. A. 2002. Patched acts catalytically to suppress the activity of Smoothened. *Nature*. 418, 892-897.

TAYLOR, M. D., LIU, L., RAFFEL, C., HUI, C. C., MAINPRIZE, T. G., ZHANG, X., AGATEP, R., CHIAPPA, S., GAO, L., LOWRANCE, A., HAO, A., GOLDSTEIN, A. M., STAVROU, T., SCHERER, S. W., DURA, W. T., WAINWRIGHT, B., SQUIRE, J. A., RUTKA, J. T., HOGG, D. 2002. Mutations in SUFU predispose to medulloblastoma. *Nature Genetics*. 31, 306-10.

TEMPE, D., CASAS, M., KARAZ, S., BLANCHET-TOURNIER, M. F., CONCORDET, J. P. 2006. Multisiteprotein kinase A and glycogen synthase kinase 3beta phosphorylation leads to Gli3 ubiquitination by SCFbetaTrCP. *Mol Cell Biol*. 26, 4316-4326.

THAYER, S. P., DI MAGLIANO, M. P., HEISER, P. W., NIELSEN, C. M., ROBERTS, D. J., LAUWERS, G. Y., QI, Y. P., GYSIN, S., FERNANDEZ-DEL CASTILLO, C., YAJNIK, V., ANTONIU, B., MCMAHON, M., WARSHAW, A. L., HEBROK, M. 2003. Hedgehog is an early and late mediator of pancreatic cancer tumorigenesis. *Nature*. 425, 851-6.

THEUNISSEN, J. W., DE SAUVAGE, F. J. 2009. Paracrine Hedgehog signalling in cancer. *Cancer Res.* 69, 6007-10.

TING-BERRETH, S. A., CHUONG, C. M. 1996. Sonic Hedgehog in feather morphogenesis: induction of mesenchymal condensation and association with cell death. *Dev Dyn*. 207(2): 157-70.

TOBIN, J. L., BEALES, P. L. 2009. The nonmotile ciliopathies. *Genet Med.* 11(6):386-402.

TOBIN, D. J., HAGEN, E., BOTCHKAREV, V. A., PAUS, R. 1998. Do hair bulb melanocytes undergo apoptosis during hair follicle regression (catagen)? *J Invest Dermatol*. 111(6):941-7.

TOJO, M., MORI, T., KIYOSAWA, H., HONMA, Y., TANNO, Y., KANAZAWA, K. Y., YOKOYA, S., KANEKO, F., WANAKA, A. 1999. Expression of sonic hedgehog signal transducers, patched and smoothened, in human basal cell carcinoma. *Pathol Int.* 49(8):687-94.

TOLL, R., JACOBI, U., RICHTER, H., LADEMANN, J., SCHAEFER, H., BLUME-PEYTAVI, U. 2004. Penetration profile of microspheres in follicular targeting of terminal hair follicles. *J Invest Dermatol.* 123(1):168-76.

TOMSON, A. M., SCHOLMA, J., MEIJER, B., KONING, J. G., DE JONG, K. M., VAN DER WERF, M. 1996. Adhesion properties, intermediate filaments and malignant behaviour of head and neck squamous cell carcinoma cells in vitro. *Clin Exp Metastasis.* 14:501–11.

TOSTAR, U., MALM, C. J., MEIS-KINDBLOM, J. M., KINDBLOM, L. G., TOFTGARD, R., UNDEN, A. B. 2006. Deregulation of the hedgehog signalling pathway: a possible role for the PTCH and SUFU genes in human rhabdomyoma and rhabdomyosarcoma development. *J Pathol.* 208, 17-25.

TOWERS, M., TICKLE, C. 2009. Growing models of vertebrate limb development. *Development*. 136:179-90.

TUKACHINSKY, H., LOPEZ, L. V., SALIC, A. 2010. A mechanism for vertebrate Hedgehog signaling: recruitment to cilia and dissociation of SuFu-Gli protein complexes. *J Cell Biol.* 191, 415-428.

TUOMINEN, H., PÖLLÄNEN, R., KALLIOINEN, M. 1997. Multicellular origin of tenascin in skin tumors--an in situ hybridization study. *J Cutan Pathol.* 24(10):590-6.

UEDA Y, RICHMOND A. 2006. NF-kappaB activation in melanoma. *Pigment Cell Res.* 19(2):112-24.

UHMANN, A., FERCH, U., BAUER, R., TAUBER, S., ARZIMAN, Z., CHEN, C., HEMMERLEIN, B., WOJNOWSKI, L., HAHN, H. 2005. A model for PTCH1/Ptch1-associated tumors comprising mutational inactivation and gene silencing. *Int J Oncol.* 27(6):1567-75.

UNDÉN, A. B., ZAPHIROPOULOS, P. G., BRUCE, K., TOFTGÅRD, R., STÅHLE-BÄCKDAHL, M. 1997. Human patched (PTCH) mRNA is overexpressed consistently in tumor cells of both familial and sporadic basal cell carcinoma. *Cancer Res.* 57(12):2336-40.

VALIN, A., BARNAY-VERDIER, S., ROBERT, T., RIPOCHE, H., BRELLIER, F., CHEVALLIER-LAGENTE, O., AVRIL, M. F., MAGNALDO, T. 2009. PTCH1 +/- dermal fibroblasts isolated from healthy skin of Gorlin syndrome patients exhibit features of carcinoma associated fibroblasts. *PLoS One.* 4(3):e4818.

VAN DE WETERING, M., CAVALLO, R., DOOIJES, D., VAN BEEST, M., VAN, E. S. J., LOUREIRO, J., YPMA, A., HURSH, D., JONES, T., BEJSOVEC, A., PEIFER, M., MORTIN, M., CLEVERS, H. 1997. Armadillo coactivates transcription driven by the product of the Drosophila segment polarity gene TCF. *Cell*. 88(6):789-99.

VAN GENDEREN, C., OKAMURA, R. M., FARIÑAS, I., QUO, R. G., PARSLOW, T. G., BRUHN, L., GROSSCHEDL, R. 1994. Development of several organs that require inductive epithelial-mesenchymal interactions is impaired in LEF-1-deficient mice. *Genes Dev*. 8(22):2691-703.

VANTUCHOVA, Y., CURIK, R. 2006. Histological types of basal cell carcinoma. *Scripta Medica (Brno).* 79 (5-6): 261-270.

VARJOSALO, M., TAIPALE, J. 2007. Hedgehog signaling. *J. Cell Sci.* 120:3–6.

VEEMAN, M. T., AXELROD, J. D., MOON, R. T. 2003. A second canon. Functions and echanisms of beta-catenin-independent Wnt signaling. *Dev Cell*. 5:367-77.

VILLANI, R. M., ADOLPHE, C., PALMER, J., WATERS, M. J., WAINWRIGHT, B. J. 2010. Patched1 inhibits epidermal progenitor cell expansion and basal cell carcinoma formation by limiting Igfbp2 activity. *Cancer Prev Res (Phila)*. 3(10):1222-34.

VOLKOVOVA, K., BILANICOVA, D., BARTONOVA, A., LETAŠIOVÁ, S., DUSINSKA, M. 2012. Associations between environmental factors and incidence of cutaneous melanoma. *Environ Health*. 11 Suppl 1:S12.

VON HOFF, D. D., LORUSSO, P. M., RUDIN, C. M., REDDY, J. C., YAUCH, R. L., TIBES, R., WEISS, G. J., BORAD, M. J., HANN, C. L., BRAHMER, J. R., MACKEY, H. M., LUM, B. L., DARBONNE, W. C., MARSTERS, J. C. JR, DE SAUVAGE, F. J., LOW, J. A. 2009. Inhibition of the hedgehog pathway in advanced basal-cell carcinoma. *N Engl J Med*. 361(12):1164-72.

WANG, X., GOODE, E. L., FREDERICKSEN, Z. S., VIERKANT, R. A., PANKRATZ, V. S., LIU-MARES, W., RIDER, D. N., VACHON, C. M.,CERHAN, J. R., OLSON, J. E., COUCH, F. J. 2008. Association of genetic variation in genes implicated in the beta-catenin destruction complex with risk of breast cancer. *Cancer Epidemiol Biomarkers Prev*. 17(8):2101-8.

WANG, C., PAN, Y., WANG, B. 2010. Suppressor of fused and Spop regulate the stability, processing and function of Gli2 and Gli3 full-length activators but not their repressors. *Development*. 137, 2001-2009.

WANG, G. Y., WANG, J., MANCIANTI, M. L., EPSTEIN, E. H. JR. 2011. Basal cell carcinomas arise from hair follicle stem cells in Ptch1(+/-) mice. *Cancer Cell.* 19(1):114-24.

WANG, P., WU, P., SIEGEL, M. I., EGAN, R. W., BILLAH, M. M. 1995. Interleukin (IL)-10 inhibits nuclear factor kappa B (NF kappa B) activation in human monocytes. IL-10 and IL-4 suppress cytokine synthesis by different mechanisms. *J Biol Chem.* 21;270(16):9558-63.

WANG, Y. N., YAMAGUCHI, H., HSU, J. M., HUNG, M. C. 2010. Nuclear trafficking of the epidermal growth factor receptor family membrane proteins. *Oncogene*. 29(28):3997-4006.

WASEEM, A., DOGAN, B., TIDMAN, N., ALAM, Y., PURKIS, P., JACKSON, S., LALLI, A., MACHESNEY, M., LEIGH, I. M. 1999. Keratin 15 expression in stratified epithelia: downregulation in activated keratinocytes. *J Invest Dermatol.* 112:362–9.

WATKINS, D. N., BERMAN, D. M. & BAYLIN, S. B. 2003. Hedgehog signaling: progenitor phenotype in small-cell lung cancer. *Cell Cycle.* 2, 196-8.

WATT, F. M., LO CELSO, C., SILVA-VARGAS, V. 2006. Epidermal stem cells: an update. *Curr Opin Genet Dev.* 16(5):518-24.

WEINSTOCK, J. V., BLUM, A., METWALI, A., ELLIOTT, D., ARSENESCU, R. 2003. IL-18 and IL-12 signal through the NF-kappa B pathway to induce NK-1R expression on T cells. *J Immunol*. 170(10):5003-7.

WEINSTEIN, G. D., MOONEY, K. M. 1980. Cell proliferation kinetics in the human hair root. *J Invest Dermatol.* 74(1): 43-6.

WETMORE, C., EBERHART, D. E., CURRAN, T. 2000. The normal patched allele is expressed in medulloblastomas from mice with heterozygous germ-line mutation of patched. *Cancer Res.* 60(8):2239-46.

WICKING, C., MCGLINN, E. 2001. The role of hedgehog signalling in tumorigenesis. *Cancer Lett*. 2001:173; 1–7.

WICKING, C., SMYTH, I., BALE, A. 1999. The hedgehog signalling pathway in tumorigenesis and development. *Oncogene*. 18(55):7844-51.

WILLIAMS, J. A., GUICHERIT, O. M., ZAHARIAN, B. I., XU, Y., CHAI, L., WICHTERLE, H., KON, C., GATCHALIAN, C., PORTER, J. A., RUBIN, L. L., WANG, F. Y. 2003. Identification of a small molecule inhibitor of the hedgehog signaling pathway: effects on basal cell carcinoma-like lesions. *Proc Natl Acad Sci U S A.* 100(8):4616-21.

WODARZ, A., NUSSE, R. 1998. Mechanisms of Wnt signaling in development. *Annu Rev Cell Dev Biol.* 14:59-88.

WONG, D. J., CHANG, H. Y. 2009. In: Stem Book [Internet]. Cambridge (MA): Harvard Stem Cell Institute. Skin tissue engineering.

XIE, J., MURONE, M., LUOH, S. M., RYAN, A., GU, Q., ZHANG, C., BONIFAS, J. M., LAM, C. W., HYNES, M., GODDARD, A., ROSENTHAL, A., EPSTEIN, E. H. JR., DE SAUVAGE, F. J. 1998. Activating Smoothened mutations in sporadic basal-cell carcinoma. *Nature*. 391(6662):90-2.

XU, Y., SHAO, Y., ZHOU, J., VOORHEES, J. J., FISHER, G. J. 2009. Ultraviolet irradiation-induces epidermal growth factor receptor (EGFR) nuclear translocation in human keratinocytes. *J Cell Biochem. 107*(5):873-80.

YANG, S. H., ANDL, T., GRACHTCHOUK, V., WANG, A., LIU, J., SYU, L. J., FERRIS, J., WANG, T. S., GLICK, A. B., MILLAR, S. E., DLUGOSZ, A. A. 2008. Pathological responses to oncogenic Hedgehog signaling in skin are dependent on canonical Wnt/beta-catenin signaling. *Nat Genet*. 40(9):1130-5.

YANG, J., MCNEISH, B., BUTTERFIELD, C., MOSES, M. A. 2012. Lipocalin 2 is a novel regulator of angiogenesis in human breast cancer. *FASEB J.*

YARDEN, Y., SLIWKOWSKI, M. X. 2001. Untangling the ErbB signalling network. *Nat Rev Mol Cell Biol.* 2(2):127-37.

YAUCH, R. L., DIJKGRAAF, G. J., ALICKE, B., JANUARIO, T., AHN, C. P., HOLCOMB, T., PUJARA, K., STINSON, J., CALLAHAN, C. A., TANG, T., BAZAN, J. F., KAN, Z., SESHAGIRI, S., HANN, C. L., GOULD, S. E.,LOW, J. A., RUDIN, C. M., DE SAUVAGE, F. J. 2009. Smoothened mutation confers resistance to a Hedgehog pathway inhibitor in medulloblastoma. *Science*. 326: 572–4.

YAUCH, R. L., GOULD, S. E., SCALES, S. J., TANG, T., TIAN, H., AHN, C. P., MARSHALL, D., FU, L., JANUARIO, T., KALLOP, D., NANNINI-PEPE, M., KOTKOW, K., MARSTERS, J. C., RUBIN, L. L., DE SAUVAGE, F. J. 2008. A paracrine requirement for hedgehog signalling in cancer. *Nature*. 455, 406-10.

YOUNG, M. R., COLBURN, N. H. 2006. Fra-1 a target for cancer prevention or intervention. *Gene*. 379:1-11.

YOUSSEF, K. K., VAN KEYMEULEN, A., LAPOUGE, G., BECK, B., MICHAUX, C., ACHOURI, Y., SOTIROPOULOU, P. A., BLANPAIN, C. 2010. Identification of the cell lineage at the origin of basal cell carcinoma. *Nat Cell Biol.* 12(3):299-305.

ZENG, X., GOETZ, J. A., SUBER, L. M., SCOTT, W. J. JR., SCHREINER, C. M., ROBBINS, D. J. 2001. A freely diffusible form of Sonic hedgehog mediates long-range signalling. *Nature*. 411(6838):716-20.

ZENG, H., JIA, J., LIU, A. 2010. Coordinated translocation of mammalian Gli proteins and suppressor of fused to the primary cilium. *PLoS One.* 5, e15900.

ZHAN, M., HAN, Z. C. 2004. Phosphatidylinositide 3-kinase/AKT in radiation responses. *Histol Histopathol.* 19(3):915-23.

ZHANG, H. M., LI, L., PAPADOPOULOU, N., HODGSON, G., EVANS, E., GALBRAITH, M., DEAR, M., VOUGIER, S., SAXTON, J., SHAW, P. E. 2008. Mitogen-induced recruitment of ERK and MSK to SRE promoter complexes by ternary complex factor Elk-1. *Nucleic Acids Res.* 36(8):2594-607.

ZHANG, H., PING, X. L., LEE, P. K., WU, X. L., YAO, Y. J., ZHANG, M. J., SILVERS, D. N., RATNER, D., MALHOTRA, R., PEACOCKE, M., TSOU, H. C. 2001. Role of PTCH and p53 in Early-onset Basal Cell Carcinomas. *Am J Pathol.* 2001:158;381-85.

ZHOU, P., BYRNE, C., JACOBS, J., FUCHS, E. 1995. Lymphoid enhancer factor 1 directs hair follicle patterning and epithelial cell fate. *Genes Dev*. 9(6):700-13.

ZIEGLER, A., LEFFELL, D. J., KUNALA, S., SHARMA, H. W., GAILANI, M., SIMON, J. A., HALPERIN, A. J., BADEN, H. P., SHAPIRO, P. E., BALE, A. E. 1993. Mutation hotspots due to sunlight in the p53 gene of nonmelanoma skin cancers. *Proc Natl Acad Sci U S A.* 90(9):4216-20.

[The p53 signalling pathway] n.d [image online]. Available at: <http://www.sigmaaldrich.com/life-science/cell-biology/learning-center/pathway-slides-and/the-p53-signaling-pathway.html> [Accessed December 2012].

Chapter 8

Appendix

Chapter 8 Appendix

8.1 Standard buffers and reagents

Buffer	Protocol
PBST	PBS containing 0.5 % (v/v) Tween
Protein lysis buffer	5 ml 1 mM Tris-HCl 20 ml 10 % (v/v) APS 200 µl 0.5 M sodium orthovanadate Made up to 100 ml with distilled water, adjusted to pH 8.4
Running buffer	30 g Tris 188 g glycine 10 g SDS Made up to 100 ml with distilled water Diluted 1:10 (v/v) with distilled water
Stripping buffer	3.75 g Tris 10 g SDS 3.57 ml β-mercaptoethanol Made up to 50 ml with distilled water, adjusted to pH 6.8
TAE	48.4 g Tris 11.4 ml 17.4 M glacial acetic acid 3.7 g EDTA Made up to 1 L with distilled water Diluted 1:10 (v/v) with distilled water
TBST	12.1 g Tris 40 g sodium chloride Made up to 50 ml with distilled water, adjusted to pH 7.6 50 ml of buffer diluted with 450 ml of distilled water 2.5 ml (0.5 %) Tween
Transfer buffer	30 g Tris 144 g glycine Made up to 1 L with distilled water 100 ml of buffer added to 200 ml of methanol and made up to 1 L with distilled water

Table 8.1: Table of standard buffers and reagents

8.2 PCR primer sequences

Gene	Forward primer	Reverse primer	Annealing temperature (°C)	Product size (base pairs)
CFP	CCTGAAGTTCATCTGCACCA	GGTGATATAGACGTTGTGGCTGA	60	331
COX2	TGAAACCCACTCCAAACACA	GAGAAGGCTTCCCAGCTTTT	60	187
CXCL11	GTGCTACAGTTGTTCAAGGC	CTAGGTTTTTCAGATGCTCT	60	291
DUSP6	CCGCAGGAGCTATACGAGTC	TTGAGCTTCTTGAGCAGCAG	60	248
EGFR	TCAAATTGTGCCGAACAAGA	ATCTGACATTGGGGTTCCAG	57	180
EGR1	CCGCAGAGTCTTTTCCTGAC	TGGGTTGGTCATGCTCACTA	60	200
ELK	GAAGCCATTCCTTTGTCTGC	CCCTATTGAAAAGCCCCATT	60	183
FOS	GGAATTAACCTGGTGCTGGA	TCAGACCACCTCAACAATGC	60	240
GAPDH	GTGAACCATGAGAAGTATGACA	CATGAGTCCTTCCACGATACC	60	123
GFP	TATATCATGGCCGACAAGCA	GAACTCCAGCAGGACCATGT	64	219
GLI1	GAAGACCTCTCCAGCTTGGA	GGCTGACAGTATAGGCAGAG	60	243
GLI2	TGGCCGCTTCAGATGACAGATGTTG	CGTTAGCCGAATGTCAGCCGTGAAG	58	200
IHH	CACCCCCAATTACAATCCAG	CGGTCTGATGTGGTGATGTC	59	231
iNOS	CTCTATGTTTGCGGGGATGT	TTCTTCGCCTCGTAAGGAAA	57	179
JUN	ACAGAGCATGACCCTGAACC	CCACCATGCCTGCCCCGTTG	60	326
KRT15	CATGACCACCACATTTCTGC	TCCTCCTGACCCTGAAGAGA	58	175
Luciferase	AGTGCTCATCATCGGGAATC	CATCCAACATTTTCGTGTCG	58	202
MMP-2	AGGGCACATCCTATGACAGC	ATTTGTTGCCCAGGAAAGTG	60	186
MMP-9	TTGACAGCGACAAGAAGTGG	TCACGTCGTCCTTATGCAAG	60	174
MYC	CCTGCGTGACCAGATCCCGGAGT	CTCCTCTGCTTGGACGGACA	60	103
PTCH1	ACTCGCCAGAAGATTGGAGA	TCCAATTTCCACTGCCTGTT	58	173
SHH	GCTCGGTGAAAGCAGAGAAC	CCAGGAAAGTGAGGAAGTCG	59	180
SNAI1	TTTACCTTCCAGCAGCCCTA	CCCACTGTCCTCATCTGACA	60	207
SMO	GGCTGCTGAGTGAGAAG	CTGGTTGAAGAAGTCGTAGAAG	58	565
SRF	ACGACCTTCAGCAAGAGGAA	AAGCCAGTGGCACTCATTCT	60	248
STAT3	TGTGCGTATGGGAACACCTA	AGAAGGTCGTCTCCCCCTTA	60	170
THY1	CCCAGTGAAGATGCAGGTTT	GACAGCCTGAGAGGGTCTTG	60	185
VIM	CCCTCACCTGTGAAGTGGAT	CAACCAGAGGGAGTGAATCC	60	330

Table 8.2: Table of PCR primer sequences

8.3 Primary antibodies

Primary antibody	Company	Type	Size(kDa)
α-Tubulin	Santa Cruz	Rabbit polyclonal	55
EGFR	Santa Cruz	Goat polyclonal	170
ERK	Cell Signaling	Rabbit polyclonal	42, 44
GFP ab290	Abcam	Rabbit polyclonal	27
GLI1 C18	Santa Cruz	Goat polyclonal	150
GLI1 H300	Santa Cruz	Rabbit polyclonal	150
MEK	Cell Signaling	Rabbit monoclonal	45
pEGFR Y845	Santa Cruz	Rabbit polyclonal	170
pEGFR Y1173	Santa Cruz	Goat polyclonal	170
pERK E10	Cell Signaling	Mouse monoclonal	42, 44
pERK 20G11	Cell Signaling	Rabbit monoclonal	42, 44
pMEK	Cell Signaling	Rabbit polyclonal	45
PTCH C20	Santa Cruz	Goat polyclonal	140
SHH	Santa Cruz	Goat polyclonal	27
SMO ab72130	Abcam	Rabbit polyclonal	86
SMO C17	Santa Cruz	Goat polyclonal	85
SMO N19	Santa Cruz	Goat polyclonal	85

Table 8.3: Table of primary antibodies

8.4 Pharmacological inhibitors

Inhibitor	Target	Company	Details
AG1478 (658552)	EGFR	Merck	Cell permeable, reversible, competitive inhibitor
Cyclopamine-KAAD (239804)	SMO	Merck	Cell permeable, competitive inhibitor
SANT1 (559303)	SMO	Merck	Cell permeable, competitive inhibitor
U0126 (662005)	MEK	Merck	Cell permeable, non-competitive inhibitor

Table 8.4: Table of pharmacological inhibitors

8.5 SMO nuclear localisation signal

```
  1  MAAARPARGPELPLLGLLLLLLLLGDPGRGAASSGNATGPGPRSAGGSARR   50
 51  SAAVTGPPPPLSHCGRAAPCEPLRYNVCLGSVLPYGATSTLLAGDSDSQE  100
101  EAHGKLVLWSGLRNAPRCWAVIQPLLCAVYMPKCENDRVELPSRTLCQAT  150
151  RGPCAIVERERGWPDFLRCTPDRFPEGCTNEVQNIKFNSSGQCEVPLVRT  200
201  DNPKSWYEDVEGCGIQCQNPLFTEAEHQDMHSYIAAFGAVTGLCTLFTLA  250
251  TFVADWRNSNRYPAVILFYVNACFFVGSIGWLAQFMDGARREIVCRADGT  300
301  MRLGEPTSNETLSCVIIFVIVYYALMAGVVWFVVLTYAWHTSFKALGTTY  350
351  QPLSGKTSYFHLLTWSLPFVLTVAILAVAQVDGDSVSGICFVGYKNYRYR  400
401  AGFVLAPIGLVLIVGGYFLIRGVMTLFSIKSNHPGLLSEKAASKINETML  450
451  RLGIFGFLAFGFVLITFSCHFYDFFNQAEWERSFRDYVLCQANVTIGLPT  500
501  KQPIPDCEIKNRPSLLVEKINLFAMFGTGIAMSTWVWTKATLLIWRRTWC  550
551  RLTGQSDDEPKRIKKSKMIAKAFSKRHELLQNPGQELSFSMHTVSHDGPV  600
601  AGLAFDLNEPSADVSSAWAQHVTKMVARRGAILPQDISVTPVATPVPPEE  650
651  QANLWLVEAEISPELQKRLGRKKKRRKRKKEVCPLAPPPELHPPAPAPST  700
701  IPRLPQLPRQKCLVAAGAWGAGDSCRQGAWTLVSNPFCPEPSPPQDPFLP  750
751  SAPAPVAWAHGRRQGLGPIHSRTNLMDTELMDADSDF               787
```

Positively and negatively influencing subsequences are coloured according to the following scale:

Negative  Positive

Figure 8.1: SMO nuclear localisation signal

The nuclear localisation signal was identified in SMO using the NucPred software (Brameier et al., 2007).

8.6 Affymetrix array data

Fold change	Symbol	Description
9.4698	MMP7	matrix metallopeptidase 7 (matrilysin, uterine)
9.1472	SCGB1A1	secretoglobin, family 1A, member 1 (uteroglobin)
8.2059	CXCL10	chemokine (C-X-C motif) ligand 10
7.0453	PTGIS	prostaglandin I2 (prostacyclin) synthase
6.4681	ANKRD1	ankyrin repeat domain 1 (cardiac muscle)
6.3496	THY1	Thy-1 cell surface antigen
5.4516	NNMT	nicotinamide N-methyltransferase
5.0397	SRPX	sushi-repeat-containing protein, X-linked
4.9818	ESX1	ESX homeobox 1
4.8906	CXCL11	chemokine (C-X-C motif) ligand 11
4.8456	ADAM19	ADAM metallopeptidase domain 19
4.8456	IL7R	interleukin 7 receptor
4.7349	GPRC5B	G protein-coupled receptor, family C, group 5, member B
4.5315	FAM20C	family with sequence similarity 20, member C
4.4076	SAA1	serum amyloid A1
4.2477	LAPTM5	lysosomal protein transmembrane 5
4.1315	MMP2	matrix metallopeptidase 2 (gelatinase A, 72kDa gelatinase, 72kDa type IV collagenase)
3.9908	LIFR	leukemia inhibitory factor receptor alpha
3.8548	CYP24A1	cytochrome P450, family 24, subfamily A, polypeptide 1
3.8194	CFB	complement factor B
3.7842	ALDH2	aldehyde dehydrogenase 2 family (mitochondrial)
3.7581	MCAM	melanoma cell adhesion molecule
3.6050	APOBEC3G	apolipoprotein B mRNA editing enzyme, catalytic polypeptide-like 3G
3.5718	VIM	vimentin
3.5718	SLCO2A1	solute carrier organic anion transporter family, member 2A1
3.4661	FAP	fibroblast activation protein, alpha
3.4502	TRIM31	tripartite motif-containing 31
3.3792	APOD	apolipoprotein D
3.3714	PMEPA1	prostate transmembrane protein, androgen induced 1
3.3636	SERPINA3	serpin peptidase inhibitor, clade A (alpha-1 antiproteinase, antitrypsin), member 3
3.3636	SIRPA	signal-regulatory protein alpha
3.3173	INHBA	inhibin, beta A
3.2868	TGFB2	transforming growth factor, beta 2
3.2716	IFITM1	interferon induced transmembrane protein 1 (9-27)
3.2565	HLA-B	major histocompatibility complex, class I, B
3.0314	ATP8A2	ATPase, aminophospholipid transporter, class I, type 8A, member 2
3.0175	SLC2A12	solute carrier family 2 (facilitated glucose transporter), member 12
2.9417	LOXL2	lysyl oxidase-like 2
2.9012	RNASE7	ribonuclease, RNase A family, 7
2.8613	LPXN	leupaxin
2.8613	C15orf48	chromosome 15 open reading frame 48
2.8415	TRIM22	tripartite motif-containing 22
2.8219	IL32	interleukin 32
2.7830	CDH2	cadherin 2, type 1, N-cadherin (neuronal)
2.7574	GBP1	guanylate binding protein 1, interferon-inducible, 67kDa
2.7447	PLOD2	procollagen-lysine, 2-oxoglutarate 5-dioxygenase 2
2.7258	ZNF114	zinc finger protein 114
2.7195	ATP6V0D2	ATPase, H+ transporting, lysosomal 38kDa, V0 subunit d2
2.6945	SPATA18	spermatogenesis associated 18 homolog (rat)
2.6945	GULP1	GULP, engulfment adaptor PTB domain containing 1

Table 8.5: Table of top 50 DEGs with a 2-fold cut off when comparing NEB1-shPTCH1 cells to NEB1-shCON cells

Fold change	Symbol	Description
-2.2191	ASNS	asparagine synthetase (glutamine-hydrolyzing)
-2.2243	ACADSB	acyl-CoA dehydrogenase, short/branched chain
-2.2346	SLC19A3	solute carrier family 19, member 3
-2.2605	GJB6	gap junction protein, beta 6, 30kDa
-2.3295	HMGN5	high-mobility group nucleosome binding domain 5
-2.3839	ANKRD22	ankyrin repeat domain 22
-2.4061	RPS6KA6	ribosomal protein S6 kinase, 90kDa, polypeptide 6
-2.4116	SCNN1B	sodium channel, nonvoltage-gated 1, beta
-2.4340	MTSS1	metastasis suppressor 1
-2.4566	BMP7	bone morphogenetic protein 7
-2.4852	WASF3	WAS protein family, member 3
-2.5024	SCNN1G	sodium channel, nonvoltage-gated 1, gamma
-2.5082	LRRC6	leucine rich repeat containing 6
-2.5374	UPK3B	uroplakin 3B
-2.5491	MANEA	mannosidase, endo-alpha
-2.5907	SPRR1B	small proline-rich protein 1B
-2.6268	FAM63B	family with sequence similarity 63, member B
-2.6635	POF1B	premature ovarian failure, 1B
-2.6759	IGFBP2	insulin-like growth factor binding protein 2, 36kDa
-2.7069	CAPNS2	calpain, small subunit 2
-2.7447	TGM1	transglutaminase 1
-2.7638	SEC11C	SEC11 homolog C (S. cerevisiae)
-2.8024	C1orf21	chromosome 1 open reading frame 21
-2.9079	PPFIBP2	PTPRF interacting protein, binding protein 2 (liprin beta 2)
-2.9485	CXCR7	chemokine (C-X-C motif) receptor 7
-2.9485	TCF7L1	transcription factor 7-like 1 (T-cell specific, HMG-box)
-3.0105	SPRR1A	small proline-rich protein 1A
-3.0175	WDR17	WD repeat domain 17
-3.0667	ANKFN1	ankyrin-repeat and fibronectin type III domain containing 1
-3.1023	KRT15	keratin 15
-3.2266	SERPINB13	serpin peptidase inhibitor, clade B (ovalbumin), member 13
-3.2415	SH3BGRL	SH3 domain binding glutamic acid-rich protein like
-3.3173	AGR2	anterior gradient homolog 2 (Xenopus laevis)
-3.3250	SPRR3	small proline-rich protein 3
-3.4661	ZNF165	zinc finger protein 165
-3.4661	EPB41L4A	erythrocyte membrane protein band 4.1 like 4A
-3.4822	SCD5	stearoyl-CoA desaturase 5
-3.6553	AMOT	angiomotin
-3.7149	SULT1E1	sulfotransferase family 1E, estrogen-preferring, member 1
-3.8106	KRT4	keratin 4
-3.8282	MCOLN3	mucolipin 3
-3.9267	H2AFY2	H2A histone family, member Y2
-4.3269	PNLIPRP3	pancreatic lipase-related protein 3
-4.3469	CNTN1	contactin 1
-4.3772	MUC15	mucin 15, cell surface associated
-4.5525	KLHL13	kelch-like 13 (Drosophila)
-5.8159	LASS3	LAG1 homolog, ceramide synthase 3
-8.6538	ARHGEF9	Cdc42 guanine nucleotide exchange factor (GEF) 9
-8.7341	C9orf125	chromosome 9 open reading frame 125
-10.1965	FBN2	fibrillin 2

Table 8.6: Table of bottom 50 DEGs with a 2-fold cut off when comparing NEB1-shPTCH1 cells to NEB1-shCON cells

Fold change	Symbol	Description
7.2267	THY1	Thy-1 cell surface antigen
6.3938	ANKRD1	ankyrin repeat domain 1 (cardiac muscle)
6.0769	SCGB1A1	secretoglobin, family 1A, member 1 (uteroglobin)
5.1814	NNMT	nicotinamide N-methyltransferase
5.1456	ADAM19	ADAM metallopeptidase domain 19
4.9474	PTGIS	prostaglandin I2 (prostacyclin) synthase
4.9019	ESX1	ESX homeobox 1
4.9019	MMP7	matrix metallopeptidase 7 (matrilysin, uterine)
4.8793	SRPX	sushi-repeat-containing protein, X-linked
4.8232	LIFR	leukemia inhibitory factor receptor alpha
4.3369	MCAM	melanoma cell adhesion molecule
4.2281	IL7R	interleukin 7 receptor
4.1892	GPRC5B	G protein-coupled receptor, family C, group 5, member B
4.1315	FAM20C	family with sequence similarity 20, member C
4.0652	LAPTM5	lysosomal protein transmembrane 5
3.9908	ALDH2	aldehyde dehydrogenase 2 family (mitochondrial)
3.8637	MMP2	matrix metallopeptidase 2 (gelatinase A, 72kDa gelatinase, 72kDa type IV collagenase)
3.8459	CXCL10	chemokine (C-X-C motif) ligand 10
3.8018	CYP24A1	cytochrome P450, family 24, subfamily A, polypeptide 1
3.7668	CDH2	cadherin 2, type 1, N-cadherin (neuronal)
3.7494	SLCO2A1	solute carrier organic anion transporter family, member 2A1
3.7321	PMEPA1	prostate transmembrane protein, androgen induced 1
3.5145	FAP	fibroblast activation protein, alpha
3.5064	SAA1	serum amyloid A1
3.4027	VIM	vimentin
3.3173	TGFB2	transforming growth factor, beta 2
3.3173	INHBA	inhibin, beta A
3.3173	PLOD2	procollagen-lysine, 2-oxoglutarate 5-dioxygenase 2
3.2191	LOXL2	lysyl oxidase-like 2
2.9690	HLA-B	major histocompatibility complex, class I, B
2.9622	CYGB	cytoglobin
2.9282	SIRPA	signal-regulatory protein alpha
2.8812	ATP8A2	ATPase, aminophospholipid transporter, class I, type 8A, member 2
2.8024	SPOCK1	sparc/osteonectin, cwcv and kazal-like domains proteoglycan (testican) 1
2.7959	CACNA2D1	calcium channel, voltage-dependent, alpha 2/delta subunit 1
2.7574	MMD	monocyte to macrophage differentiation-associated
2.7447	PLAT	plasminogen activator, tissue
2.7321	QPRT	quinolinate phosphoribosyltransferase
2.7321	ZNF114	zinc finger protein 114
2.7069	GRAMD1B	GRAM domain containing 1B
2.7007	DGAT2	diacylglycerol O-acyltransferase 2
2.6945	DOCK10	dedicator of cytokinesis 10
2.6635	GLIPR1	GLI pathogenesis-related 1
2.6451	SLC41A2	solute carrier family 41, member 2
2.6329	CFB	complement factor B
2.5967	APOD	apolipoprotein D
2.5550	LPXN	leupaxin
2.5198	CXCL11	chemokine (C-X-C motif) ligand 11
2.4909	SPATA18	spermatogenesis associated 18 homolog (rat)

Table 8.7: Table of top 50 DEGs with a 2-fold cut off when comparing NEB1-shPTCH1 + Cyc-KAAD cells to NEB1-shCON cells

Fold change	Symbol	Description
-2.5491	UPK3B	uroplakin 3B
-2.5787	PARP16	poly (ADP-ribose) polymerase family, member 16
-2.6268	ERO1LB	ERO1-like beta (S. cerevisiae)
-2.6759	BLNK	B-cell linker
-2.7702	SPRR1B	small proline-rich protein 1B
-2.7766	ANKRD22	ankyrin repeat domain 22
-2.8415	ANKFN1	ankyrin-repeat and fibronectin type III domain containing 1
-2.8812	SEL1L	sel-1 suppressor of lin-12-like (C. elegans)
-2.8945	SEC11C	SEC11 homolog C (S. cerevisiae)
-2.9079	TMEM50B	transmembrane protein 50B
-2.9147	SCNN1B	sodium channel, nonvoltage-gated 1, beta
-2.9622	GPR1	G protein-coupled receptor 1
-2.9759	PPFIBP2	PTPRF interacting protein, binding protein 2 (liprin beta 2)
-2.9828	IGFBP2	insulin-like growth factor binding protein 2, 36kDa
-3.0175	ASNS	asparagine synthetase (glutamine-hydrolyzing)
-3.1023	SDF2L1	stromal cell-derived factor 2-like 1
-3.1602	STARD5	StAR-related lipid transfer (START) domain containing 5
-3.1675	CAPNS2	calpain, small subunit 2
-3.1675	DNAJB9	DnaJ (Hsp40) homolog, subfamily B, member 9
-3.2490	SCD5	stearoyl-CoA desaturase 5
-3.2716	TCF7L1	transcription factor 7-like 1 (T-cell specific, HMG-box)
-3.3636	SH3BGRL	SH3 domain binding glutamic acid-rich protein like
-3.3636	TGM1	transglutaminase 1
-3.4343	AMOT	angiomotin
-3.4343	SPRR1A	small proline-rich protein 1A
-3.4422	FICD	FIC domain containing
-3.4502	CXCR7	chemokine (C-X-C motif) receptor 7
-3.5472	EPB41L4A	erythrocyte membrane protein band 4.1 like 4A
-3.6893	MCOLN3	mucolipin 3
-3.7149	HERPUD1	homocysteine-inducible endoplasmic reticulum stress-inducible ubiquitin-like domain 1
-3.7235	MUC15	mucin 15, cell surface associated
-3.8548	H2AFY2	H2A histone family, member Y2
-4.1030	CHAC1	ChaC, cation transport regulator homolog 1 (E. coli)
-4.2575	SERPINB13	serpin peptidase inhibitor, clade B (ovalbumin), member 13
-4.4795	CNTN1	contactin 1
-4.4795	KRT15	keratin 15
-4.5842	KLHL13	kelch-like 13 (Drosophila)
-4.7240	KRT4	keratin 4
-4.7568	SPRR3	small proline-rich protein 3
-5.2174	SULT1E1	sulfotransferase family 1E, estrogen-preferring, member 1
-5.3641	ZNF165	zinc finger protein 165
-5.7491	LASS3	LAG1 homolog, ceramide synthase 3
-5.8835	AGR2	anterior gradient homolog 2 (Xenopus laevis)
-6.0769	PNLIPRP3	pancreatic lipase-related protein 3
-6.6807	DDIT3	DNA-damage-inducible transcript 3
-7.9815	ARHGEF9	Cdc42 guanine nucleotide exchange factor (GEF) 9
-8.0000	C9orf125	chromosome 9 open reading frame 125
-10.0329	FBN2	fibrillin 2

Table 8.8: Table of bottom 50 DEGs with a 2-fold cut off when comparing NEB1-shPTCH1 + Cyc-KAAD cells to NEB1-shCON cells